Enhancement of Solar Photovoltaic System Performance under Partial Shaded Conditions using Evolutionary Optimization Techniques

Thesis

Submitted in partial fulfillment of the requirements

for the award of the degree of

Doctor of Philosophy

in

Electrical Engineering

by

Rambabu Motamarri
(Roll No. 717011)

Supervisor

Dr. Bhookya Nagu
Assistant Professor

Department of Electrical Engineering
National Institute of Technology Warangal
(An Institute of National Importance)
Warangal – 506004, Telangana State, India.

March - 2021

APPROVAL SHEET

This Thesis entitled "**Enhancement of Solar Photovoltaic System Performance under Partial Shaded Conditions using Evolutionary Optimization Techniques**" by **Rambabu Motamarri (Roll No.717011)** is approved for the degree of Doctor of Philosophy.

Examiners

_____

_____

_____

Supervisor

Dr. Bhookya Nagu
Assistant Professor
EED, NIT Warangal

Chairman

Dr. D. M. Vinod Kumar
Professor,
EED, NIT Warangal

Date: _____

DEPARTMENT OF ELECTRICAL ENGINEERING
NATIONAL INSTITUTE OF TECHNOLOGY WARANGAL
WARANGAL – 506 004

DEPARTMENT OF ELECTRICAL ENGINEERING

NATIONAL INSTITUTE OF TECHNOLOGY WARANGAL

CERTIFICATE

This is to certify that the thesis entitled **"Enhancement of Solar Photovoltaic System Performance under Partial Shaded Conditions using Evolutionary Optimization Techniques"**, which is being submitted by **Mr. Rambabu Motamarri** (Roll No. 717011), is a bonafide work submitted to National Institute of Technology Warangal in partial fulfilment of the requirements for the award of the degree of **Doctor of Philosophy** in Electrical Engineering. To the best of my knowledge, the work incorporated in this thesis has not been submitted elsewhere for the award of any degree.

Date:

Place: Warangal

Dr. BHOOKYA NAGU
(Thesis Supervisor)
Assistant Professor
Department of Electrical Engineering
National Institute of Technology Warangal
Warangal – 506004, Telangana State

DECLARATION

This is to certify that the work presented in the thesis entitled "**Enhancement of Solar Photovoltaic System Performance under Partial Shaded Conditions using Evolutionary Optimization Techniques"** is a bonafide work done by me under the supervision of **Dr. Bhookya Nagu**, Assistant Professor, Department of Electrical Engineering, National Institute of Technology Warangal, India and was not submitted elsewhere for the award of any degree.

I declare that this written submission represents my ideas in my own words and where others ideas or words have been included; I have adequately cited and referenced the original sources. I also declare that I have adhered to all principles of academic honesty and integrity and have not misrepresented or fabricated or falsified any idea/date/fact/source in my submission. I understand that any violation of the above will be a cause for disciplinary action by the institute and can also evoke penal action from the sources which have thus not been properly cited or from whom proper permission has not been taken when needed.

Date:

Place: Warangal

Rambabu Motamarri
(Roll No: 717011)

ACKNOWLEDGEMENTS

It gives me immense pleasure to express my deep sense of gratitude and thanks to my supervisor **Dr. Bhookya Nagu,** Assistant Professor, Department of Electrical Engineering, National Institute of Technology Warangal, for his valuable guidance, support, and suggestions. His knowledge, suggestions, and discussions enabled me to become a capable researcher. He has shown me the interesting side of this wonderful and potential research area. His encouragement helped me overcome the difficulties encountered in my research as well in my personal life.

I am very thankful to **Prof. D. M. Vinod Kumar**, DSC Committee Chairman, Department of Electrical Engineering for his constant technical suggestions, encouragement, support and cooperation.

I take this privilege to thank all my DSC Committee members, **Dr. S. Srinivasa Rao**, Professor, Department of Electrical Engineering, **Dr. B. L. Narasimharaju**, Associate Professor, Department of Electrical Engineering and **Dr. S. Ravichandra**, Associate Professor, Department of Computer Science and Engineering for their detailed technical review, constructive suggestions and excellent advice during the progress of this research work.

I am very much thankful to **Prof. M. Sailaja Kumari**, Head, Department of Electrical Engineering for her constant encouragement, support, and cooperation.

I wish to express my sincere thanks to **Prof. N. V. Ramana Rao**, Director, NIT Warangal for his official support and encouragement.

I also appreciate the encouragement from teaching, non-teaching members, and fraternity of Department of Electrical Engineering of NIT Warangal. They have always been encouraging and supportive.

I would also like to thank **Dr. M. Raja Vishwanathan**, Assistant Professor, Department of Humanities & Social Science for his valuable time in proofreading the thesis.

I convey my special thanks to contemporary Research Scholars Mr. V Venkataramana, Ms. T Ratna Rahul, Mr. M Hareesh, Mr. B Anil Kumar, Mr. M Santosh, Mr. A Pranay Kumar, Mr. K Sateesh Kumar, Mr. Y Bhaskar S S Gupta, Mr. V K Satyakar, Mr. Phanendra Babu,

Mr. K. Hemasundara Rao, Mr. S Venu, Mr. K Narender Reddy, Ms. S Niveditha, Mr. B Laxman, Mr. G Mahanandeswara Gowd, Ms. P Mounica, Dr. D Sumon, and Mr. S Madhu Babu, Mr. P Srinivas, Mr. K Srinivas, Mr. G.Ramesh, Mr. C Bhanu Prasad, Mr. M Dileep Krishna, Mr. K Eshwar.

I acknowledge my gratitude to all my teachers and colleagues at various places for supporting and co-operating with me to complete the work.

I express my deep sense of gratitude and reverence to my beloved father **Shri. M. Adinarayana,** Mother **Smt. Venkayamma**, wife **Thirumala,** uncle **Shri. M. Sivaiah,** aunty **Smt. Rama Koteswari**, brother **Shri. M. Venkateswarlu,** Sister in law **Smt. Hima Bindu,** and my grandfather **Shri. M. Chinnarayana,** grandmother **Smt. Annapurna**, for their sincere prayers, blessings, constant encouragement, and for shouldering the responsibilities of educating me and providing me with moral support throughout my life, without which the research work would not have been possible.

I would like to express my greatest admiration to **all my family members** for their positive encouragement that they showered on me throughout this research work. Without my family's sacrifice and support, this research work would not have been possible. It is a great pleasure for me to acknowledge and express my appreciation to all **my well-wishers** for their understanding, relentless support, and encouragement during my research work. Last but not least, I wish to express my sincere thanks to all those who helped me directly or indirectly at various stages of this work.

Above all, I express my deepest regard and gratitude to "**ALMIGHTY**" whose divine light and warmth showered upon me the perseverance, inspiration, faith and strength to keep the momentum of work high even at tough moments of research work.

Rambabu Motamarri

ABSTRACT

Maximum Power Point Tracking (MPPT) is necessary for solar Photovoltaic (PV) systems. It is a well-known and well-researched concept that under uniform irradiance conditions, there is a single Maximum Power Point (MPP) in the Power-Voltage (P-V) characteristics. However, when there are fluctuations in the solar irradiance received on the surface of a PV system, such as partial shading caused by moving clouds, shade of trees or tall buildings, dust, etc., the P-V curve displays multiple local peaks. Thus, the MPPT algorithm must have the capability to locate the global MPP from multiple local peaks. There is no unique MPPT algorithm, which can contribute to 'better' performance for all operating conditions for a PV system. In a PV array, the distribution of irradiance is unequal varying from module to module under Partial Shading (PS) conditions. Because of the PS of PV array the number of peaks in P-V characteristics increases. In such cases, it would be difficult to track highest peak point of P-V curve using traditional MPPT algorithms such as Perturb and Observe (P&O), Hill Climbing (HC), Incremental Conductance (IC), etc. But these work effectively only under constant irradiance conditions. However, in order to track global peak point of P-V curves, evolutionary optimization techniques are best suited to track global peak of P-V curve under partial shading condition (PSC) of the PV system. From the literature it is observed that, evolutionary algorithms are facing some problems such as, delay in convergence due to more control parameters, and more tuning parameters, which are unable to tune exact value through a course of iteration. In order to track the Global Maximum Power Point (GMPP) with a better convergence factor, and minimum oscillations at transient and steady-state point, bio-inspired algorithms have to search properly by maintaining an exploration and exploitation process in the designed search space. For better performance of PV system in increasing efficiency, the present research proposes improvements to existing evolutionary algorithms.

In this thesis, the Modified Grey Wolf Optimization (MGWO) algorithm is developed and validated experimentally to track the Global MPPT under partial shaded conditions of PV array. The MGWO algorithm enhances the existing Grey Wolf Optimization (GWO) algorithm by using modified updated-position and non-linear variation of control parameter for better convergence factor. The proposed MGWO algorithm tracks the Global Peak (GP) power under shaded conditions of PV array with reduced number of iterations and less tracking period. The steady-state oscillations are also reduced around the global peak point

successfully with only one tuning control parameter, and initial particles are independent of the PV system. To highlight the proposed method a detailed comparison with conventional GWO and HC algorithms is presented under static and re-initialization of parameters during dynamic shaded conditions of PV array.

Due to presence of varying control parameters, one is unable to tune exact value through a course of iteration, which creates delay in convergence. Based on this information, the Velocity of PSO algorithm based on Lévy Flight (VPSO-LF) is proposed with reduction in adaptive control parameters for better convergence under PSC. In the proposed algorithm, the velocity of PSO is updated with Lévy Flights (LF) distribution to reach the GMPP with low tracking time and reduced number of iterations without any limitations to control parameters. The proposed VPSO-LF algorithm also reduces steady-state oscillations around the GP effectively, allows initial duty independent of the PV system and also does not need the tuning of parameters. The proposed VPSO-LF algorithm is examined through MATLAB/SIMULINK as well as from experiments along with conventional PSO and HC to validate the results under static and re-initialization of parameters during dynamic cases.

Many control parameters create a poor exploitation process while searching for the global best position. So from the literature it is observed that, Jaya algorithm has few specific parameters but its performance is good for the exploration process, though it is poor at exploitation process. To improve both exploration and exploitation process, Jaya algorithm is implemented based on LF called Jaya-LF. The proposed Jaya-LF algorithm tracks GP power with fewer iterations and lower convergence time, and also reduces the oscillations at steady-state and transient period. The results of the performance of Jaya-LF algorithm are validated with Jaya and PSO algorithms to demonstrate the effectiveness of the proposed algorithm under static and re-initialization of parameters during dynamic conditions. The reduced control parameters are considered in Jaya-LF algorithm compared with VPSO-LF and MGWO algorithms.

Contents

ACKNOWLEDGEMENTS **i**

ABSTRACT **iii**

List of Figures **ix**

List of Tables **xiv**

Abbreviations **xv**

List of Symbols **xvii**

Chapter 1 Introduction **1**

1.1 Introduction to PV System 2

1.2 Literature Survey 3

1.3 Motivations 13

1.4 Research Objectives 14

1.5 Organization of the Thesis 14

Chapter 2 The Solar Photovoltaic System **16**

2.1 Introduction 17

2.2 A Solar PV Cell Working Principle 18

2.3 Solar Radiation 19

2.4 Modelling of PV Systems 21

2.4.1 Ideal PV Cell 21

2.4.2 Modelling of PV Array 22

2.4.3 Fill Factor 26

2.5 Characteristics of Solar PV Module 27

2.5.1 The Effect of Temperature on PV Module 27

2.5.2 The Effect of Irradiance on PV Module 28

2.6 Types of Solar Cells 29

2.6.1 Mono-crystalline Silicon 30

2.6.2 Poly-crystalline Silicon 30

2.6.3 Amorphous and thin-film Silicon 30

2.6.4 Other Cells and Materials 31
2.7 MPPT in PV Systems 32
2.7.1 MPPT under Non-Uniform Irradiance 34
2.7.1.1 PV System under Partial Shaded Conditions 34
2.7.1.2 Effect of Rapidly Changing Irradiance on PV Stytem 36
2.7.2 Classical MPPT Techniques 37
2.7.2.1 Perturb and Observe Algorithm 37
2.7.2.2 Incremental Conductance Algorithm 39
2.7.3 Evolutionary Optimization Techniques 40
2.7.3.1 Particle Swarm Optimization Algorithm 40
2.7.3.2 Ant Colony Optimization Algorithm 41
2.7.3.3 Artificial Bee Colony Algorithm 44
2.7.3.4 Firefly Algorithm 46
2.7.3.5 Other Types of Algorithms 49
Chapter 3 Modified Grey Wolf Optimization Algorithm for Global MPPT under Partial Shading Conditions in Photovoltaic System 50
3.1 Introduction 51
3.2 Tracking Methods for GMPP 51
3.2.1 Hill Climbing Algorithm for GMPPT 51
3.2.2 GWO Algorithm for GMPPT 52
3.2.3 Proposed MGWO algorithm for GMPPT 53
3.2.3.1 Steps to Implement Proposed MGWO Algorithm 54
3.3 The Solar PV Array under Partial Shaded Condition 56
3.4 Simulation Results 57
3.4.1 Simulation Results of 3S PV Array Configuration 59
3.4.2 Simulation Results of 4S2P PV Array Configuration 62
3.5 Experimental Results 64
3.5.1 Experimental Results of 3S PV Array Configuration 65
3.5.2 Experimental Results of 4S2P PV Array Configuration 69

3.6 Comparative Study of Proposed MGWO Algorithm with Existing Algorithms 74
3.7 Results and Conclusions 76
Chapter 4 GMPPT using PSO based on Lévy Flight for Photovoltaic System under Partial Shading Conditions 77
4.1 Introduction 78
4.2 GMPPT Methods 78
4.2.1 GMPPT through Hill Climbing Algorithm 78
4.2.2 GMPPT through PSO Algorithm 79
4.2.3 GMPPT through Proposed VPSO-LF Algorithm 80
4.2.3.1 Steps to Implement Proposed VPSO-LF Algorithm 82
4.3 The Solar PV Array under Partial Shaded Conditions 84
4.4 Simulation Results 86
4.4.1 Simulation Results of 3S PV Array Configuration 88
4.4.2 Simulation Results of 4S PV Array Configuration 93
4.4.3 Simulation Results of 6S PV Array Configuration 95
4.5 Experimental Results 98
4.5.1 Experimental Results of 3S PV Array Configuration 99
4.5.2 Experimental Results of 4S PV Array Configuration 105
4.5.3 Experimental Results of 6S PV Array Configuration 109
4.6 Comparative Study of Proposed VPSO-LF Algorithm with Existing Algorithms 112
4.7 Results and Conclusions 114
Chapter 5 Jaya Algorithm based on Lévy Flight for Global MPPT under Partial Shading in Photovoltaic System 115
5.1 Introduction 116
5.2 Implementation of GMPPT Algorithms 116
5.2.1 Jaya Algorithm for GMPPT 116
5.2.2 Jaya Algorithm based on Lévy Flight (Jaya-LF) for GMPPT 117
5.2.2.1 Steps to Implement Proposed Jaya-LF Algorithm 120

5.3 The Solar PV Array under Partial Shaded Condition 120
5.4 Simulation Results 122
5.4.1 Simulation Results of 3S2P PV Array Configuration 123
5.4.2 Simulation Results of 4S2P PV Array Configuration 125
5.5 Experimental Results 128
5.5.1 Experimental Results of 3S2P PV Array Configuration 129
5.5.2 Experimental Results of 4S2P PV Array Configuration 133
5.6 Comparative Study of Proposed Jaya-LF Algorithm with Existing Algorithms 138
5.7 Results and Conclusions 140
Chapter 6 Conclusions and Scope for the Future Research 141
6.1 Conclusions 142
6.2 Scope for Future Research 144
Journal Publications 145
References 146
Appendix-I 157
Appendix-II 158
Curriculum-Vitae 159

List of Figures

Figure 2.1	PV Cell, Module and Array	18
Figure 2.2	Physical structure of a PV cell	18
Figure 2.3	Spectral power distribution of the black body radiation and the Sun radiation in the extra-terrestrial space (AM0) and on Earth's surface (AM1.5)	20
Figure 2.4	Illustration of the AM1.5 path and the direct-normal and global incident radiations on a the Sun-facing surface at 37^o tilt	20
Figure 2.5	Model of the ideal PV cell and equivalent circuit of a practical PV system	22
Figure 2.6	The I–V characteristics of a PV cell. The total cell current (I) is composed of the Sun-radiated current I_{pv} and the diode current I_d	22
Figure 2.7	The I–V characteristics of a practical PV system with three remarkable points: short circuit $(0,\ I_{sc})$, MPP (V_{mp}, I_{mp}), and open circuit $(V_{oc}, 0)$	23
Figure 2.8	I-V and P-V characteristics at standard irradiation (1 kW/m^2) with four dissimilar temperatures	28
Figure 2.9	I-V and P-V characteristic at standard temperature (25°C) with four dissimilar irradiation values	28
Figure 2.10	Classification of MPPT techniques	34
Figure 2.11	PV array configuration of: (a) Four PV modules in series (4S), and (b) Four PV modules are in series and with two such combinations in parallel (4S2P)	35
Figure 2.12	Characteristics of PV array configuration: (a) 4S, and b) 4S2P	36
Figure 2.13	The P-V characteristics for two series connected modules under shading conditions	37
Figure 2.14	Flowchart of perturb and observation algorithm	38
Figure 2.15	Flowchart of incremental conductance algorithm	39
Figure 3.1	Flowchart of proposed MGWO algorithm	55

Figure 3.2	PV array configurations under partial shading conditions of: (a) 3S, and (b) 4S2P	56
Figure 3.3	PV array characteristics partial shading conditions of: (a) 3S, and (b) 4S2P	57
Figure 3.4	Application of PV array to boost converter with MPPT controller	58
Figure 3.5	Simulation results for 3S PV array configuration during shading of: (a) Pattern-1, (b) Pattern-2, and (c) Pattern-3	60
Figure 3.6	Simulation results for proposed MGWO algorithm compared with HC, and GWO algorithms during dynamics of shading pattern-1, and shading pattern-2 of 3S PV array	62
Figure 3.7	Simulation results of 4S2P PV array configuration during shading of: (a) Pattern-4, (b) Pattern-5, and (c) Pattern-6	63
Figure 3.8	Experimental setup for proposed MGWO algorithm	65
Figure 3.9	Experimental results for shading pattern-1 of 3S PV array: (a) HC, (b) GWO, and (c) Proposed MGWO algorithm	66
Figure 3.10	Experimental results for shading pattern-2 of 3S PV array: (a) HC, (b) GWO, and (c) Proposed MGWO algorithm	67
Figure 3.11	Experimental results for shading pattern-3 of 3S PV array: (a) HC, (b) GWO, and (c) Proposed MGWO algorithm	68
Figure 3.12	Experimental results during dynamics of shading pattern-1, and shading pattern-2 of 3S PV array of: (a) HC, (b) GWO, and (c) Proposed MGWO algorithm	70
Figure 3.13	Experimental results for shading pattern-4 of 4S2P PV array: (a) HC, (b) GWO, and (c) Proposed MGWO algorithm	71
Figure 3.14	Experimental results for shading pattern-5 of 4S2P PV array: (a) HC, (b) GWO, and (c) Proposed MGWO algorithm	72
Figure 3.15	Experimental results for shading pattern-6 of 4S2P PV array: (a) HC, (b) GWO, and (c) Proposed MGWO algorithm	73
Figure 3.16	Experimental results comparison of proposed MGWO algorithm with GWO, and HC algorithms of: (a) Power, (b) Tracking time,	75

	(c) Efficiency, and (d) Iterations with respect to each shading pattern	
Figure 4.1	Lévy flights distribution in two dimensional plane	82
Figure 4.2	Flowchart of proposed VPSO-LF algorithm	83
Figure 4.3	The PV array configuration under partial shading conditions: (a) Three PV modules in series (3S), (b) Four PV modules in series (4S), and (c) Six PV modules in series (6S)	85
Figure 4.4	The PV array characteristics under partial shading conditions: (a) 3S, (b) 4S, and (c) 6S	85
Figure 4.5	Application of PV array to boost converter with MPPT controller	86
Figure 4.6	Simulink model of: (a) The proposed VPSO-LF algorithm, and (b) Series connection of PV modules	87
Figure 4.7	Simulation results for 3S PV array configuration during shading of: (a) Pattern-1, and (b) Pattern-2	89
Figure 4.8	Comparisons of VPSO-LF, and PSO algorithms particle velocity values with the number of iterations	90
Figure 4.9	Simulation results for 3S PV array configuration during shading: (a) Pattern-3, and (b) Pattern-4	92
Figure 4.10	Simulation results for proposed VPSO-LF algorithm compared with HC, and PSO algorithms during dynamics of shading pattern-2, and shading pattern-4 of 3S PV array	93
Figure 4.11	Simulation results for 4S PV array configuration during shading of: (a) Pattern-5, and (b) Pattern-6	94
Figure 4.12	Simulation results for 6S PV array configuration during shading of: (a) Pattern-7, and (b) Pattern-8	97
Figure 4.13	Experimental setup for proposed VPSO-LF algorithm	99
Figure 4.14	Experimental results for shading pattern-1 of 3S PV array of: (a) HC, (b) PSO, and (c) Proposed VPSO-LF algorithm	101
Figure 4.15	Experimental results for shading pattern-2 of 3S PV array of: (a) HC, (b) PSO, and (c) Proposed VPSO-LF algorithm	102

Figure 4.16	Experimental results for shading pattern-3 of 3S PV array of: (a) HC, (b) PSO, and (c) Proposed VPSO-LF algorithm	103
Figure 4.17	Experimental results for shading pattern-4 of 3S PV array of: (a) HC, (b) PSO, and (c) Proposed VPSO-LF algorithm	104
Figure 4.18	Experimental results during dynamics of shading pattern-2, and shading pattern-4 of 3S PV array of: (a) HC, (b) PSO, and (c) Proposed VPSO-LF algorithm	106
Figure 4.19	Experimental results for shading pattern-5 of 4S PV array of: (a) HC, (b) PSO, and (c) Proposed VPSO-LF algorithm	107
Figure 4.20	Experimental results for shading pattern-6 of 4S PV array of: (a) HC, (b) PSO, and (c) Proposed VPSO-LF algorithm	108
Figure 4.21	Experimental results for shading pattern-7 of 6S PV array of: (a) HC, (b) PSO, and (c) Proposed VPSO-LF algorithm	110
Figure 4.22	Experimental results for shading pattern-8 of 6S PV array of: (a) HC, (b) PSO, and (c) Proposed VPSO-LF algorithm	111
Figure 4.23	Experimental results comparison of proposed VPSO-LF algorithm with PSO, and HC algorithms of: (a) Power, (b) Tracking time, (c) Efficiency, and (d) Iterations with respect to each shading pattern	113
Figure 5.1	Flowchart of proposed Jaya-LF algorithm	119
Figure 5.2	PV array configuration under partial shading conditions of: (a) Three PV modules in series and two path such modules in parallel (3S2P), and (b) Four PV modules in series and two path such modules in parallel (4S2P)	121
Figure 5.3	PV array characteristics under partial shading conditions of: (a) 3S2P, and (b) 4S2P	121
Figure 5.4	Application of PV array to boost converter with MPPT controller	122
Figure 5.5	Simulation results for 3S2P PV array configuration during shading: (a) Pattern-1, (b) Pattern-2, and (c) Pattern-3	124

Figure 5.6	Simulation results for 4S2P PV array configuration during shading of: (a) Pattern-4, (b) Pattern-5, and (c) Pattern-6	126
Figure 5.7	Simulation results for proposed Jaya-LF algorithm compared with Jaya, and PSO algorithms during dynamics of shading pattern-1, and shading pattern-2 of 3S2P PV array	128
Figure 5.8	Experimental setup for proposed Jaya-LF algorithm	129
Figure 5.9	Experimental results for shading pattern-1 of 3S2P PV array of: (a) PSO, (b) Jaya, and (c) Proposed Jaya-LF algorithm	130
Figure 5.10	Experimental results for shading pattern-2 of 3S2P PV array of: (a) PSO, (b) Jaya, and (c) Proposed Jaya-LF algorithm	131
Figure 5.11	Experimental results for shading pattern-3 of 3S2P PV array of: (a) PSO, (b) Jaya, and (c) Proposed Jaya-LF algorithm	132
Figure 5.12	Experimental results for shading pattern-4 of 4S2P PV array of: (a) PSO, (b) Jaya, and (c) Proposed Jaya-LF algorithm	134
Figure 5.13	Experimental results for shading pattern-5 of 4S2P PV array of: (a) PSO, (b) Jaya, and (c) Proposed Jaya-LF algorithm	135
Figure 5.14	Experimental results for shading pattern-6 of 4S2P PV array of: (a) PSO, (b) Jaya, and (c) Proposed Jaya-LF algorithm	136
Figure 5.15	Experimental results during dynamics of shading pattern-1, and shading pattern-2 of 3S2P PV array of: (a) PSO, (b) Jaya, and (c) Proposed Jaya-LF algorithm	137
Figure 5.16	Experimental results comparison of proposed Jaya-LF algorithm with PSO, and Jaya algorithms of: (a) Tracking time, and (b) Iterations with respect to each shading pattern	140

List of Tables

Table 3.1	PV Module specifications	57
Table 3.2	Irradiance (W/m^2) of each module in PV arrays configuration	57
Table 3.3	Designed parameters of algorithms and boost converter	58
Table 3.4	Simulation performance analysis of 3S, and 4S2P PV array configurations	61
Table 3.5	Experimental performance analysis of 3S, and 4S2P PV array configurations	74
Table 3.6	Qualitative comparison of the proposed MGWO algorithm with existing MPPT algorithms	76
Table 4.1	Irradiance (W/m^2) of each module in PV array configuration	84
Table 4.2	Designed parameters of algorithms and boost converter	86
Table 4.3	Simulation performance analysis of 3S, 4S, and 6S PV array configurations	98
Table 4.4	Experimental performance analysis of 3S, 4S, and 6S PV array configurations	109
Table 4.5	Qualitative comparison of the proposed VPSO-LF algorithm with existing MPPT algorithms	113
Table 5.1	Irradiance (W/m^2) of each module in PV array configuration	122
Table 5.2	Designed parameters of algorithms and boost converter	123
Table 5.3	Simulation performance analysis of 3S2P, and 4S2P PV array configurations	127
Table 5.4	Experimental performance analysis of 3S2P, and 4S2P PV array configurations	138
Table 5.5	Qualitative comparison of the proposed Jaya-LF algorithm with existing MPPT Algorithms	139

Abbreviations

MPPT	Maximum Power Point Tracking
P-V	Power vs. Voltage
PV	Photovoltaic
I-V	Current vs. Voltage
PS	Partial Shading
PSC	Partial Shading Conditions
P&O	Perturb and Observe
HC	Hill Climbing
IC	Incremental Conductance
PSO	Particle Swarm Optimization
GWO	Grey Wolf Optimization
ACO	Ant Colony Optimization
FA	Firefly Algorithm
MGWO	Modified Grey Wolf Optimization
VPSO-LF	Velocity of PSO based on Lévy Flights
LF	Lévy Flight
Jaya-LF	Jaya based on Lévy Flights
MAHC	Modified Adaptive Hill Climbing Method
GP	Global Peak
DIRECT	Dividing Rectangles
GMPPT	Global MPPT
DPSO	Deterministic PSO
LIPO	Lipschitz Optimization
LMPP	Local MPP
IPSO	Improved PSO
FLC	Fuzzy Logic Controller
C-FPA	Chaotic Flower Pollination Algorithm
OD-PSO	Overall Distribution PSO
ARMO	Adaptive Radial Movement Optimization
ELPSO	Enhanced Leader PSO
LSDS	Large and Small Duty Step

LMDS	Large And Mutable Duty Step
ANN	Artificial Neural Network
ABC	Artificial Bee Colony
AM	Air Mass
STC	Standard Test Condition
FF	Fill Factor
CIGS	Copper Indium Gallium Selenide
CdTe	Cadmium Telluride
LCD	Liquid-Crystal Display
CdS	Cadmium Sulphide
GaAs	Gallium Arsenide
4S	Four PV Modules in Series
4S2P	Four PV Modules are in Series and with Two such Combinations in Parallel
3S	Three PV Modules are in Series
M-I	PV Module -I
6S	Six PV Modules in Series
3S2P	Three PV Modules are in Series and with Two such Combinations in Parallel
MPV-PSO	Modified Particle Velocity-based PSO
LPSO	Leader-PSO
ICS	Improved Cuckoo Search
HAPO&PSO	Hybrid Adaptive P & O and PSO

List of Symbols

$\vec{a}$	Control Parameter of GWO
V_{oc}	Open Circuit Voltage
T_{PD}	Predefined Time
θ_z	Azimuth Angle
$I_{pv,cell}$	The Current Generated by the Incident Light
I_d	Shockley Diode Current
$I_{o,cell}$	The Reverse Saturation Current of PV cell
q	The Electron Charge
k	The Boltzmann Constant
a	The Diode Ideality Constant
N_s	Number of Cells Connected in Series
N_p	Number of Cells Connected in Parallel
R_s	The Equivalent Series Resistance
R_p	The Equivalent Parallel Resistance
I_{sc}	Short Circuit Current
V_{mp}	Voltage at Maximum Power
I_{mp}	Current at Maximum Power
P_{max}	Maximum Power
K_V	The Open-Circuit Voltage/Temperature Coefficient
K_I	The Short Circuit Current/Temperature Coefficient
T	The Actual Nominal Temperature [in Kelvin]
T_n	Nominal Temperature [in Kelvin]
G	Actual Irradiation on the Device Surface in Watts per Square Meters
G_n	Nominal Irradiation in Watts per Square Meters (W/m^2)
E_g	The Band Gap Energy of the Semiconductor
V_t	Thermal Voltage
J_o	Current Density of the Semiconductor in [A/cm^2]
p_{best}^i	The Personal Best Position of particles

k	Maximum Iteration
c_1	Acceleration coefficient of PSO algorithm
v_i^k	Velocity at Present Iteration
x_i^k	Present Particle Position
g_{best}^k	Global Best Position of all the Particles
$r_1 \, and \, r_2$	Randomly Generated Numbers
s_i	Particle Position
$G^i(x)$	The Gaussian Kernel for the i^{th} dimension of the Solution
σ_l^i	Standard Deviation
V_{ref}	Reference Voltage
t_s	Settling Time
e_{ss}	Steady State Error
d_{max}	Maximum Duty Cycle
β_o	The Initial Attractiveness Two Fireflies
r_{ij}	Distance between Fireflies
θ	Perturbation Size
$\vec{X}$	The Position of a Grey Wolf Vector
$\vec{X}_p$	The Position of the Prey Vector
$\vec{X}_{GWO}$	Update Position of GWO
d_i^k	Duty Cycle at i^{th} Position
$\vec{X}_{MGWO}$	Update Position of MGWO
I_{pv}	PV output Current
V_{pv}	PV output Voltage
P_{pv}	PV output Power
W	Inertia Weight
β	Levy Index
δ	Percentage Change of Power

Chapter 1

Introduction

Chapter 1

Introduction

1.1 Introduction to PV System

Humanity is actually confronted by a huge problem. Economic development in many developing countries has led to improvement in working conditions for many more people than in the past. In order to supply power to meet increasing demand, energy generation capacity has to increase drastically in the decades to come. While budgetary opinions could take a temporary role in the ongoing cost of fossil fuels such as coal, oil, and natural gas, it becomes clearer year after year that these costs are largely related to the fact that the supply of oil is reaching its 'ceiling'. Even if this were not the situation, the need for increased energy supply capability would arise, necessitating the use of strategies that are suitable with sustainability criteria. If the above condition is to be met, renewable energy sources such as wind and solar power are the best options. With solar power's tremendous long-term promise, it is expected to expand rapidly in the coming years. The insights on the importance of solar power for future energy supply has been growing strongly with growing concerns about the cost and availability of fossil fuels.

At present, increased reliance on generation of power from Photovoltaic (PV) systems to supply to power grid has been becoming popular and an encouraging sign for future development of renewable energy sources. Photovoltaic systems offer many benefits such as lower maintenance compared to rotating machine interfaced power generating systems, quicker installation time, greater flexibility of placing PV panels on rooftops of homes and buildings. Photovoltaic cells provide clean power because they emit no pollutants like carbon dioxide (CO_2), though small amounts of methane (CH_4) and nitrous oxide (N_2O) are released. They do not pollute the environment, making them suitable for use in suburban areas. Study on the emission from the PV manufacturing process is beyond the scope of this thesis. Further, the initial investment on solar power plants are reduced due to the mass production of semiconductor materials suitable for development of solar panels [1]. However, the PV system offers lower efficiency due to the material properties, nonlinear characteristics and fluctuating climatic conditions. Therefore, the PV system must be run at its Maximum Power Point (MPP). Efficiency is greatly influenced by partial shading due to moving clouds, dust, neighbouring buildings, trees and prevailing weather conditions. Due to these obstacles,

multiple local peaks and a global peak are available on P-V characteristics of a PV system [2] - [4]. It's a great challenge to ensure global optimization of PV system, in order to operate at the global optimal point rather than local optimal points.

1.2 Literature Survey

In the last few decades, with the help of power electronic converters, many Maximum Power Point Tracking (MPPT) techniques have been implemented to harvest power from the PV array. The parameters considered in the methods vary according to their own performance. From these techniques, Hill Climbing (HC) and Perturb and Observe (P&O) algorithms are most commonly used for their simplicity [5]. Both algorithms work on a similar principle to attain the MPP. Periodically the HC method provides power by perturbing the duty cycle to the converter, whereas P&O method performs with a PV system voltage by perturbation. Based on power levels, control parameters (duty cycle or voltage) can be increased or decreased to reach MPP. Due to the elegant performance of HC and P&O algorithms, it is easy to detect oscillations present around the steady-state point or MPP and also power loss during tracking. If the perturbation step size is small, it can show minimum oscillations and reduce the response speed and vice versa.

Xiao and Dunford proposed a modified adaptive hill climbing Method (MAHC) [6]. In their work, parameter tuning was implemented to reach the requirements of good dynamic and static conditions. The control mode switching was designed to keep away from the tracking deviation. The upgraded tracking performance of this method was verified through Simulink and experimental conditions. The proposed MAHC algorithm not only shows less steady-state error than Adaptive Hill Climbing (AHC) when the step change of perturbation was set to 0.4%, but also makes the convergence speed 34.62% faster compared to the AHC method. The drawbacks of this proposed MAHC is that power loss was observed during initial tracking and steady-state point. The MAHC method was not performed under shaded conditions of PV array.

Zhu, Shang, Li, and Guo proposed a modified hill climbing technique with decreased oscillation around MPP and increased tracking performance [7]. The adaptive hill climbing method is easy to deviate from MPP locus under conditions of incremental irradiance transition. Their work proposes a modified hill climbing algorithm and is obtained through

MATLAB/Simulink simulation: (i) Under the step-change irradiance environment, the proposed method can increase speed response and also minimize steady-state oscillations compared to traditional hill climbing method. (ii) The proposed algorithm can solve the problem in adaptive hill climbing, which diverges from the MPP locus while operating under irradiance gradation process. The drawbacks of the proposed modified hill climbing MPPT method is that it shows power loss during transient period and oscillations around steady-state point not minimized to zero. This method was not verified experimentally.

Piegari, and Rizzo proposed a P&O MPPT algorithm aimed at achieving a good variant response of the system by regulating the perturbation amplitude to the actual operating conditions [8]. An adaptive P&O MPPT technique was proposed to obtain better efficiency of PV systems. The algorithm has been designed to reduce the problems that arise in conventional P&O algorithms: dynamic or variant response and maximum power stability. The basic principle of the proposed algorithm is to regulate the perturbation amplitude to real working conditions. High amplitudes of perturbation are suitable to improve tracking time performance but it shows more oscillations around MPP while small perturbations are useful to minimize the steady-state oscillation; it also shows poor initial tracking performance.

Femia, Granozio, Petrone, Spagnuolo, and Vitelli presented the difficulty of the optimization of P&O strategy for PV system [9]. The classical constant duty cycle step size has been substituted by change in step size that linearly decreases with increase in tracking power of PV system. This allows the user to improve the constant P&O performances under uniform irradiance conditions, especially in terms of tracking power levels and stability of maximum power point. To show better performance of P&O algorithm, some improvements have been proposed by changing the perturbation step size in [10]-[12]. The main drawbacks of these methods is that they are unable to capture global power during Partial Shaded Conditions (PSC). Similarly Incremental Conductance (IC) works in the same manner as P&O method and reach MPP when P-V curve slope is zero but has drawbacks such as accuracy, initial tracking performance, and is incapable of tracking Global Peak (GP) during the shading of PV array [13]-[14].

Nguyen and Low introduced a novel search method that is close to P&O and IC algorithms in terms of implementation [15]. Particularly in the presence of multiple peaks and a sudden

shift in irradiance level, the new search algorithm shows improved efficiency and tracking speed. The proposed method is based on the dividing rectangles (DIRECT) algorithm that was implemented for tracking the global extreme of a Lipschitz function in an interval. The function that depicts the power/voltage relation of PV cells in the proposed algorithm is a Lipschitz function. The DIRECT algorithm was carried out along with P&O technique. During the shading of the PV array, the proposed technique was activated to track Global Power (GP), following which P&O holds the GP when stop condition arrives. This process involves complex computations and shows oscillations at steady state. It is not applicable for re-initialization of parameters under dynamic cases of PV array.

Patel and Agarwal proposed a new approach for locating the maximum power under shading conditions of PV array [16]. Under shading conditions, the P-V curves of a PV system become more complicated, with several peaks. The global power position on the P–V curve is not set and is influenced by a variety of factors such as insolation, temperature, and array configuration. Several important findings, helpful for GP tracking, are being made based on a detailed analysis of the I–V and P–V characteristics of a partially shaded array, and a technique for detecting the GP has been introduced. Under partial shading, this global MPPT approach is dependent on the knowledge of I-V and P-V curves. This approach first tracks all local peaks and then determines actual global peak from all observation of local peaks under certain shading of PV patterns. The proposed method was implemented based on system dependent on parameters and it takes more tracking time to reach global peak under partial shaded conditions of PV array and is not considered for re-initialization of parameters under dynamic cases of shaded condition.

Alireza, Hossein, and Behzad designed a software based MPPT method which works correctly in both uniform and non-uniform insolation conditions [17]. This new MPPT method used for global peak introduces an analytic condition under partially shaded conditions and is also uses HC method to track global peak with the help of open circuit voltage of PV module, but oscillations are nevertheless present at steady state. The above Global MPPT (GMPPT) methods [15]-[17] proposed one MPPT algorithm for searching GMPP but the initialization of particles are dependent on PV system but such system dependent method is not always suitable, particularly in extended PV systems [18]. These algorithms may locate local MPP instead of global MPP. The following point shows the

disadvantages when the proposed algorithm parameters were dependent on PV system of open circuit voltage of PV module. For example, consider four PV modules connected in series under partial shaded conditions which exhibits four different peaks on P-V characteristics:

i. When a new peak power is discovered, it is equivalent to the previous peak power. The operating point would switch to the next open circuit voltage of PV module area if this new peak power is greater than the previous peak power one.
ii. When a new peak power is lower than the previous one, the algorithm skips the next open circuit voltage of PV module area, moves to the previous peak power, and ends the tracking operation.
iii. However, if the actual Global MPP is found in the next missed open circuit voltage of PV module location, the algorithm will be stuck at the Local MPP, reducing overall performance.
iv. Furthermore, even though the actual GMPP is not missed, the open circuit voltage of PV module design is not always accurate, particularly for long PV strings. It's likely that it is searching the wrong section of the P-V curve, resulting in an inaccurate global peak.

Evolutionary optimization algorithms have been extensively used for solving non-linear multi-model optimization problems effectively; with quick response for a wide range of exploration to reach the Global MPP (GMPP) under the shading of PV array [19]. These approaches have good efficiency as well as quicker convergence. Various soft computation algorithms (evolutionary algorithms) have been developed for the application of MPPT to overcome some inherent disadvantages found in traditional methods.

Liu, Huang, Huang, and Liang have proposed a Particle Swarm Optimization (PSO) based optimization techniques during partial shaded conditions [20]. The PSO is executed with three parameters such as two acceleration factors and one weight factor which are tuned to the maximum iteration, providing higher efficiency for global MPP. The main aim of this approach is to create a reliable, system-independent MPPT algorithm for centralized power generation systems that run under Partial Shading Condition (PSC). The basic design of PSO has been updated to take into account the realistic considerations of power generation systems working in partially shaded environments. The proposed approach should achieve the GMPP in fewer iterations and has been shown to be more efficient in terms of tracking. The four

separate shading patterns are often used to assess the proposed system's validity in an experimental environment. As per the findings of the experiments, the suggested procedure will extract GMPP in all test situations, regardless of where the GMPP is located. The observations from this proposed method is that taking more number of iterations to locate GMPP, the exploitation process is poor due to more control parameters and tuning parameters which delay the convergence process.

Ishaque and Salam developed a Deterministic PSO (DPSO) to enhance the traditional PSO algorithm's capabilities [21]. The key concept is to exclude the random number from the PSO velocity equation's acceleration factor. Furthermore, the maximum variation in velocity is limited to a fixed value that is calculated after a detailed analysis of the P–V characteristics during partial shading. The proposed DPSO approach was implemented in the absence of random values, where only one factor, i.e., the inertia weight, requires to be adjusted. In this paper DPSO has the limitation of velocity though it removes random generation values to get better performance of PSO. In this proposed DPSO method, the initial particles are dependent on PV system and oscillations around MPP, showing in experimental results. Due to the limitations of parameters like velocity, there is a chance for the algorithm to get struck at local MPP (LMPP). According to Lipschitz Optimization (LIPO), the importance of randomly generating numbers will provide better search process for GMPP without getting struck at LMPP [22].

Sudhakar Babu, Rajasekar, and Sangeetha suggested introducing an efficient approach to compute initial duty cycle for rapid convergence, decreased oscillations around maximum power, and natural tracking fluctuations to increase PSO efficiency [23]. Furthermore, the global peak power was tracked under different climate factors. The drawbacks of the proposed Modified PSO (MPSO) method is that the initial values depend on the PV system and during dynamic cases, the proposed algorithm was considered without re-initializing the parameters to see the effectiveness of the proposed MPSO algorithm.

Sen, Pragallapati, Agarwal, and Kumar proposed a modified particle velocity-based PSO (MPV-PSO) algorithm and verified it for GMPP tracking of a PV array under PSC [24]. The proposed PSO algorithm employs a modified update velocity equation for the particles in which the weight factor, the cognitive acceleration coefficient and the social acceleration

coefficient change adaptively according to the particle position in the search space for achieving fast convergence, avoiding oscillations about the GP and successfully negotiating local minima. The algorithm also does away with the inherent randomness by removing the random numbers from the velocity equation. In addition to this, the particle velocity is bounded by a certain upper limit, the value of which is based on the PV string's open circuit voltage. Extensive experimentation has been performed to validate the performance of the proposed scheme in contrast with conventional PSO algorithm. The drawbacks of this method is that acceleration parameters are tuned with current particle position which depend on the PV system. The re-initialization of parameter is not considered during change of PV shading pattern to gauge the performance of the proposed algorithm. Here implemented with limitation of particle velocity, due to this limitation of velocity the chance is greater to locate local power point rather than global power point.

Huang, Wang, Yeung, Zhang, Schung, and Bensoussan came up with an algorithm to enhance the MPPT performance of PV systems in terms of faster convergence, lower oscillation, and higher efficiency; a natural cubic spline-based prediction model was incorporated into the iterative solution update of Jaya algorithm [25]. The utilization of the natural cubic spline model in the iterative process of S-Jaya algorithm can avoid worse updates and thereby improve MPPT performance. Simultaneously, the natural cubic spline model can be renewed online to maintain its prediction accuracy and produce correct decisions in terms of updating solutions. The performance of S-Jaya algorithm including its convergence speed and efficiency in tracking GMPP for PV systems under various partial shading conditions is examined through simulation studies as well as experiment. The drawbacks of the proposed method is that it is implemented with five initial particles, which depend on PV system and take more tracking time to reach global peak even with a population size of five.

Lian, Douglas, and Jagdish proposed a novel MPPT based on the Ant Colony Optimization (ACO) technique to track the MPP for a huge PV system in shading conditions [26]. It has a fast convergence rate, where independent particles are considered initially, and no knowledge of PV array characteristics is needed. Simulation of different shading patterns confirms the effectiveness of the suggested MPPT for PV array during constant and transient irradiance conditions. The results show that, compared to some traditional MPPT methods, such as P&O, constant voltage tracking (CVT) and PSO method, the proposed method finds better

performance and also requires less number of iterations. One drawback of this method is that, ACO was not implemented in real-time system. At the time of initialization, five control parameters had been initialized, and due to more parameter initialization the computational burden on the system increased per iteration.

Sundareswaran, Sankar, Nayak, Simon, and Palani looked at GMPP tracking in a PV power generation system, and recommended a new solution based on Artificial Bee Colony (ABC) [27]. The simulation results performed on two distinct configurations of differing shading patterns explicitly show that the proposed ABC algorithm outperforms the current PSO and enhanced P&O approaches. The limitations of this method is that it takes more time to reach global MPP with the proposed algorithm when the population size reaches six.

Sundareswaran, Peddapati, and Palani proposed to develop a Firefly algorithm (FA)-based scheme for tracking GMPP during PSC in a PV system [28]. The proposed approach is reliable, quick to track GMPP, and is independent to system. In this paper several case studies were presented for different PSC conditions. This proposed method also reports the application of standard P&O and PSO algorithm for MPPT under similar conditions, as well as simulation and experimental tests. FA-based detection was seen to be superior to conventional approaches, however the proposed Firefly Algorithm (FA) uses six fireflies for implementation which increases the burden on the system per iteration.

Mohanty, Subudhi, and Ray suggested Grey Wolf Optimization (GWO), a new evolutionary computation method for developing a peak power extraction technique for PV systems to operate with PSCs [29]. The efficiency of the new MPPT (Grey Wolf-based MPPT) was compared to two existing MPPTs in order to determine its effectiveness, namely P&O and Enhanced PSO-based MPPT approaches. Based on the findings of the proposed GWO process, it was discovered that the GWO-based MPPT outperforms the other two MPPTs in terms of convergence speed and oscillations at the steady-state stage. But it is observed that the proposed GWO algorithm did not maintain enough exploitation process with equations of updated position and linear tuning of control parameter. Also the algorithm did not perform with re-initialization of parameters in dynamic cases for one to determine the effectiveness of the proposed algorithm.

Eltamaly and Farh investigated MPPT-based heuristic techniques such as PSO and GWO and discovered that such methods suffers from oscillations around the GMPP. They can not also reach to GMPP under dynamic conditions of shaded PV array. In this work, GWO is hybridized with Fuzzy Logic Controller (FLC) to reduce the oscillations in power around the GMPP [30]. In addition, two efficient initialization techniques were proposed to re-initialize the GWO in order to reach GMPP during dynamic cases. The first initialization technique was based on predefined time. The second initialization technique was based on PSC change (power levels change due to shading of PV array). With re-initialization of parameters, the tracking efficiency of PV system also increased. But the proposed method was implemented with more than five initial particles, which increases the computational burden on the system for each iteration in real time system.

Yousri, Babu, Allam, Ramachandaramurthy, and Etiba introduced a new approach, where three chaos maps (logistic, sine, and tent maps) are merged with the Flower Pollination Algorithm to tune some of its parameters to generate the initial solution. As a result, Chaotic Flower Pollination Algorithm (C-FPA) variants are introduced and tested in tracking GMPP over several shade conditions and for step variations in irradiance conditions [31]. The developed variants response is compared with FPA based on several statistical analysis to show the influence of integrating the chaos maps in the tracking system. The performance of the proposed C-FPA method improved compared with FPA in terms of tracking time and tracking efficiency. Here the drawback is that proposed method implemented with five initialization of particles, which creates more computational burden on system per each iteration in real-time process.

Li, Yang, Su, Lü, and Yu have proposed a novel Overall Distribution PSO (OD-PSO) MPPT algorithm. This approach does not include any hardware knowledge about PV systems and can reliably and easily search for and locate the GMPP [32]. The OD-MPPT method is used in particular to find the GMPP portion, which makes it easier to set input data that will be incorporated into the PSO MPPT controller. The PSO MPPT controller would only need to locate the GMPP within a very narrow search area after obtaining the input data, allowing it to identify the same GMPP quickly. As a result of the combination of the OD-MPPT algorithm and the PSO MPPT algorithm, the GMPP of PV modules can be tracked and identified more quickly and reliably in complex PSCs. The proposed algorithm was

implemented with five initial particles, thereby increasing the complexity and computational burden on system.

Seyedmahmoudian, Soon, Horan, Ghandhari, Mekhilef, and Stojcevski came up with a novel rapid, simple, and efficient method called Adaptive Radial Movement Optimization (ARMO), which was designed and developed to track the GMPP at the output of a partially shaded PV system [33]. The main objective of this study was to develop a new MPPT technique with fast-tracking speed, high reliability, and low output fluctuation for the PV system operating under different shaded conditions of PV array. The drawback is that the proposed ARMO tracks location(s) of GMPP faster but it is implemented by considering initial particles of more than five along with three tuning parameters, thereby increasing computation burden on the system for each iteration.

Ram, Pillai, Rajasekar, and Strachan showed that by adding new mutation variables, one could enhance the performance of the PSO processes designed. The first approach aims at reducing power oscillations, while the second is for exploitation. As a result, the performance of the traditional PSO algorithm is increased by four additional mutations to attain global peak, and the traditional P&O approach is used to prevent the unnecessary search. In addition to mutations developed for PSO approaches, quicker convergence to global locations in a reasonable amount of time is possible. Furthermore, using the Enhanced Leader PSO (EL-PSO) process, new mathematical formulations are created in which the global best solution is defined in the first stage and only after confirmation, and the P&O transition is anticipated in the second stage. Since shifting between the approaches is dependent on threshold voltage and current constrains, the ELPSO-P&O approach is expected to set a new norm in the MPPT region. The hybrid enhanced leader PSO-P&O was proposed with many control parameters along with tuning parameters though the designers had not reckoned with determining efficiency [34].

The study of Husain, Jain, Tariq, and Iqbal had the objective of evaluating the GMPP in a very short period of time. Three alternate strategies have been suggested and tested in this implemented methods to solve such issues as slower tracking process, lower efficiency, and excessive sweeping of PV output power curve [35]. Large and small duty stage (LSDS), large and mutable duty step (LMDS), and fast and intelligent GMPPT (FIGMPPT) are the three

types. The LSDS method covers nearly the entire P-V curve using a combination of LSDS approach. Small duty measures were used in all LMPPs on the P-V curve in predefined regions. In addition, the LMDS method sweeps the whole P-V curve at a rapid speed. This is achieved in such a way that the duty step scale is wide for points far away from each LMPP and mutable duty steps are used near each LMPP. The mutable duty size allows for quick tracking with low fluctuations at or around the global peak power, as well as ensuring that no LMPP is missed. The FI-GMPPT is an enhanced accurate GMPPT approach that restricts the search area to be swept during the process. When compared to LMDS-GMPPT, this approach results in a shorter sweep cycle. During the sweep operation, the unwanted region is avoided in this step. This method of narrowing the search area is focused on significant observations made through PSC using PV string's unique P-V and I-V characteristics. These approaches were developed by changing the traditional IC approach to make it function better in PSCs. The drawback of these methods is the tracking time, which is more even if unnecessary sweep time is skipped and power loss is also observed during the initial tracking period. This experimental results of the proposed methods are not shown during dynamic cases of shaded PV array.

Venkata and Muralidhar have developed a new optimizing algorithm for GMPP tracking under PSC, which has better accuracy, improved convergence time, better to implementation and over more economical. As a consequence, this study presents a novel GMPPT strategy focused on the detection of shading patterns using Artificial Neural Networks (ANN). In this scheme, powers at two different voltages for various shading patterns and at different temperatures are pre-calculated and ANN is trained such that it identifies the shading patterns corresponding to input powers and temperature on the panel. The MPP voltages corresponding to each shading patterns are also pre-calculated and stored in a two dimensional lookup table (2DLT). The lookup table is also provided with interpolation and extrapolation techniques and it provides maximum power voltage corresponding to the shading pattern identified by ANN. A new optimizing algorithm is implemented to improve accuracy and convergence time but requires pre-calculated voltages for implementation of ANN method [36].

Selvakumar, Madhusmita, Koodalsamy, Simon, and Sood proposed a fast tracking method, which works effectively both in normal irradiance and PSCs for MPPT with all improvement

in all aspects of performance [37]. By virtue of the property of inductor and boost converter with the help of high-resolution analog-to-digital converter (ADC), the P-V curve is sampled. The PV voltage at maximum power is provided to PI controller as a reference for tracking the global maximum operating point further. The proposed High Speed (HS) tracks faster to global peak compared to duty sweep and PSO methods, but it uses PI controller to track global peak, and its tracking time depends on the inductance of converter, magnitude of PV voltage and magnitude of current at previous operating point.

1.3 Motivations

From the above literature survey, it is concluded that conventional algorithms such as P&O, HC and IC are easy to implement for maximum power tracking in single peak curve and its improvement methods [6]-[14]. But they offer steady-state oscillation, suffer power loss during transient period, reduce system efficiency, and are not suitable for Partial Shading Conditions (PSC) of PV array due to fixed step size; power loss is presents in variable step size methods. The algorithms are implemented for Global Maximum Power Point Tracking (GMPPT) under partial shading conditions [15]-[17]. These proposed GMPPT methods are implemented based on open circuit voltage of PV module but the system dependent method is not always suitable, particularly in extended PV systems [18]. These algorithms may locate local MPP instead of global MPP under PSC.

The evolutionary optimization techniques are most suitable to track global peak power under PSC such as PSO, FA, ABC, FPA, OD-PSO, S-Jaya, ARMO and GWO-FLC etc. [20]-[32]. But the proposed algorithms are implemented by taking into account population size, which makes complex computational burden during experimentations. The presence of tuning parameters in the proposed algorithm leads to delay in convergence because it is unable to tune optimum value during the course of iterations in [20], [24] & [33]. The re-initializations of parameters is not considered in the proposed methods of literature during dynamic change of PV patterns under PSC, otherwise unable to judge the tracking performance of proposed algorithm [15] [23] & [29]. With the presence of limitation, search process will go out of MPP in [21]& [24]. In order to reduce tracking period and number of itrerations to reach global peak, a minimum number of control parameters is required, which also reduuces system complexity. To improve PV system performance, the algorithm has to maintain better exploration and exploitation process.

1.4 Research Objectives

The research aims at Enhancement of Global Maximum Power Point Tracking (GMPPT) performance using evolutionary optimization techniques under shaded conditions of PV system through:

- Using Modified Grey Wolf Optimization (MGWO) algorithm for global MPPT under PSC in PV system to improve the tracking performance of PV system, reduction of number of iterations to reach global peak of multiple P-V curve and improvement of exploration process using modified updated positon and control parameter.
- Using GMPPT through PSO based on Lévy Flights for PV system under PSC to reduce tuning parameter, improve the tracking performance of PV system by maintaining both exploration process and exploitation process, and reduce the number of iterations to reach global peak of multiple P-V curve.
- Using Jaya algorithm based on lévy flight for global MPPT under PSC in PV system with fewer control parameters, without tuning any control parameter, improve the tracking performance of PV system by proper search process, and reduce the number of iteration to reach global peak of multiple P-V curve with initial particles that are independent of PV system.

1.5 Organization of the Thesis

The thesis is divided into six chapters

Chapter-1: This chapter provides an introduction to MPPT controllers for solar photovoltaic (PV) systems, literature survey based on global maximum power point tracking for an PV array under partial shading conditions, motivations based on literature survey to formulate research objectives and the objectives of thesis and its chapter wise summary.

Chapter-2: The second chapter provides details and brief introduction to solar photovoltaic (PV) systems, P-V array system modelling, P-V characteristics under uniform irradiance and shading conditions of PV array, list of MPPT control methods to PV applications, and explanation of some of those

methods based on global maximum power point tracking for an PV array under partial shading conditions.

Chapter-3: Supplies a detailed explanation of the proposed Modified Grey Wolf Optimization (MGWO) algorithm and its advantages while searching for global optimum in solar PV applications to extract maximum power, details of the PV array configuration of 3S and 4S2P, simulation and experimental performance of the proposed MGWO over GWO and HC algorithms, and comparisons with existing algorithms in terms of performance.

Chapter-4: Deals with a detailed explanation of the proposed VPSO-LF algorithm and its advantages for global optimization. PV array configurations under shaded conditions are explained in detail. The simulation and experimental performance of the proposed algorithm is compared over PSO and HC algorithms. A comparison of the proposed method with existing methods in terms tracking performance is also made.

Chapter-5: This chapter gives details of the proposed Jaya-LF algorithm and its advantages for obtaining global optimum. The explanation of PV array configurations under different shaded conditions is also provided. The simulation and experimental performance of the proposed method over Jaya and PSO methods are compared in the chapter. The comparison of the proposed method with existing methods in terms of parametric consideration is also made.

Chapter-6: The overall conclusion of the proposed work and future scope of research have been summarized in the area of PV system applications.

Chapter 2

The Solar Photovoltaic System

Chapter 2

The Solar Photovoltaic System

2.1 Introduction

A Solar Photovoltaic (PV) system directly changes light rays from the Sun into electrical energy. The PV cell is the most essential element of a PV system. The cells can be connected in series or in parallel to make modules and make a group of modules to form arrays; the corresponding PV cell formation is shown in Figure 2.1. The power available at the output of PV system can be used directly to loads such as DC machines and lighting systems. Most sophisticated equipment require power electronic converters to extract power from the PV system for the load. These electronic converters are useful to control the output levels at both load level, as well as the power supply in grid-connected devices, and also to extract PV system's peak power output. To read PV power converters, one must first understand how to design a PV unit which is connected to the converter. The PV systems have non-linear *I–V* characteristics since a large number of factors must be changed based on observational information from real-world PV systems. The PV device's theoretical model is important in the evolution of power converter numerical model with maximum power point tracking algorithms, and to simulate the PV system and its components using circuit parameters.

This chapter introduces the working of a PV system, and its corresponding equations with the purpose of contributing to a more thorough understanding of the PV system mechanism through semiconductor phenomena. The modeling comes after the presentation on PV system, characteristics of PV system and MPPT algorithms, which is the primary subject of this chapter. A PV cell is an element that converts directly energy from the Sunlight into electricity through photovoltaic effect. The PV cells are the most basic PV unit. A PV module is made up of a group of PV cells that are attached in series and parallel. The arrays are basically formed with a group of PV modules, which are in series that is needed to achieve high voltage levels. The arrays with higher currents are generated by extending the diameter of PV cells or connecting PV devices in parallel. A PV array is formed by a group of modules, which are associated in a group for higher power ratings of PV systems. Electronic converter manufacturers generally show an interest in the modeling of PV arrays, which are generally

sought after in the market. This chapter plays much attention to PV arrays that demonstrate how to calculate values in the I–V equation using experimental information from data sheets.

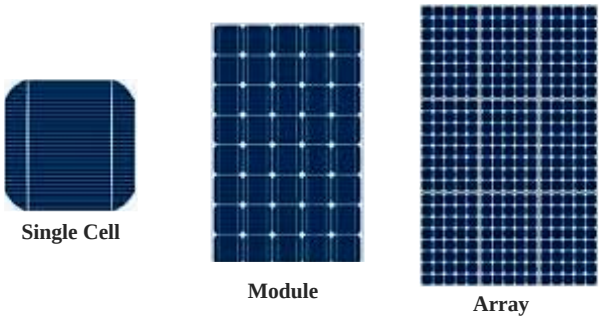

Figure 2.1 PV Cell, Module and Array.

2.2 A Solar PV Cell Working Principle

A solar PV cell is primarily a semiconductor device with Sunlight to a $p-n$ junction [38]. The PV cells are fabricated from a variety of semiconductors and manufactured in a number of ways. At this time, the mono-crystalline and poly-crystalline silicon solar cells seem to be the only ones that have been commercialized. A thin sheet of high volume 'Si' or a slim 'Si' layer attached to electric contacts makes up a silicon photovoltaic cell. To form *p–n* intersection, each of the faces of its 'Si' sheet must be doped. The light portion of every semiconductor is covered with a protective metal grid. A true identity of PV cell can be seen in Figure 2.2.

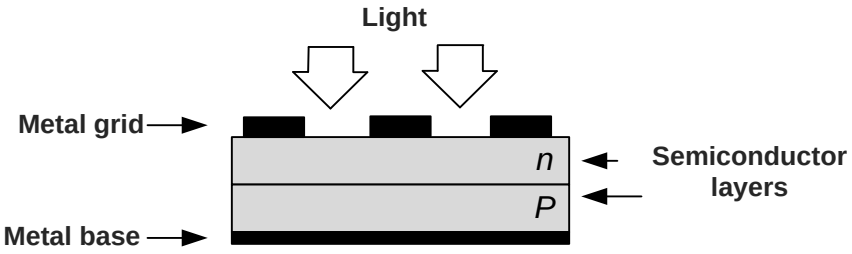

Figure 2.2 Physical structure of a PV cell.

If the PV cell is short-circuited, light causes charge carriers to form, which create an electric field. These charges have been formed if the initial energy is able to differentiate the semiconductor's covalent ions. This mechanism is reliant upon the dielectric material and intensity of the Sun's energy. Essentially, the photovoltaic mechanism is defined as Sunlight absorbing, the production and travel of free electrons at its $p-n$ intersection, as well as the generation of such free electrons now at photovoltaic system's terminals [39]. The speed of production of electronic carriers is determined by the intensity of light energy in Sun's radiation and the semiconductor's absorbing power. The potential of absorbance is based

primarily upon the semiconductor energy band gap, cell surface refractive indices, intrinsic semiconductor charge density, electronic movement, recombination rate and temperature. Sunlight is a set of photons with high energy levels. The photons with sources of energy below the energy gap of every solar cell become ineffective, and so neither electrical potential nor electrical field will be developed. The energy of photons which are more than the energy gap produce power, but primarily the energy associated with the energy gap is used; the rest of energy is lost to the atmosphere in the PV cell. Semiconductors to smaller band differences will benefit from a wider radiation range, though the accessible voltages will be significantly smaller. The semiconductor material 'Si' is being used in photovoltaic cell, which is the only reason the installation process is cost-effective on a huge scale. Other products have a higher output, though they are more expensive and not financially feasible. It is sufficient to understand the electrical performance of the PV unit in order to research electronic converters for PV systems (Cell, Module, and Array). The PV device vendors often have a collection of observational results that can be used to calculate the PV system's the mathematical equation for I–V curve. Few designers have experimentally obtained I–V curves for various operating conditions. These experimental curves can be used to adjust and verify the mathematical model.

2.3 Solar Radiation

The spectral power distribution of the Sunlight-based radiation determines the efficacy of a PV system. The Sun is a light and heat source whose emission distribution is comparable to that of a black body about 6000 K. A black body allows all forms of light to pass into it and emits electromagnetic radiation of all wavelengths. Planck's law, which establishes the relationships and interdependencies between the wavelength (frequency), temperature, and spectral power distribution of black body radiation, numerically depicts the theoretical distribution of wavelengths of black body radiation [40]. Figure 2.3 shows the black body radiation's spectral power distribution in comparison to extraterrestrial and terrestrial solar radiations [38].

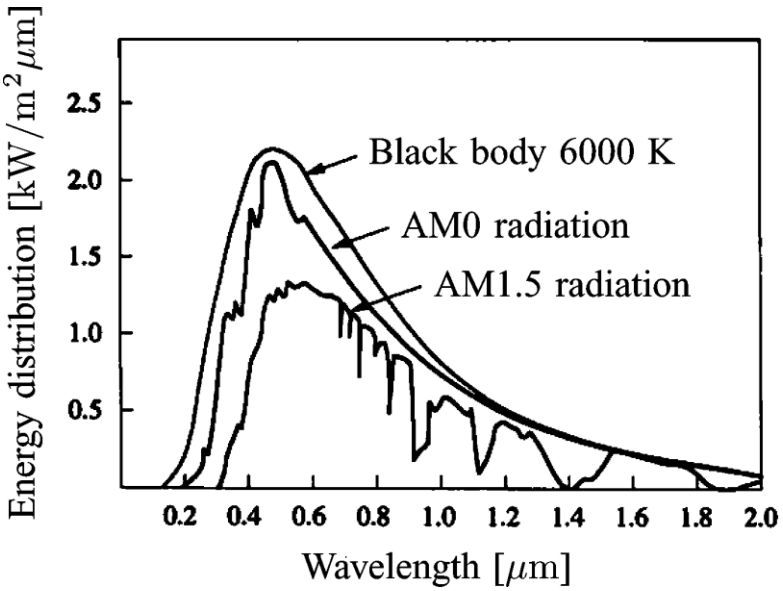

Figure 2.3 Spectral power distribution of the black body radiation and the Sun radiation in the extra-terrestrial space (AM0) and on Earth's surface (AM1.5).

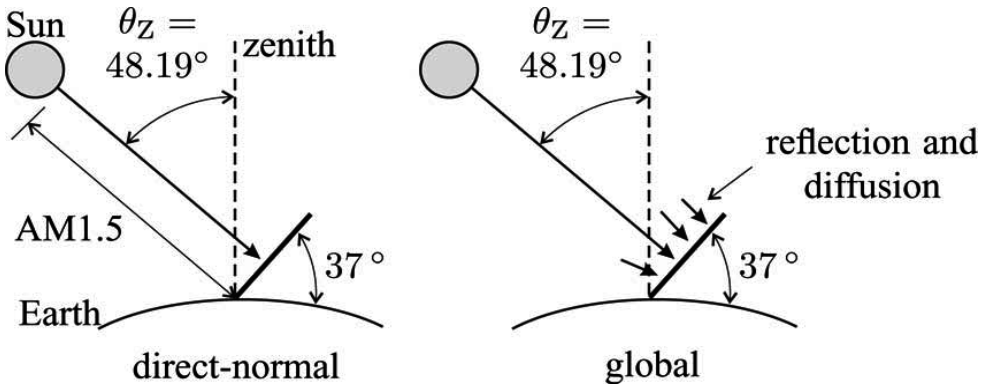

Figure 2.4 Illustration of the AM1.5 path and the direct-normal and global incident radiations on a Sun-facing surface at 37º tilt.

Investigating the effects of solar radiation on PV systems is difficult because the distribution of solar radiation on the Earth's surface is distorted by certain influences such as temperature fluctuations on the solar disc and the influence of the atmosphere [41]. Solar radiation is around 1.353 kW/m^2 in extraterrestrial space at the natural distance between the Sun and the Earth. The irradiation on the Earth's surface is about 1000 W/m^2.

In most cases, PV systems are estimated using a regular spectral distribution. The American Society for Testing and Materials (ASTM) recognizes two regular terrestrial spectral distributions: direct-normal and global AM1.5 (AM stands for air mass) [42]. The electromagnetic radiation that perpendicularly enters a facing the Sun surface straight

forwardly from the Sun is referred to as the direct-normal standard. The world standard, also known as the complete standard, refers to the spectrum of direct and diffuse solar radiation. Diffuse radiation is solar radiation that is affected by the earth's atmosphere when it reaches the Earth's surface. The AM1.5 specifications are for a PV device with a surface inclined at 37^{o} and directly facing the Sun's rays. The AM initials stand for air mass, which refers to the mass of air between a surface and the Sun that influences solar radiation spectral power distribution and intensity. The AMx number describes the journey of sunlight across the atmosphere; as the path wavelength increases, the majority of the light rays deviates and absorption increases. This is where the spectral power distribution of the PV systems collected radiation changes. The 'x' coefficient of AMx describes the path distance of solar radiations.

$$\text{Coefficient of AM (x)} = \frac{1}{cos\theta_Z} \tag{2.1}$$

where θ_Z is the angle between vertical (or zenith angle) and the Sun, as seen in Figure 2.4. Higher direction lengths and greater air mass between the Sun and the surface of the terrestrial PV system are associated with larger 'x'. The AM1.5 distributions are based on the spectrum of sunlight with a solar angle of $\theta_z = 48.19°$. The significance of the AM1.5 direction, as well as the direct normal and global radiations, are shown in Figure 2.4.

Solar radiation strength and spectral power delivery are affected by geographical location, time, day of the year, environmental patterns, atmosphere formation, and altitude [43]. The AM1.5 spectral power distributions are only average estimates that fill in as sources for the estimation and analysis of PV systems due to the variables that impact solar radiation. In the PV sector, the AM1.5 distributions are used as instructions. Normally, datasheets provide details about the properties and performance of PV devices under the so-called Standard Test Condition (STC), which entails a 1000 W/m^2 irradiation with an AM1.5 spectrum at 25℃ [44].

2.4 Modelling of PV Systems

2.4.1 Ideal PV Cell

Figure 2.5 depicts the ideal PV cell's corresponding circuit. The I–V characteristic of a desired PV cell is numerically represented by the following equation based on semiconductor concept, as seen in Figure 2.6 [45].

$$I = I_{pv,cell} - I_{o,cell}\left[exp\left(\frac{qV}{akT}\right) - 1\right] \tag{2.2}$$

where

$I_{pv,cell}$	The current obtained by sun's radiation
I_d	The diode current of Shockley
$I_{o,cell}$	The diode's saturation current.
q	The charge of electrons ($1.60217646 \times 10^{-19}$C)
k	The Boltzmann constant ($1.3806503 \times 10^{-23}$ J/K)
T	The temperature of the *p–n* intersection (in Kelvin)
a	The ideality constant factor of a diode

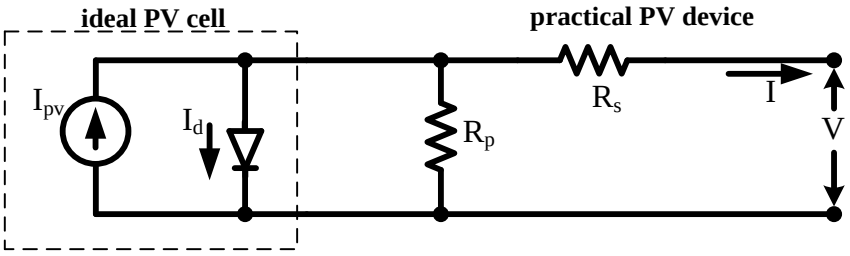

Figure 2.5 Model of the ideal PV cell and equivalent circuit of a practical PV system.

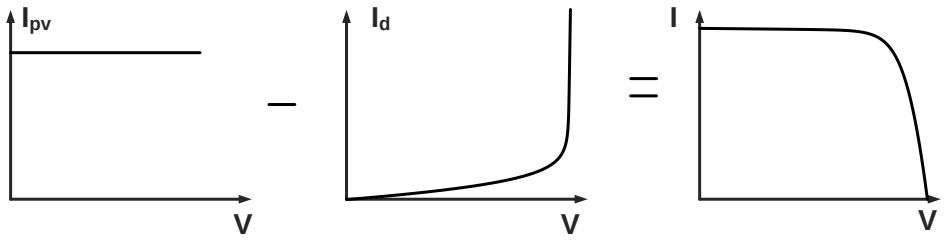

Figure 2.6 The I–V characteristics of a PV cell. The total cell current (I) is composed of the Sun-radiated current I_{pv} and the diode current I_d.

2.4.2 Modelling of PV Array

The *I–V* characteristic of a functional PV array is not addressed by the primary equation (2.2) of the elementary PV cell. Practical PV arrays are made of a few related PV cells, and taking into account the characteristics of the PV array's terminals necessitates the addition of additional parameters to the primary equation (2.2) [45]:

$$I = I_{pv} - I_o\left[exp\left(\frac{V + R_s I}{V_t a}\right) - 1\right] - \frac{V + R_s I}{R_p} \quad (2.3)$$

where

I_{pv}	Photovoltaic (PV) current of the array
I_o	Saturation current of the array
V_t	The thermal voltage of the array
N_s	Cells connected in series
N_p	Parallel connections of cells
R_s	The equivalent series resistance of the array
R_p	The equivalent parallel resistance of the array

If the array is composed of N_p number of cells, the PV and saturation currents are indicated as $I_{pv} = I_{pv,cell}N_p$, $I_o = I_{o,cell}N_p$. Equation (2.3) develops the $I-V$ curve in Figure 2.7, where three important positions are highlighted on the curve: short circuit $(0,\ I_{sc})$, MPP $(V_{mp}\ , I_{mp})$, and open circuit $(V_{oc}, 0)$.

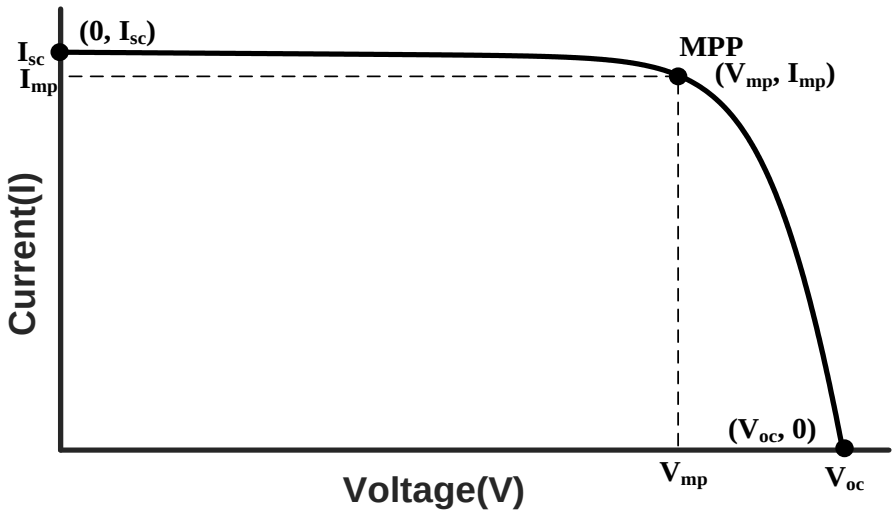

Figure 2.7 The I–V characteristics of a practical PV system with three remarkable points: short circuit $(0,\ I_{sc})$, MPP $(V_{mp}\ , I_{mp})$, and open circuit $(V_{oc}, 0)$.

The single-diode model of a practical PV cell shown in Figure 2.5 is stated in equation (2.3). The single diode method of Figure 2.5 is analysed for simplicity's sake. This model demonstrates a strong balance between flexibility and precision. This model additionally has been utilized by some researchers in past exploration works, now and then for simplifications; this model is consistent with the essential design made out of a current source and an equal

diode. The single-diode model is ideal for electronic system engineers who have been searching for an easy and convenient model to simulate PV systems to power electronic devices.

The PV array designers have only a limited range of functional details regarding electrical and thermal properties instead of the I–V equation. Unfortunately, a few key parameters for modifying PV array models, as with the light-generated or PV current, series-shunt resistances, diode ideality factor, diode's saturation current, and semiconductor bandgap energy, are not included in the designer's datasheets. The following information can be found on all PV array datasheets: voltage in the open-circuit condition at its nominal $(V_{oc,n})$, current in the short-circuit condition at its nominal $(I_{sc,n})$, the voltage at which maximum power occurs (V_{mp}), the current at which maximum power occurs (I_{mp}), the voltage/temperature coefficient in an open circuit (K_V), the current/temperature coefficient in short circuits (K_I), and the maximum power available in practical case $(P_{max,e})$. These specifics are often given in conjunction with normal test conditions for temperature and irradiation from the sun. These $I-V$ graphs for various irradiation and temperature structure are given by some designers. Such graphs make adjusting and verifying the appropriate mathematical $I-V$ equation much easier. Essentially, it is all the information that can be gathered from PV array user manuals.

Power generators are limited in their ability to generate current or voltage. As seen in Figure 2.7, the functional (practical) PV cell has a hybrid behaviour that can be either a current or voltage source based on the operating stage. The functional PV cell has a series resistance (R_s), which has a greater effect when the cell is working in the voltage source field, and a parallel resistance (R_p), which has a greater impact when the cell is working in the current source region. R_s is the sum of the device's various structural resistances. The configuration of a PV cell is depicted in Figure 2.2. Generally R_s rely on the metal rear's interaction resistance to p semiconductor sheet, the p and n bodies' resistances, the n layer's contact resistance with that of the surface metal contacts, and the grid's resistance [39]. The R_p exists primarily due to the $p-n$ junction's leakage current and is based on the PV cell's manufacturing process, and R_p has a higher value and R_s has a lower value. The $I-V$ feature of the functional PV cell depicted in Figure 2.7 is based on the PV cell's internal factors

(R_s, R_p) as well as environmental events including solar irradiance level and temperature. The intensity of incident light has a direct impact on charge carrier output and, as a result, the current emitted by the device. It is difficult to establish the PV current (I_{pv}) of the basic cells without the assistance including its R_s and R_p resistances. Datasheets only address the nominal current present in a short circuit condition $(I_{sc,n})$, which is the maximum current possible at the PV cell's output terminals. The short circuit condition where $I_{sc} \approx I_{pv}$ is normally used in the modelling of PV systems because in practical systems R_s is less and the R_p is high. Since R_s is very low value than that of R_p in practical systems, $I_{sc} \approx I_{pv}$ is commonly used in PV device modelling during the short circuit state. The PV cell current generation is linearly proportional to solar irradiation and is also affected by temperature, as seen in the equation below [46]–[47]:

$$\text{Generation of PV current } (I_{pv}) = \left(I_{pv,n} + K_I \, \Delta_T\right) \frac{G}{G_n} \tag{2.4}$$

$$\Delta_T = T - T_n$$

where

$I_{pv,n}$	The light-generated current at the nominal condition in amperes
T	Actual temperature in Kelvin
T_n	Nominal temperatures in Kelvin
G	The irradiation on the device surface in watts per square meters
G_n	The nominal irradiation in watts per square meters

The diode saturation current I_o and it is relies upon the temperature would be illustrated as below equation [47]:

$$\text{The diode saturation current } (I_o) = I_{o,n} \left(\frac{T_n}{T}\right)^3 exp\left[\frac{qE_g}{ak}\left(\frac{1}{T_n} - \frac{1}{T}\right)\right] \tag{2.5}$$

where

E_g	A semiconductor's bandgap energy (For the polycrystalline Si $E_g = 1.12eV$ at 25°C [23], [42])
$I_{o,n}$	The nominal saturation current in amperes

$$\text{The nominal saturation current } \left(I_{o,n}\right) = \frac{I_{sc\_n}}{exp(V_{oc,n}/aV_{t,n})-1} \tag{2.6}$$

where $V_{t,n}$ is the thermal voltage of N_s series-connected cells in at nominal temperature T_n .

The saturation current I_o of the PV cells that make up the device is determined by the semiconductor's current density (J_o , which is usually expressed in [A/cm^2]) and the cells' effective field. The intrinsic properties of the PV cell, such as the electron diffusion coefficient in the semiconductor, the lifespan of minority carriers, and the intrinsic carrier density, are used to calculate current density (J_o). For commercial PV applications, this kind of data is not available. The nominal saturation current $I_{o,n}$ is achieved from the practical data using equation (2.6), that is derived by analysing equation (2.3) at the actual open-circuit state, to $V = V_{oc,n}$, $I = 0$, and $I_{pv} \approx I_{sc,n}$.

The factor of a ideality 'a' would be selected randomly. Many experts debate how to accurately assess this factor's worth [48]. In general, $1 \leq a \leq 1.5$ is used and the decision is based on other $I-V$ model parameters. Based on analytical studies a few values have been presented for 'a' [42]. As mentioned previously, there are a variety of perspectives on the best way to choose 'a' [48]. Since 'a' represents the diode's degree of ideality and is fully analytical, any starting value of 'a' can be selected to modify the design. Changing 'a' can marginally improve model accuracy by influencing the curvature of the $I-V$ characteristic.

2.4.3 Fill Factor

The fill factor (FF) can be calculated using maximum values of current and voltage (I_{mp} and V_{mp}), when the output terminals are shorted and opened conditions(V_{oc} and I_{sc}):

$$\text{Fill factor (FF)} = \frac{V_{mp}I_{mp}}{V_{oc}I_{sc}} \tag{2.7}$$

The fill factor is a commonly used metric for assessing the overall quality of a solar cell [49]. It should be the ratio of the maximum obtainable power (V_{mp}, I_{mp}), to the product of V_{oc} and I_{sc}. Because of the series and parallel resistances, as well as the diode shown in Figure 2.5, the usable maximum power voltage and current are still below theoretical values. For marketing solar photovoltaic cells, the fill factor is typically greater than 0.7.

2.5 Characteristics of Solar PV Module

The irradiation and temperature of the PV module are two important considerations to remember, since they have a direct impact on the PV module's characteristics. As a result, the MPP varies during the day, which is the primary reason why the MPP should be followed at all times to ensure that the module's full power is obtained.

2.5.1 The Effect of Temperature on PV Module

The voltage is mostly influenced by the temperature. The output voltage is proportional to the temperature at open condition, as seen in the equation below:

$$\text{Open circuit voltage } [V_{oc}(T)] = V_{oc}^{STC} + \frac{K_{V,\%}}{100}(T - 273.15) \tag{2.8}$$

Since K_V is negative, the effect of the temperature on V_{oc} is negative, as seen by equation (2.8), i.e., as the temperature goes up, the voltage is reduced. The current increases in proportion to the temperature, but it is insufficient to compensate for the voltage drop caused by a provided temperature increase. As a result, the power also decreases. The temperature coefficients, which are parameters that show how the open circuit voltage, short circuit current, and peak power fluctuate as the temperature varies, are given by PV device designers in their datasheets. Since the effect of temperature on current was too low, it is generally negligible [50]. The current-voltage and power-voltage characteristics differ through temperature, as seen in Figure 2.8. From the figure the observation is difference of power, i.e., maximum power reduces with rise in temperature, thereby also causing variation in efficiency. The maximum power of PV array changes by 0.5% for each change in 1°C of temperature [51].

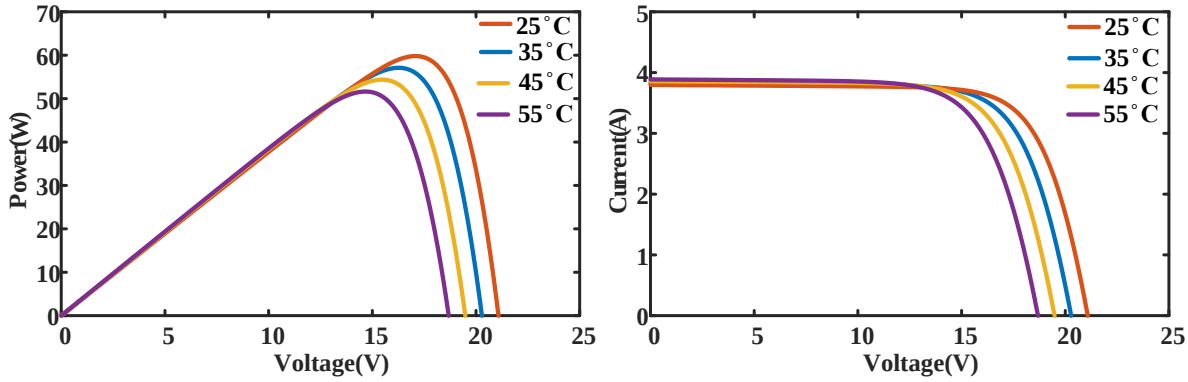

Figure 2.8 I-V and P-V characteristics at standard irradiation (1 kW/m^2) with four dissimilar temperatures.

2.5.2 The Effect of Irradiance on PV Module

The impact of the irradiance on current-voltage (I-V) and power-voltage (P-V) characteristics is illustrated in Figure 2.9. As previously mentioned, photo-generated current is equal to solar radiation, so a higher degree of irradiation results in a higher photo-generated current. Furthermore, the photo induced current is approximately equal to the short circuit current; As a result, it is related to irradiance. The photo induced current is always a major factor in the PV current when the working point is the short-circuited, where no power is available at the output terminals, as shown in equations (2.2) and (2.3). As a result, the current-voltage characteristic shifts in response to irradiation. In comparison, the voltage is normally unaffected since the light induced current is logarithmic, as seen in the following equation:

$$\text{Open circuit voltage } (V_{oc}) \approx \frac{akT}{q} ln\left(\frac{I_{pv}}{I_o} + 1\right) \tag{2.9}$$

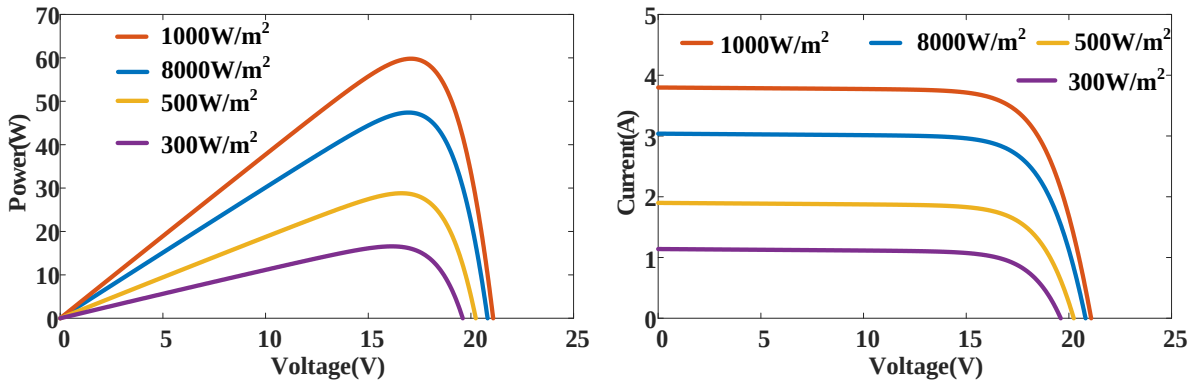

Figure 2.9 I-V and P-V characteristic at standard temperature (25°C) with four dissimilar irradiation values.

The improvement in current is more pronounced than in voltage improvement, as seen in Figure 2.9. In reality, the voltage dependence on irradiation is normally negligible [50]. Since the effect on voltages and currents is positive, i.e., each increases as irradiation increases; the influence on power is also positive as higher irradiation equals more power production.

As previously stated, temperature and irradiation are dependent on environmental patterns, which are not stable over the year or even within a specific day; these can change easily due to constantly shifting conditions along with clouds. This allows the MPP to shift continuously, variation based on irradiation and temperature. Power losses occur if the operation point is not close to MPP. As a consequence, tracking the MPP under any situation is critical to ensuring that the PV system produces the highest possible power. This task is concerned with MPPT algorithms in current solar power conversion.

2.6 Types of Solar Cells

For the last few decades, silicon has essentially been the only substance used to create solar cells. Despite the fact that new materials and techniques are being developed, silicon is used in over 80% of the manufacturing processes [49]. Silicon (Si) is well-known for being one of the most common minerals in the Earth's crust, as silicon dioxide, and it really is non-toxic. Silicon solar cells can be divided into two types: mono-crystalline and poly-crystalline. Amorphous silicon is a third type of film, although it has a lower efficiency than the other two, and therefore is used less often. Copper indium gallium (di) selenide (CIGS) or cadmium telluride (CdTe) are other new solar cell materials. While much effort is being put into developing new technologies, there are currently no commercial alternatives to the above forms of solar cells. This distinctive solar cells are taken into consideration in this section. One of the really important elements of solar cells is their performance, which is the amount of solar energy that is converted into electric energy. It is calculated using Standard Test Conditions (STC), which include a 1000 W/m^2 irradiance, A.M 1.5, air mass coefficient (which characterizes the sunlight after it has passed through its aerosphere), and a cell junction temperature of 25°C. The smaller the surface area needed for generating a given amount of electricity, the higher its performance. This would be significant because, in certain cases, space is limited, and various expenses and specifications of the establishment are dependent on the mounted PV surface.

2.6.1 Mono-crystalline Silicon

Solar cells built of mono-crystalline silicon seem to be the most effective. They are created from single crystal wafers (slim cuts) acquired with perfect molten material. Since the crystal nature is strongly ordered, the properties of these single crystal wafers are uniform and consistent. However, the planning process should be done with great care even at extreme temperatures, which is costly really. These cells have an around 20 percent efficiency [52], and the surface area used to generate 1 kW in STC would be around 7 m^2.

2.6.2 Poly-crystalline Silicon

Wafers of perfect molten silicon are used to manufacture poly-crystalline cells. In either case, the crystalline structure is arbitrary: as silicon cools, it encapsulates itself in a variety of locations simultaneously, resulting in an unusual structure: irregularly shaped, sized, and oriented crystals. Since the designs have not been as good as those in mono-crystalline cells, the performance is smaller, and gives around 15 percent efficiency [52]. However, as the designing procedure is less costly, the lower performance is due to poor silicon purity levels. The surface area used to generate 1 kW in STC is approximately 8m^2. As a result, more space is required for installing this particular solar cell.

2.6.3 Amorphous and thin-film Silicon

Amorphous silicon is a non-crystalline silicon that is often stored as nanostructures on a wide range of substrates. It is possible to store it at lower temperatures. Compared to crystalline cells, the modelling process is less complicated, simpler, and less costly. The disadvantage of such cells is their poor performance as they give around 10 percent efficiency [52]. The STC is used to calculate efficiency. However, in softer or diffuse irradiation, such as that seen on gloomy days, efficiency could become greater than it does in crystalline cells, and its temperature is lower [49]. Amorphous silicon is really good at bright light absorption over crystalline silicon, so that the thin film, despite its poor efficiency, is successful. Thin-film processing was used for the first time in solar cells. Since the 1980s, they have been used in electronic products including calculators. Because of the previously mentioned characteristics, amorphous silicon is used in high-power applications in several fields. One typical use these days will be as building cladding, such as in facades, since its cost is comparable with many other high-quality claddings and it produces energy. The major

benefits of thin film solar cells are the simplicity at which they can be designed at low temperatures using low-cost substances, an efficient manufacturing process that eliminates the need for each wafer installation, and the capacity for light-weight and portable solar cells. These advantages apply to the vast majority of thin-film photovoltaic panels, not just those made of amorphous silicon.

In the past few years, a new kind of silicon, microcrystalline silicon, has been created [49]. It can also be deposited as thin films on a variety of substrates, reducing the amount of crystalline silicon required while increasing the performance of amorphous solar cell. Microcrystalline silicon, on the other hand, has a lower light absorption than amorphous silicon. To absorb the bright light incident on film, the arrangement could become an important light catching device. This method of silicon is not yet a commercially useful product, and further research and development is expected.

2.6.4 Other Cells and Materials

Other elements can also be used to make solar cells in addition to silicon. Since these substances are thin film coated, they provide comparable benefits to silicon thin film solar cells, but with higher performance. Two of these substances are currently used in industrial photovoltaic modules. Copper indium gallium selenide (CIGS) or cadmium telluride (CdTe) are the two materials. The performance efficiency would be about 13 percent [52], and as the technologies advance, this should continue in the coming years. Thin film manufacturing is often shown as the cheapest way to achieve grid parity, such as where the cost of producing electricity is comparable to, or less costly than, grid power [49]. The toxicity of these innovations is one of their most significant disadvantages. Indium is used as a result of CIGS. This part, however, is not quite as common as silicon on Earth's crust, and it can be used in other electronics devices such as liquid-crystal display (LCD) displays, resulting in a scarcity. In addition, CIGS is integrated to cadmium sulphide (CdS), to form the p-n junction. Cadmium is a toxic element which is harmful in high doses. Because of CdTe, the other compounds are used in industrial thin film solar cells, as these are not as poisonous as its constituents.

Gallium Arsenide (GaAs) is being used in aircraft parts for two things: first, this is less vulnerable to harmful effects of space radiation than silicon, and second, because of its band gap of 1.42 eV, it will gain from a larger portion of the solar spectrum than silicon. Despite

the fact that it is a highly important investment, aerospace ventures could accommodate it because cost is not the primary consideration when selecting materials. It is currently being researched for use in terrestrial photovoltaic systems with sunlight concentrators (reflectors or lenses) to concentrate light through smaller units, lowering costs and requiring less content. A three-way intersection using light concentrators, and GaAs cells have achieved 40 percent productivity in the test facility [49]. The only disadvantage of this technology at this time is the high expense of concentration devices, which would track the Sun during the day.

Dye-sensitized cells is another technology that is being thoroughly studied [49]. These solar cells are made from synthetic organic materials and are considered part of the "third generation" of solar cells. They outperform amorphous silicon and thin-film cells in terms of performance. One brilliant feature is that they perform effectively in low and diffused light and have lower temperature coefficients. The products used are non-toxic and plentiful, and the production methods are fairly easy. Flexible modules, which can be created in a variety of forms, measurements, and design specifications, could be conveniently built using flexible substrates and used for building integrated PV on rooftops and walls.

The last two sections reflect innovations which are typically being studied at the present. They are still in non-commercial developments, but it will be anticipated that they will become efficient and used in the coming years, increasing opportunities for electricity generation. The innovations depicted previously, silicon and thin film photovoltaic (PV) cells, are currently being used in commercial PV implementations. Nonetheless, what is relevant for this study is that all of the above-mentioned solar cells have nonlinear current-voltage (I-V) characteristics and are similarly affected by irradiation and temperature. The only distinction is that different kinds of solar cells have different degrees of sensitivity; nonetheless, MPP can be tracked using identical algorithms.

2.7 MPPT in PV systems

Solar photovoltaic (PV) energy production networks have been successfully commercialized around the world as a result of their significant long-term benefits, large-scale support programs, and other enticing initiatives taken by governments around the world to facilitate the use of productive power energy supplies. Photovoltaic systems are used for a variety of purposes, ranging from satellite control to PV power sources for power grid services [53].

The PV systems have many advantages, including long-term viability, low maintenance requirements, the potential to position PV panels on the roofs of residential buildings, the absence of complex components, lower initial investment costs for solar power plants in response to technological advancements and environmental friendliness [1]. As a result, working the device at its Maximum Power Point (MPP) at specific solar irradiation levels has become critical. This has motivated the use of Maximum Power Point Tracking (MPPT) algorithm in conjunction with PV systems [54]. To advance the presentation of enormous reach to installed PV units, the MPPT algorithm is commonly used in conjunction with an electronic converter. Any difference in environmental conditions, such as atmospheric temperature and solar irradiation, causes the MPPT algorithm to allow the PV system to supply maximum electricity. As its MPP position shifts nonlinearly as a function of nature parameters, tracking the MPP is a complex job which is being effectively done using different techniques [55] - [59]. As PV arrays are subjected to non-uniform solar irradiance, the MPPT technique struggles to detect maximum power. Such a phenomenon is known as partial shading [17]. This happens as a consequence of the shadow cast by clouds, tree branches, large buildings, as well as other nearby structures on individual areas of the PV array, whereas the remaining parts are subjected to uniform radiation. This concern is more noticeable in a PV array with a long series of modules. Partial shading can also be caused by irregularities in PV units, such as when the PV panels break. Under partial shading, the PV array's power-voltage (P-V) characteristics become more complicated, resulting in several peaks [16]. Most previous MPP tracking techniques were better adapted for PV systems with a single P-V peak under constant solar irradiation, but they were unable to achieve the global peak power point under PSC [21].

Soft computation (Evolutionary optimization) techniques such as the Artificial Neural Network (ANN), Fuzzy Logic Control (FLC), and bio-inspired approaches have recently been shown to be effective enhancement optimization algorithms for solving complex problems. The soft computing approach used in PV systems for maximum power point has been revealed in Figure 2.10. The FLC and ANN approaches are well known among researchers in the field of MPPT. Under uniform as well as PSC conditions, these methodologies produced suitable results for tracking global peak points. These methods, on the other hand, necessitate experience and include complex computations [60].

For this situation, research studies recommended bio-inspired optimization approaches for MPPT implementations, as they correctly work to nonlinear and stochastic optimization issues and demonstrate amazing execution without requiring huge complex computations, resulting in simple structure, ease of interpretation, accuracy, and improved response. Following that, in this thesis, bio-inspired approaches for global maximum power point tracking (GMPPT) in PV systems have been discussed.

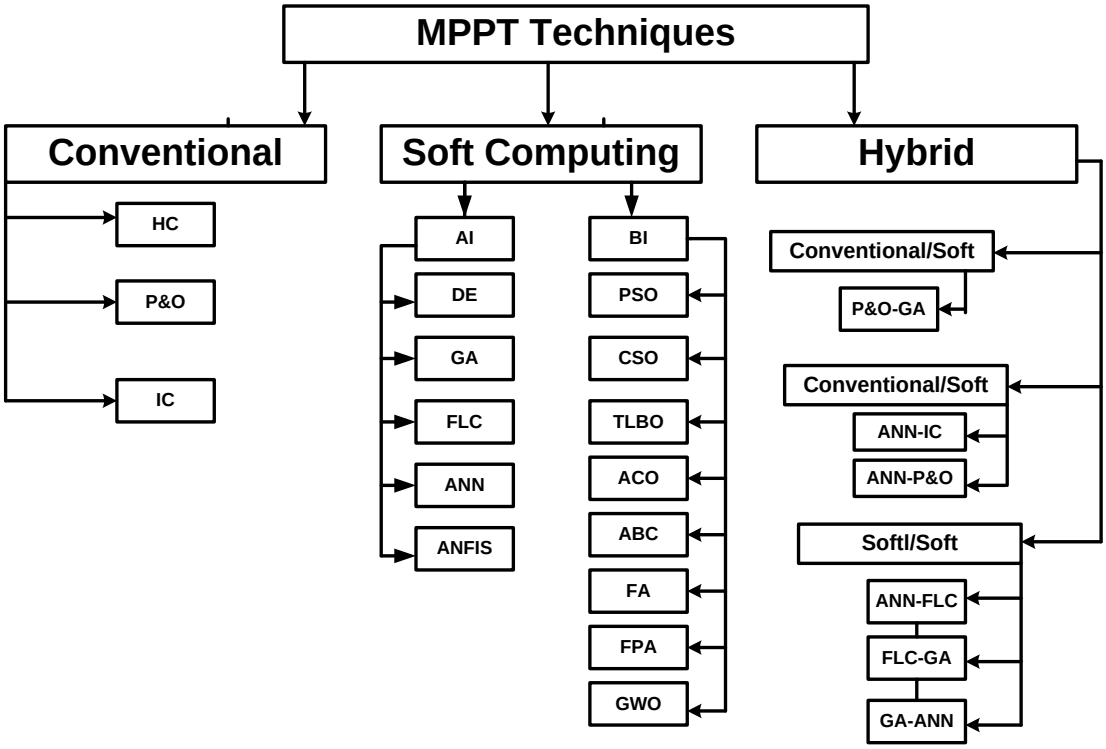

Figure 2.10 Classification of MPPT techniques.

2.7.1 MPPT under Non-Uniform Irradiance

Traditional MPPT algorithms function best in uniform irradiance situations, but PV systems are universal and operate in a variety of weather conditions. This has posed two significant problems in MPPT: partial shade conditions and sudden irradiance changes.

2.7.1.1 PV System under Partial Shaded Conditions

Traditional MPPT techniques like Perturb and Observe (P&O) and Incremental Conductance (IC) are sufficient for tracking the single peak of PV array under uniform irradiance conditions [5], [13]. The PV modules, which are used to form PV arrays, are made up of several PV cells attached in series and in parallel. In a PV system, each PV array incorporates many PV modules connected in series and parallel to utilize higher voltage and higher current, for the use of higher output power of PV arrays. There are two kinds of diodes in a PV array, bypass

diodes and blocking diodes, for distinct reasons. Blocking diodes are used for reverse flow of current. Bypass diodes are utilized to inhibit hotspot heating impact and minimize the power loss because of shading. The present situation is characterized as partial shading conditions (PSC) where each module is subjected to non-uniform solar irradiations and temperatures simultaneously [61]. Figure 2.11 depicts the configuration of a photovoltaic array that contains diodes [62], with corresponding characteristics are shown in Figure 2.12 under PSC. It consists of four PV modules connected in sequence. In most PV array configurations, at least one bypass diode is connected in parallel to each individual module, and a blocking diode is connected in series to the string. However, using bypass diodes has a few drawbacks, such as a lack of power, an increase in price, and multiple peaks on P-V curve, making MPP tracking performance more difficult. As a result, standard MPPT algorithms get stuck at local peaks rather than locating global peaks, reducing performance. To locate the global peak power for PV systems under PSC, evolutionary optimization algorithms are needed.

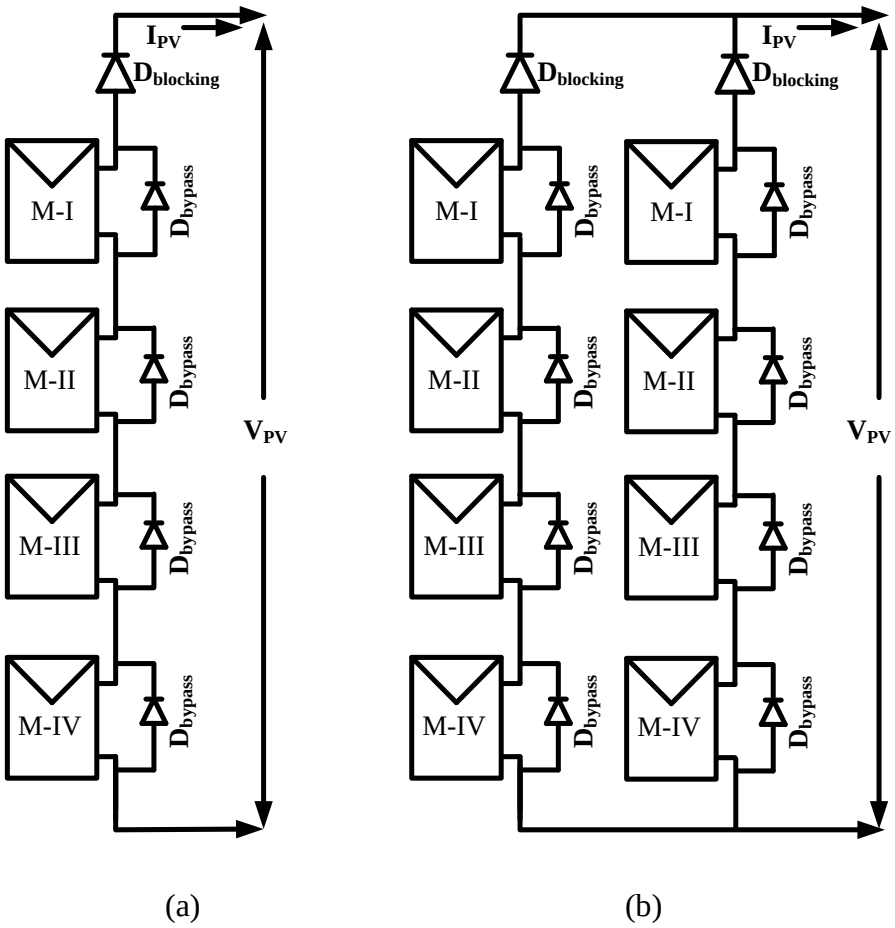

Figure 2.11 PV array configuration of: (a) Four PV modules in series (4S), and (b) Four PV modules are in series and with two such combinations in parallel (4S2P).

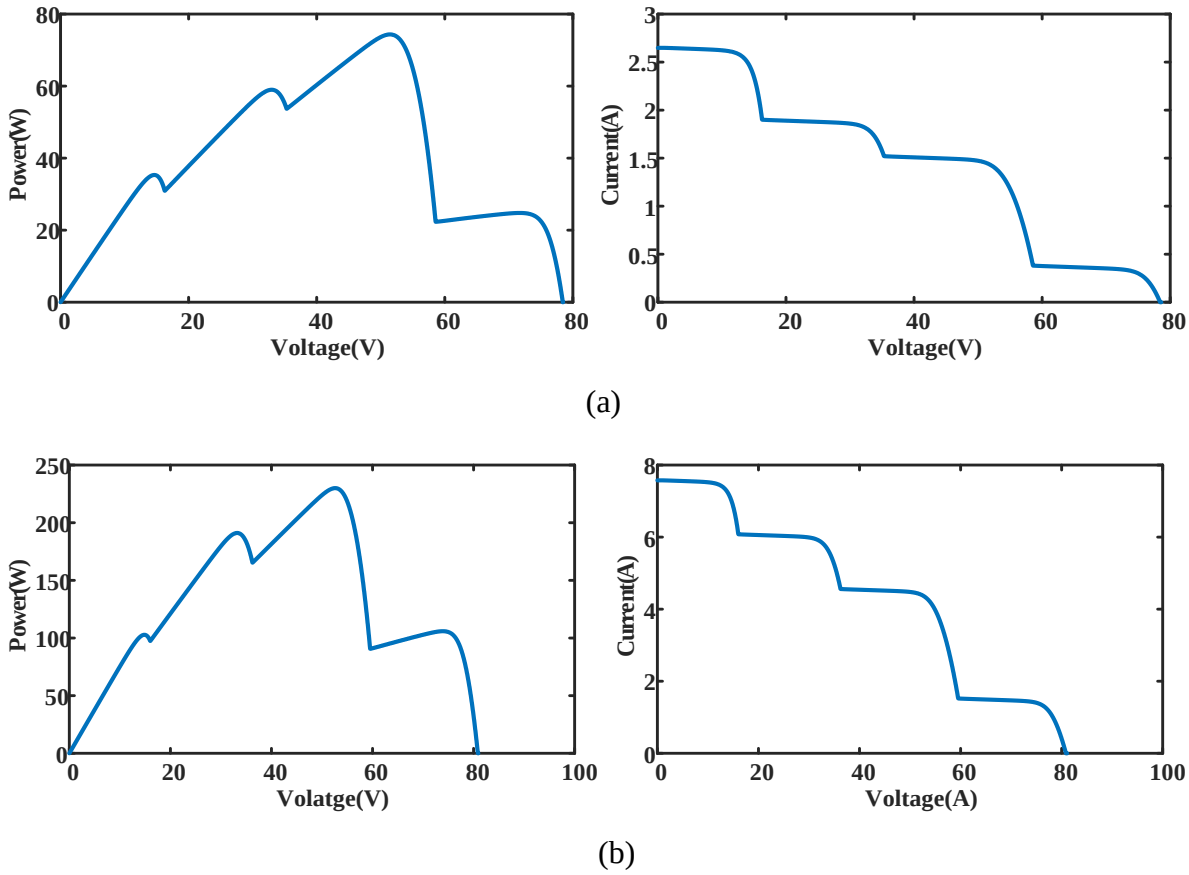

Figure 2.12 Characteristics of PV array configuration: (a) 4S, and (b) 4S2P.

2.7.1.2 Effect of Rapidly Changing Irradiance on PV System

Another point that impacts the PV system tracking efficiency is the point at which the irradiance changes suddenly. In this situation, traditional MPPT algorithms, like P&O, track incorrectly in course of the transient period. In Figure 2.13, the PV module design for 60W then the operating point at maximum power for a PV array power 'P_1' (P_1 is the maximum power when PV module subjected to 800W/m^2) oscillates on either side of the maximum power at point 'A'. When a rapid transition in irradiance occurs, the algorithm switches from position 'A' to 'B,' which corresponds to a shift in the peak of the maximum power curve from 'P_1' to 'P_2' (P_2 is the maximum power when PV module subjected to 1000W/m^2) and the present operating position 'C'. The P&O algorithm detects an increase in power with this perturbation and then proceeds to perturb to position 'D' before finally returning to the path to its original MPP (position 'E'), leading to a loss of power. Same process will happen when P&O algorithm detects decrease in power from 'P_1' to 'P_3' ($P_{3\,is}$ the maximum power when

PV module subjected to 500W/m^2) with this perturbation. If there are a large number of recurrent irradiance shifts, this concern will become much more critical.

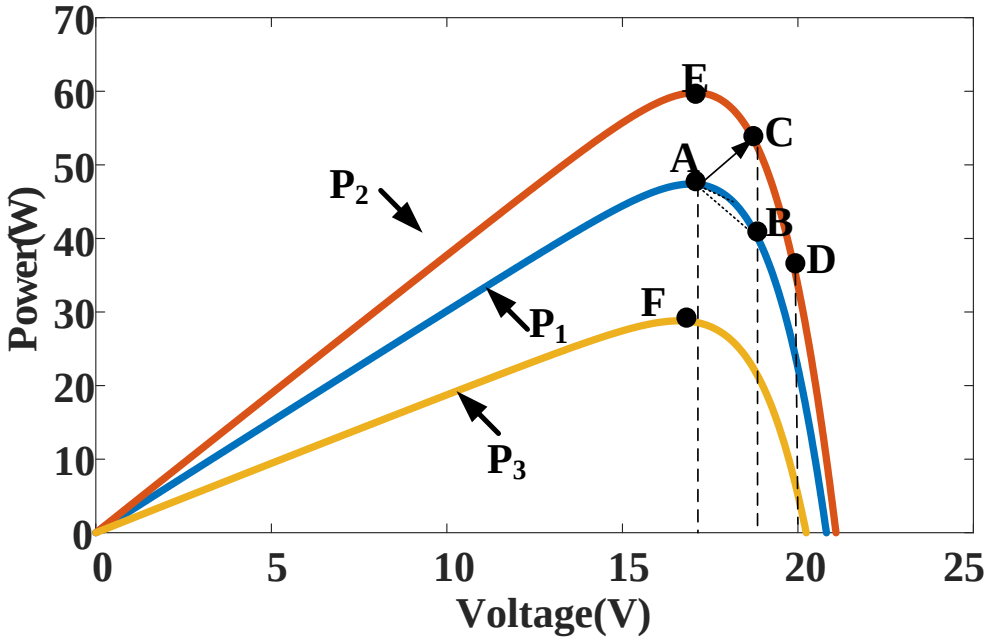

Figure 2.13 The P-V characteristics for two series connected modules under shading conditions.

2.7.2 Classical MPPT Techniques

There are two well-known MPPT techniques that are commonly used in commercial products. To enhance tracking performance, these are combined with soft computing techniques. The two MPPTs are Perturb and Observe (P&O) algorithm and Incremental Conductance (IC) algorithm.

2.7.2.1 Perturb and Observe Algorithm

The essential philosophy of Perturb and Observe (P&O) algorithm (same as Hill Climbing (HC) algorithm) is to regularly perturb (weather increment or decrement) the output voltage of the PV array based on power difference between the present power P(k) and the earlier power P(k-1), in order to identify the path of perturbation in the subsequent stage. When a perturbation induces an increment in the shift in PV array power, the present perturbation's path is maintained until another perturbation; else, the perturbation's path is modified [5]. Based on this process, the P&O algorithm will ultimately track maximum power of single peak and oscillate around the steady-state point. The general flowchart of perturb and observe algorithm is appeared in Figure 2.14. The benefit of this method is that it is easy to implement and has good tracking performance under invariable irradiance conditions. However, P&O method would tracked the local peak power instead of global peak under shading conditions

of PV array, thereby reducing tracking efficiency. The P&O algorithm presents an oscillations around MPP, where power loss occurs due to step size. A small step size reduces the oscillations at a steady state but shows poor tracking performance at transient period, while a large step size improves the tracking performance but leads to more oscillations around steady-state point. To enhance the tracking performance and accuracy, various modifications to P&O algorithm are being implemented, like the adaptive P&O algorithm [8]-[12]. The flexible design of step size's key function is to adjust the step size according to the tracking procedure. When the operating point is well away from the MPP, a broad step size is used to increase the tracking performance in accordance with the P-V curve's slope. A small step is applied to the operating conditions as it moves towards the MPP to reduce oscillation. The step size is defined as follows [6]-[12]:

$$D(k) = D(k-1) \pm N.\Delta d \tag{2.10}$$

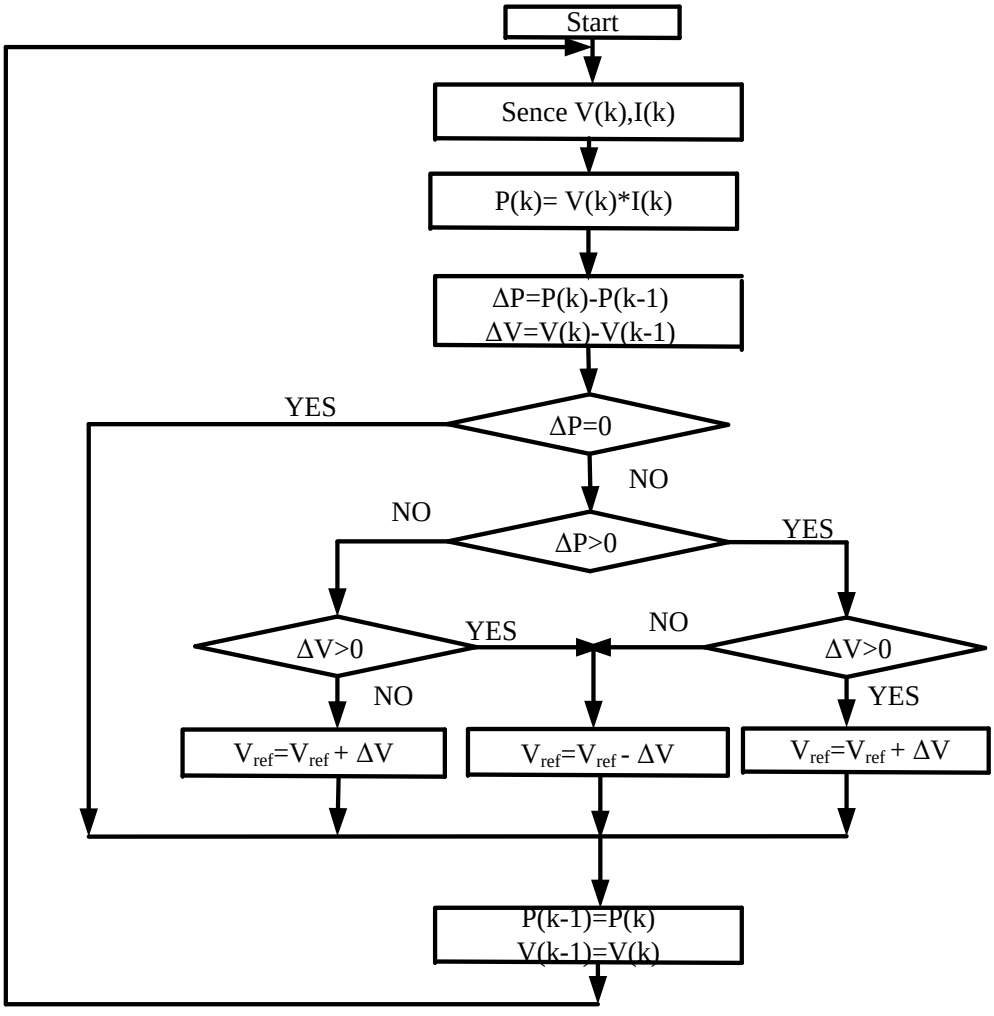

Figure 2.14 Flowchart of perturb and observation algorithm.

where N is a scaling variable that influences the output of the MPPT algorithm and thus is placed under adaptive nature, and Δd seems to be the adaptable portion of the duty cycle of the power converter, which will be ΔP/ΔV, $\Delta P/\Delta I, \Delta P/\Delta D$, or ΔP etc., where, $\Delta P, \Delta I, \Delta V$ and ΔD are respectively the variations of power, current, voltage and duty ratio in the recent sampling time.

2.7.2.2 Incremental Conductance Algorithm

The working of the Incremental Conductance (IC) MPPT algorithm is predicted on the theory that towards the MPP, the derivative to PV power, 'P', in aspects of PV voltage level, 'V', is zero (e.g., dP/dV = 0) [13]. As a consequence, if individuals take the derivative of $P=IV$, then follows:

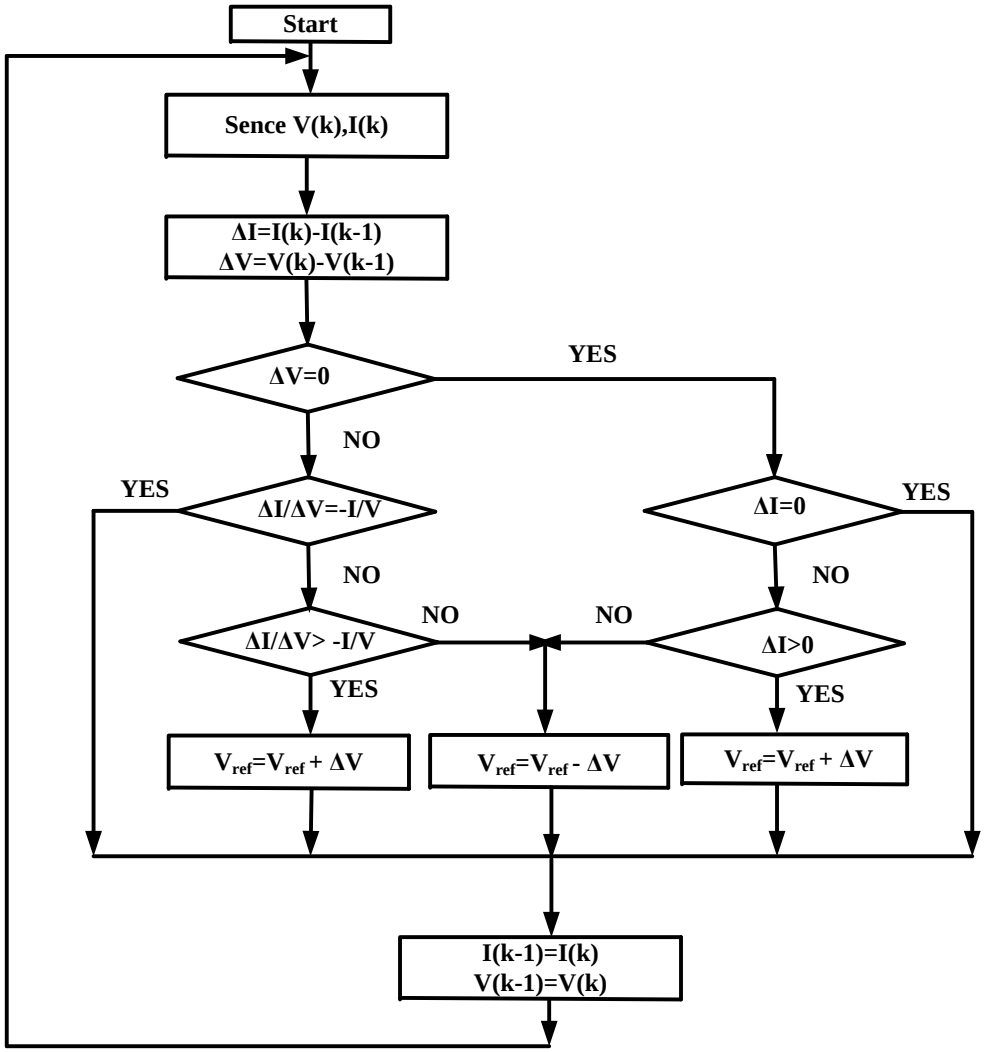

Figure 2.15 Flowchart of incremental conductance algorithm.

$$\frac{dP}{dV} = V\frac{dI}{dV} + I = 0 \text{ at the MPP} \tag{2.11}$$

Hence, within one iteration:

$$\frac{\Delta I}{\Delta V} = -\frac{I}{V} \tag{2.12}$$

Therefore, the perturbation trajectory for the next level is being decided by contrasting the change in conductance ($\Delta I/\Delta V$) with the present conductance($-I/V$). If $\Delta I/\Delta V > -I/V$, then maximize V_{ref}, while if $\Delta I/\Delta V < -I/V$, then minimize the 'V_{ref}. Otherwise, MPP is achieved. The general flowchart of incremental conductance algorithm is presented in Figure 2.15.

Unlike the P&O algorithm, the IC algorithm does not deviate from the maximum power point (MPP) when the irradiance changes suddenly. Since the IC technique requires the slope of the current-voltage (I-V) characteristic to be calculated from the trajectory of perturbation in the subsequent stage, it needs high-accuracy current/voltage sensors. Otherwise, the perturbation procedure becomes muddled because of the flatness of the I-V curve on the MPP's left hand side. Like P&O algorithm, the adaptive step size searching process can indeed be implemented on this incremental conductance algorithm [14].

2.7.3 Evolutionary Optimization Techniques

2.7.3.1 Particle Swarm Optimization Algorithm

The PSO algorithm is a population-dependent evolutionary algorithm based on bird flocking activity [63]. The PSO algorithm manages a swarm of entities, or particles, with two movement variables for each particle: present particle velocity v_i^k (velocity of i^{th} particle at k^{th} generation) and updated particle position position x_i^{k+1}(i^{th} particle position in next $(k+1)$ generation). The global best position (g_{best}^k) among all particles at k^{th} generation, as well as its personal best position (p_{best}^i) influence the production of a particle position, with exchange of data in the search strategy. The following equations are used to update the velocity (v_i^{k+1}) and position (x_i^{k+1}) of a particle [64]:

$$v_i^{k+1} = wv_i^k + c_1r_1\left(p_{best}^i - x_i^k\right) + c_2r_2\left(g_{best}^k - x_i^k\right) \tag{2.13}$$

$$x_i^{k+1} = x_i^k + v_i^{k+1} \tag{2.14}$$

where v_i^k is the i^{th} particle velocity and x_i^k is the i^{th} particle position at the k^{th} generation, respectively; c_1 and c_2 are acceleration coefficients; w is the weight factor, where a high value suitable for global searching, and a low value suitable for local searching; $r_1$and r_2 are random numbers in the range of (0, 1); p_{best}^i is the personal best position of the i^{th} particle; g_{best}^k is the global best position of whole particles at the present k^{th} generation. A restriction to v_{max} is generally applied on velocity v_i^k to confirm the algorithm convergence factor. The velocity is limited to $[-v_i^{max}\ ,\ v_i^{max}]$, where $v_i^{max}$is the higher velocity of the initial particles. There are both conceptual and observational approaches for determining these parameters [65]. Any particle within that population is typically used in a progressive manner, which implies that the control parameter (e.g., voltage/current/duty ratio) is provided to the agitator and executed independently in each generation. On this assumption each module of PV array is provided with a power converter, and all PV modules are controlled with only one MPPT algorithm. Hence, each module's output voltage (V_1, V_2,…,V_N) is treated as N-dimensional independent variables. The particle's position at k^{th} time moment (x^k)is:

$$x^k = \left[V_1^k, V_2^k, \ldots\ldots, V_i^k, \ldots, V_N^k\right] \tag{2.15}$$

where N represents the total of modules within PV array, $V_i^k$is the output voltage of an i^{th} module at the k^{th} generation. The velocity (v) is defined as the variation in output voltage levels of present and previous generations and is determined as follows:

$$v^k = \left[V_1^k - V_1^{k-1}, V_2^k - V_2^{k-1} \ldots\ldots, V_N^k - V_N^{k-1}\right] \tag{2.16}$$

The objective of MPPT evolutionary optimization technique is to track maximum power from each and every module of PV array. When PSO algorithm reaches the final iteration or generation then power changes will be small, and stop the tracking process. Alternatively, the PV array's output power and current, as well as the duty ratio sent to the power converter(s), can be assumed to be control parameters. The PSO algorithm can also be used to create a centralized PV system with several PV modules arranged in a single configuration and a single power converter.

2.7.3.2 Ant Colony Optimization Algorithm

An Ant Colony Optimization (ACO) algorithm is a probability-based strategy solving the global best solution for nonlinear systems. The ACO algorithm mimics the foraging action of ants in order to improve the path in a graph [66]. The combined actions of a great amount of ants create a positive feedback phenomenon: ants look for a path randomly at first, then leave

pheromone for many other ants to try. The greater the number of ants passing along a path, the thicker the pheromone on the path, and therefore the greater the probability that a following ant would choose that path. Ultimately, a vast number of ants explore the track before the ant entities discover the most narrow path by pheromone data trading.

During solution generation, a pheromone database is characterized to address the persistent issue. The vectors s_i $(i = 1, 2, \dots, l, \dots, K)$ and $f(s_i)$ represent the K potential solutions as well as their associate objective functions. After that, for N-dimensional scenario, the steps for developing an ACO-based maximum power point tracking are as follows [26]:

Step 1: *Initialization:* Initialize the variables and produce K ($K \geq NP$, where NP is the total population) arbitrary solutions, ranking them as per optimal solution ($f(s_i)$) (from worst to best), $f(s_1) \leq f(s_2) \leq \dots \leq f(s_l) \leq \dots \leq f(s_K)$, and keeping them in the solution database.

Step 2: *Generate a new solution:* In two steps, sample the Gaussian Kernel probabilistic model to every dimension to create a fresh solution:

(i) Select the sub-function of Gaussian probability density

(ii) As described by the parameterized normal distribution, sample the selected Gaussian probability density sub-function. Each dimension's probability density function is made up of numerous (K) Gaussian sub-functions, followed by

$$G^i(x) = \sum_{l=1}^{K} w_l g_l^i(x) = \sum_{l=1}^{K} w_l \frac{1}{\sigma_l^i \sqrt{2\pi}} exp\left(-\frac{\left(x-\mu_l^i\right)^2}{2{\sigma_l^i}^2}\right) \quad (2.17)$$

where $G^i(x)$ is the Gaussian function for the i^{th} dimension of the solution, $g_l^i(x)$ is the l^{th} sub-Gaussian function for the i^{th}dimension of the solution, μ_l^i and σ_l^i are the i^{th} dimensional mean value and the standard deviation for the l^{th} solution, respectively. The three parameters, (i) The mean, μ^i, (ii) Standard deviation, σ^i, and (iii) Weight, w_l, of the Gaussian Kernel for each dimension in equation (2.17) are calculated based on following equations:

$$\mu^i = \left\{\mu_1^i, \dots \dots \mu_l^i, \dots \dots \mu_K^i\right\} = \left\{s_1^i, \dots \dots s_l^i, \dots \dots s_K^i\right\} \quad (2.18)$$

$$\sigma_l^i = \xi \sum_{j=1}^{K} \left|s_j^i - s_l^i\right| / (K-1) \quad (2.19)$$

$$w_l = \frac{1}{QK\sqrt{2\pi}} \exp\left(-\frac{(l-1)^2}{2Q^2K^2}\right), \quad (2.20)$$
$$w_K \leq \cdots \leq w_l \leq \cdots \leq w_2 \leq w_1$$

where s_l^i is the i^{th} dimensional value for the l^{th} solution, σ_l^i is the standard deviation for the i^{th} dimension of the l^{th} solution, ξ is the speed of convergence, w_l is the weight of solution s_l, l is the rank of solution s_l, and Q is the importance of the top ranked solutions. Based on the likelihood, the Gaussian sub-function is selected at random.

$$p_l = \frac{w_l}{\sum_{r=1}^{r=K} w_r} \quad (2.21)$$

Step 3: *Ranking and archive updating:* NP new solutions are created by doing it all again. Bring the newly created solution to the archive's original solutions, rate the NP + K solutions, and save just the K best solutions.

Step 4: *Termination:* Put an end to the searching process if ACO algorithm reaches maximum iteration (generation) or termination criteria $\left(\left|V_{ref}(k) - V_{ref}(k-1)\right|\right) < \epsilon$ occurs. Otherwise, go to Step 2.

An ACO algorithm is implemented for MPPT in PV systems with various parallel connections of PV strings followed by a power converter for every PV string [26]. The control vector is formed here by collecting current from the PV string. The objective function is considered terminal output power of PV array. The observation form the ACO technique based MPPT is that it is a faster tracking process compared to standard PSO and P&O algorithms. The ACO process is combined with P&O and IC to enhance search process. For example [67], the ACO algorithm is used to search, and the best solution is used to launch the P&O algorithm after a certain amount of ant activities.

Rather than directly applying ACO algorithm to global solution, it can also be utilized to improve parameters for various kinds of controllers employed in PV systems [68]. The ACO algorithm is also used to adjust the parameters of the PI controller [68]. The objective is to improve the dynamic response by reducing the performance condition; $F = \lambda_{t_s} f_1 + \lambda_{e_{ss}} f_2$, where $\lambda_{t_s}$and $\lambda_{e_{ss}}$are weights and f_1 and f_2 are functions of the settling time (t_s) and steady state error $(e_{ss})$of the unit step response, described as:

$$f_1 = t_s/t_{s0}, \text{ and } f_2 = \begin{cases} e_{ss}/e_{ss0}, & if\ e_{ss0} \neq 0 \\ 0, & if\ e_{ss0} = 0 \end{cases} \quad (2.22)$$

where t_{s0} and e_{ss0} are the reference performance values. Under rapid irradiance changes, the improved controller provides a strong performance.

2.7.3.3 Artificial Bee Colony Algorithm

Karaboga suggested the Artificial Bee Colony (ABC) optimization algorithm, as a new member of swarm based strategies that was initiated for solving multi-dimensional and multimodal optimization problems [69]. The employment of ABC applications is made to MPPT [27]. ABC imitates the honey bee based on foraging behavior, learning, memorizing and information sharing characteristic of honey bees to locate the best response. The ABC study estimates the positions of food sources to be possible alternatives. The consistency (objective function (f_i)) of the corresponding solution i (i=1, 2,…, NP), where NP is the quantity of food sources is propotional to the nectar volume of food source. In the ABC algorithm, the bees are classified into three groups: working bees, onlookers, and scouts, as well as three kinds of foraging behavior: looking for a new food supply, hiring bees to get food from a source of food, and leaving a food source based on the nature of the food. During the search process, the function of honey bee varies among the three kinds of bees. Remember that each food source has only one employed bee in a D-dimensional problem with NP food sources. At the t^{th} iteration, the position of the i^{th} food supply is defined by:

$$X_i^t = [x_{i1}^t, x_{i2}^t, \dots, x_{id}^t, \dots, x_{iD}^t]^T \quad (2.23)$$

The ABC algorithm is implemented using the following procedure:

Step 1: *Initialization:* Set criteria including the initial population (NP), the 'Limit' for each solution, and the overall number of iterations. Set t=1 and allocate the original food supply as follows:

$$x_{id} = L_d + r(U_d - L_d) \quad (2.24)$$

where L_d, U_d represent the d^{th} dimension's minimum and maximum search space limits and r is a randomly generated in the range of (0, 1).

Step 2: *Identify new food sources:* There are two stages of each loop of the searching operation.

(i) *Employed bee phase:* Each possible food source X_i should have an employed bee assigned to it. Begin looking for a new objective function

V_i along the selected X_i on a randomly chosen dimension d ($d \in [1, D]$), as described by:

$$v_{id} = x_{id} + \varphi(x_{id} - x_{jd}) \tag{2.25}$$

where $i \neq j \in (1, 2, \cdots NP)$, j is selected at random vector index, and φ is a uniform random value in the range of (−1,1). If the present objective function V_i is superior to that of the original position X_i, then X_i is updated with V_i; otherwise leave X_i alone.

(ii) *Onlooker phase:* After exchanging the food supporting data with onlooker bees, that onlookers use a roulette wheel collection system to choose the sources of food based on the following likelihood:

$$P_i = \frac{fitness_i}{\sum_{n=1}^{NP} fitness_n} \tag{2.26}$$

At the same time, the number of working bees is updated using a greedy selection method.

Step 3: *Abandon phase:* If the fitness function does not change after a predetermined number of trials 'limit', the present reference food supply X_i is discarded, and go to Step 4; otherwise get over to Step 5.

Step 4: *Scout bee phase:* The bees associated with discarded sources of food turn into scout bees and begin looking for new sources of food, according to equation (2.24).

Step 5: *Termination:* The best fitness gets restored if the ultimate fitness is appropriate or exceeds the required number of iterations. Otherwise, proceed to Step 2, increase the number of iterations ('t') and repeat this process.

The effect of control parameters on the optimization's representation was investigated, and it was discovered that ABC is unaffected by the problem dimension or population size. The 'limit' for discarding a possible solution, on the other hand, has an impact on the ABC algorithm's results. Its resulting search capacity is weakened by low value, and its global search potential is influenced by a huge value. The ABC algorithm's presentation can be enhanced in three different ways: the sorting process, the upgrading of fresh sources of food, and the upgrade calculations with scout bees to find new food sources.

The ABC is simple to use, has simple tuning parameters, is accurate, is independent of the PV scheme, and offers a global optimization approach. As a result, ABC algorithm has been

used to improve MPPT for PV systems. The ABC algorithm-based MPPT varies in two ways in the literature: (i) control variables, and (ii) update calculations in the 'employed/onlooker/scout' processes. The ABC, like other optimization algorithms, applies each particle in a sequential order. The duty ratio of the dc-dc converter is used to characterize each candidate solution, and the fitness is determined by the PV array's output power [70]. The maximum power of the PV device is tracked using a regular ABC algorithm [70]. The findings show that, in comparison to PSO, the ABC-based MPPT has improved convergence in shaded PV array situations for a number of iterations, but has a poor transient response. The scout bee process is changed in an updated version of the regular ABC-based MPPT [27]. It is assumed that half of the colony is made up of workers and the other half is made up of onlookers. Onlooker bees start moving to the working bee's location where the nectar amount is greatest, eliminating the probabilistic selection process. The i_{th} onlooker bee's movement is described as:

$$x_i^{t+1} = x_h^t + \frac{\varphi(d_{max} - d_{min})}{NP/2 - 1} \tag{2.27}$$

where x_h denotes the food supply with the most nectar. The initialization method for the bee locations (x_i) in the optimal solution has also been enhanced:

$$x_i = d_{min} + \frac{(i-1)(d_{max} - d_{min})}{NP - 1} \tag{2.28}$$

As compared to the regular ABC-based MPPT, these changes speed up convergence.

2.7.3.4 Firefly Algorithm

The flashing activity of fireflies motivated the Firefly Algorithm (FA) [71]. During the mating process, the male firefly's light is used to lure female fireflies. This FA method predicted that (i) All unisexual fireflies would be drawn to the remaining fireflies; and (ii) each firefly's attraction is proportional to the brightness of the flash. If the brighter one is not present in their colony, the less brighter one would have been drawn and shifted towards the brightest one; (iii) if the brighter one is not present in their colony, each firefly will move at random. The light of the firefly is used to represent the objective feature. The following is the general procedure for the FA algorithm:

Step 1: *Initialization:* Set the number of fireflies x_i, (i = 1, 2,…, n), the corresponding algorithm's constants, and the maximum number of iterations; Determine each firefly's fitness value.

Step 2: *Evaluate brightness and absorption coefficient:* The attraction reduces as the distance travelled increases because there is light absorption in atmosphere. In aspects of distance from the source, the FA algorithm employs exponential decay with a medium instead of the inverse-square law. Every firefly's attraction (or brightness) β is expressed as:

$$\beta(r) = \beta_o exp(-\gamma r^m), \qquad m \geq 1 \tag{2.29}$$

where β_o is the initial attraction at $r = 0$, r is the length of two fireflies, γ is a user-estimated light absorption coefficient that addresses intensity of light decline, and m is an numerical constant. The Euclidean distance between every two fireflies positioned at $x_i$and x_j is denoted as:

$$r_{ij} = \|x_i - x_j\| = \sqrt{\sum_{k=1}^{d} \left(x_{i,k} - x_{j,k}\right)^2} \tag{2.30}$$

where 'd' is the concern dimension and $x_{i,k}(x_{j,k})$ is the k^{th} generation of the spatial coordinates of the $i^{th}(j^{th})$ firefly.

Step 3: *Move towards brighter fireflies:* Fireflies with lower glow are attracted to (as well as move towards) to higher and stronger fireflies. If the i^{th} firefly's brightness (fitness) value is higher than the j^{th} firefly's, the j^{th} firefly would move closer to the i^{th} firefly. In the next stage, a firefly's behavior is determined by:

$$x_i^{k+1} = x_i^k + \beta_o exp\left(-\gamma r_{ij}^2\right)\left(x_j^k - x_i^k\right) + \alpha(randn - 0.5) \tag{2.31}$$

where α is the constant factor ($\alpha \in [0, 1]$) and 'randn' is a random number uniformly distributed in the range (0, 1). In this scenario, a firefly's flight is affected by the lure of a brighter firefly, as well as its spontaneous existence. The fitness value of the new fireflies is calculated after the upgrade, and the lower brightness intensities are modified.

Step 4: *Rank and find best solution:* After upgrading all the firefly populations, rate it and decide the present best global solution.

Step 5: *Terminate:* Stop checking when the FA algorithm reaches its iteration limit or meets the termination conditions. Otherwise, get into Step 3 and increment the current iteration.

The FA algorithm was implemented to track maximum power during partial shading of PV array [28]. In this incident, the dimension is chosen as one ($d = 1$) and hence the distance between fireflies (r_{ij}) is denoted by:

$$r_{ij} = \sqrt{(x_i - x_j)^2} \tag{2.32}$$

The main focus of standard FA is that, the number of fireflies in population change their positions with each other, and each movement bring about stepwise manner in the direction of the bright fireflies. However, the zigzag direction of travel occurs when more population takes more tracking time, with high computational burden in each iteration. To address this issue, an updated firefly method was implemented, in which the average of the coordinates of all stronger fireflies was used as the indicative intensity point, and the firefly moved towards that point instead of wandering towards all the brighter flies [72]. To reduce tracking time, the update calculation for FA is changed, and each firefly is given by:

$$x_i^{k+1} = x_i^k + \beta_o exp(-\gamma r_{ij,avg}^2)(x_{j,avg}^k - x_i^k) + \alpha(randn - 0.5) \tag{2.33}$$

where $r_{ij,avg}$ denotes the interval between x_i and the averaged coordinate of its higher bright fireflies $(x_{i,avg})$, expressed as:

$$r_{ij,avg} = \sqrt{(x_i - x_j, avg)^2} \tag{2.34}$$

$$x_{j,avg} = \frac{1}{L}\sum_{m=1}^{L} x_j \tag{2.35}$$

where L is the number of brighter flies. Thus, rather than modifying x_i in regard to each brighter fly, the average coordinate of all brighter flies is used, which decreases tracking time and increases the search procedure. The modified FA implementation utilizes a programmable PV emulator with such an interleaved topology boost converter to show the importance of using the average coordinate of all the brighter flies to reach the global MPP. While the updated version based on the MPPT's static tracking precision is marginally lower than that of the original FA, the overall approach improves the search process and saves 67

percent of tracking time compared to FA. Furthermore, as compared to PSO and P&O, updated FA outperforms them.

2.7.3.5 Other Types of Algorithms

A variety of other popular soft computing techniques, such as the Intelligent Monkey King Evolution (IMKE) algorithm, Bat Algorithm (BA), Flower Pollination Algorithm (FPA), Grey Wolf Optimization (GWO), and others, have recently been proposed in addition to the above evolutionary dependent MPPT techniques. These heuristic algorithms can be represented in a similar way for MPPT [29], [31], [73], and [74].

Chapter 3

Modified Grey Wolf Optimization Algorithm for Global MPPT under Partial Shading Conditions in Photovoltaic System

Chapter 3

Modified Grey Wolf Optimization Algorithm for Global MPPT under Partial Shading Conditions in Photovoltaic System

3.1 Introduction

In the study of Photovoltaic (PV) system, Power-Voltage (P-V) curves exposed to view several peaks under Partial Shaded Condition (PSC), which brings about muddled and most extreme Maximum Power Point Tracking (MPPT) process. Under uniform weather conditions, regular MPPT algorithms such as Perturb and Observe (P&O), Hill Climbing (HC), Incremental Conductance (IC), etc. work in an effective manner. However, these conventional methods are unable to track global peak successfully under PSC. In this context, the evolutionary algorithms such as Grey Wolf Optimization (GWO) perform better than conventional algorithms. However, the conventional GWO is not sufficient for exploration point of view to locate global best particles; and moreover, GWO deteriorates the convergence process. To overcome these drawbacks a Modified GWO (MGWO) algorithm is proposed to track global best particle, which improves the convergence process under static condition and as well as re-initialization under dynamic conditions. The proposed method is verified using simulations as well as using experimental results. The obtained results demonstrate superiority compared to conventional GWO and HC algorithms under static and re-initialization of parameters during dynamic shaded conditions of PV array.

3.2 Tracking Methods for GMPP

3.2.1 Hill Climbing Algorithm for GMPPT

The best MPPT technique is Hill Climbing (HC) due to its directness (means duty can be given to converter without using PI controllers) and less cost. The duty cycle to converter is directly provided by the algorithm [5]. By providing duty to the converter, maximum power can be measured. The presentation of traditional methods in the literature are described [5]-[14]. The duty cycle (d) of HC is varied by the size of perturbation 'θ'. The perturbation size plays important role for maximum power and the equations are given as follows:

$$d_{new} = d_{old} + \theta \quad if \quad P > P_{old} \tag{3.1}$$

$$d_{new} = d_{old} - \theta \ \ if \ \ P < P_{old} \tag{3.2}$$

where d_{new} and d_{old} are the present and previous duty cycles, P and P_{old} are the present and previous powers. The benefit of HC algorithm is that no additional controllers (such as P or PI) are required for generation of pulses to control the duty of converter.

3.2.2 GWO Algorithm for GMPPT

The Grey Wolf Optimization (GWO) is an advanced algorithm motivated by behavior of grey wolves and introduced by Mirjalili, Mirjalili and Lewis [75]. It mimics the nature of social leadership and hunting behavior of grey wolves. In GWO algorithm, the optimum solution (leader wolf) is denoted by alpha (α). The second and third best solutions (wolves) are represented as beta (β) and delta (δ), respectively. The other solutions (wolves) within the population are represented as omega (ω). Mathematically, the encircling mechanism of grey wolves is given by the equation below:

$$\vec{D} = \left|\vec{C} \cdot \vec{X}_p(t) - \vec{X}(t)\right| \tag{3.3}$$

$$\vec{X}(t+1) = \vec{X}_p(t) - \vec{A} \cdot \vec{D} \tag{3.4}$$

where $\vec{X}$ is the position of a grey wolf vector, t is the current iteration, $\vec{X}_p$ specify the position of the prey vector (food source), A and C are coefficient vectors

$$\vec{A} = 2\vec{a} \cdot \vec{r}_1 - \vec{a} \tag{3.5}$$

$$\vec{C} = 2 \cdot \vec{r}_2 \tag{3.6}$$

where r_1 and r_2 are random vectors in $[0, 1]$, respectively, and $\vec{a}$ is control parameter linearly reduced from 2 to 0 according to equation (3.7)

$$\vec{a}(t) = 2 - \frac{2t}{MaxIter} \tag{3.7}$$

$MaxIter$ denotes the number of maximum iterations. The positions updated according to the positions of α, β, and δ in the following equations:

$$\vec{X}_1 = \vec{X}_\alpha - \vec{A}_1 \cdot \left|\vec{C}_1 \cdot \vec{X}_\alpha - \vec{X}\right| \tag{3.8}$$

$$\vec{X}_2 = \vec{X}_\beta - \vec{A}_2 \cdot \left|\vec{C}_2 \cdot \vec{X}_\beta - \vec{X}\right| \tag{3.9}$$

$$\vec{X}_3 = \vec{X}_\delta - \vec{A}_3 \cdot \left|\vec{C}_3 \cdot \vec{X}_\delta - \vec{X}\right| \tag{3.10}$$

$$\vec{X}_{GWO}(t+1) = \frac{\vec{X}_1(t) + \vec{X}_2(t) + \vec{X}_3(t)}{3} \tag{3.11}$$

The grey wolves are duty ratios to converter, the controller implements by sensing V_{pv} and I_{pv}. To update the position of GWO based on MPPT, duty cycle (D) is denoted as grey wolf. Therefore equation (3.4) changed as below:

$$D_i(k+1) = D_i(k) - A \cdot D \tag{3.11}$$

The fitness function of GWO is denoted as power

$$P\left(d_i^k\right) > P\left(d_i^{k-1}\right) \tag{3.12}$$

where *P* is power and d is duty cycle, i and k denotes present grey wolf and maximum number of iterations.

3.2.3 Proposed MGWO algorithm for GMPPT

The Grey Wolf Optimization (GWO) is a population-based optimization algorithm motivated by hunting strategy of grey wolves to optimize the best particle [75]. The conventional GWO does not maintain enough exploration process in the search space with current position update equation $(\vec{X}_{GWO})$, and linear tuning of control parameter $(\vec{a})$, due to which slow convergence occurs [29]. To enhance exploration process of GWO, proposes the Modified Grey Wolf Optimization (MGWO) algorithm for better convergence over existing GWO shown in Figure.3.1. The updated-position equation of GWO is modified by the inspiration of PSO in the proposed MGWO algorithm for better exploration process [76]. In the proposed method each particle (wolf) is updated using modified updated-position equation (3.13). According to the modified updated-equation of the proposed MGWO algorithm, the new updated particles move towards the global best particle (leader wolf α). Therefore the exploration is well in the proposed method for global best solution.

$$\vec{X}_{MGWO}(t+1) = b_1 \times \vec{X}_{GWO}(t+1) + b_2 \times \left(\vec{X}' - \vec{X}\right) \tag{3.13}$$

$\vec{X}'$ is the particle selected from the wolves randomly but different to $\vec{X}$, $b_1 \in (0, 1)$ and $b_2 \in (0, 1)$ are constant coefficients used to regulate the exploration and exploitation capabilities of above equation (3.13); several simulations are conducted by varying the parameters b_1 and b_2 and optimal solutions are at $b_1 = 0.9$ and $b_2 = 0.1$ according to [76]. In order to trade-off the exploration and exploitation capabilities, the specific control parameter $(\vec{a})$ has to be tuned according to the search process. Here the control parameter $(\vec{a})$

is modified in equation (3.14) and decreased nonlinearly from 2 to 0, which makes crucial contribution in the proposed algorithm to balance the exploration and exploitation in design process. A suitably large value of $\vec{a}$ helps exploration, however a relatively small value of $\vec{a}$ helps exploitation process. Where exploration addresses the ability to explore unknown regions of the design (search) space to realize the global optimum. While exploitation addresses the ability to relate the knowledge of the existing particles in order to obtain better particle. In the conventional GWO algorithm, $\vec{a}$ reduces linearly fashion 2 to 0 [29]. But the linear changes in $\vec{a}$ would not reflect proper search process. Better performance can be obtained using the model of Mittal, Singh and Sohi. if $\vec{a}$ decreases as nonlinearly instead of linearly [77]. Based on the above information the control parameter ($\vec{a}$) is modified in the following way:

$$\vec{a}(t) = a_{initial} - \left(a_{initial} - a_{final}\right) \times \left(\frac{Max\_iter - t}{Max\_iter}\right)^{\mu} \tag{3.14}$$

where 't' is present iteration number, Max_iter specify the maximum iterations, 'μ' denotes modulation index, in (0, 2.0) and assumed as 2 for better solution, $a_{initial}$ and a_{final} are initial and final value of control parameter according to [76].

3.2.3.1 Steps to Implement Proposed MGWO Algorithm

Step-1: Initialize the particles of the wolves at fixed positions between 0.1 and 0.9 of the duty cycle.

Step-2: Measure the power 'P_{pv}' from output of PV array at each location of wolf (duty) by sensing 'V_{pv}' and 'I_{pv}' and corresponding duty cycle to boost converter, ' $P_{pv} = V_{pv} \times I_{pv}$'.

Step-3: Update the best fitness powers.

Step-4: Update global best fitness from best fitness.

Step-5: Update the modified updated-positions of wolves as duty of converter according to equation (3.13).

Step-6: Update A, C, and $\vec{\boldsymbol{a}}$ according to equations (3.5), (3.6) and (3.14).

Step-7: Repeat steps 2 and 6 till to reach global peak of P-V curve.

Step-8: If any new shading pattern occurs then re-initialize the parameters.

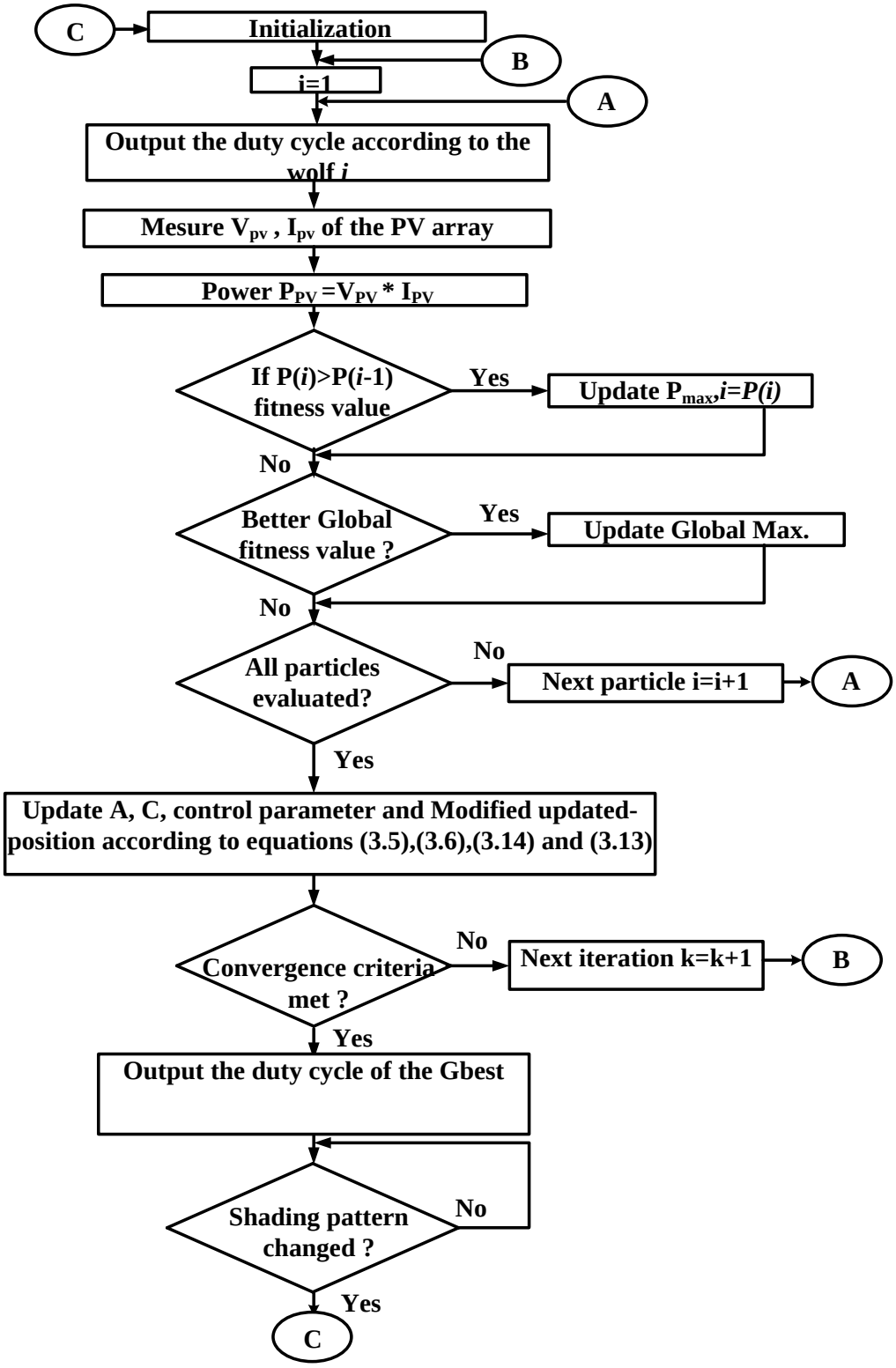

Figure 3.1 Flowchart of proposed MGWO algorithm.

Step-9: The change of PV pattern is recognized by proposed algorithm with the following power equation:

$$\frac{|P_{n+1} - P_n|}{P_n} \geq \delta \tag{3.15}$$

Term P_n, P_{n+1} are present and future power output of PV system, δ (percentage change in power) is considered as 2% according to [78].

3.3 The Solar PV Array under Partial Shaded Condition

The performance of MGWO algorithm can be proven with two PV arrays under PSC. The two PV arrays are designed by three PV modules are in series (3S), four PV modules are in series and with two such combinations in parallel (4S2P) according to Figure 3.2 and related P-V curves with shading conditions are shown in Figure 3.3. The each PV module is designed for 60W, which is shown in Table 3.1 and where the irradiance considered to shading cases (patterns) are shown in Table 3.2.

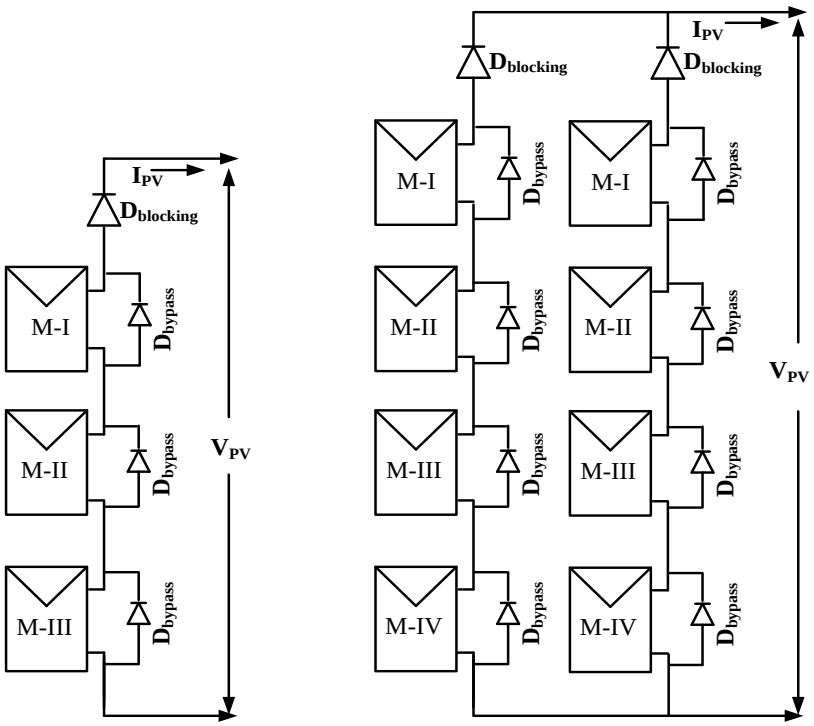

Figure 3.2 PV array configurations under partial shading conditions of: (a) 3S, and (b) 4S2P.

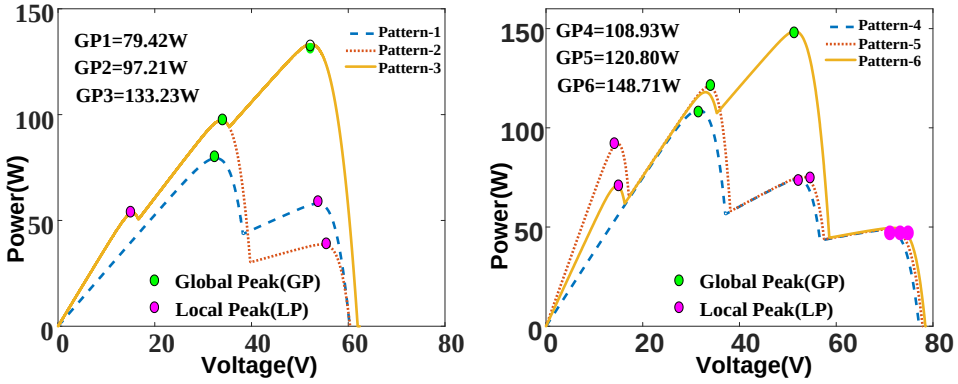

(a) (b)

Figure 3.3 PV array characteristics under partial shading conditions of: (a) 3S, and (b) 4S2P

Table 3.1 PV Module Specifications

P_{max}	V_{OC}	I_{SC}	V_{max}	I_{max}
60 $Watt$	21 $Volt$	3.8 Amp	17.1 $Volt$	3.5 Amp

Table 3.2 Irradiance (W/m^2) of each module in PV arrays configuration

Module (M)	Pattern-1	Pattern-2	Pattern-3	Pattern-4	Pattern-5	Pattern-6
M-I	700	1000	1000	500	900	700
M-II	700	800	800	500	500	500
M-III	300	200	700	200	200	400
M-IV	-	-	-	100	100	100

3.4 Simulation Results

The schematic diagram of boost converter to PV application is shown in Figure 3.4. The results were carried out using the proposed method for GMPPT in simulation for six feasible shaded conditions of PV array. In these shaded conditions, 3S cofiguration of PV array for three patterns and the remaining three patterns were formed by 4S2P configrations of PV array. In these, one on leftmost peak, one in center peak and another on rightmost peak of 3S configuration. Global peak point of 4S2P configuration has first, second and third peaks from left side of the P-V curve. Initial wolves of the proposed MGWO and GWO agorithms labelled as duty to converter were three $x_1 = 0.2, x_2 = 0.3$ and $x_3 = 0.7$. The designed values of algorithm and boost converter are presented in Table 3.3.

Table 3.3 Designed parameters of algorithms and boost converter

Particulars	Parameters
Proposed	$\mu = 2,\ b_1 = 0.9\ and\ \ b_2 = 0.1$ $Population\ size = 3$
GWO	$Population\ size = 3$
HC	$\theta = 0.05$
Boost coverter	$L = 1.928\ mH, C_1 = C_2 = 100\ \mu F,$ $F_s = 10\ kHz, Diode - MUR860,$ $MOSFET - IRFP460,$ $100\ \Omega\ 10\ A\ Variable\ Rheostat\ load.$
Sampling period (T_s)	$For\ simulation\ T_s = 50ms,$ $For\ experimental\ T_s = 100ms.$

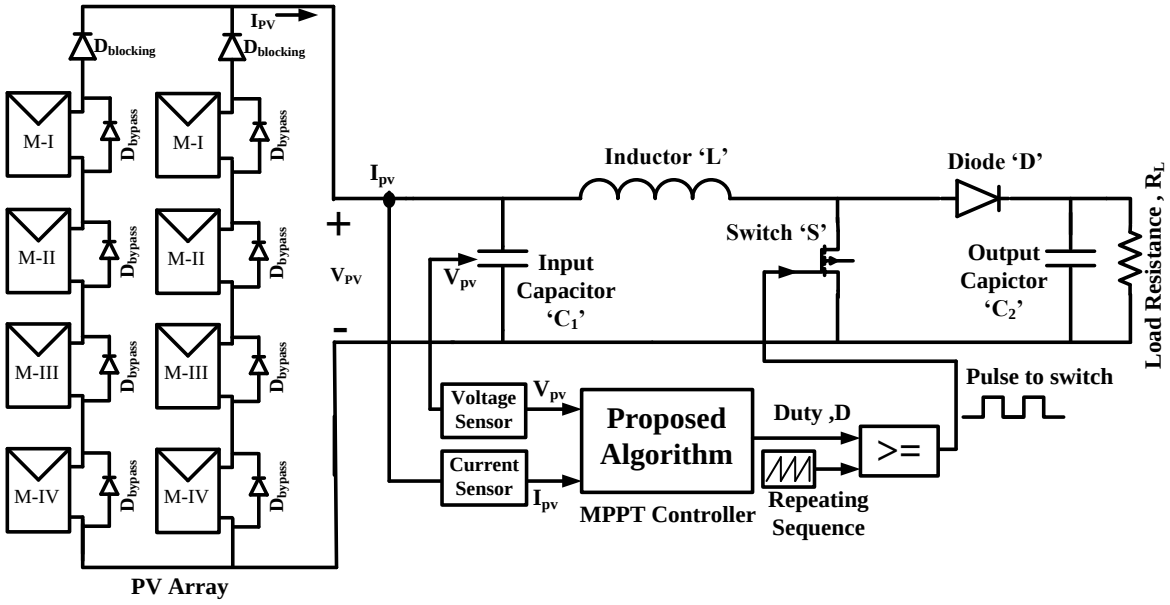

Figure 3.4 Application of PV array to boost converter with MPPT controller.

The implementation of PV array with boost converter of the proposed algorithm in simulink is modelled as per Figure 3.4. The PV modules connected in series or parallel with bypass and blocking diodes to form PV array. Implementation of the proposed technique in MATLAB/SIMULINK using s-function is as per flowchart (Figure 3.1). The proposed algorithm provide duty to switch the boost converter by taking voltage and current signals from output of PV array. To prove the performance of the proposed MGWO algorithm, it was compared with conventional Grey Wolf Optimization (GWO) and Hill Climbing (HC) algorithms. The results were verified with six different shaded conditions of PV array.

3.4.1 Simulation Results of 3S PV Array Configuration

Pattern-1: In this pattern, the PV array consists of three PV modules and these are placed in series to form a 3S configuration. The irradiances are considered 700W/m^2, 700W/m^2 and 300W/m^2. Due to two different irradiances in pattern-1, there will be two peaks in P-V characteristics of PV array in Figure 3.3 (a). The first peak from left side is global peak (GP) and the second peak is local peak (LP). The global point is left most peak and its corresponding power is 79.42Watt. By considering pattern-1 as PV source and connecting this as a source to boost converter, the converter switch (MOSFET) can be operated by taking the signal from MPPT algorithm. The proposed MGWO algorithm can be operated by sensing voltage and current from the output of PV array. The power observed by HC algorithm is 76.91Watt with tracking time of 0.1 sec but there are oscillations at steady state. The tracking power obtained by GWO is 79.05Watt with a time of 1.50 sec to reach global power along with 10 cycles; in GWO steady-state oscillations are reduced but they take more time to reach global peak power due to does not have enough exploration search process in GWO with improper peturbation. *The global peak power obtained by the proposed MGWO algorithm is 79.05Watt with a 0.96 sec in 6 iterations*, the corresponding simulation results are shown in Figure 3.5 (a). *From the results relized that the proposed MGWO technique is superior to GWO and HC algorithm in terms of steady-state oscillations, tracking time and iterations*. The GWO algorithm does not have enough exploration due to which there is convergence delay. In this proposed algorithm, due to modified updated-position and the control parameter updated maintains better exploration and exploitation process for global best particle to reach global power, so the time consumed by the proposed MGWO algorithm is less.

Patttern-2 and Pattern-3: The global peak power is the center peak in pattern-2 and rightmost peak in pattern-3 and its corresponding irradiances (W/m^2) are shown in Table 3.2; global peak powers and P-V characteristics are shown in Figure 3.3 (a). The power extracted by HC algorithm in pattern-2 is 94.18Watt with a tracking time of 0.1 sec but oscillations at steady state. The power achieved by GWO and the proposed MGWO algorithm is 96.17Watt but the *proposed MGWO algorithm reaches global peak with 1.01 sec and 7 iteration* whereas GWO takes 1.81 sec with 12 iterations. The power obtained by HC algorithm of pattern-3 is 126.34Watt with 0.1 sec, while GWO takes 12 iterations to catch highest peak power 132.30Watt with 1.82 sec and *the proposed MGWO algorithm reaches highest peak power of*

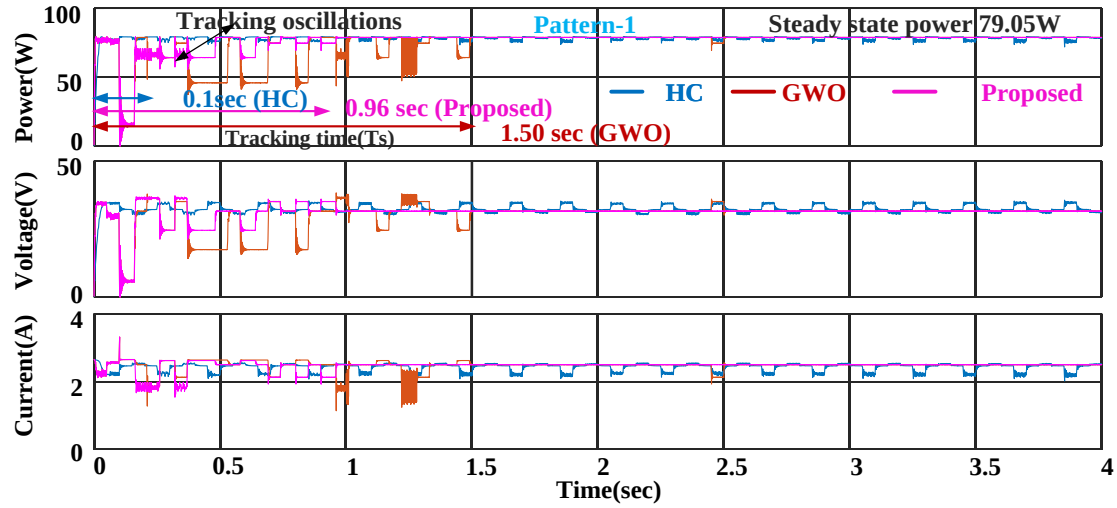

(a)

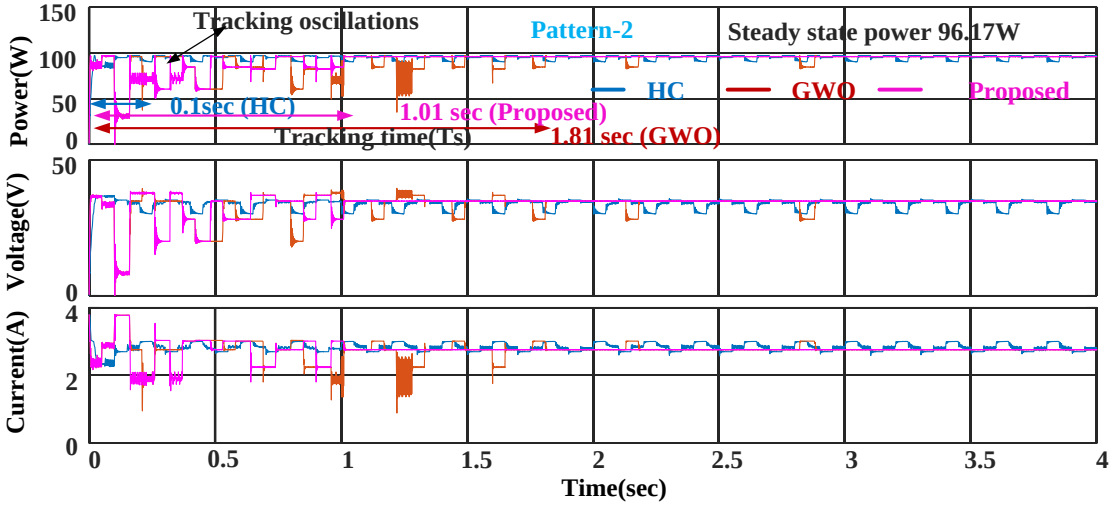

(b)

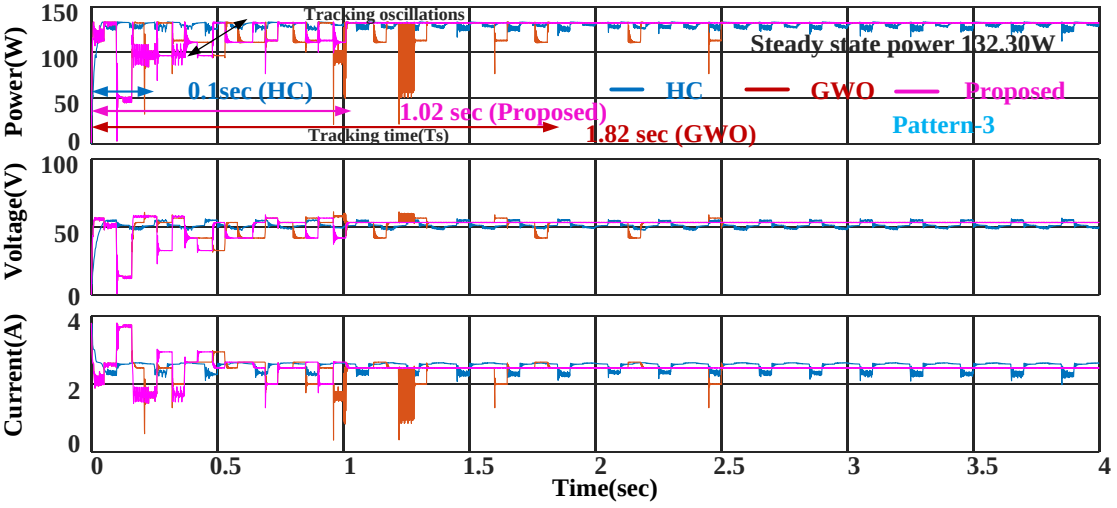

(c)

Figure 3.5 Simulation results for 3S PV array configuration during shading of: (a) Pattern-1, (b) Pattern-2, and (c) Pattern-3.

132.30Watt in 7 iterations within 1.02 sec. The advantages of these patterns are similar to pattent-1, and the simulation results are in Figures 3.5 (b) & (c) and the corresponding comparision results are presented in Table 3.4.

Table 3.4 Simulation performance analysis of 3S, and 4S2P PV array configurations

Method	**Rated Power (Watt)**	**Extracted Power from PV(Watt)**	**Voltage from PV(Volt)**	**Current from PV(Amp)**	**Tracking time (Sec)**	**Iterations**	**Tracking Efficiency (%)**
Proposed	79.42 Pattern-1	79.05	31.62	2.50	**0.96**	**06**	99.53
GWO		79.05	31.62	2.50	1.50	10	99.53
HC		76.91	32.18	2.39	0.10	-	96.83
Proposed	97.21 Pattern-2	96.17	34.84	2.76	**1.01**	**07**	98.93
GWO		96.17	34.84	2.76	1.81	12	98.93
HC		94.18	33.28	2.83	0.10	-	96.88
Proposed	133.23 Pattern-3	132.30	53.56	2.47	**1.02**	**07**	99.30
GWO		132.30	53.56	2.47	1.82	12	99.30
HC		126.34	51.15	2.47	0.10	-	94.82
Proposed	108.93 Pattern-4	108.09	32.56	3.32	**1.01**	**07**	99.22
GWO		108.09	32.56	3.32	1.81	12	99.22
HC		105.70	31.75	3.32	0.10	-	97.03
Proposed	120.80 Pattern-5	119.75	34.61	3.46	**1.01**	**07**	99.13
GWO		119.75	34.61	3.46	1.82	12	99.13
HC		114.90	33.20	3.46	0.10	-	95.11
Proposed	148.71 Pattern-6	148.60	51.60	2.86	**1.02**	**07**	99.92
GWO		148.60	51.60	2.86	1.33	09	99.92
HC		140.70	52.69	2.67	0.10	-	94.61

Simulation Results of Pattern-1 and Pattern-2 during Dynamics: In order to verify the dynamic operation of proposed MGWO algorithm, pattern-1 and pattern-2 were considered in dynamic case. First pattern-1 is assumed as source to boost converter, it tracks highest peak power with minimum tracking time as 1.01 sec using the proposed MGWO algorithm where as GWO takes 1.50 sec; after 4 sec, pattern-2 acts as source and the proposed MGWO algorithm re-initializes the parameter by considering power equation (3.15), where again it tracks new global peak power of pattern-2 with less tracking time of 1.01 sec and GWO tracks with 3 sec. *Hence the proposed MGWO algorithm works well even in dynamic cases also and compared with GWO and HC algorithms*, its corresponding simulations results are shown in Figure 3.6.

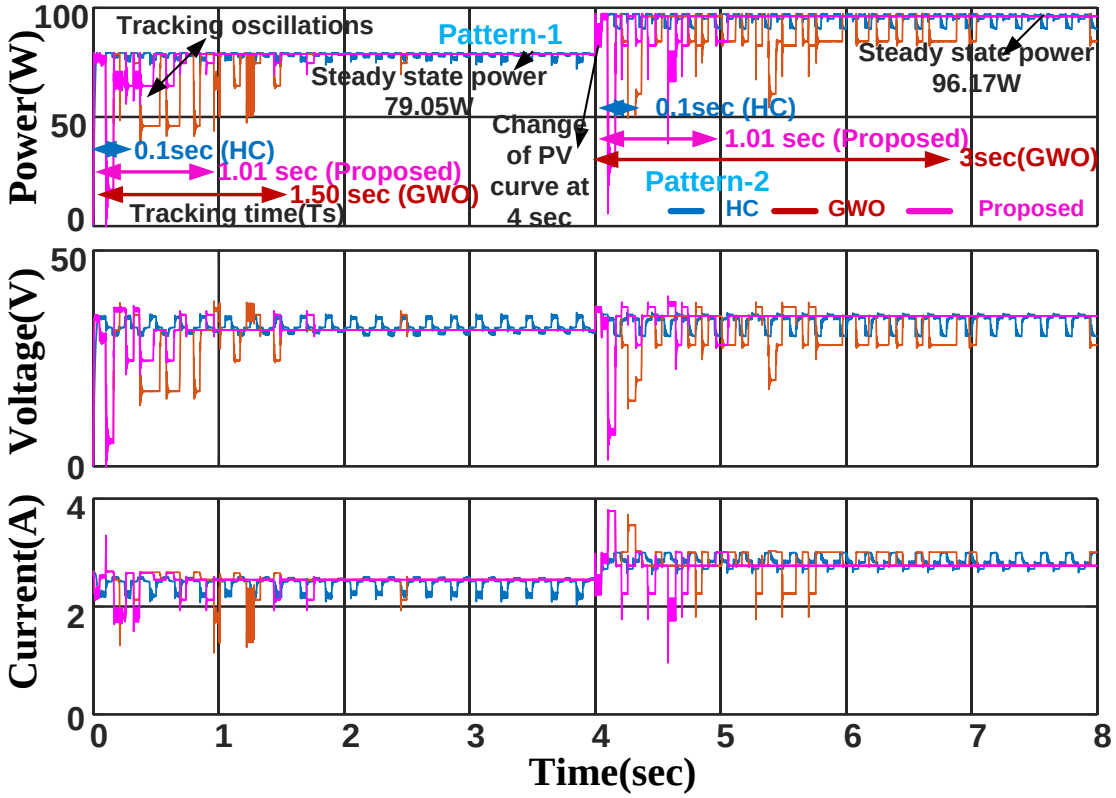

Figure 3.6 Simulation results for proposed MGWO algorithm compared with HC, and GWO algorithms during dynamics of shading pattern-1, and shading pattern-2 of 3S PV array.

3.4.2 Simulation Results of 4S2P PV Array Configuration

The complexity of PV system pattern is increased compared to previous patterns; here four series PV modules and two such parallel paths are called 4S2P configuration. Based on this configuration, three patterns are formed, in which the first, second and third peak from the left side of characteristics of PV array are shown in Figure 3.3 (b) along with global peak powers. The individual PV module irradiances (W/m^2) of each 4S2P pattern are presented in Table 3.2. In pattern-4, due to three dissimilar irradiances, there would be three peaks with the first peak being global peak. The power observed by HC algorithm is 105.70Watt with a tracking time 0.1 sec, but there are oscillations at steady-state position; the GWO algorithm reaches global peak power of 108.09 Watt with a taking time of 1.81 sec along with 12 cycles and *the proposed MGWO algorithm attains gobal peak power of 108.09Watt with 7 iterations and tracking time of 1.01 sec*. The advantages of pattern-5 and pattern-6 are that of same as

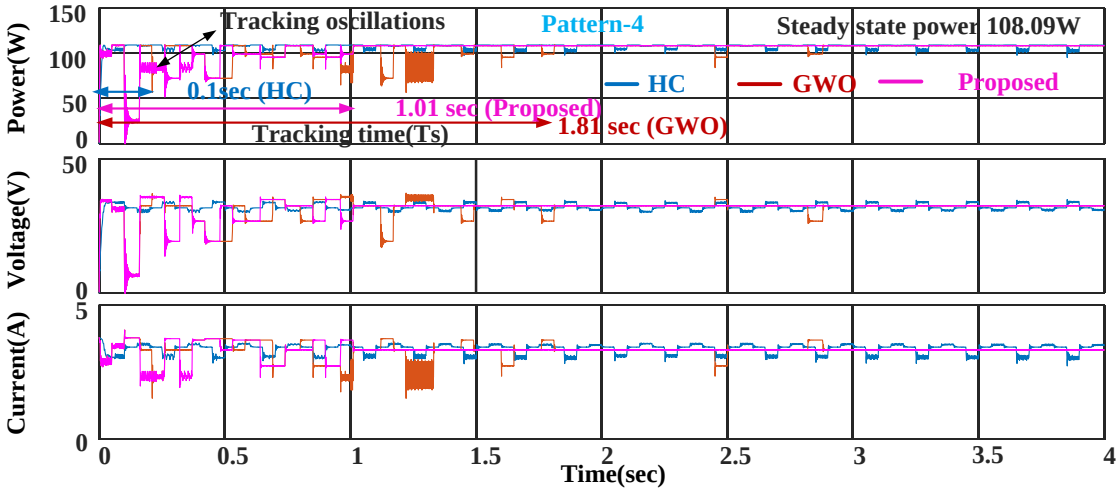

(a)

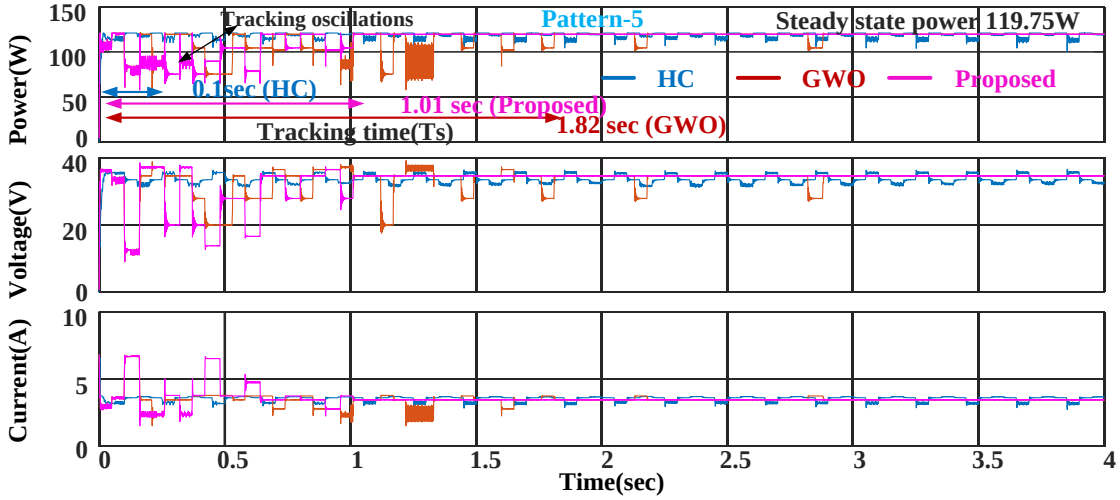

(b)

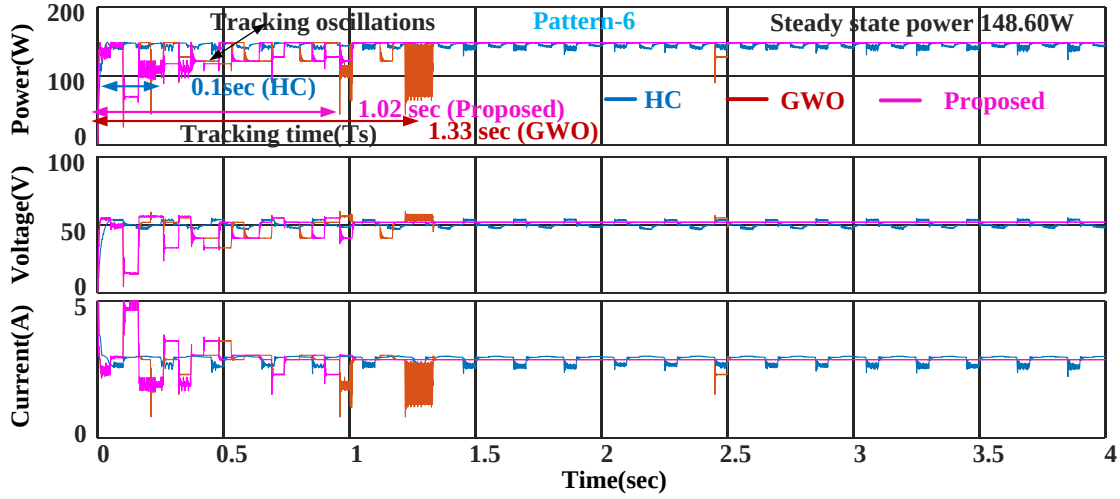

(c)

Figure 3.7 Simulation results of 4S2P PV array configuration during shading of: (a) Pattern-4, (b) Pattern-5, and (c) Pattern-6.

above patterns even if complexity of the system increases and simulation results are shown in Figure 3.7, corresponding values are presented in Table 3.4.

The simulation performance of HC, GWO and proposed MGWO algorithms were tested under six patterns of PV array and also results presented in Table 3.4. *From the results relized that the proposed MGWO technique is superior to GWO and HC algorithm in terms of steady state oscillations, tracking time and iterations*. HC dipalys oscillations around steady state point and there is a loss of power during trasient period due to improper step size under PSC. GWO algorithm does not have enough exploration due to which there is convergence delay, taking more number of iterations to reach global power and also observed from Table 3.4. In this proposed MGWO algorithm, due to modified updated-position and the control parameter updated maintains better exploration and exploitation process for global best particle to reach global power, *so the time consumed by the proposed MGWO algorithm is less and takes fewer number of iterations compared to GWO*.

3.5 Experimental Results

An experimental-setup for proposed MGWO algorithm is shown in Figure 3.8, it is comprising of programmable PV simulator (Magna power electronics XR600-9.9/415+PPPE+HS), boost converter, voltage sensor (LV25-p) and current sensor (LA55-p) and D-space 1104 controller which is interfaced with MATLAB. The P-V curves are taken from PV simulator for different PV array patterns. The proposed MGWO algorithm was verified by D-space 1104 controller by sensing voltage and current from output of PV simulator with the help of sensors. The output of proposed MGWO algorithm duty is given to switch of boost converter and the converter details are mentioned same as simulations values, which are shown in Table 3.3. The verification of GMPP using the proposed algorithm with two PV array configurations at various peaks on P-V curve under different shaded patterns. The corresponding irradiances (W/m^2) are represented in Table 3.2 and the P-V curves are in Figure 3.3.

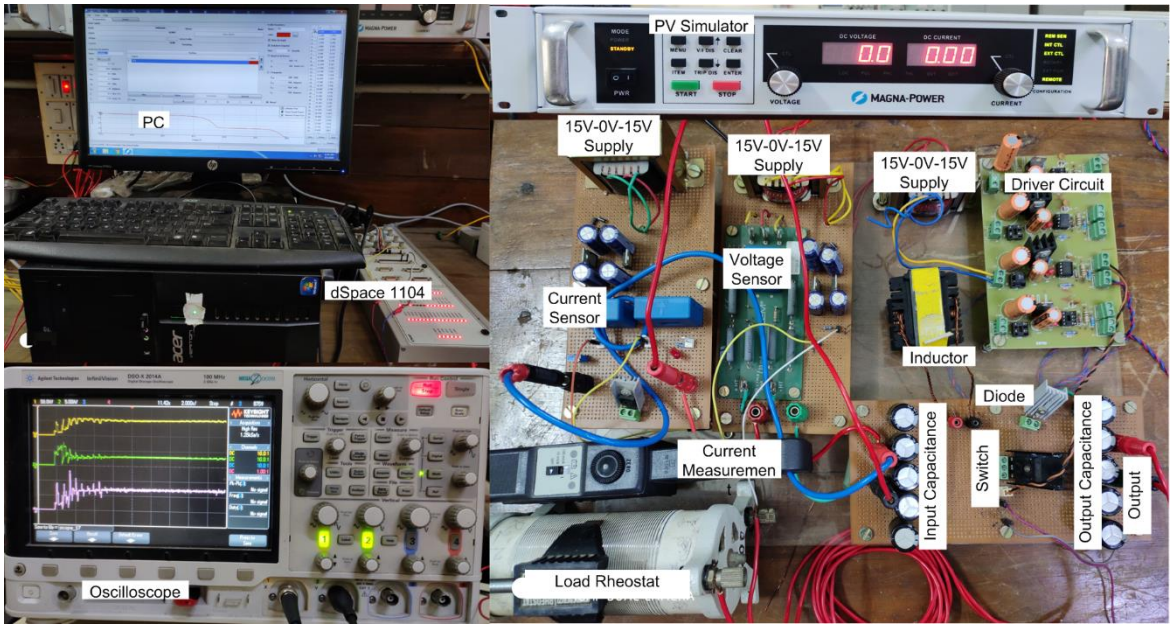

Figure 3. 8 Experimental setup for proposed MGWO algorithm.

3.5.1 Experimental Results of 3S PV Array Configuration

The superiority of the MGWO algorithm over HC and GWO algorithms is that, the fewer cycles (iterations) are needed to track highest peak of P-V curve and oscillations around global peak and the convergence time is also minimum as was noticed in Section 3.4 results. The proposed MGWO algorithm was developed in experiment to compare with Section 3.4 results and the GMPP on P-V curves was also observed to justify the efficiency. Table 3.5 shows the results of experimental analysis of two PV array configurations.

The experimental results of the proposed MGWO, GWO and HC algorithms of pattern-1 are shown in Figure 3.9 along with an operating point on P-V characteristic which is inscribed in each figure at the righthand corner. The power obtained by HC algorithm of pattern-1 is 75Watt with a time of 1.12 sec; the GWO algorithm tracks global power of 78.12Watt with a time of 3 sec and takes 10 iterations and *the proposed MGWO method observed 78.72Watt of global peak power within 5 iterations with a time of 1.5 sec*. In hardware implementation also, the steady-state oscillations were observed in HC whereas GWO takes more time and iterations to achieve GMPP, *so that the proposed MGWO method overcomes problems associated with HC and GWO algorithms in experiment.* The performance results are shown in Figure 3.9. In order to demonstrate the performance of the proposed MGWO algorithm, it is verified with two more shaded patterns of 3S configuration with middle and rightmost peak

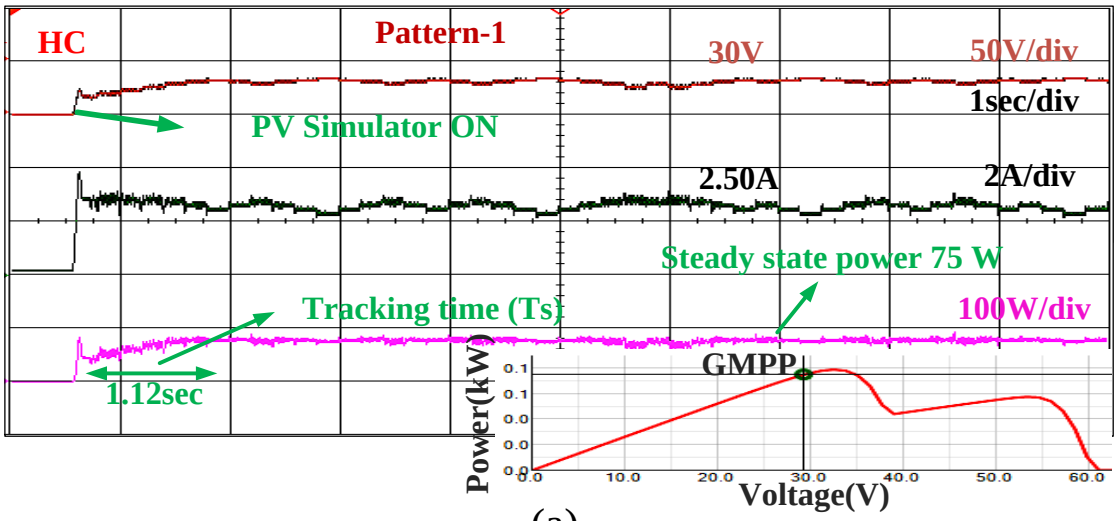

(a)

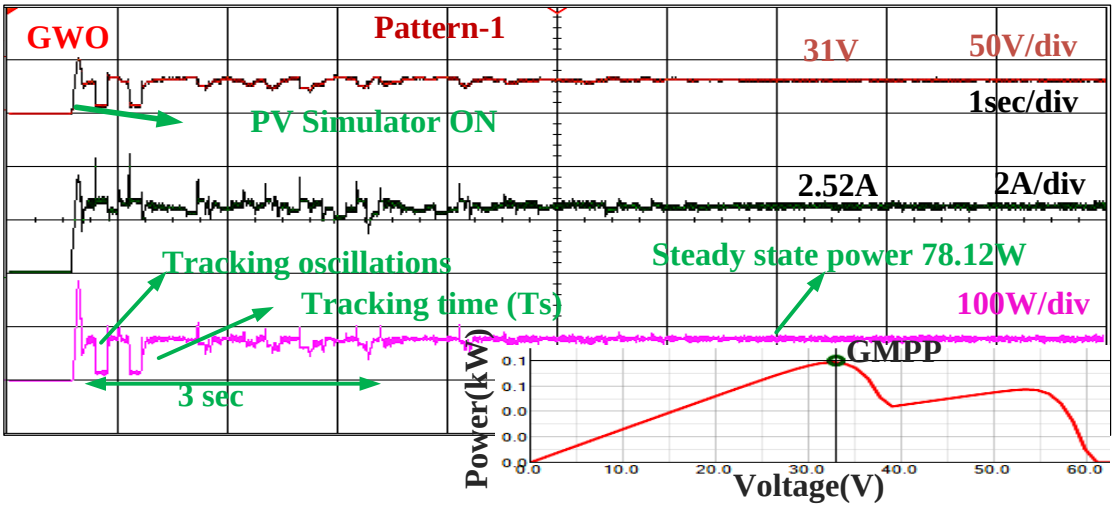

(b)

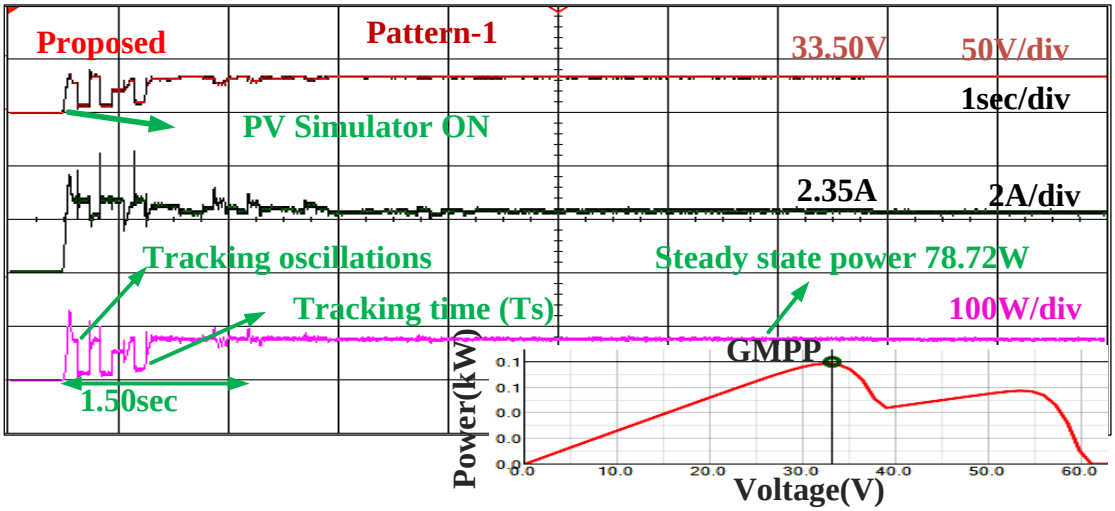

(c)

Figure 3.9 Experimental results for shading pattern-1 of 3S PV array: (a) HC, (b) GWO, and (c) Proposed MGWO algorithm.

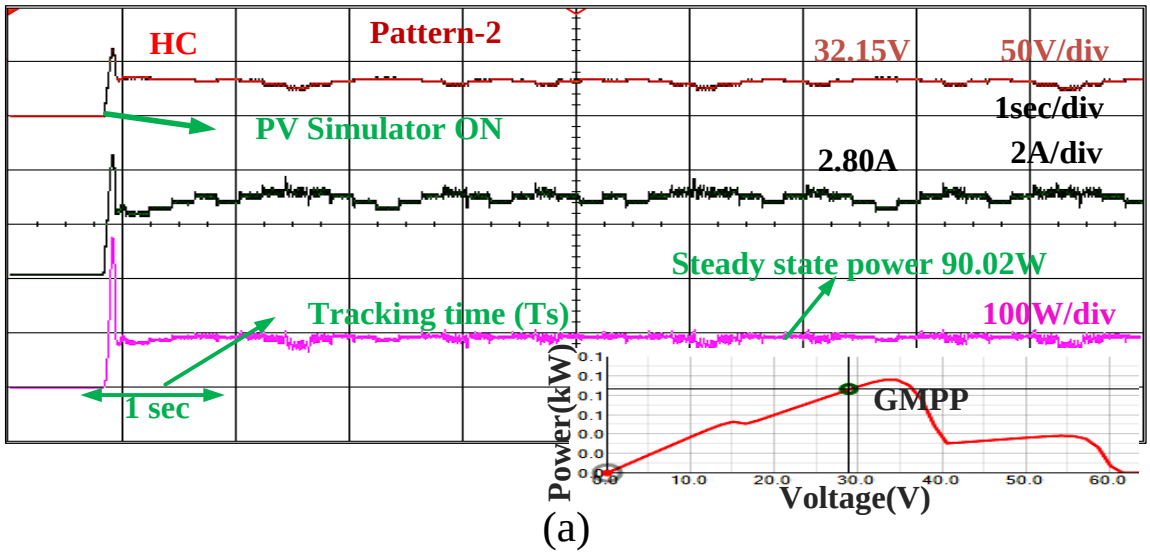

(a)

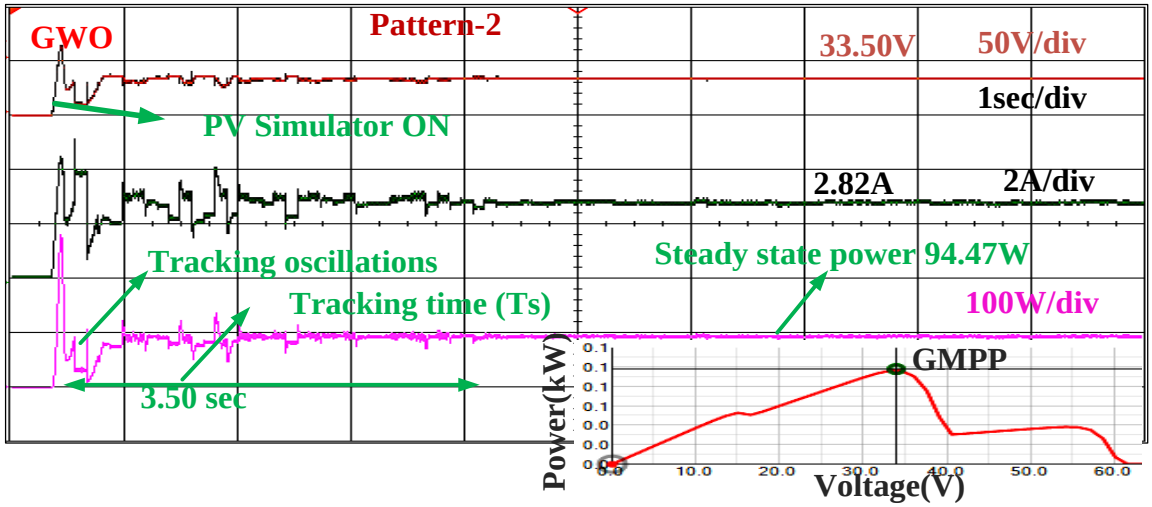

(b)

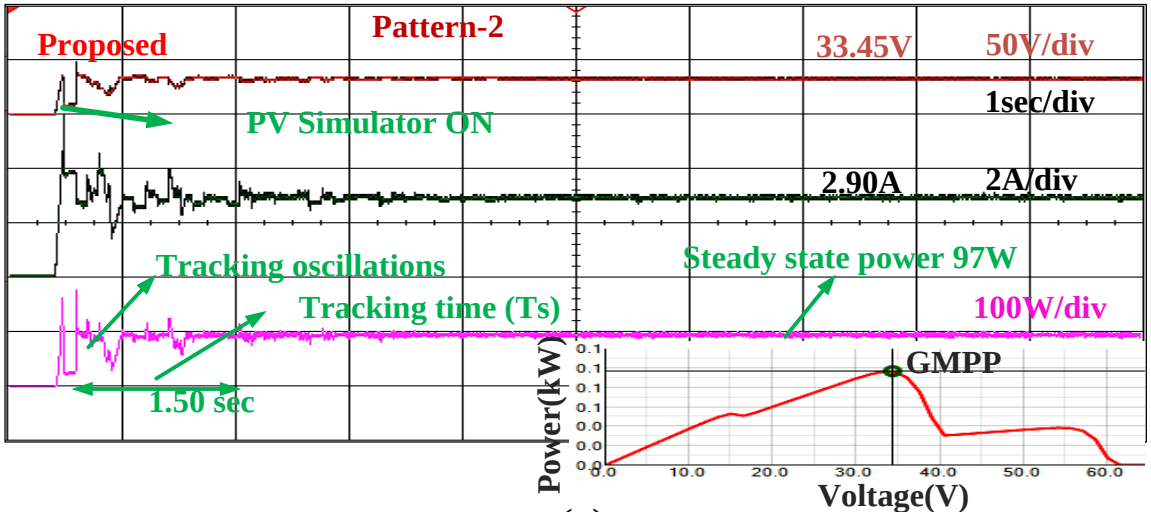

(c)

Figure 3.10 Experimental results for shading pattern-2 of 3S PV array: (a) HC, (b) GWO, and (c) Proposed MGWO algorithm.

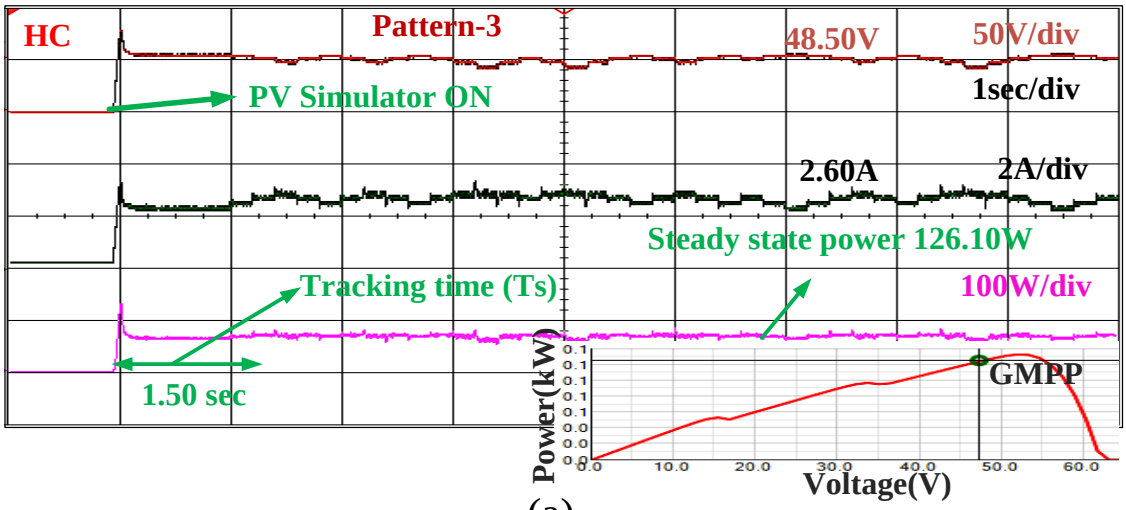

(a)

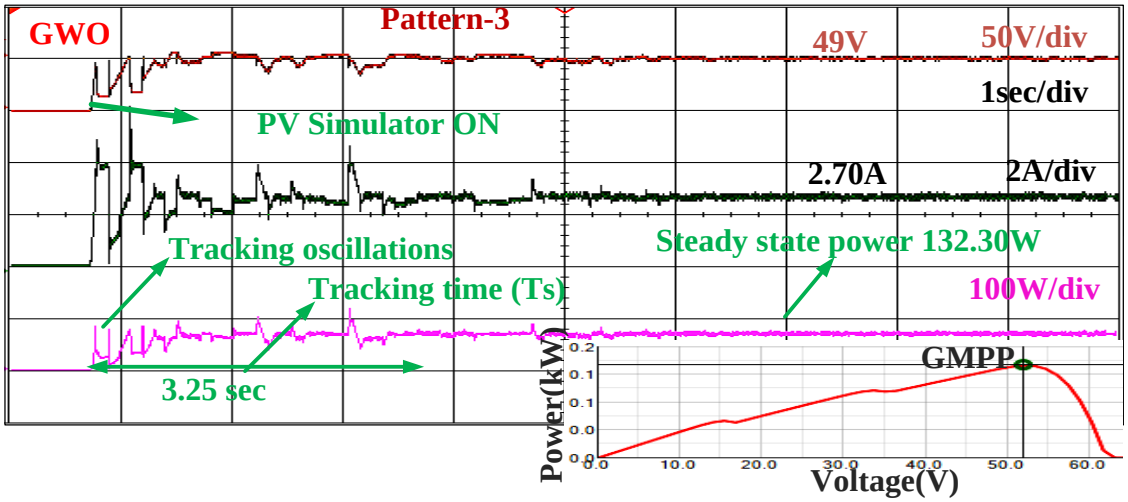

(b)

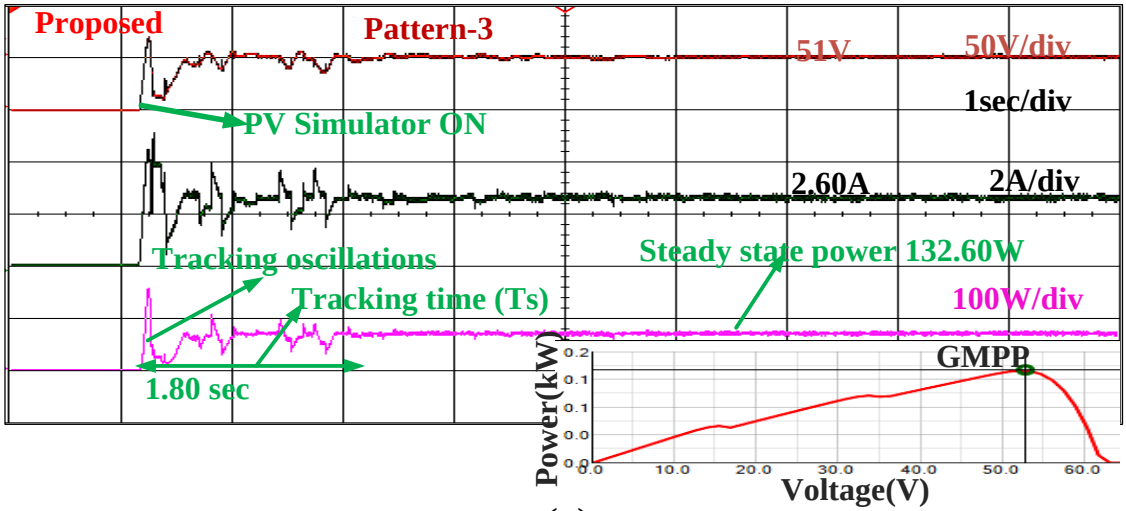

(c)

Figure 3.11 Experimental results for shading pattern-3 of 3S PV array: (a) HC, (b) GWO, and (c) Proposed MGWO algorithm.

as global peak in each P-V characteristic. The advantages of the proposed MGWO algorithm with pattern-2 and pattern-3 as PV source also have minimum tracking time and fewer cycles compared to HC and GWO methods; the related waveforms are presented in Figures 3.10 & 3.11 and the corresponding obervations are presented in Table 3.5.

Experimental Results of Pattern-1 and Pattern-2 during Dynamics: To test the proposed MGWO algorithm with a sudden change of one shading pattern to another shading pattern at a particular period is also observed in Figure 3.12. The proposed MGWO alorithm tracks global power (78.72Watt) with minimum tracking time of 2 sec where as GWO takes 4 sec with a power of 78.12Watt when pattern-1 is acting as PV source under PSC, then maintains constant power as global power and at 12.5 sec PV source changes to pattern-2; the proposed MGWO algorithm has to re-initilize the parameter and track new global power (97Watt) according to pattern-2 with less tracking time of 2 sec where as GWO takes 3.5 sec to reach 94.47Watt power. In the dynamic case also proposed MGWO algorithm compared with GWO and HC algorithms as shown in Figure 3.12.

3.5.2 Experimental Results of 4S2P PV Array Configuration

In this configuration, the complexity of PV source is increased compared to 3S configuration and also multiple peaks present in P-V characteristics. Based on 4S2P PV array, three shaded patterns are considered and the power observed by HC algorithm of pattern-4 is 104.40 Watt with a time of 1.25 sec; the global peak power observed by GWO algorithm is 108Watt with a time of 3.37 sec along with 11 iterations, *whereas the proposed MGWO algorithm converges to global peak power 108.67Watt with 7 iterations along with minimum tracking period of 2.12 sec*. In this case also the proposed MGWO algorithm outerperforms GWO and HC algorithms, its results of pattern-4 are shown in Figure 3.13. Similarly pattern-5 and pattern-6 are performed to show the effectiveness of the proposed MGWO algorithm for different shading conditions; these overcome problems faced by conventional HC and GWO algorithms, and the corresponding results are in Figures 3.14 & 3.15 and the observation are presented in Table 3.5.

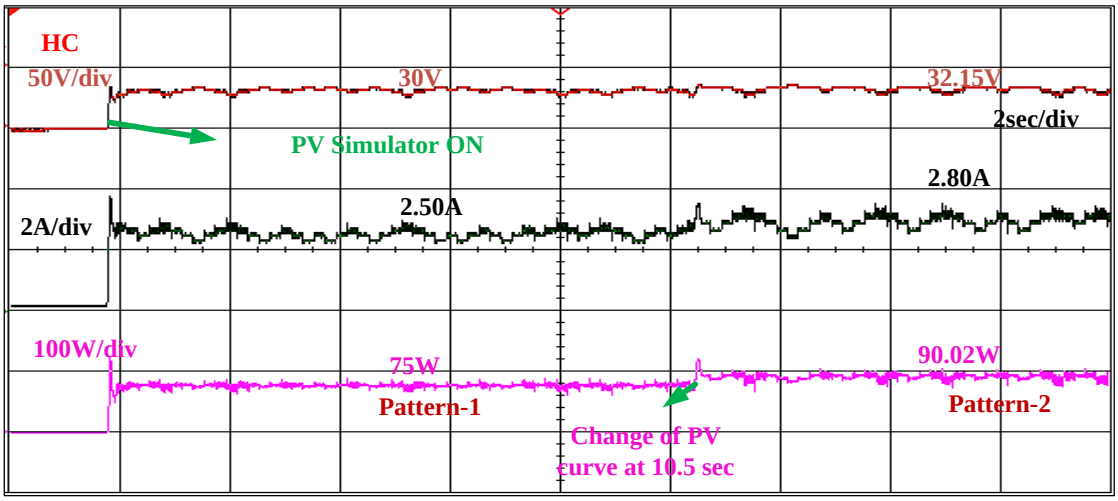

(a)

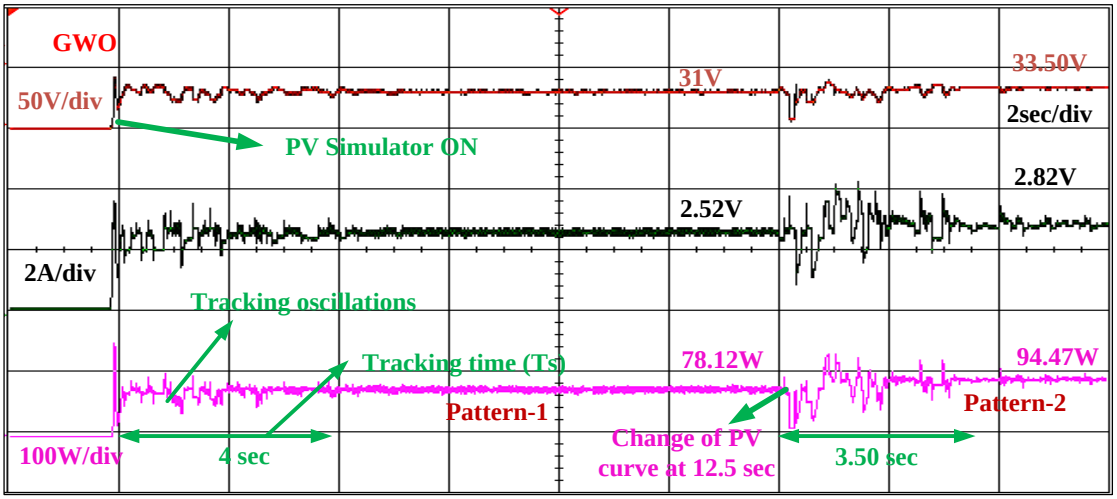

(b)

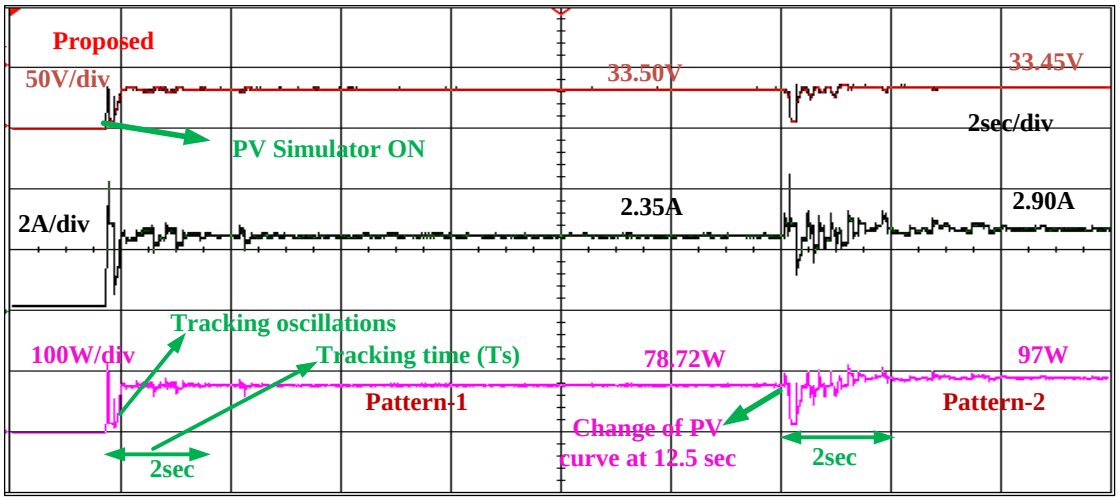

(c)

Figure 3.12 Experimental results during dynamics of shading pattern-1, and shading pattern-2 of 3S PV array of: (a) HC, (b) GWO, and (c) Proposed MGWO algorithm.

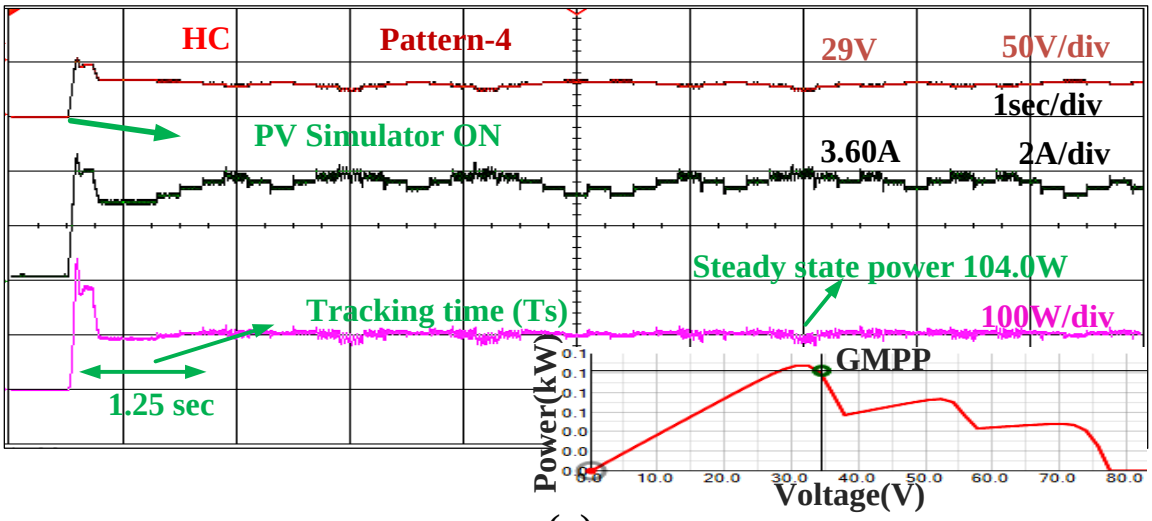

(a)

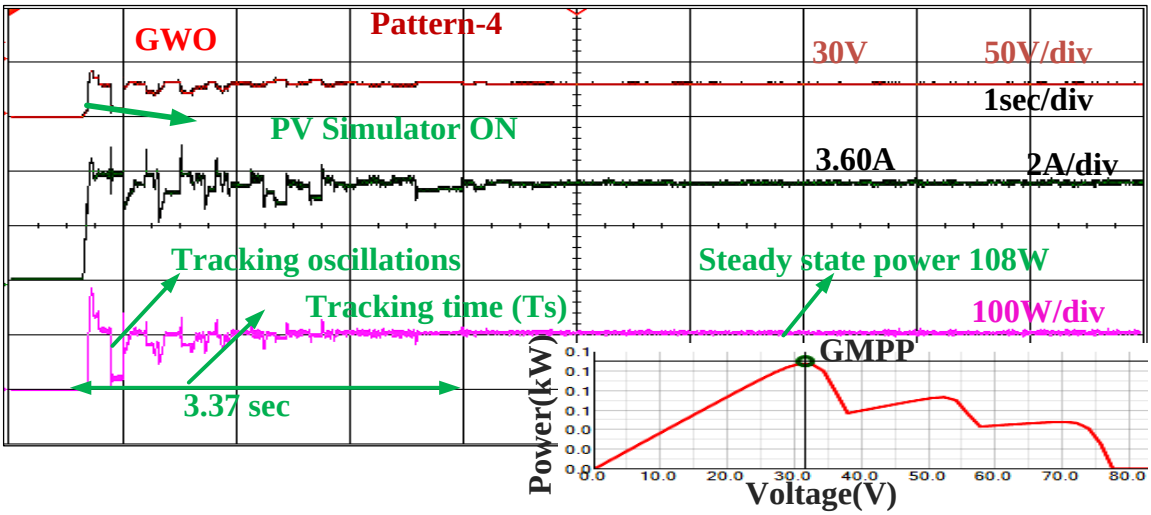

(b)

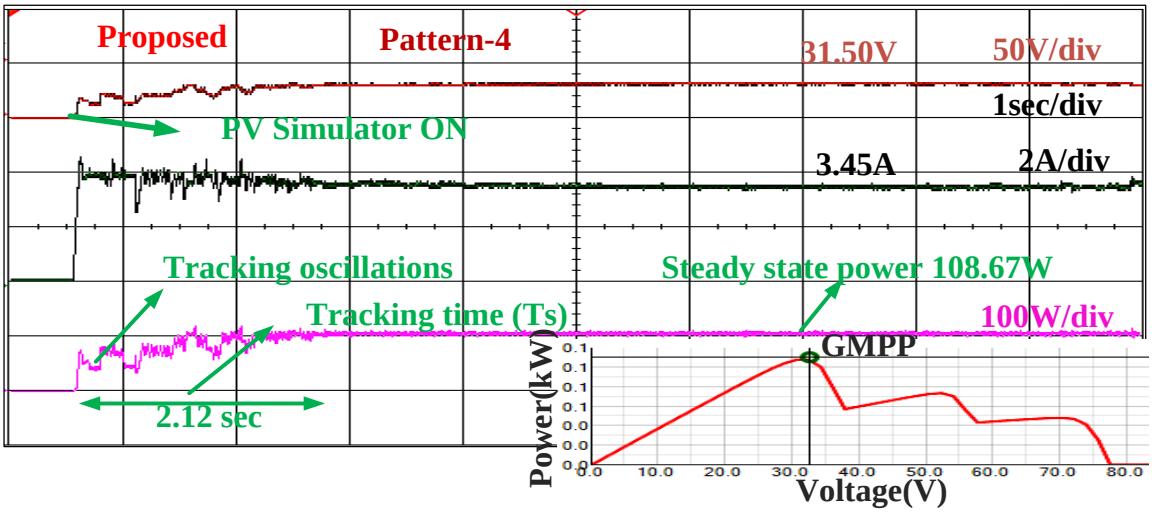

(c)

Figure 3.13 Experimental results for shading pattern-4 of 4S2P PV array: (a) HC, (b) GWO, and (c) Proposed MGWO algorithm.

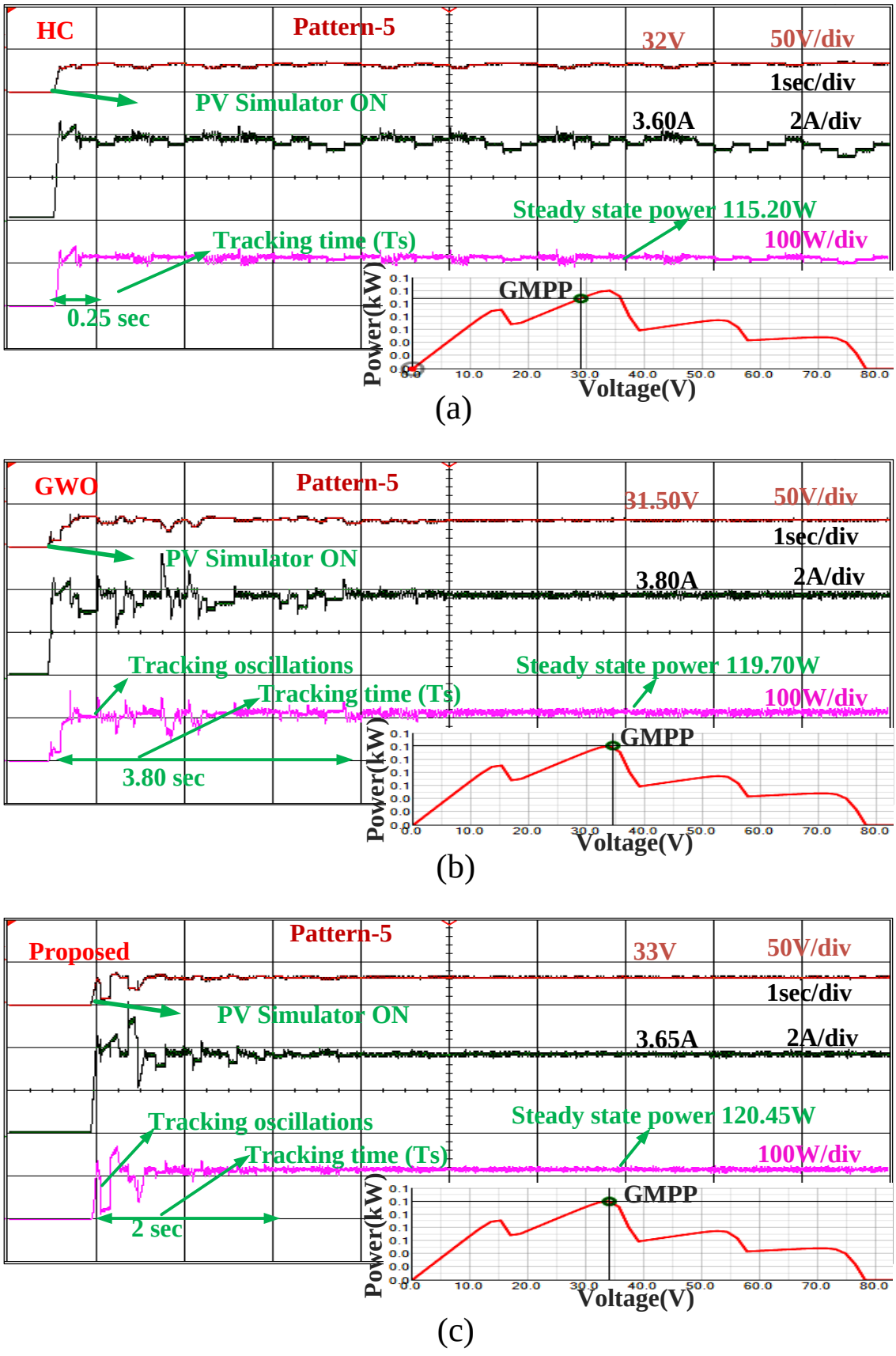

Figure 3.14 Experimental results for shading pattern-5 of 4S2P PV array: (a) HC, (b) GWO, and (c) Proposed MGWO algorithm.

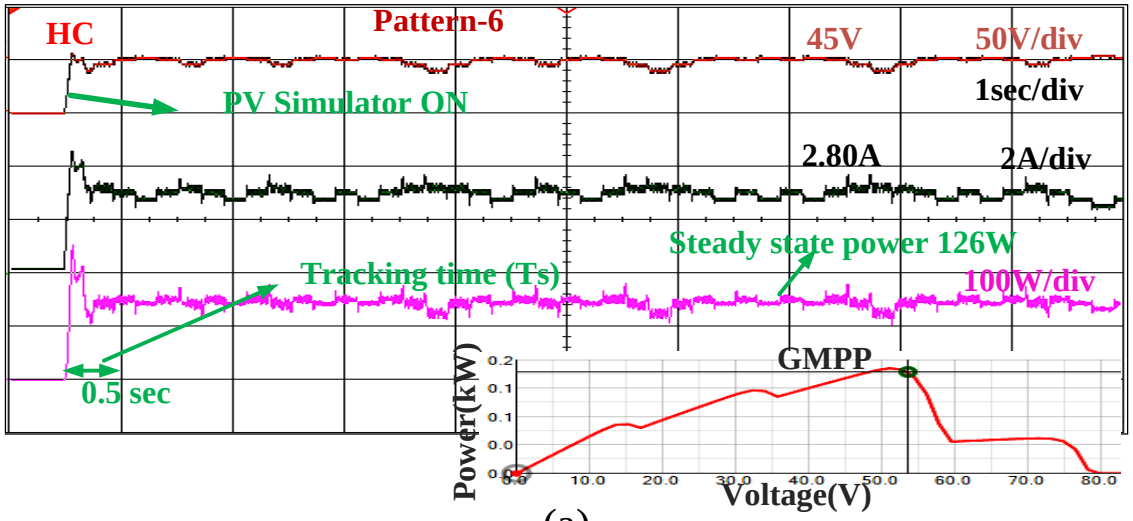

(a)

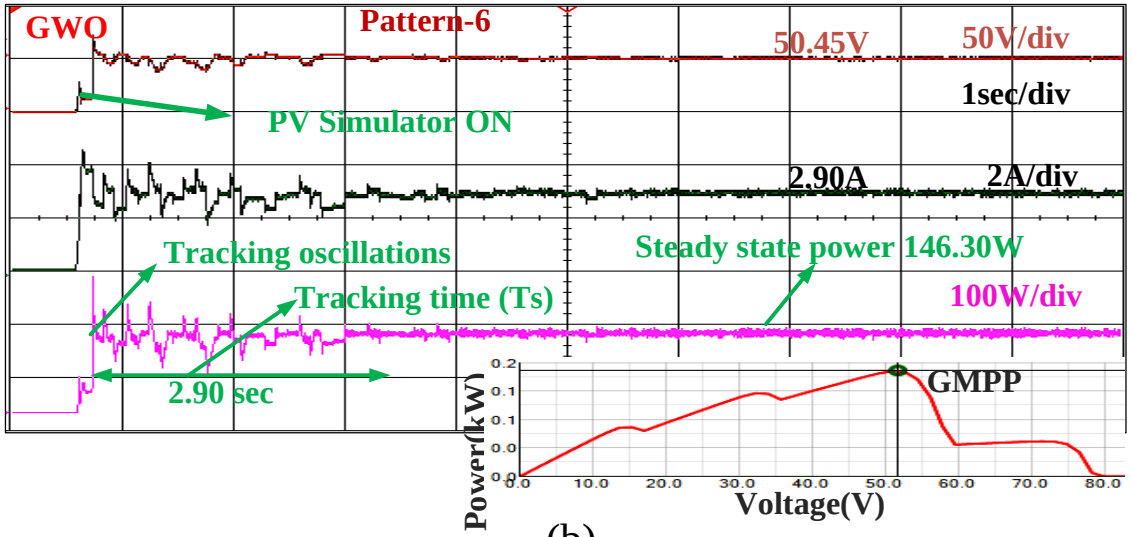

(b)

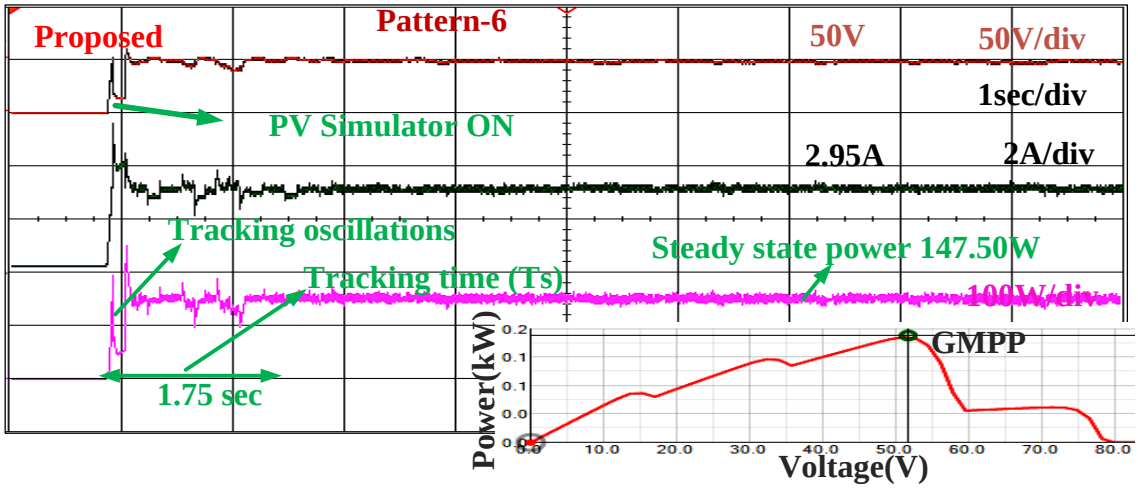

(c)

Figure 3.15 Experimental results for shading pattern-6 of 4S2P PV array: (a) HC, (b) GWO, and (c) Proposed MGWO algorithm.

Table 3.5 Experimental performance analysis of 3S, and 4S2P PV array configurations

Method	**Rated Power (Watt)**	**Extracted Power from PV (Watt)**	**Voltage from PV (Volt)**	**Current from PV (Amp)**	**Tracking Time (Sec)**	**Iterations**	**Tracking Efficiency (%)**
Proposed	79.42 Pattern-1	78.72	33.50	2.35	**1.50**	**05**	99.11
GWO		78.12	31.00	2.52	3.00	10	98.36
HC		75.00	30.00	2.50	1.12	-	94.43
Proposed	97.21 Pattern-2	97.00	33.45	2.90	**1.50**	**05**	99.78
GWO		94.47	33.50	2.82	3.50	12	97.18
HC		90.02	32.15	2.80	1.00	-	92.60
Proposed	133.23 Pattern-3	132.60	51.00	2.60	**1.80**	**06**	99.52
GWO		132.30	49.00	2.70	3.25	11	99.30
HC		126.10	48.50	2.60	1.50	-	94.64
Proposed	108.93 Pattern-4	108.67	31.50	3.45	**2.12**	**07**	99.76
GWO		108.00	30.00	3.60	3.37	11	99.14
HC		104.40	29.00	3.60	1.25	-	95.84
Proposed	120.80 Pattern-5	120.45	33.00	3.65	**2.00**	**07**	99.71
GWO		119.70	31.50	3.80	3.80	12	99.08
HC		115.20	32.00	3.60	0.25	-	95.36
Proposed	148.71 Pattern-6	147.50	50.00	2.95	**1.75**	**06**	99.18
GWO		146.30	50.45	2.90	2.90	08	98.37
HC		126.00	45.00	2.80	0.50	-	84.72

3.6 Comparative Study of Proposed MGWO Algorithm with Existing Algorithms

The proposed MGWO algorithm finds GMPP with fewer iterations, less tracking period and minimum oscillations around global peak compared to conventional GWO and HC. The conventional GWO algorithm have delay in convergence process due to poor exploration process; also it is not performed with re-initialization of parameters under dynamic case [29]. Whereas the proposed MGWO algorithm implemented with modified updated-position along with nonlinear decreasing nature of control paramerter ($\vec{a}$) is used for fast convergence process and also performed with re-initialization under dynamic conditions. The change of step size is difficult under dynamic coditions and PSC in HC algorithm [5]. The comparison of power, tracking time, efficiency and iterations with respect to the number of patterns is shown in Figure 3.16. The PSO algorithm implemented for GMPP with three tuning parameter and five initial particles, takes more number of iterations to reach globla peak power [20]. Adaptive Radial Movement Optimization (ARMO) algorithm reaches global

peak with low tracking period but is implemented with three tuning parameter and initial particles are greater than five, which are dependent on PV voltage [33]. Hybrid GWO-P&O tracks global power fast but not re-initialized the parameter during change of PV shaded patterns [79]. Modified Particle Velocity-based Particle Swarm Optimisation (MPV-PSO) algorithm tracks fast with the removal of tuning of weight factor, while cognitive factors are in tune with current particle, and initial particles are dependent [24]. Hybrid GWO and Fuzzy Logic Controller (FLC) (GWO-FLC) algorithm is implemented with higher power ratings with different re-initialization methods by considering an average of 5 to 10 grey wolves as a population [30]. Due to higher number of initial particle the computational burden on the system is increased in each iteration. The comparison of these algorithms are presented in Table 3.6 and the experimental performance of the proposed MGWO algorithm over GWO and HC algorithms is presented in Table 3.6.

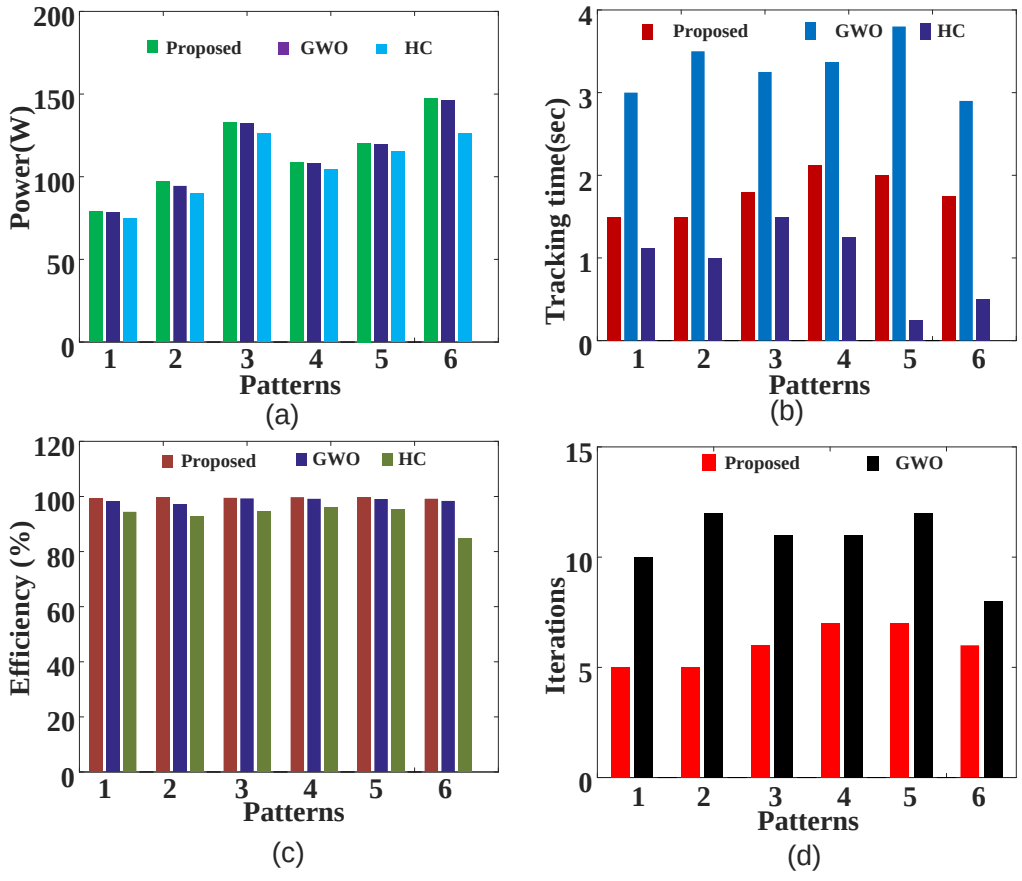

Figure 3.16 Experimental results comparison of proposed MGWO algorithm with GWO, and HC algorithms: (a) Power, (b) Tracking time, (c) Efficiency, and (d) Iterations with respect to each shading pattern.

Table 3.6 Qualitative comparison of the proposed MGWO algorithm with existing MPPT algorithms

Parameters/ Method	**PSO [20]**	**ARMO [33]**	**GWO [29]**	**GWO-P&O [79]**	**MPV-PSO [24]**	**GWO-FLC [30]**	**Proposed**
Tracking time	Moderate	Less	Moderate	Less	Less	Less	**Less**
Iterations	More	Less	Moderate	Less	Less	Less	**Less**
Tuning parameters	3	3	1	1	2	1	**1**
Initial duties	Independent	Dependent	Independent	Independent	Dependent	Independent	**Independent**
Population size	5	Greter than 5	3	3	3	Greter than 5	**3**
Re-initialization	Considered	Considered	Not considered	Not considered	Considered	Considered	**Considered**

3.7 Results and Conclusions

This chapter proposed a novel GMPP tracking algorithm for shaded conditions of PV array. The proposed MGWO algorithm enhances existing Grey Wolf optimization (GWO) algorithm by using modified updated-position and nonlinear decreasing nature of control paramerter $(\vec{a})$ to enhance fast convergence. *The proposed algorithm (MGWO) tracks the global peak (GP) power under shaded condition of PV array with reduced number of iterations and less tracking period. The steady-state oscillations also reduced around global peak point successfully with only one tuning control parameter; initial duties are not dependent on PV system.* To highlight the proposed method detailed comparison with conventional GWO and HC algorithms are presented. The proposed MGWO method demonstrated better performance than conventional GWO and HC methods and can track GP with any shading condition of PV pattern, outperformed even in dynamic shaded conditions and offered high efficiency. This proposed MGWO algorithm implemented with only one tuning of control parameter $(\vec{a})$. Due to tuning of parameter, during search process it was unable to find optimum value through a course of iterations, which results in delay in convergence and influence on exploitaion process. The tuning nature is removed in next chapters.

Chapter 4

GMPPT using PSO based on Lévy Flight for Photovoltaic System under Partial Shading Conditions

Chapter 4

GMPPT using PSO based on Lévy Flight for Photovoltaic System under Partial Shading Conditions

4.1 Introduction

The adaptive control parameters, cannot be tuned exactly through a course of iteration which creates delay in convergence factor. Based on this information, proposes a Velocity of PSO based on Lévy Flights (VPSO-LF) algorithm for tracking GMPP under partial shading conditions (PSC) of PV array. In conventional PSO, the velocity is updated randomly and with more tuning parameters, which shows slow search process. Due to this, convergence time and iterations increase before reaching steady-state position and the algorithm also possesses more tracking oscillations. But in the proposed VPSO-LF algorithm, step size (velocity of PSO) is updated by Lévy Flights (LF) instead of determining velocity randomly. This would increase search efficiency and reduce convergence time of GMPPT with fewer iterations, less transient and steady-state oscillations, initial duty independent of the PV system and no need of the tuning the parameters. The proposed VPSO-LF algorithm is tested along with conventional PSO and HC to validate the results under static and re-initialization of parameters during dynamic cases. The proposed VPSO-LF technique is simulated in MATLAB/SIMULINK as well as experimentally validated and followed by comparison with existing optimization techniques.

4.2 GMPPT Methods

4.2.1 GMPPT through Hill Climbing algorithm

Hill Climbing (HC) is a conventional MPPT and most commonly adopted method because of its simplicity and low cost. The algorithm provides direct duty cycle [5] to the boost converter. Based on this, maximum power can be observed at the output of the PV array. The conventional methods are available in the literature [5]-[14]. The duty cycle (d) of HC is changed by perturbation size 'θ'. The step size is dependent on the change of maximum power by the following equations

$$d_{new} = d_{old} + \theta \quad if \quad P > P_{old} \tag{4.1}$$

$$d_{new} = d_{old} - \theta \;\; if \;\; P < P_{old} \tag{4.2}$$

where d_{new} and d_{old} are the present and previous duty cycles, P and P_{old} are the present and previous powers. An advantage of this algorithm is that there is no requirement of any P or PI controller for pulse generation to control duty ratio of boost converter.

4.2.2 GMPPT through PSO algorithm

Eberhart and James proposed a Particle Swarm Optimization (PSO) algorithm in 1995 [63]. This optimization method has been used for the purpose of control to locate global peak where it was first applied for MPPT in PV system [64]. The PSO is a population based evolutionary algorithm, modelled on the behavior of bird flocks. The PSO algorithm maintains a swarm of individuals i.e., particles, where each particle is appointed to act as a solution of a candidate. These particles follow a set behavior to emulate the success of neighboring particles and their own to achieve success. The particle position is affected by the best particle in the neighborhood, i.e., P_{besti}. The global best particle is created by all the particles in the whole population denoted as G_{best}.

The particle position X_i^k is updated as

$$X_i^{k+1} = X_i^k + \theta_i^{k+1} \tag{4.3}$$

where the component of velocity (θ_i^k) represents the perturbation size. The velocity (θ_i^k) is updated as follows:

$$\theta_i^{k+1} = w\theta_i^k + C_1R_1[P_{besti} - X_i^K] + C_2R_2\left[G_{best} - X_i^k\right] \tag{4.4}$$

$$w = w_{max} - \left(\frac{iter}{itermax}\right)(w_{max} - w_{min})$$

$$C_1 = C_{1,max} - \left(\frac{iter}{itermax}\right)\left(C_{1,max} - C_{1,min}\right)$$

$$C_2 = C_{2,max} - \left(\frac{iter}{itermax}\right)\left(C_{2,max} - C_{2,min}\right)$$

where w is the inertia weight, w_{max} and w_{min} are maximum and minimum values of inertia weight; C_1 and C_2 are the acceleration coefficients, $C_{1,max}$ and $C_{1,min}$ are maximum and minimum values of C_1, $C_{2,max}$ and $C_{2,min}$ are maximum and minimum values of C_2; R_1 and R_2 are random numbers, $R_1 \& R_2 \in U(0,1)$, P_{besti} is personal best position of particle i, and G_{best} is the optimum position of the particle in the whole population; *iter* is present iteration number and *itermax* is the maximum number of iterations.

If position is represented as a duty cycle and the step size is the velocity, then equation (4.3) can be represented as:

$$d_i^{k+1} = d_i^k + \theta_i^{k+1} \tag{4.5}$$

Comparing equations (4.1) and (4.5) HC and PSO, are equivalent.

4.2.3 GMPPT through Proposed VPSO-LF Algorithm

From the literature, it can be observed that the PSO algorithm is employed to keep from slow convergence due to more tuning parameters, but unable to converge best values through a course of iteration [20]. Different algorithms related to an improved PSO are also proposed with updated step size in different forms [21], [23], [24]. But in the proposed method, velocity (step size) can be updated by Lévy Flights (LF) which is the same as standard PSO. Initial duty cycles (particles) are randomly taken within a range, and fitness (power) value is evaluated for each particle (duty cycle). So the presence of random numbers in velocity equation as shown in equation (4.4) makes good for exploration process but poor exploitation process due to tuning of ($w, C_1\ and\ C_2$) parameters. The presence of tuning parameters make the PSO unable to find optimum values through the course of iteration, which makes causes delay in convergence. Here several simulations are conducted by varying (trial and error process) the parameters and optimal solutions are at $w = 0.4, C_1 = 1.6, and\ C_2 = 1.8$. In proposed method, velocity (step size) of PSO can be updated by Lévy Flights, called VPSO-LF, for better search process using the following equation:

$$\theta_i^{t+1} = w \times Levy_{walk}(X_i^t) + C_1 R_1\left(P_{besti} - X_i^t\right) + C_2 R_2\left(G_{best} - X_i^t\right) \tag{4.6}$$

Updated position shown below,

$$X_i^{t+1} = X_i^t + \theta_i^{t+1} \tag{4.7}$$

By updating the velocity with Lévy Flights, the particle takes a small steps and searches for P_{best} and G_{best}, thereby intensifying the variation of the swarm and facilitating the algorithm to accomplish global exploitation search throughout the space. Lévy flights are random walks. There are two steps for the production of random numbers with lévy flight, i.e., the selection of random direction and the production of steps which obey the chosen lévy distribution [80]-[84]. Random walks are taken from lévy stable distribution. The simple formula for power-law $(s) \sim |s|^{-1-\beta}$, where $0 < \beta < 2$ is an index. Mathematically, lévy distribution can be defined as,

$$L(s,\gamma,\mu) = \begin{cases} \sqrt{\frac{\gamma}{2\pi}} \quad exp\left[-\frac{\gamma}{2(s-\mu)}\right] \frac{1}{(s-\mu)^{3/2}} & , \ 0 < \mu < s < \infty \\ 0 & otherwise, \end{cases} \tag{4.8}$$

where μ is a parameter location, $\gamma > 0$ is parameter scale and s is step length.

In general, lévy distribution can be specified in the form of a Fourier transform,

$$F(k) = exp\left[-\alpha|k|^{\beta}\right], \quad 0 < \beta \leq 2 \tag{4.9}$$

where α is a parameter among [-1, 1] interval, and recognised as skewness or scale factor, k is distribution varible. Stability index β ∈ (0, 2) is considered as lévy index.

In this study, Lévy Flights (LF) are applied to each variable of the present iteration using the following equation:

$$Levy\ walk\left(X_i^k\right) = \ step\ size \tag{4.10}$$

where

$$step\ size = 0.01 \times step \times \left(X_i^k \ - \ P_{best}\right) \tag{4.11}$$

The factor 0.01 comes from the fact that *step*/100 should be the typical *step size* of walks where *step* is a typical length scale; otherwise, Levy flights may become too aggressive, which makes new solutions jump out side of the design domain (and thus wasting evaluations). For random walk, the value of *step* can be calculated by Mantegna's algorithm as:

$$step = \frac{u}{|v|^{1/\beta}} \tag{4.12}$$

Here β plays an important role in distributions and 1.5 is chosen as the optimum value for β [84]. The other two parameters u and v are drawn from normal distributions with standard deviation σ_u and σ_v given by:

$$u \sim N(0, \sigma_u^2), \quad v \sim N(0, \sigma_v^2)$$

where

$$\sigma_u = \left(\frac{\Gamma(1+\beta) \times \sin(\pi \times \beta/2)}{\Gamma\left(\left(\frac{1+\beta}{2}\right)\right) \times \beta \times (2)^{\left(\frac{\beta-1}{2}\right)}} \right)^{\frac{1}{\beta}} \text{ and } \ \sigma_v = 1 \tag{4.13}$$

The search area of LF with a small step size is for exploitation process. The step size is updated with a long jump from one area to another area of searching for exploration process as shown in Figure 4.1. Based on this process, the tracking speed is high and takes fewer iterations to track GMPP and the flowchart of proposed VPSO-LF algorithm is shown in Figure 4.2.

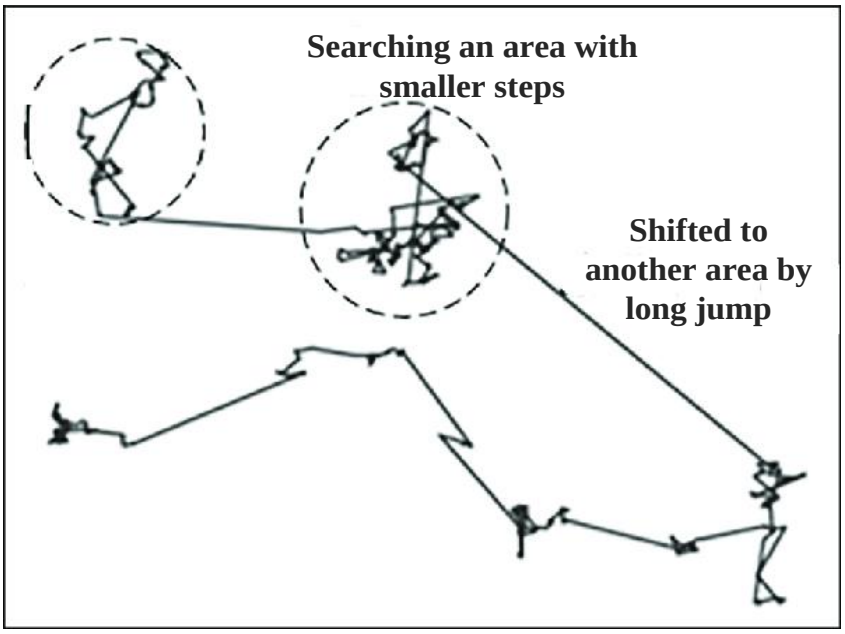

Figure 4.1 Lévy flights distribution in two dimensional plane.

4.2.3.1 Steps to Implement Proposed VPSO-LF Algorithm

Step-1: Initialize the particles at fixed positions between 0.1 and 0.9 of the duty cycle.

Step-2: Measure the power 'P_{pv}' from the output of PV array at each location of particle (duty) by sensing 'V_{pv}' and 'I_{pv}' and corresponding duty cycle to boost converter to ' $P_{pv} = V_{pv} \times I_{pv}$'.

Step-3: Update the best fitness powers.

Step-4: Update global best fitness from best fitness powers.

Step-5: Update the modified updated positions of particles according to equations (4.3), (4.4), (4.6), and (4.7) as per condition given in flowchart Figure 4.2.

Step-6: Repeat steps 2 and 5 till to reach global peak of P-V curve.

Step-7: If any new shading pattern occurs then re-initialize the parameters.

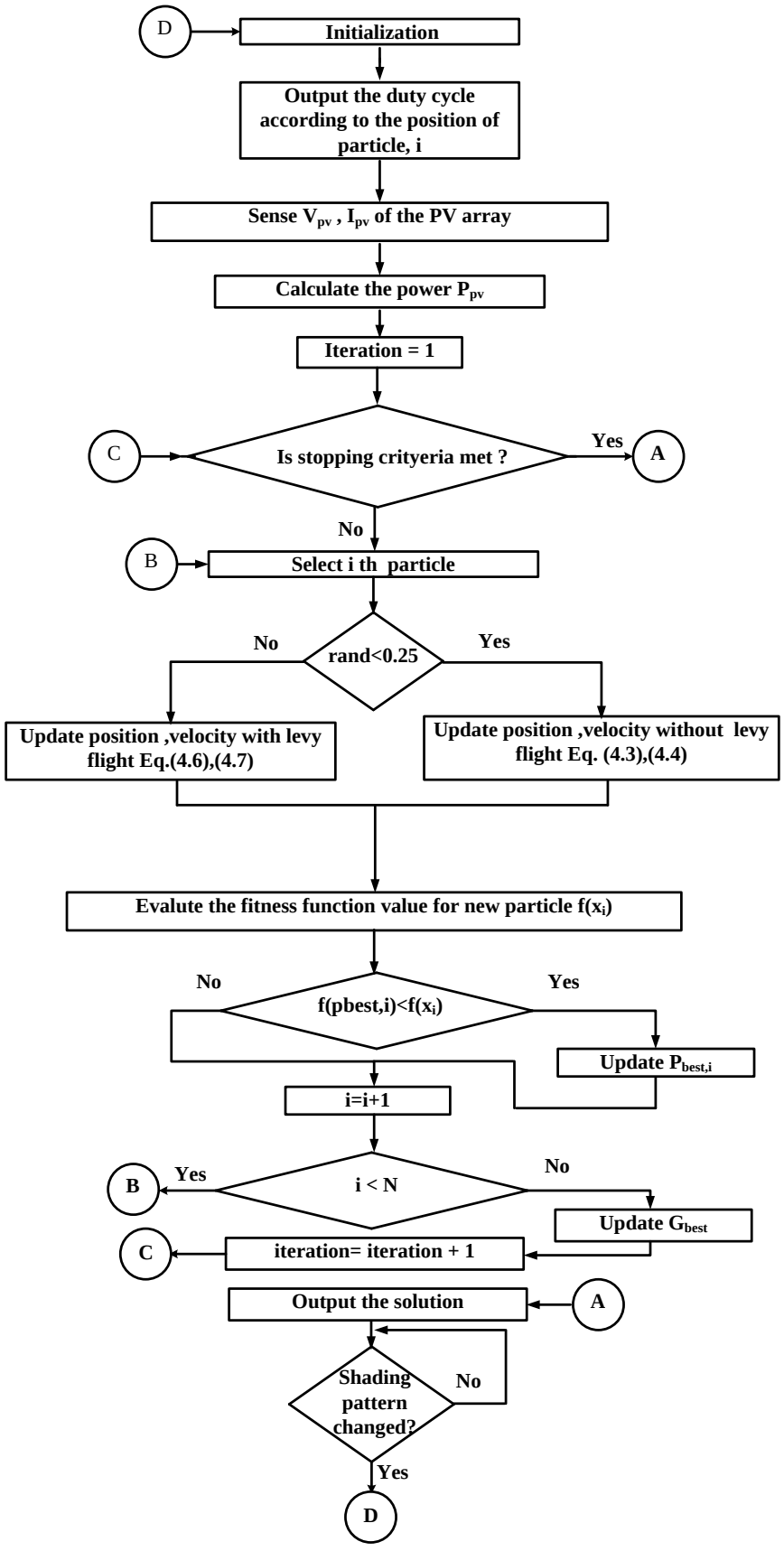

Figure 4.2 Flowchart of proposed VPSO-LF algorithm.

Step-8: The change of PV pattern is recognized by proposed algorithm with the following power equation:

$$\frac{|P_{n+1} - P_n|}{P_n} \geq \delta \tag{4.14}$$

Term $\boldsymbol{P_n}$, $\boldsymbol{P_{n+1}}$ are present and future power output of PV system, δ (percentage change of power) is considered as 2% [78].

4.3 The Solar PV Array under Partial Shaded Condition

The proposed VPSO-LF algorithm can be verified with three different PV array configurations. The three PV arrays are formed by connecting three PV modules in series (3S), four PV modules in series (4S) and six PV modules in series (6S) as shown in Figure 4.3 and the P-V characteristics are shown in Figure 4.4. The module irradiance level (data) of each PV array pattern is presented under partial shaded conditions (PSC) in Table 4.1 and Each PV module is designed for 60W, which is shown in Table 3.1 in Chapter 3.

Table 4.1 Irradiance (W/m^2) of each module in PV array configuration

Module (M)	**Pattern -1**	**Pattern -2**	**Pattern -3**	**Pattern -4**	**Pattern -5**	**Pattern -6**	**Pattern -7**	**Pattern -8**
M-I	1000	1000	800	1000	1000	1000	1000	1000
M-II	400	600	600	700	900	900	1000	1000
M-III	200	300	500	600	800	900	600	900
M-IV	-	-	-	-	400	400	600	700
M-V	-	-	-	-	-	-	300	400
M-VI	-	-	-	-	-	-	300	300

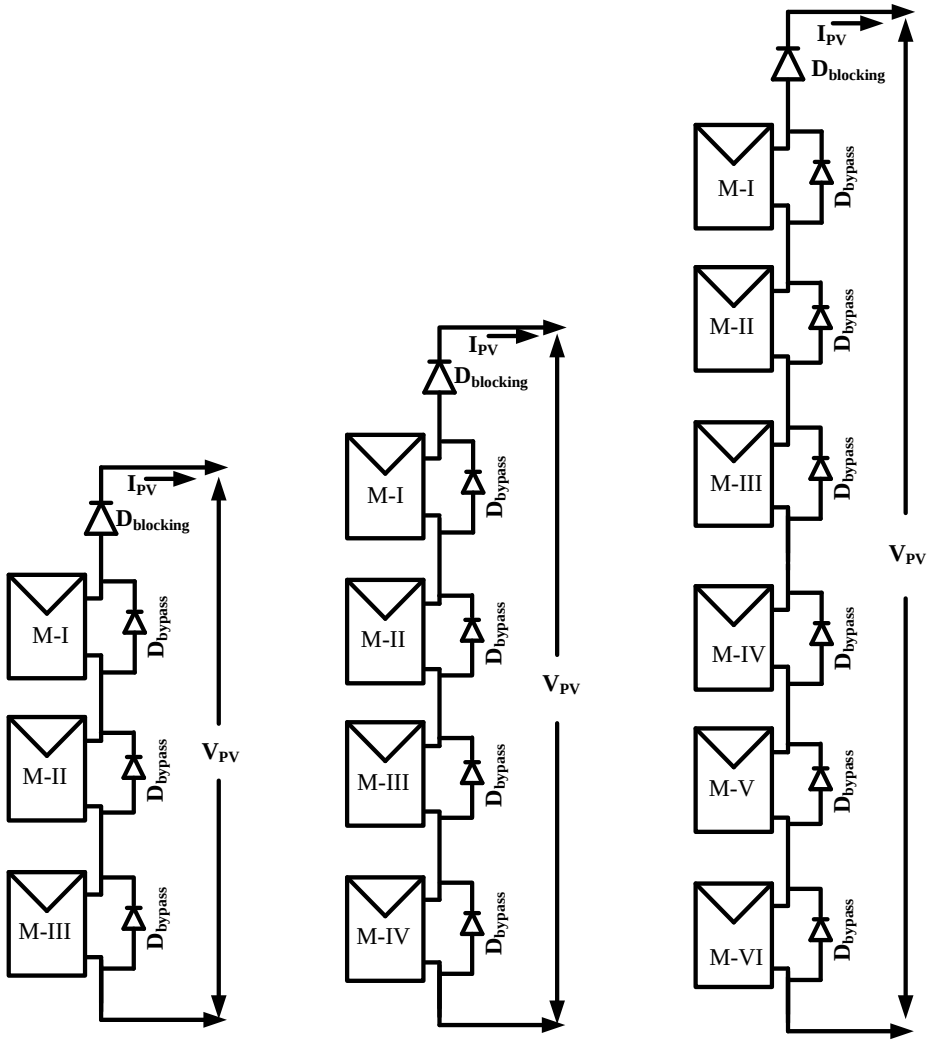

Figure 4.3 The PV array configurations under partial shading conditions: (a) Three PV modules in series (3S), (b) Four PV modules in series (4S), and (c) Six PV modules in series (6S).

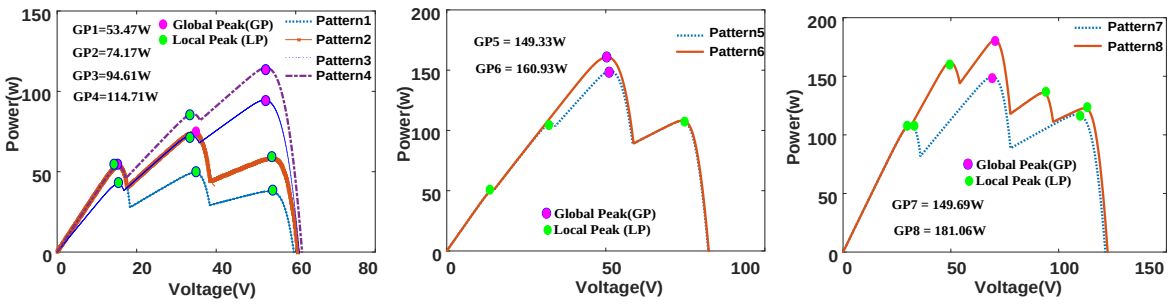

Figure 4.4 The PV array characteristics under partial shading conditions: (a) 3S, (b) 4S, and (c) 6S.

4.4 Simulation Results

The Schematic diagram of boost converter to PV application is shown in Figure 4.5. The simulation studies are performed by using the proposed VPSO-LF algorithm for GMPPT in MATLAB/SIMULINK for eight possible cases (patterns) of PSCs. In each PSC case, PV modules are connected in a series called PV array pattern as in Figure 4.3. These patterns are one left most peak, one middle peak and two rightmost peaks of PV array of 3S configuration, second and third from the left side of P-V curve of 4S configuration and two middle peaks of P-V curve of 6S configuration as shown in Figure 4.4. Initialization particles of VPSO-LF and PSO called duty cycle of boost

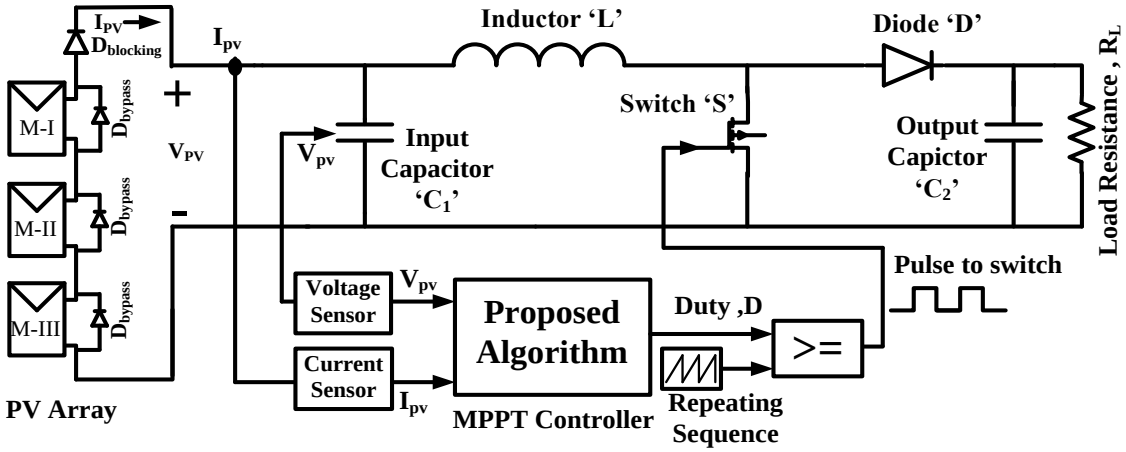

Figure 4.5 Application of PV array to boost converter with MPPT controller.

Table 4.2 Designed parameters of algorithms and boost converter

Particulars	Specifications
VPSO − LF	$w = 0.4, C_1 = 1.6, C_2 = 1.8,$ $\beta = 1.5, K = 0.01.$ $Population\ size = 3$
PSO	$C_{1,min} = 1\ , C_{1,max} = 2,$ $C_{2,min} = 1, C_{2,max} = 2,$ $w_{min} = 0.1,\ w_{max} = 1,$ $Population\ size = 3.$
HC	$D_{initial} = 0.7\ , \theta = 0.035$
Boost coverter	$L = 1.928mH, C_1 = C_2 = 100\mu F,$ $F_s = 10kHz, Diode - MUR860,$ $MOSFET - IRFP460,$ $240V\ 20A\ Variable\ Resistive\ load$
$Sampling\ period\ (T_s)$	$For\ simulation\ T_s = 50ms,$ $For\ experimental\ T_s = 200ms.$

converter were three $x_1 = 0.2, x_2 = 0.3$ and $x_3 = 0.7$, (x_1 , x_2 *and* x_3 are initial population) other designed parameters of algorithms and boost converter are shown in Table 4.2.

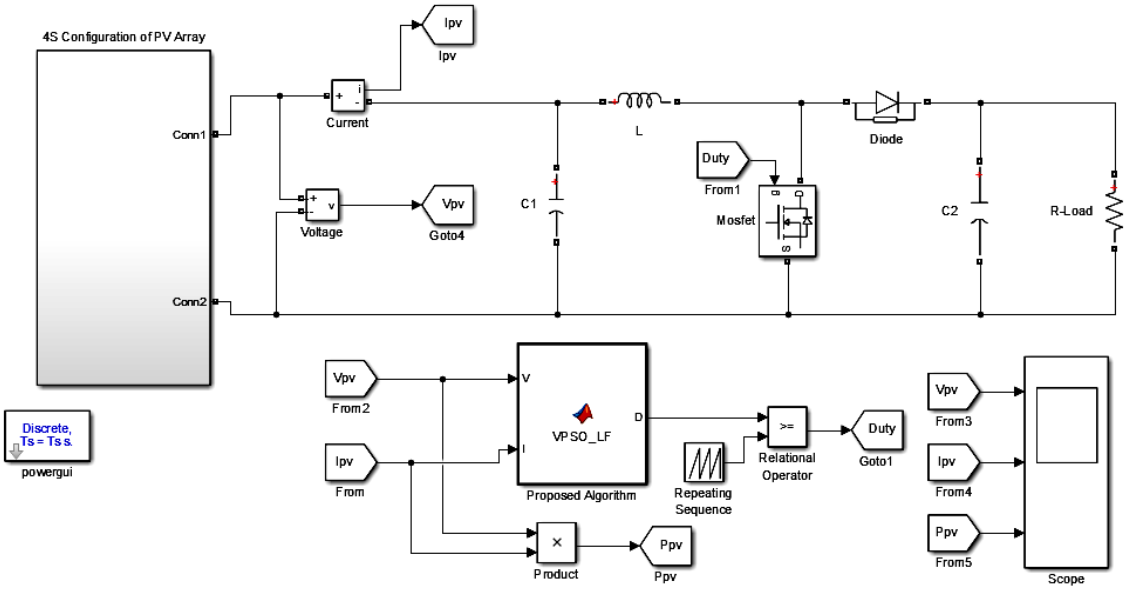

(a)

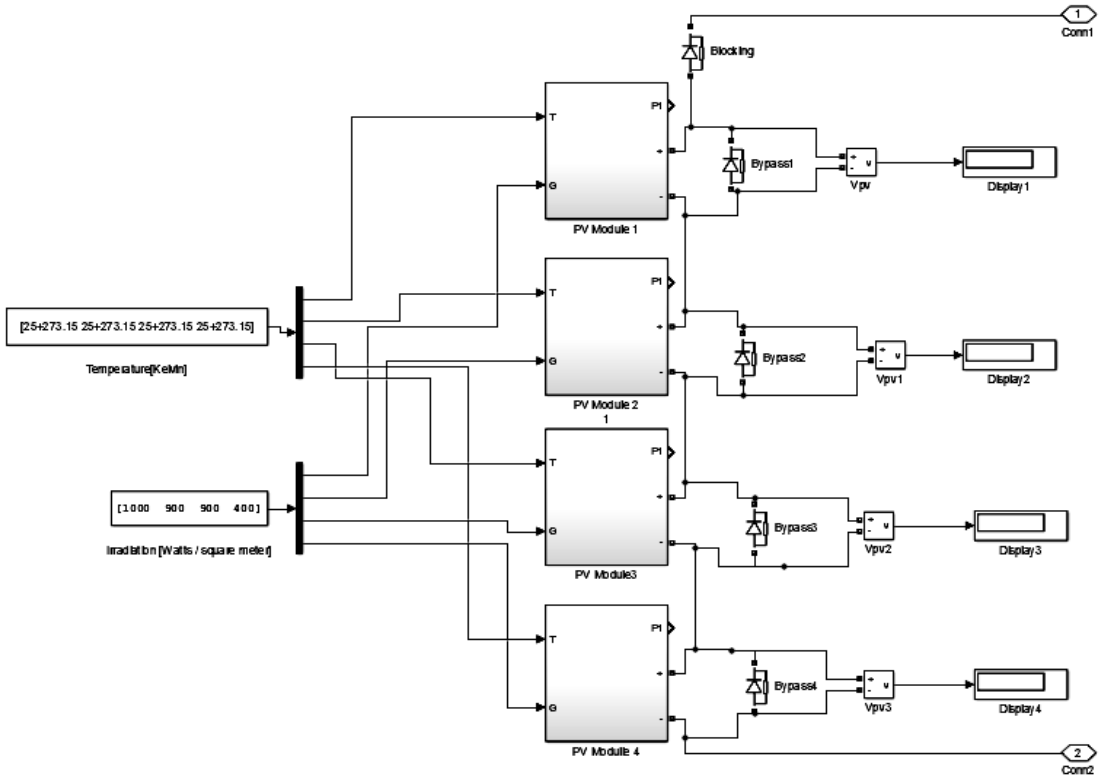

(b)

Figure 4.6 Simulink model of: (a) The proposed VPSO-LF algorithm, and (b) Series connection of PV modules.

The Simulink model of the proposed system of PV array connected to boost converter is shown in Figure 4.6 (a) and the PV array in Simulink with blocking and bypass diode is shown in Figure 4.6 (b). The proposed VPSO-LF algorithm is implemented using s-function in MATLAB/SIMULINK as per flowchart shown in Figure 4.2. In order to validate the results of the proposed VPSO-LF algorithm, it is compared with Hill Climbing (HC) and Particle Swarm Optimization (PSO) algorithms. The results are verified with eight patterns of PV array under Partial Shading Conditions (PSC).

4.4.1 Simulation Results of 3S PV Array Configuration

Pattern-1: Pattern-1 of PV array consists of three modules connected in series as shown in Figure 4.3 (a). Module-I takes irradiance (subjected irradiance) of 1000W/m^2, Module-II takes 400W/m^2 and Module-III uses 200W/m^2. Due to three irradiances three different peaks are available as characteristics of Power-Voltage (P-V) curve shown in Figure 4.4 (a). In this P-V curve, the leftmost peak is the highest peak called Global Peak (GP) and its value is 53.47 Watt; the remaining peaks which are middle and rightmost peaks are local peaks (LP). So this pattern-1 (case-1) is applied as a PV source to the input of boost converter, and the results are observed in simulation with HC, PSO and the proposed VPSO-LF algorithm; the corresponding PV power, PV voltage and PV current waveforms, shown in Figure 4.7 (a). The power obtained by HC algorithm is 52.05 Watt, and its tracking time is 0.3 sec, but there is a loss of power during tracking and steady-state oscillations are observed. The power obtained by a PSO algorithm is 53.39 Watt with a tracking time of 2.16 sec and 15 iterations are required to reach the global peak, but there are more oscillations during tracking and less steady-state oscillations compared to HC method. *By using the proposed VPSO-LF algorithm the power obtained is 53.39 Watt with a tracking time of 0.3 sec and the required iterations are 2 to reach the global peak of pattern-1*. In the proposed VPSO-LF method, the power oscillation during tracking and steady state are less compare to hill climbing and particle swarm optimization methods and the method also takes less tracking time. From pattern-1 results, it is observed that the proposed VPSO-LF algorithm is superior to hill climbing and particle swarm optimization algorithms. The proposed VPSO-LF algorithm searches the feasible search area in small step increments at initial stage. This improves the exploitation capability of the PSO algorithm by changing the velocity in small the increments. In later stages Levy Flights (LF) adopts large step size, which improves the exploration ability of PSO algorithm by changing the velocity in large increments. The corresponding searching of

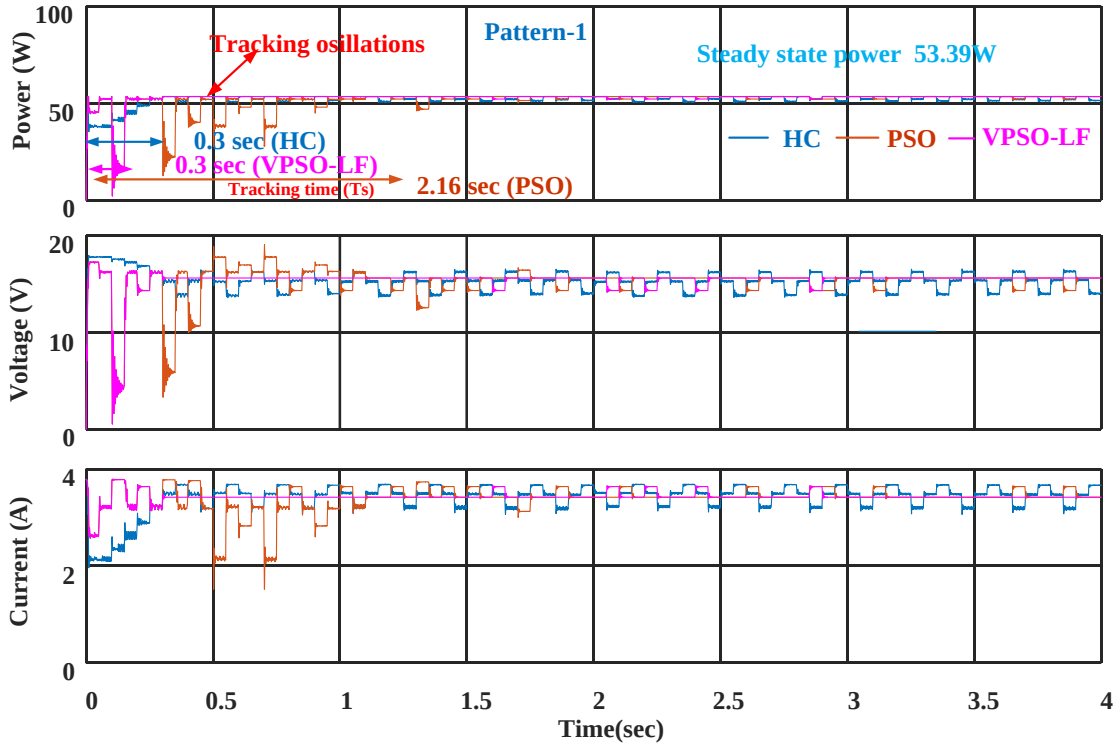

(a)

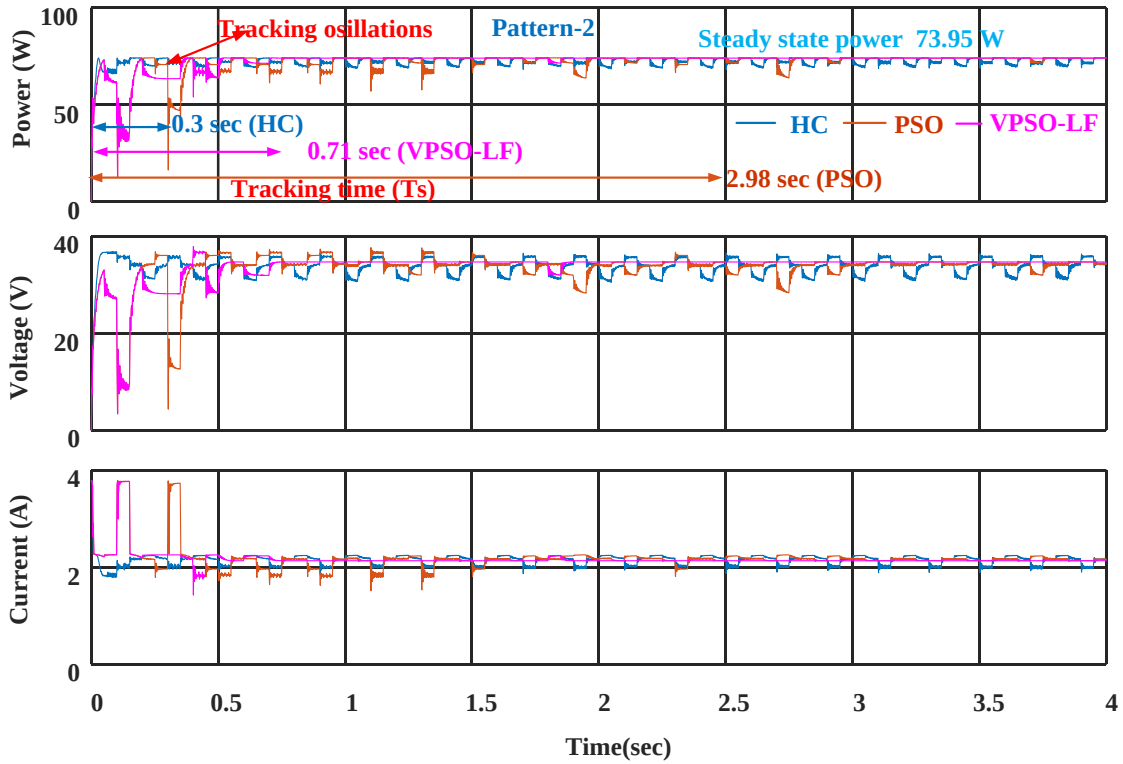

(b)

Figure 4.7 Simulation results for 3S PV array configuration during shading of: (a) Pattern-1, and (b) Pattern-2.

velocity particle values of VPSO-LF and PSO with respect to the number of iterations is shown in Figure 4.8 according to [24]. Similarly the proposed system is going to verify with 3S configuration of different shading patterns, already considered as leftmost peak as a global peak while going to test with middle and rightmost peaks as global peak in the next patterns of PV array. The 3S configuration of four patterns results is presented in Table 4.3.

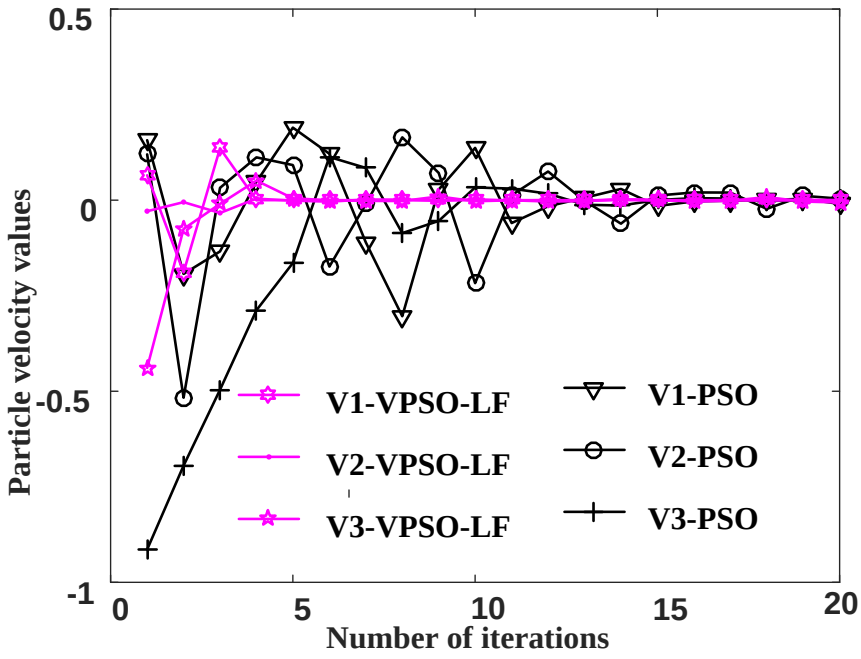

Figure 4.8 Comparisons of VPSO-LF, and PSO algorithms particle velocity values with the number of iterations.

Pattern-2: The shading pattern-2 is considered as a middle peak and the corresponding irradiance values are also shown in Table 4.1. In pattern-2, three module irradiances are different while the three peaks are available in P-V curve as shown in Figure 4.4 (a), and the global peak is middle peak, while the remaining peaks (leftmost and rightmost) are local peaks. The global peak value power is 74.17 Watt. The PV power extracted by HC algorithm is 71.45 Watt, also shown as PV voltage and current in Figure 4.7 (b). Based on the observation from HC, the tracking time is 0.30 sec but steady state oscillations are more due to step size under PSC. PSO algorithm applied to PV system and the related waveforms are shown in Figure 4.7 (b). The maximum power obtained by PSO algorithm is 72.67 Watt, and the time taken to reach global peak is 2.98 sec along with 20 iterations. The tracking time and

iterations needed are more to reach global peak due to three tuning parameters. *The proposed VPSO-LF algorithm is applied to PV system and the time taken for tracking is 0.71 sec to reach global peak in 5 iterations, while the maximum power is achieved by the proposed VPSO-LF algorithm of 73.95 Watt; voltage and current waveforms are shown in Figure 4.7 (b). From these three algorithm, proposed VPSO-LF algorithm yields better results when compared to PSO and HC algorithms.*

Pattern-3: The P-V curve of shading parttern-3 also has three peaks in which the third peak is global peak, the leftmost and middle are local peaks. The maximum power delivered by pattern-3 is 94.61 Watt. The conventional HC algorithm is applied to pattern-3, with tracking time and GMPP value being 0.30 sec and 90.70 Watt, respectively. The waveforms of pattern-3 of conventional HC algorithm are shown in Figure 4.9 (a). By observing power waveform, the tracking time is less, but has steady state oscillations of HC method similar to above pattern-1 and pattern-2. PSO algorithm is applied to pattern-3, with tracking time of 3.52 sec to get GMPP with 24 iterations and global peak power of 94.11 Watt. The power is achieved but the tracking time and iterations are more to get global peak power with PSO algorithm. *By using the proposed VPSO-LF algorithm, the tracking time is 0.75 sec with 5 iterations and a GMPP of 94.58 Watt, the proposed algorithm overcomes limitations of PSO and conventional HC algorithm, takes less tracking time and fewer iterations for the location of global peak*; the corresponding results are shown in Figure 4.9 (a).

Pattern-4: Pattern-4 of P-V curve is similar to pattern-3. The global peak power of this pattern-4 is 114.71 Watt. Conventional HC algorithm takes 0.35 sec to track global peak power of 109.90 Watt. The tracking time to reach global power using PSO is 3.50 sec and the maximum power is 114.70 Watt with 24 iterations. *The proposed VPSO-LF method tracking time is 0.23 sec and the global peak power is 114.70 Watt within 2 iterations*. So the VPSO-LF algorithm has better tacking time and fewer iterations compared to PSO and HC algorithms; corresponding results are shown in Figure 4.9 (b).

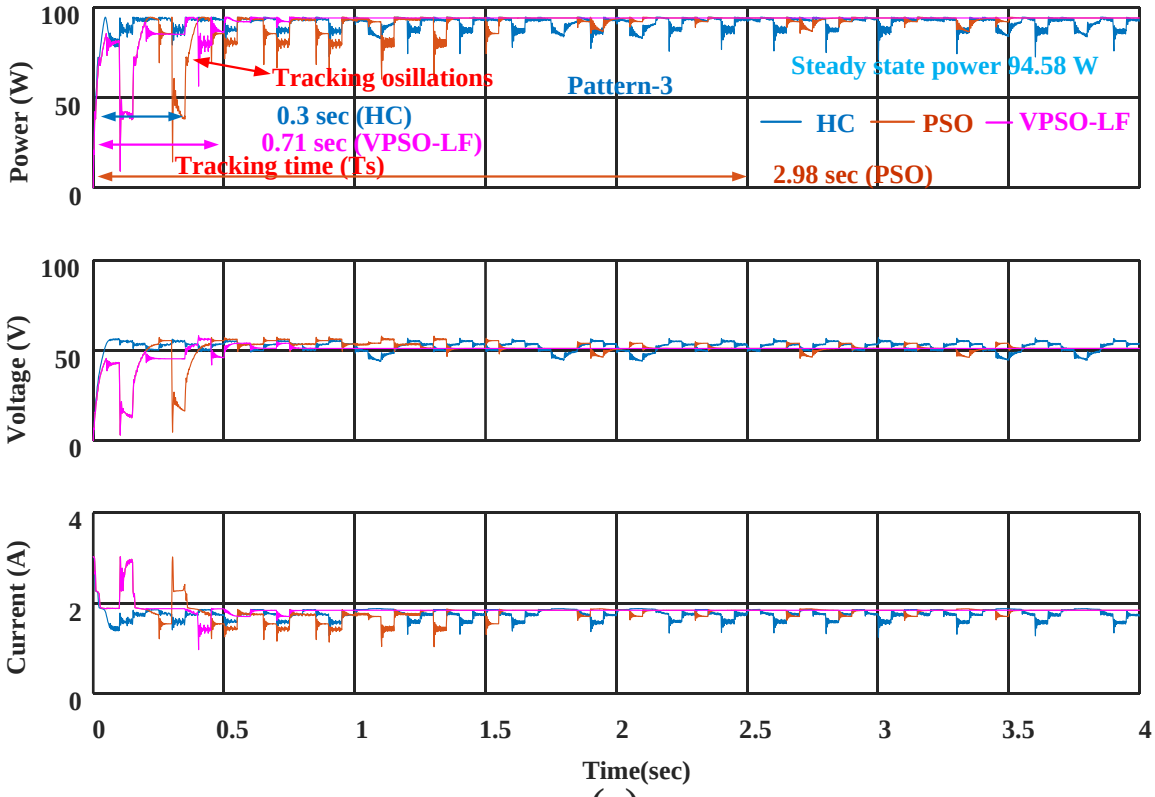

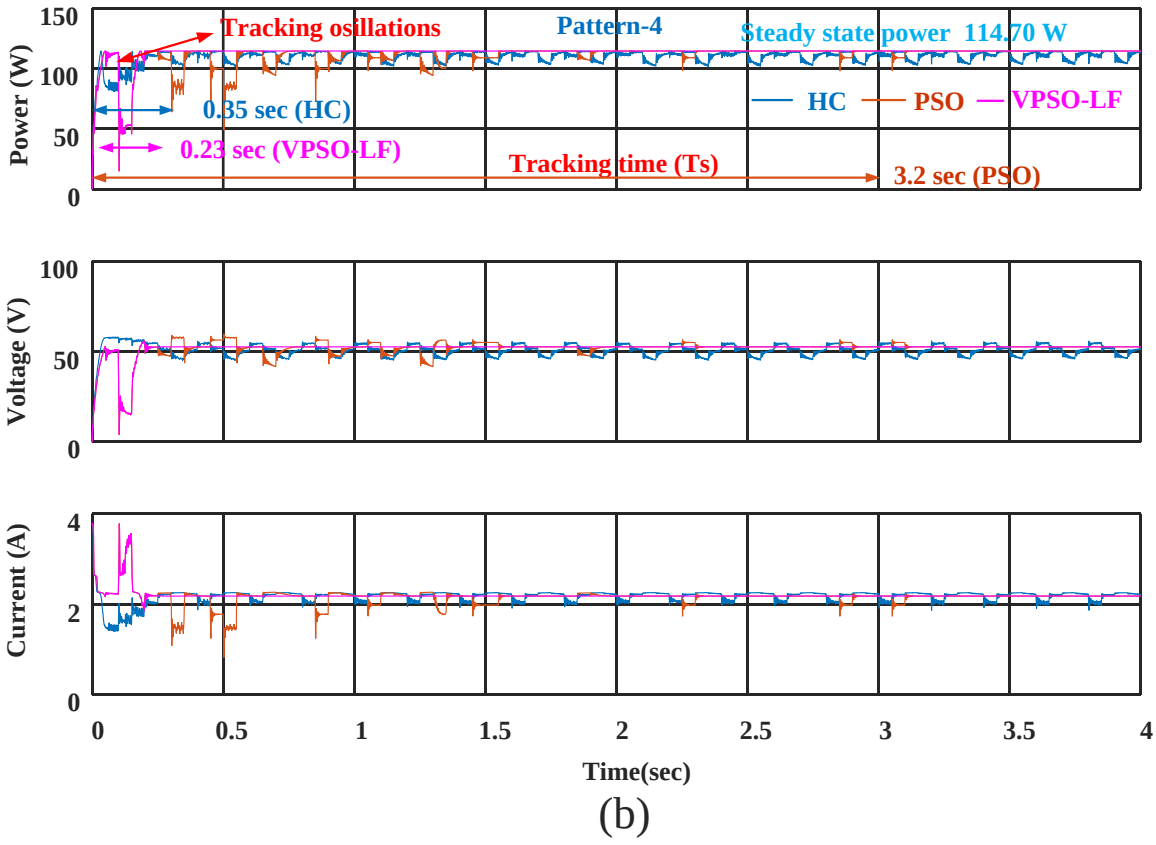

Figure 4.9 Simulation results for 3S PV array configuration during shading: (a) Pattern-3, and (b) Pattern-4.

Simulation Results of Pattern-2 and Pattern-4 during Dynamics: Whenever there is a change in one shading pattern to other shading pattern of PV array under partial shading condition at a particular time, the algorithm has to be re-initialized the parameters to track new GMPP. The proposed VPSO-LF algorithm, conventional PSO algorithm and HC algorithm are verified with a change of from shading pattern-2 to shading pattern-4 at 4 sec. The results prove (change of power from 73.95 Watt to 114.70 Watt) that the dynamic case is also working in perfect manner. The waveforms, which presents the superior performance of VPSO-LF when compared with PSO algorithm and conventional HC algorithm are shown in Figure 4.10.

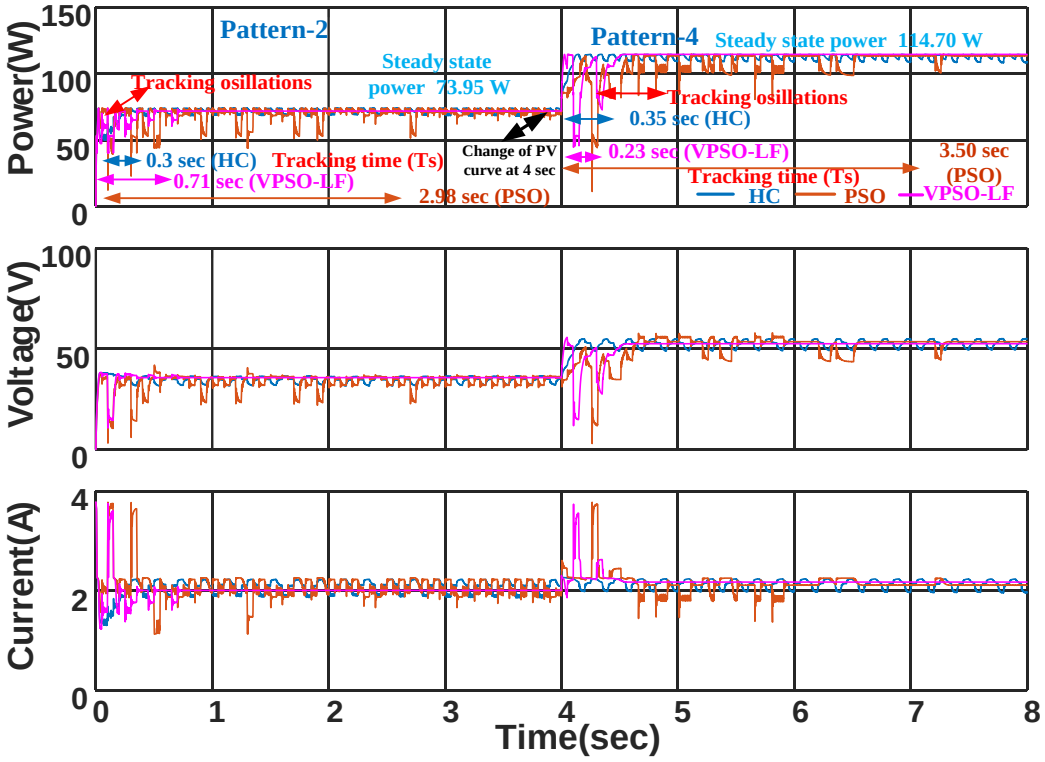

Figure 4.10 Simulation results for proposed VPSO-LF algorithm compared with HC, and PSO algorithms during dynamics of shading pattern-2, and shading pattern-4 of 3S PV array.

4.4.2 Simulation Results of 4S PV Array Configuration

In the previous cases (patterns), the proposed VPSO-LF algorithm was tested with three modules in series; in each case three irradiances were different and there were different global peaks. Now four modules are connected in series to form a PV array as shown in Figure 4.3 (b); four different irradiances are considered to form pattern-5 and three different

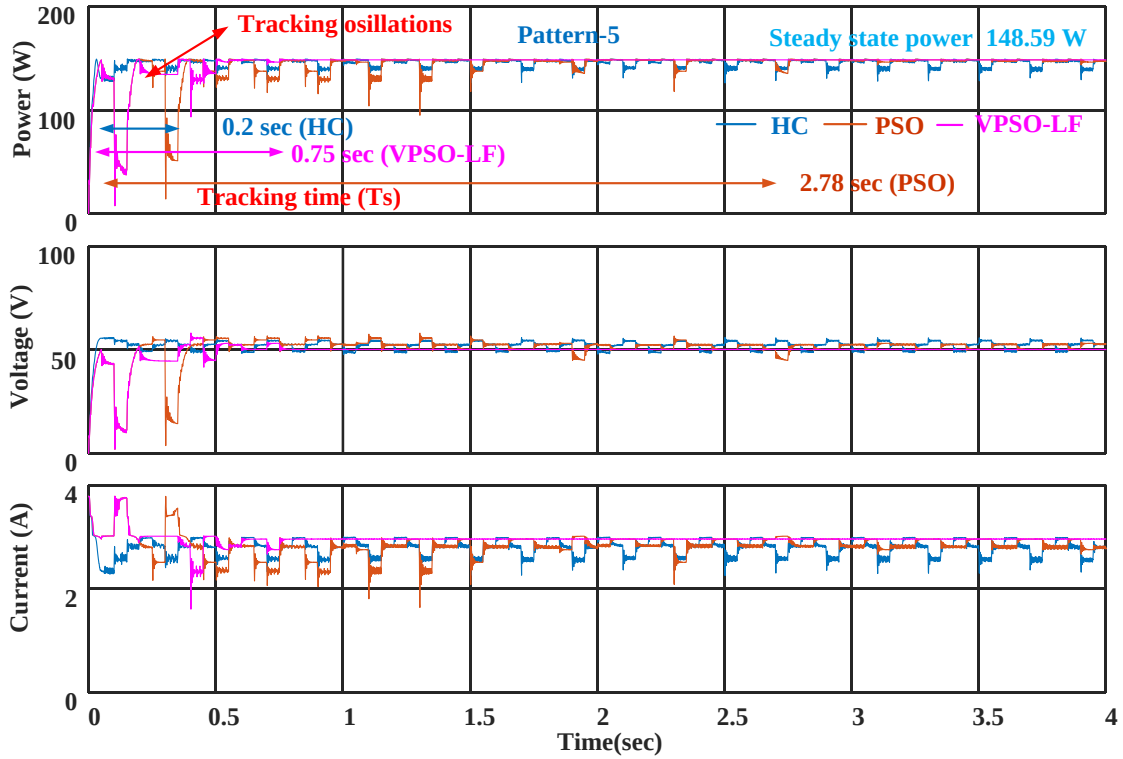

(a)

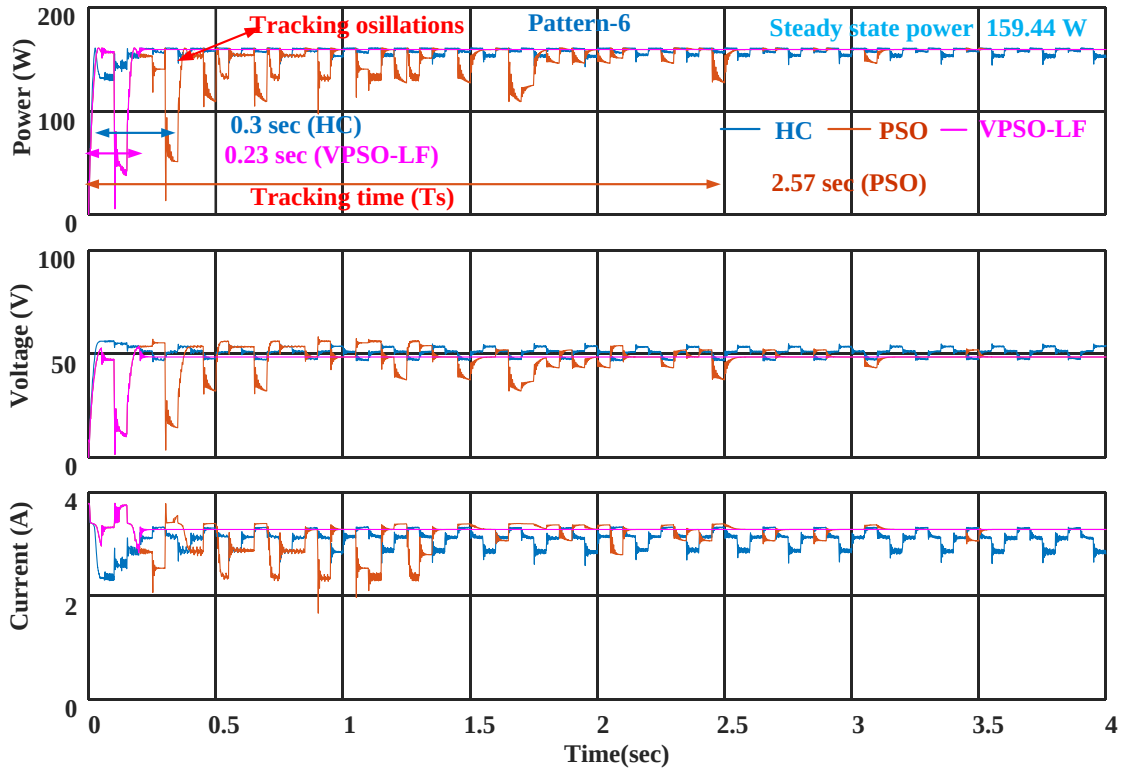

(b)

Figure 4.11 Simulation results for 4S PV array configuration during shading of: (a) Pattern-5, and (b) Pattern-6.

irradiances to form pattern-6, its module values are shown in Table.4.1, the proposed VPSO-LF algorithm was tested with four peaks and three peaks of 4S configuration, its P-V curves shown in Figure 4.4 (b).

Pattern-5: Pattern-5 irradiances of each module are Module-I-1000W/m^2, Module-II-900W/m^2, Module -III-800W/m^2 and Module-IV-400W/m^2. The four irradiances are different because there of which are four peaks in P-V curve of pattern-5; the respective P-V curve of pattern-5 is shown in Figure 4.4 (b). In pattern-5 the global peak is third from the left of the P-V curve and its maximum power is 149.33 Watt. So the PV system's complexity has increased compared to the previous configuration. The proposed system was tested with pattern-5 and the results of the proposed VPSO-LF method along with two existing methods are shown in Figure. 4.11 (a). HC method takes 0.2 sec to reach global peak with a power of 143.98 Watt, but it has problems of steady state oscillations. The PSO method tracks global power of 147.83 Watt with a tracking time of 2.78 sec and uses 19 iterations. *The proposed VPSO-LF algorithm takes 0.75 sec to reach power of 148.59 Watt along with 5 iterations as shown in Figure 4.11 (a). The proposed VPSO-LF algorithm can overcome the problem of PSO and HC algorithms*. A detailed results of 4S configuration is shown in Table 4.3.

Pattern-6: In this, three different irradiances of PV array, Module-I -1000W/ m^2, Module-II and Module-III of 900W/m^2, Module-IV-400W/m^2 are considered. The global peak is in the middle, its maximum power being 160.93 Watt. Under simulation conditions, the HC tracking time is 0.2 sec, the power used up is 157.19 Watt. PSO takes 2.57 sec to reach the global point of 159.50 Watt with 17 iterations. *The proposed VPSO algorithm takes only 2 iterations and 0.23 sec to locate GP of 159.44 Watt*. In pattern-6, proposed VPSO-LF algorithm is best suited for GMMP tracking compared to HC and PSO algorithms. A comparative analysis of 4S configuration of pattern-5 and pattern-6 shown in Table 4.3. The tracking of PV power, voltage and current waveforms of pattern-6 are shown in Figure 4.11 (b).

4.4.3 Simulation Results of 6S PV Array configuration

The number of modules of PV array are increased to six to form a 6S configuration as shown in Figure 4.3 (c), corresponding values of irradiances under partial shading conditions shown

in Table 4.1. There are three different irradiances considered for pattern-7 and five different irradiances for pattern-8; its P-V curves are shown in Figure 4.4 (c). A detailed comparison of 6S PV array results are presented in Table 4.3. Now PV array complexity increases compared to previous 3S and 4S configurations.

Pattern-7: In pattern-7, the Module-I and Module-II receive irradiance of 1000W/m^2, Module-III and Module-IV of 600W/m^2, Module-V and Module-VI are 300W/m^2. For three different irradiances there will be three peaks in P-V curve of pattern-7, shown in Figure 4.4 (c), in which the middle peak is global peak, with corresponding power of 149.69 Watt. The results of HC method take 0.4 sec to locate GP of 143.06 Watt; steady state oscillations are near GP. PSO algorithm finds GP with a tracking time of 3.13 sec and takes 14 iterations consuming 149.30 Watt, but it has problems with regard to tracking time and oscillations due to velocity tuning with three parameters $(w, C_1 \,\&\, C_2)$. *The proposed VPSO-LF takes 0.87 sec to locate GP of 149.48 Watt with 4 iterations. In this too, the proposed algorithm is superior to HC and PSO algorithms*. The tracking power, voltage and current of pattern-7 of waveforms are which shown in Figure 4.12 (a).

Pattern-8: In pattern-8, there are five different irradiances which form pattern-8; there are five peaks available in P-V curve of pattern-8 as shown in Figure 4.4 (c). Its corresponding irradiances are 1000W/m^2, 1000W/m^2, 900W/m^2, 700W/m^2, 400W/m^2 and 300W/m^2. The third peak is global peak with a power of 181.06 Watt. In this case the results obtained by HC is 173.54 Watt near GP with a time of 0.3 sec. PSO algorithm locates GP with a time of 3.57 sec and takes 15 iterations. *The proposed VPSO-LF algorithm settles GP at 180.89 Watt with a tracking time of 0.52 sec, taking 2 iterations*. VPSO-LF has better response compared to HC and PSO algorithms. The tracking waveforms of pattern-8 are shown in Figure 4.12 (b).

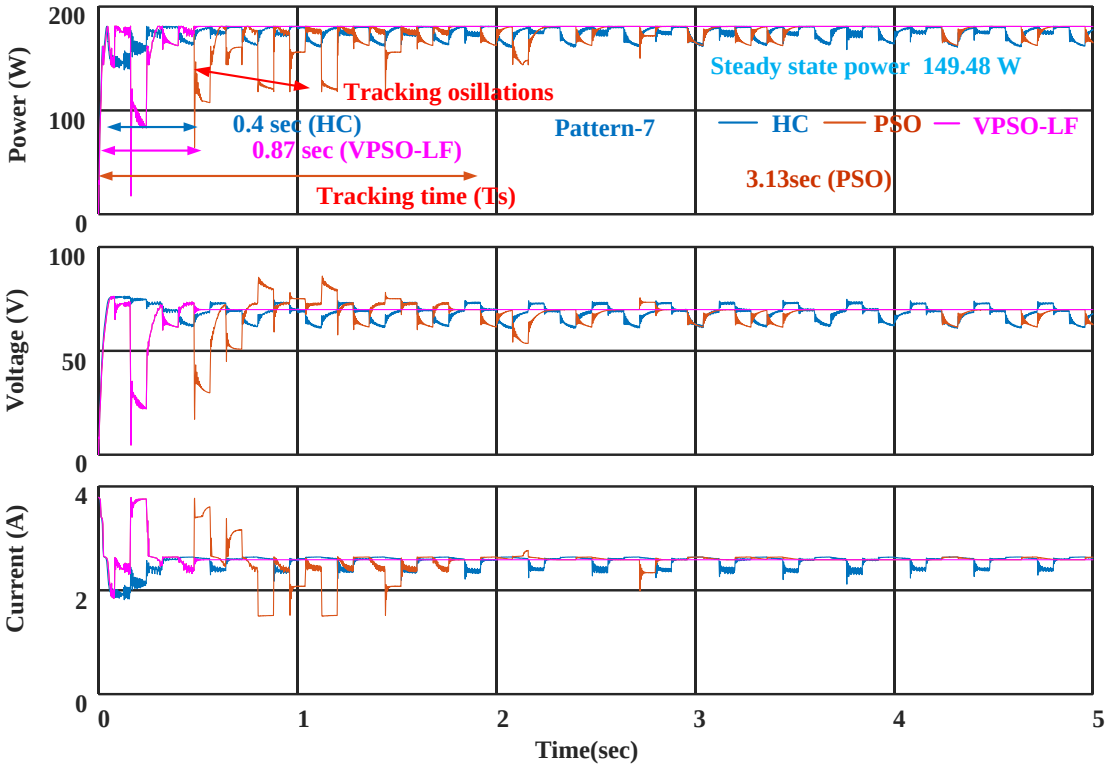

(a)

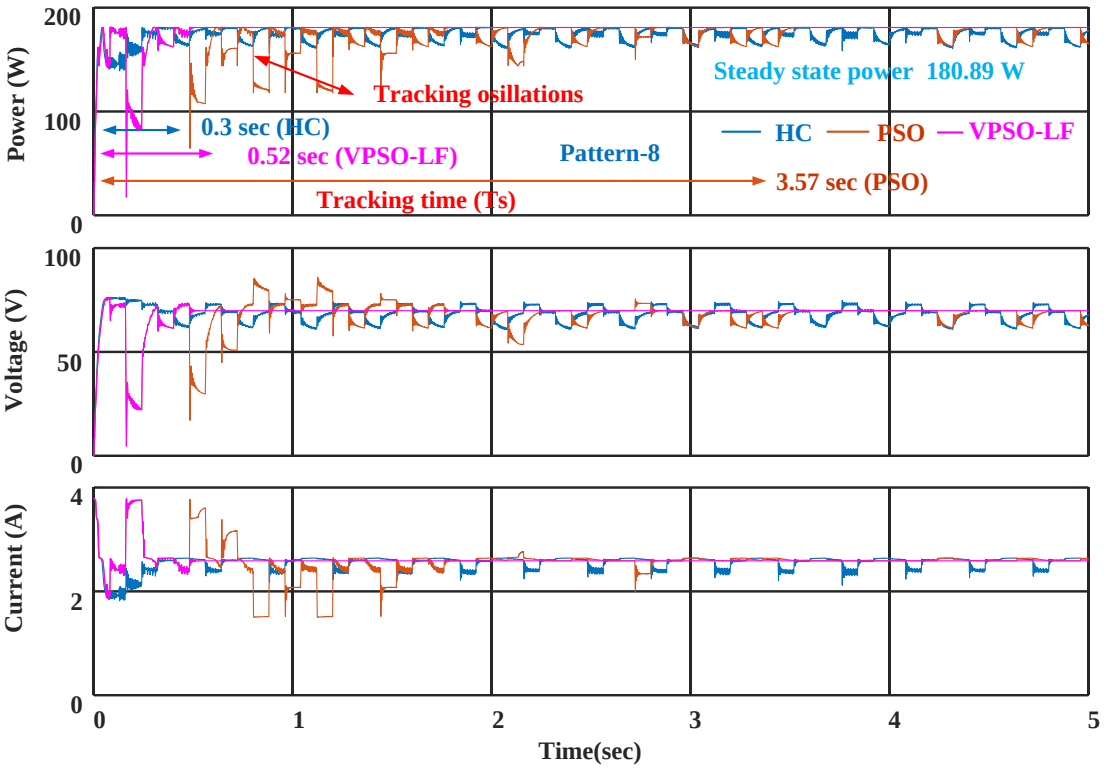

(b)

Figure 4.12 Simulation results for 6S PV array configuration during shading of: (a) Pattern-7, and (b) Pattern-8.

Table 4.3 Simulation performance analysis of 3S, 4S, and 6S PV array configurations

Technique to extract maximum power	**Rated power (Watt)**	**Maximum power extracted from PV(Watt)**	**Maximum voltage extracted from PV(V)**	**Maximum current extracted from PV(A)**	**Tracking time(sec)**	**Iterations required to reach GMPP**	**Tracking efficiency (%)**
Proposed	53.47 Pattern-1	53.39	15.61	3.42	**0.30**	**2**	99.85
PSO		53.39	15.61	3.42	2.16	15	99.85
HC		52.05	15.31	3.40	0.30	-	99.35
Proposed	74.17 Pattern-2	73.95	34.72	2.13	**0.71**	**5**	99.70
PSO		72.67	34.12	2.13	2.98	20	97.98
HC		71.45	33.96	2.10	0.30	-	96.33
Proposed	94.61 Pattern-3	94.58	51.40	1.84	**0.75**	**5**	99.97
PSO		94.11	51.15	1.84	3.52	24	99.47
HC		90.70	52.43	1.73	0.30	-	95.81
Proposed	114.71 Pattern-4	114.70	52.63	2.18	**0.23**	**2**	99.99
PSO		114.70	52.63	2.18	3.50	24	99.99
HC		109.90	50.87	2.16	0.35	-	95.81
Proposed	149.33 Pattern-5	148.59	50.37	2.95	**0.75**	**5**	99.50
PSO		147.83	51.69	2.86	2.78	19	98.99
HC		143.98	51.24	2.81	0.20	-	96.42
Proposed	160.93 Pattern-6	159.44	48.55	3.28	**0.23**	**2**	99.07
PSO		159.50	48.57	3.28	2.57	17	99.11
HC		157.19	50.22	3.13	0.20	-	97.68
Proposed	149.69 Pattern-7	149.48	68.57	2.18	**0.87**	**4**	99.86
PSO		149.30	68.49	2.18	3.13	14	99.74
HC		143.06	66.54	2.15	0.40	-	95.57
Proposed	181.06 Pattern-8	180.89	69.87	2.58	**0.52**	**2**	99.91
PSO		180.89	69.87	2.58	3.57	15	99.91
HC		173.54	69.03	2.51	0.30	-	95.85

4.5 Experimental Results

A hardware-setup was developed comprising PV simulator followed by boost converter to validate the performance of the proposed VPSO-LF algorithm, PSO algorithm and conventional HC algorithm. These algorithms are implemented with MATLAB interface with dspace-1104 controller by voltage sensor (LV25-p) and current sensor (LA55-p) are input to the algorithms. The P-V characteristics are verified by using PV simulator (Magna power electronics XR600-9.9/415+PPPE+HS). The experimental setup is shown in Figure 4.13. The real time parameters are the same as simulations as shown in Table 4.2. In order to verify GMPP of multiple peaks on P-V curve, three PV array configurations were considered with different irradiance conditions in each case, as shown in Figure 4.3. The irradiance of each module in each shading pattern is shown in Table 4.1.

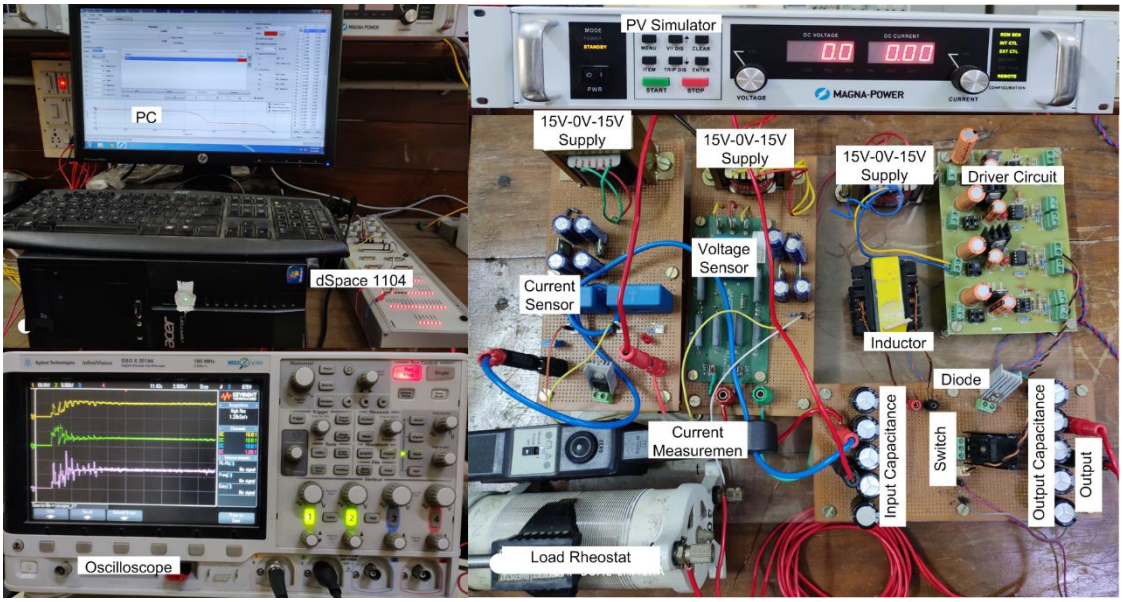

Figure 4.13 Experimental setup for proposed VPSO-LF algorithm.

4.5.1 Experimental Results of 3S PV Array Configuration

The advantages of the proposed VPSO-LF over PSO and HC algorithms is that, the number of iterations required to reach global MPP is minimum and tracking and steady state oscillations are also fewer as was observed in simulation results. The proposed VPSO-LF algorithm was implemented in hardware to verify simulation results and a screen shot of Global Maximum Power Point (GMPP) on P-V curve was also taken to validate the efficiency in real time from PV simulator. In Table 4.4, the performance analysis of 3S PV array configuration of four patterns are presented.

Pattern-1: The experiment results of pattern-1 tracking power, voltage, current using proposed VPSO-LF, PSO and HC algorithms are shown in Figure 4.14 along with a screen shot of GMPP on P-V curve which is attached to each subfigures on the right side corner. The HC algorithm tracks a power 45.92 Watt and the time taken to reach this power is 2.4 sec. From the HC results steady state oscillation more occurred due to the step size under PSC. So the power obtained using PSO algorithm is 46.78 Watt with a time of 7.6 sec along with 13 iteration. From PSO algorithm it is observed that the steady state and transient oscillations are high due to the PV simulator operating with minimum voltage (i.e. PV simulator has own limits of voltage and current). *Whereas proposed VPSO-LF algorithm tracking power is 52.20 Watt with a tracking time of 3.2 sec with 6 iterations*; the operating point is close to that of the GMPP even under minimum voltage. The proposed VPSO-LF algorithm works better compare to PSO and HC algorithms.

Pattern-2: The tracking voltage, current and power of pattern-2 results along with GMPP on P-V curve are shown in Figure 4.15. On observing these results, *it is clear that the tracking time is 1.6 sec and 3 iterations are required to reach the global peak of 73.50 Watt for the proposed VPSO-LF algorithm*. On the other hand the tracking time of PSO algorithm is 6.4 sec and the number of iterations required to get global peak is 11, for a power of 72.24 Watt. HC algorithm takes 8 sec to track global peak and its iterations depends on step size for a power of 72.93 Watt. From this pattern the tracking time and steady-state oscillations of HC algorithms are more compared to VPSO-LF and PSO algorithm; PSO algorithm takes more iterations, less steady state oscillations compared to HC. The steady state power oscillations and iterations of the proposed VPSO-LF algorithm is fewer compared to PSO and HC algorithms. The performance results of VPSO-LF algorithm over PSO and HC algorithms is shown in Table 4.4

Pattern-3: Pattern-3 tracking power, voltage and current results of three algorithms are shown in Figure 4.16. *The tracking time of proposed VPSO-LF algorithm is 3 sec and the number of iterations required for GMPP is 5, the power obtained is 94.12 Watt*. The PSO algorithm takes a tracking time of 6 sec to reach the global peak 90.84 Watt with 10 iterations. The HC algorithm takes 8.1 sec to reach global peak of 91.69 Watt but the steady state oscillations are more. The advantage of the proposed VPSO-LF algorithm that it is similar to above patterns. The proposed VPSO-LF algorithm takes low tracking time and fewer iterations compared to PSO and HC algorithms.

Pattern-4: The tracking voltage, current and power of the experimental results based on pattern-4 is shown in Figure 4.17. The proposed VPSO-LF algorithm tracks GMPP with 3.2 sec, whereas the PSO and HC algorithms take 6.5 sec and 5.6 sec of tracking time. The iterations required for VPSO-LF are 6 and 11 for PSO. The advantage of the proposed VPSO-LF algorithm over PSO and HC is that it needs less tracking time, fewer iterations and low steady state oscillations. The power levels of VPSO-LF, PSO and HC is 114.24 Watt, 111.15 Watt and 107.13 Watt.

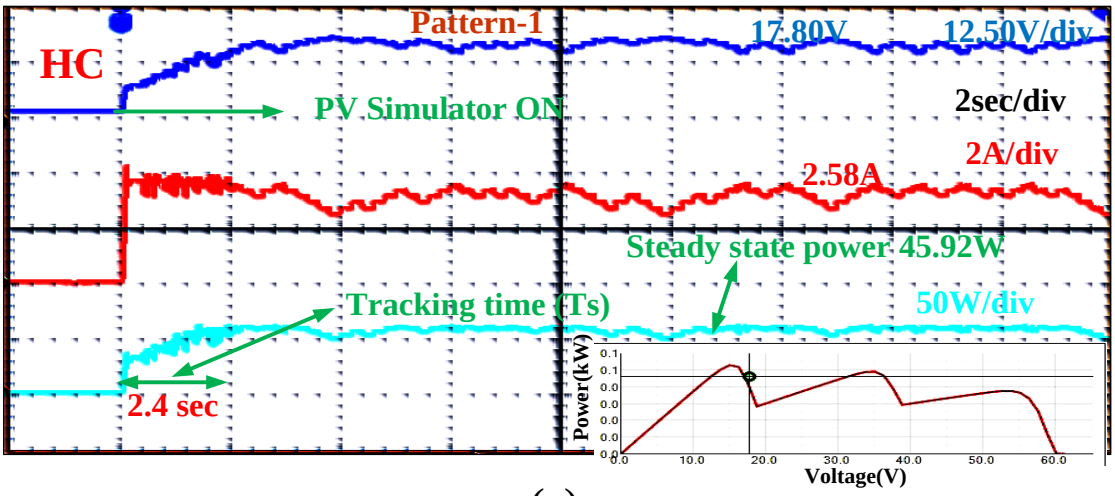

(a)

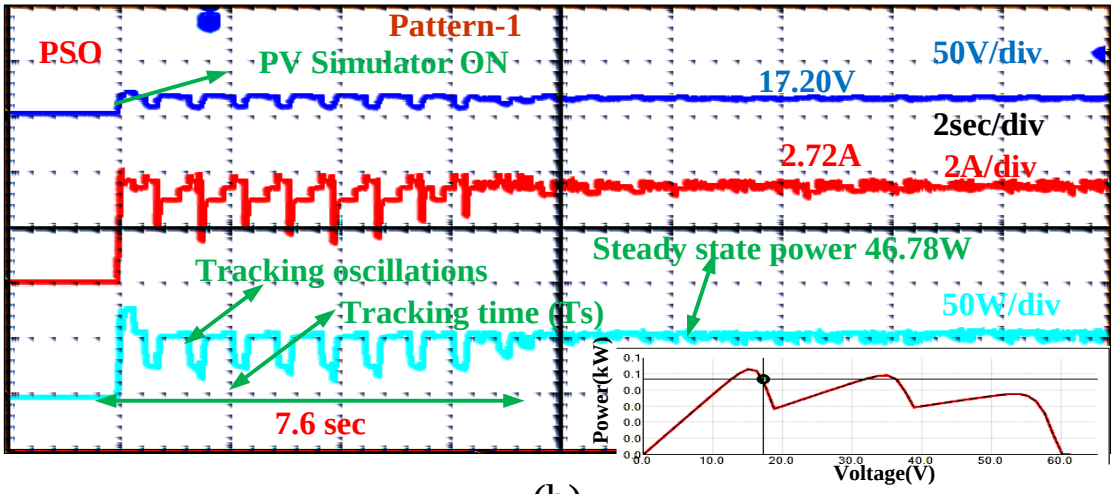

(b)

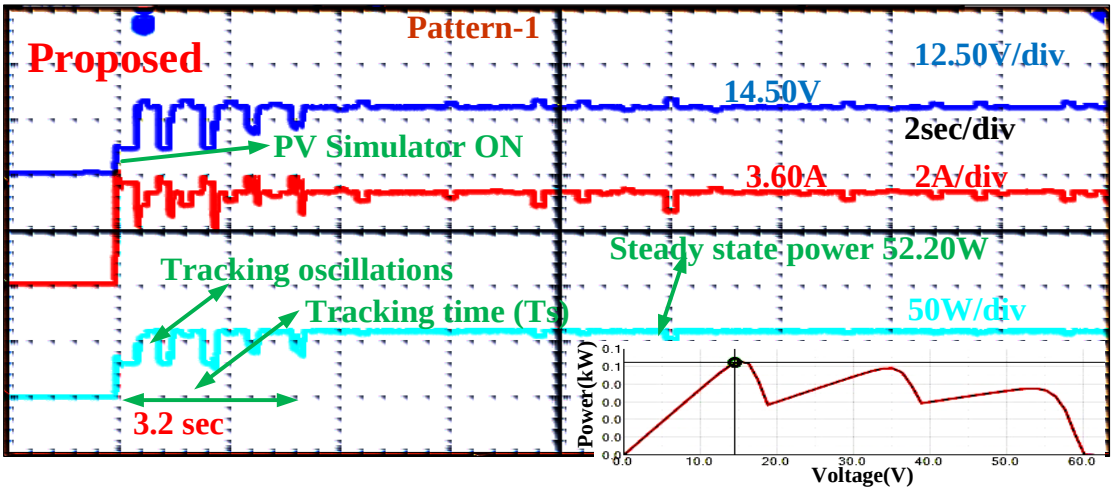

(c)

Figure 4.14 Experimental results for shading pattern-1 of 3S PV array of: (a) HC, (b) PSO, and (c) Proposed VPSO-LF algorithm.

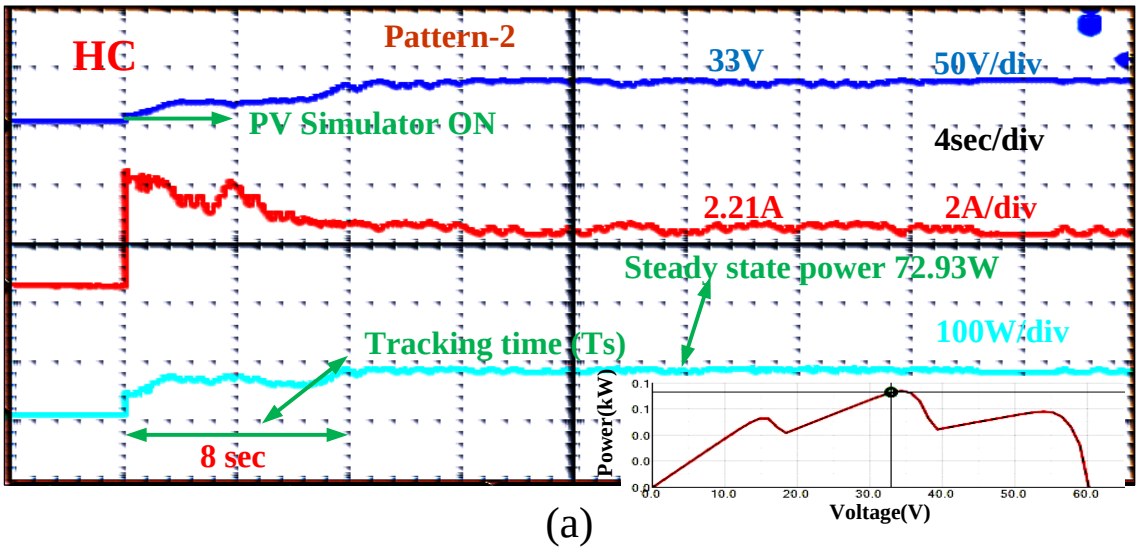

(a)

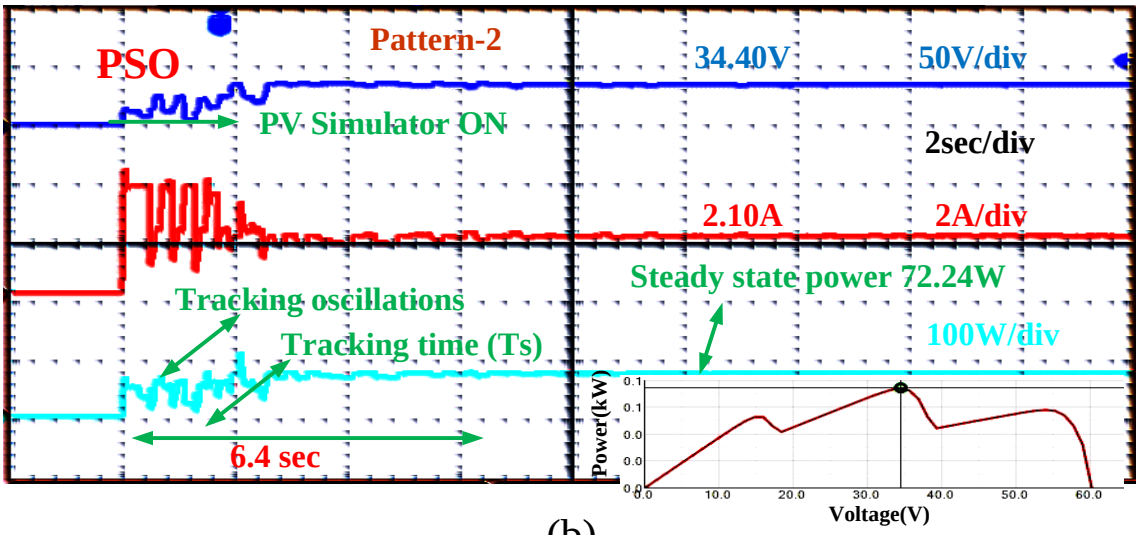

(b)

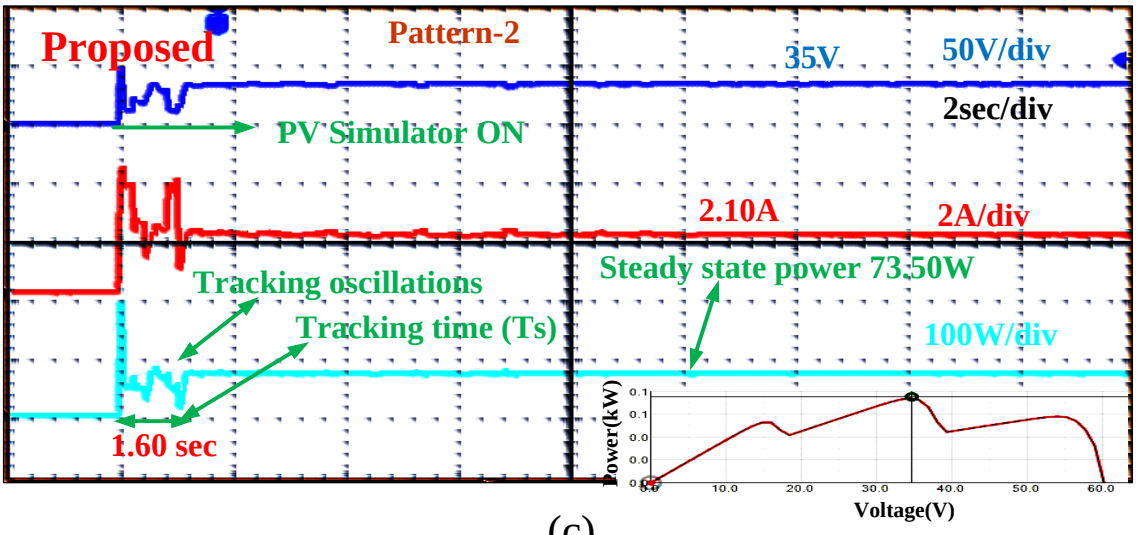

(c)

Figure 4.15 Experimental results for shading pattern-2 of 3S PV array of: (a) HC, (b) PSO, and (c) Proposed VPSO-LF algorithm.

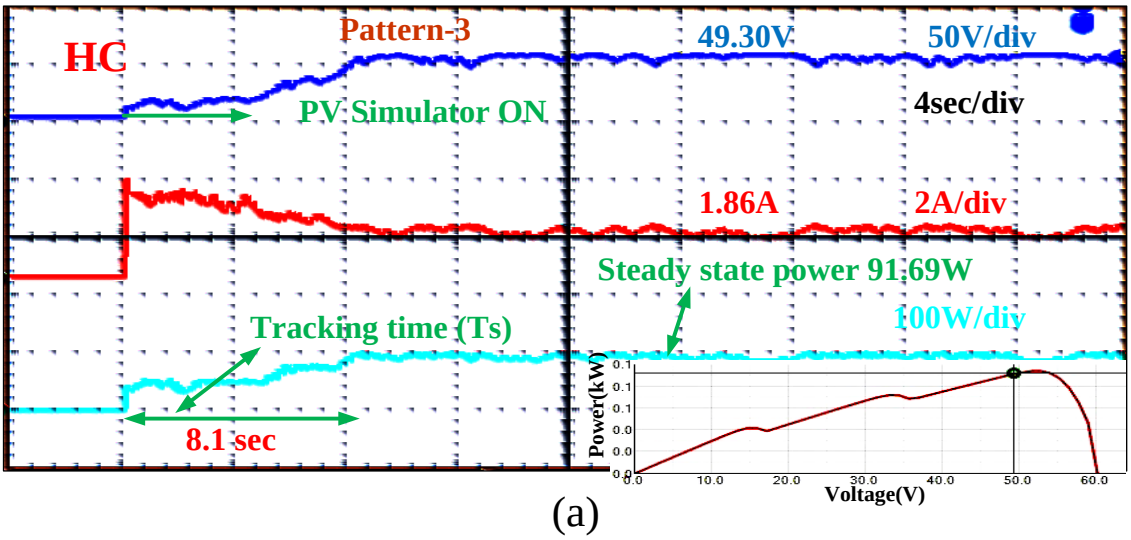

(a)

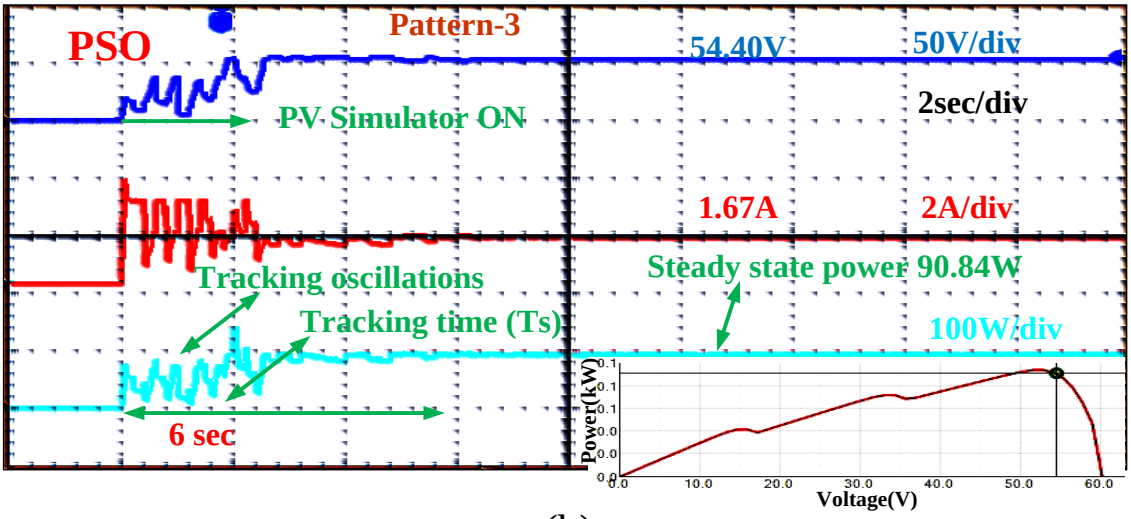

(b)

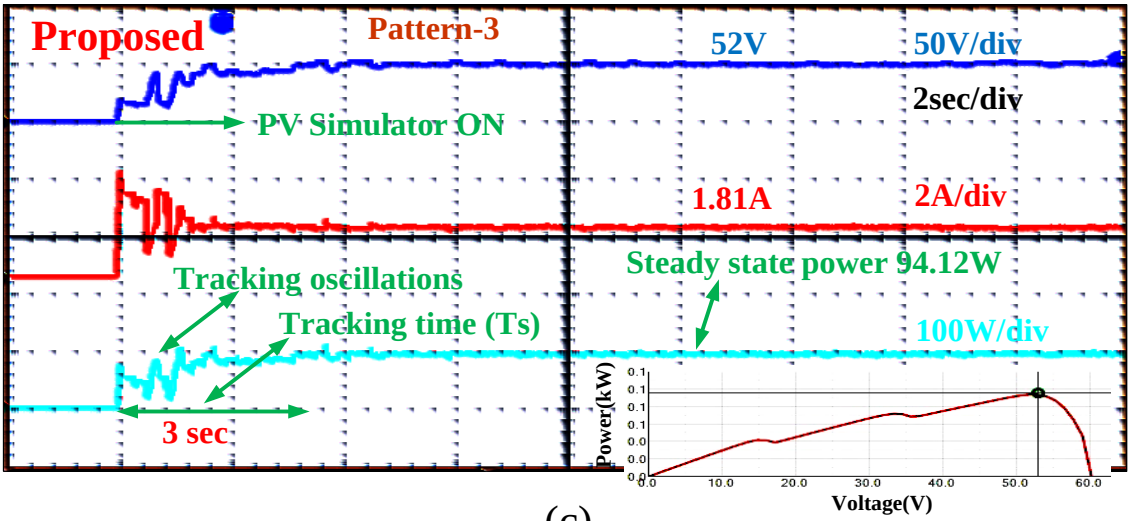

(c)

Figure 4.16 Experimental results for shading pattern-3 of 3S PV array of: (a) HC, (b) PSO, and (c) Proposed VPSO-LF algorithm.

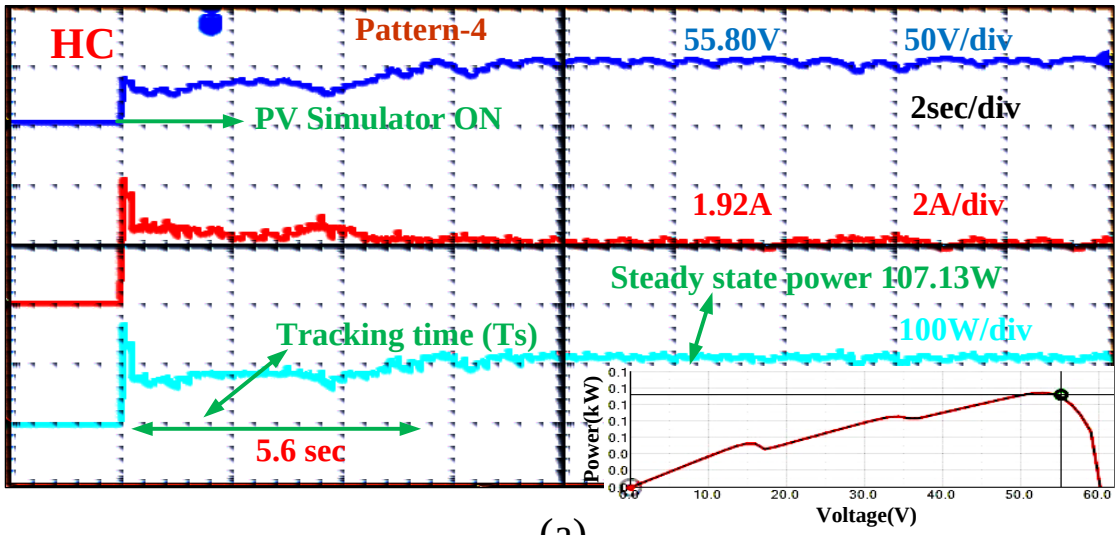

(a)

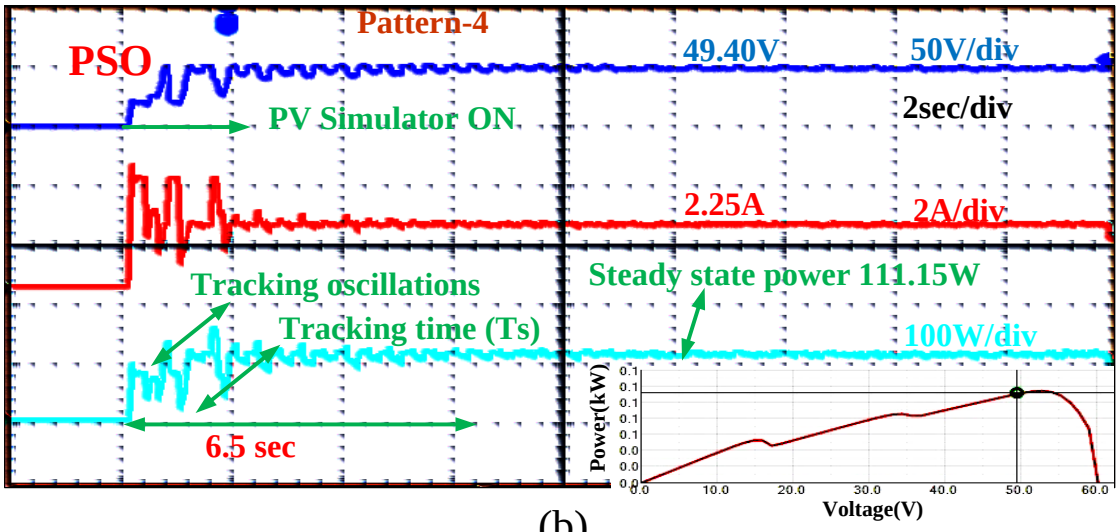

(b)

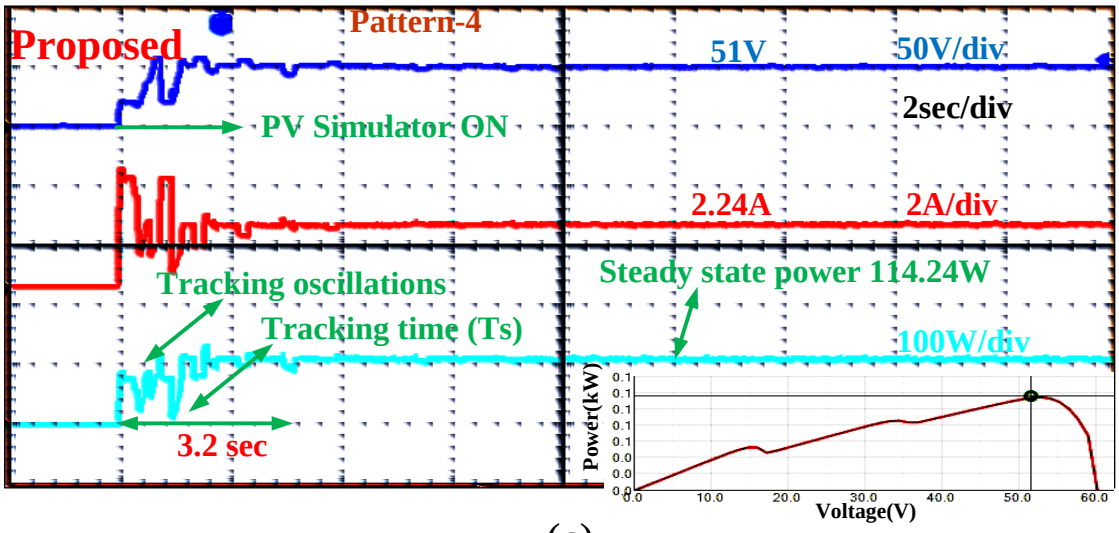

(c)

Figure 4.17 Experimental results for shading pattern-4 of 3S PV array of: (a) HC, (b) PSO, and (c) Proposed VPSO-LF algorithm.

Experimental Results of Pattern-2 and Pattern-4 during Dynamics: Its assignment is to verify whether the proposed VPSO-LF algorithm tracks GMPP when there is a sudden change of one pattern to another pattern of PV system at a particular time. Like the proposed VPSO-LF algorithm, this pattern is tested with pattern-2 and tracks GMPP now at steady state point; after some time the pattern-4 is applied to the experiment through PV simulator, the proposed VPSO-LF algorithm re-initializes initial parameters and tracks new GMPP in less time compared to PSO and HC algorithms. So the proposed VPSO-LF algorithm works perfectly despite any change in irradiance of PV system. The dynamics of PSO algorithm and HC algorithm are also verified with experimental results. The dynamic results of VPSO-LF, PSO and HC algorithms are shown in Figure 4.18.

4.5.2 Experimental Results of 4S PV Array Configuration

In 4S configuration of PV array two patterns are considered under PSC, in order to verify the proposed VPSO-LF algorithm as having results similar to simulation results. The tracking power, voltage and current of pattern-5 results are shown in Figure 4.19. The tracking power of pattern-5 by HC method is 146.05 Watt with tracking time of 7 sec to reach GP, also shown its PV simulator screen shot of GMPP location on P-V curve of pattern-5 in each subfigures on the right side corner below. Similarly with PSO method, the obtained tracking power of 148.40 Watt, with tracking time of 7 sec and 12 iterations to reach global peak. *The proposed VPSO-LF algorithm takes tracking time of 1.6 sec and 3 iterations to find the location of GMPP with power 148.97 Watt*. Experimental results closely match simulation results. The 4S configuration of pattern-6 results is shown in Figure 4.20. Using HC method tracking power is 158.17 Watt and it takes 4 sec to reach global point. The PSO method uses up tracking power of 150 Watt with 6.4 sec and 11 iterations required to reach GMPP. *The proposed VPSO-LF method uses tracking power of 157.79 Watt with a tracking time of 2.4 sec and 4 iterations to reach GMPP*. In 4S configurations also, the proposed VPSO-LF algorithm overcomes the problems of PSO and HC, the results of which are presented in Table 4.4.

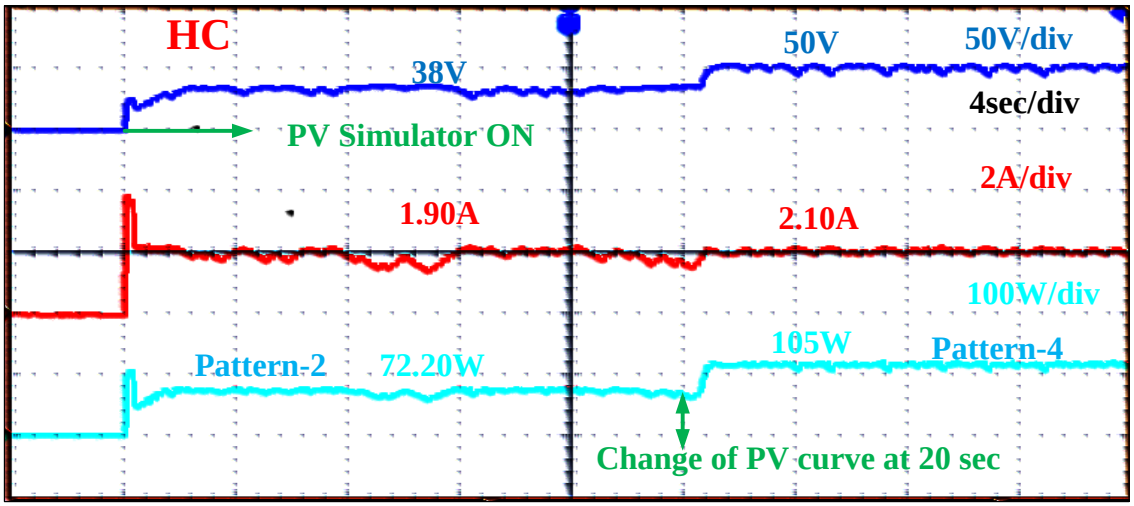

(a)

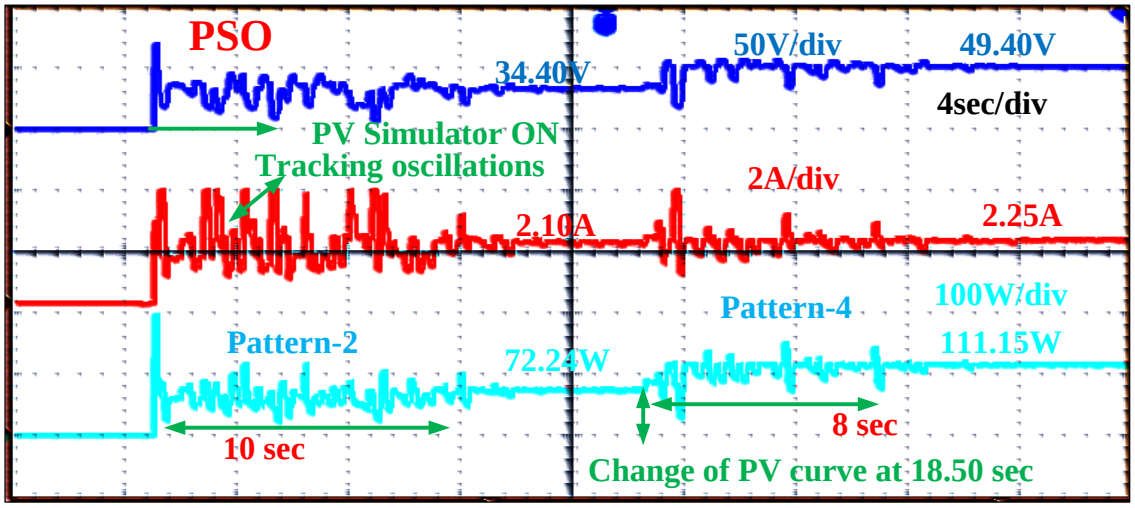

(b)

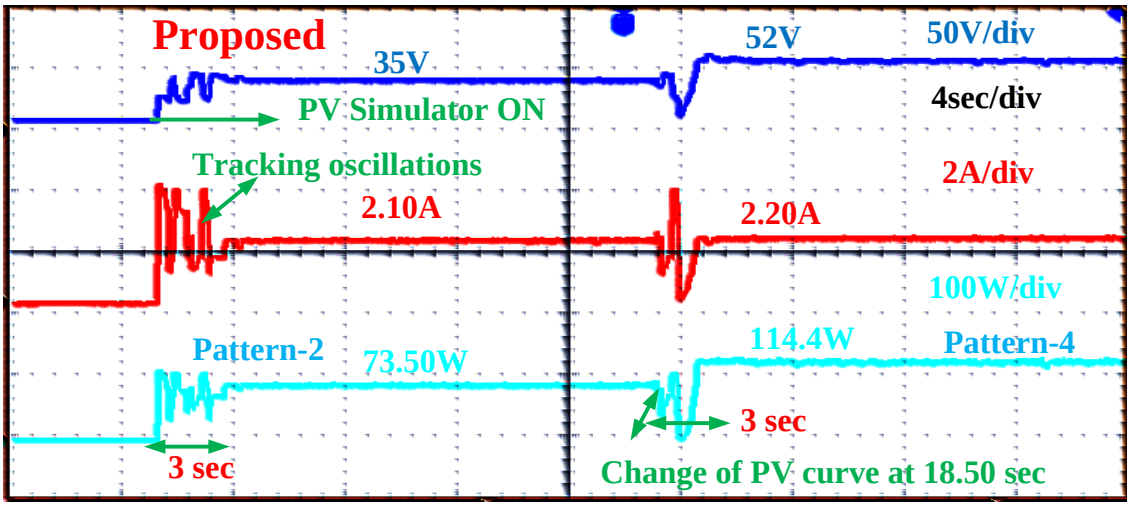

(c)

Figure 4.18 Experimental results during dynamics of shading pattern-2, and shading pattern-4 of 3S PV array of: (a) HC, (b) PSO, and (c) Proposed VPSO-LF algorithm.

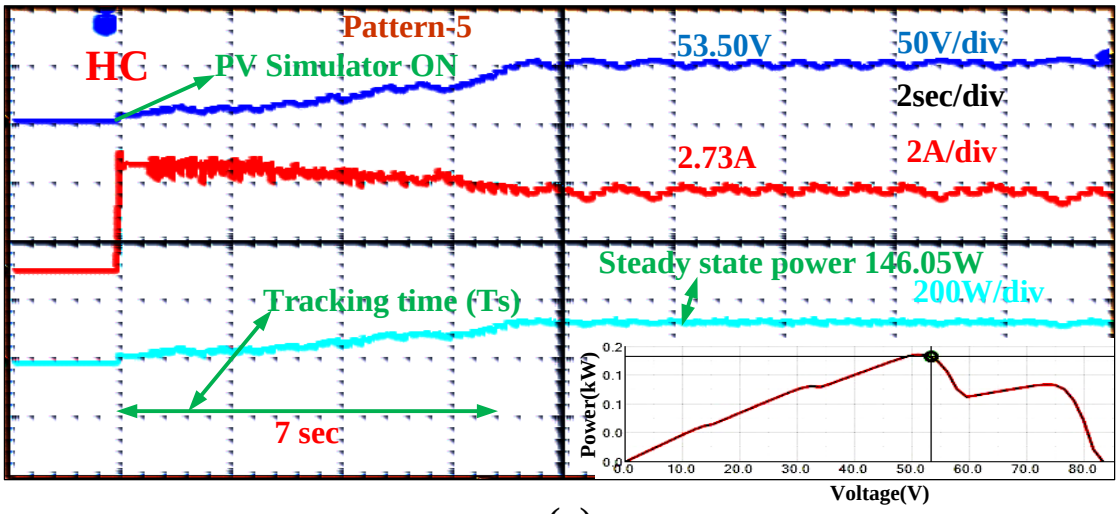

(a)

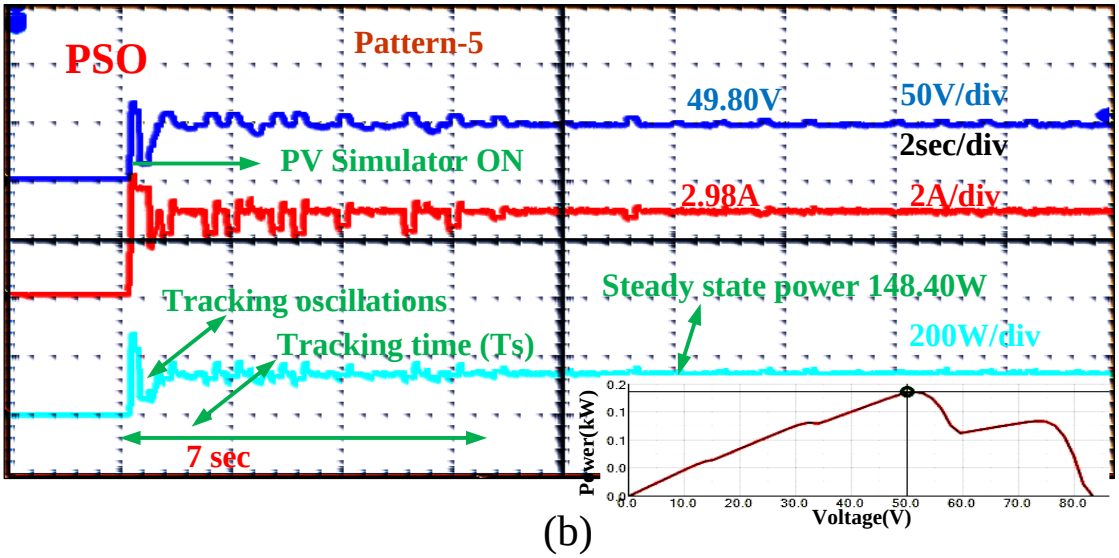

(b)

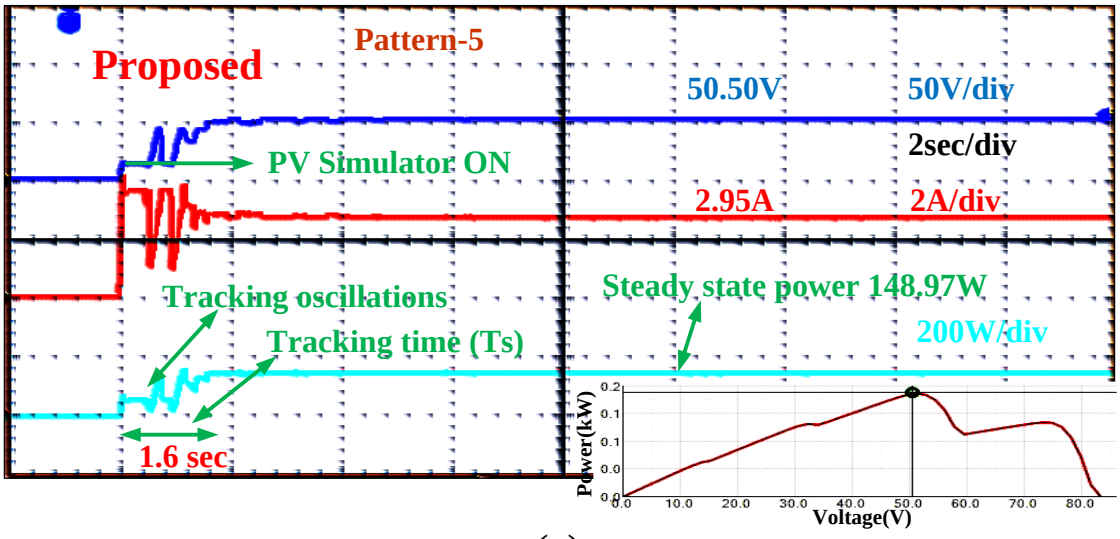

(c)

Figure 4.19 Experimental results for shading pattern-5 of 4S PV array of: (a) HC, (b) PSO, and (c) Proposed VPSO-LF algorithm.

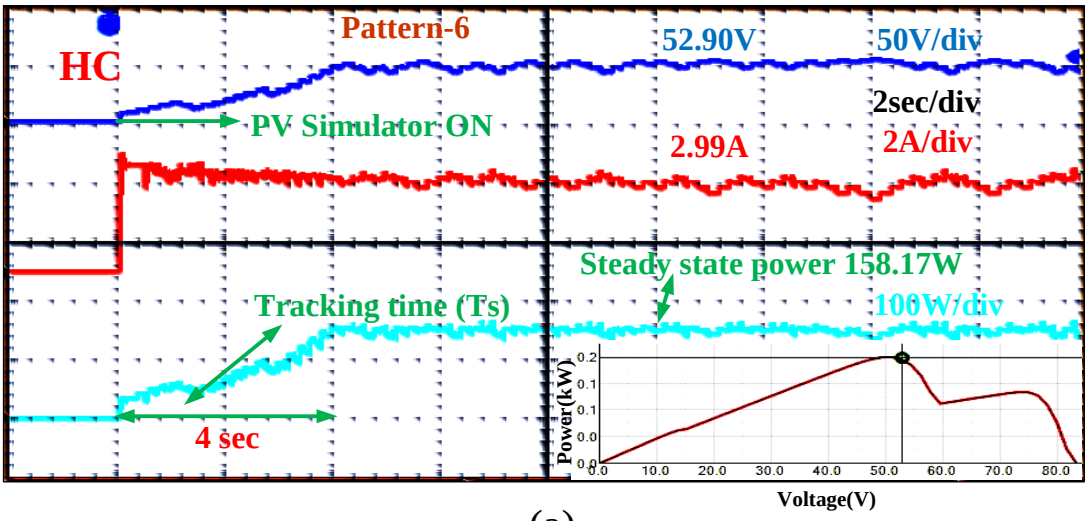

(a)

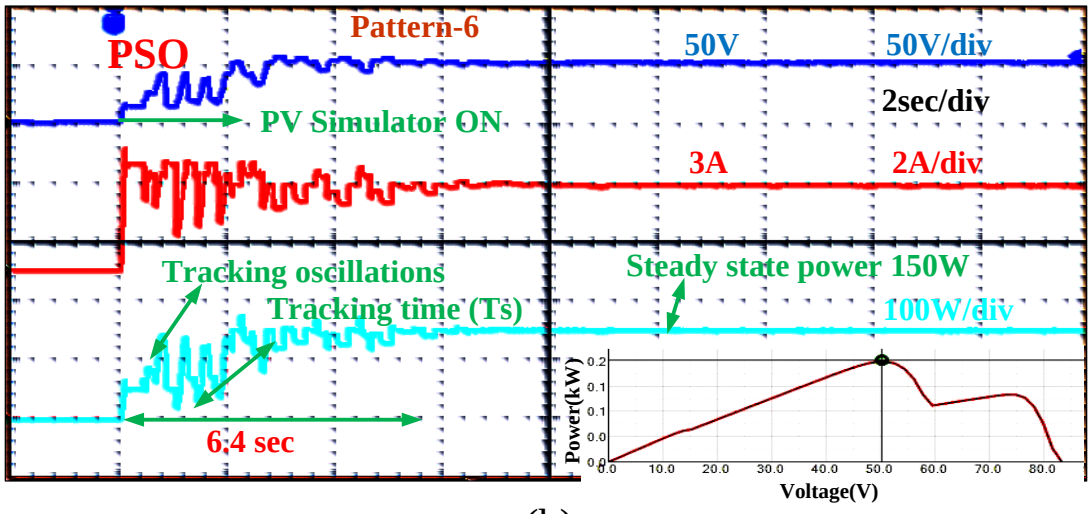

(b)

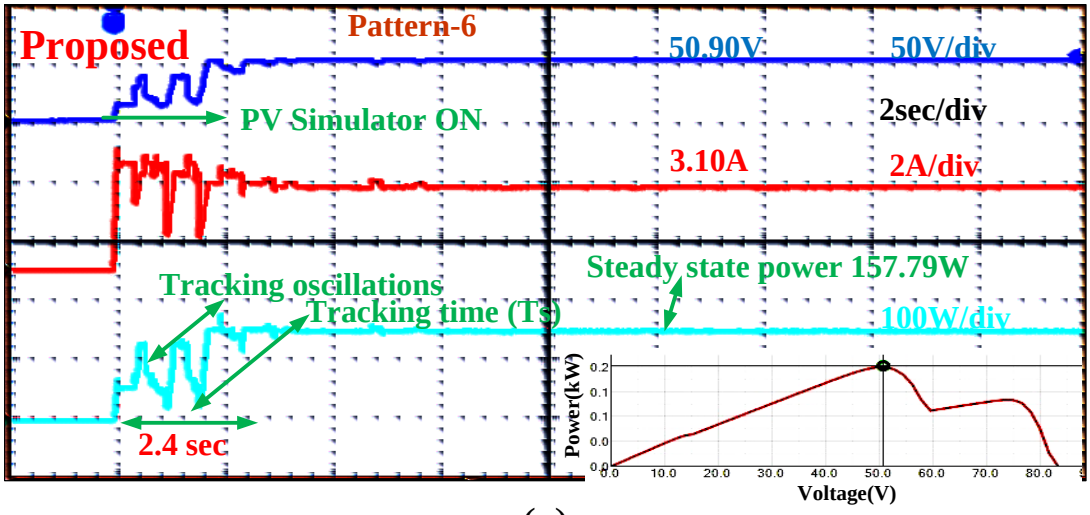

(c)

Figure 4.20 Experimental results for shading pattern-6 of 4S PV array of: (a) HC, (b) PSO, and (c) Proposed VPSO-LF algorithm.

4.5.3 Experimental Results of 6S PV Array Configuration

The 6S configuration of PV array consists of two patterns under PSC. The tracking power achieved by HC method is 132.96 Watt with a tracking time of 4 sec in pattern-7. The PSO method tracks power of 147.63 Watt in 5 sec while 9 iteration are required to attain GP; the screen shot of the GMPP on the P-V curve on right side below the corner of each subfigures is shown in Figure 4.21. *The tracking power achieved by the proposed VPSO-LF method of pattern-7 is 147.66 Watt with a tracking time of 2.2 sec with 4 iterations*. Pattern-8 tracking results are shown in Figure 4.22. The tracking power achieved by HC method is 169 Watt with a tracking time of 4 sec in pattern-8. PSO method uses up 156.20 Watt has a tracking time of 8 sec with 14 iterations but the *proposed method tracks GMPP in just 1.6 sec with 3 iterations and a global power of 179.90 Watt*. The performance results of 6S configuration is shown in Table 4.4.

Table 4.4 Experimental performance analysis of 3S, 4S, and 6S PV array configurations

Technique to extract maximum power	**Rated power (Watt)**	**Maximum power extracted from PV(Watt)**	**Maximum voltage extracted from PV(V)**	**Maximum current extracted from PV(A)**	**Tracking time(sec)**	**Iterations required to reach GMPP**	**Tracking Efficiency (%)**
Proposed	53.47 Pattern-1	52.20	14.50	3.60	**3.2**	**6**	97.62
PSO		46.78	17.20	2.72	7.6	13	87.49
HC		45.92	17.80	2.58	2.4	-	85.88
Proposed	74.17 Pattern-2	73.50	35.00	2.10	**1.6**	**3**	99.09
PSO		72.24	34.40	2.10	6.4	11	97.39
HC		72.93	33.00	2.21	8.0	-	98.32
Proposed	94.61 Pattern-3	94.12	52.00	1.81	**3.0**	**5**	99.48
PSO		90.84	54.40	1.67	6.0	10	96.02
HC		91.69	49.30	1.86	8.1	-	96.92
Proposed	114.71 Pattern-4	114.24	51.00	2.24	**3.2**	**6**	99.59
PSO		111.15	49.40	2.25	6.5	11	96.89
HC		107.13	55.80	1.92	5.6	-	93.39
Proposed	149.33 Pattern-5	148.97	50.50	2.95	**1.6**	**3**	99.76
PSO		148.40	49.80	2.98	7.0	12	99.37
HC		146.05	53.50	2.73	7.0	-	97.80
Proposed	160.93 Pattern-6	157.79	50.90	3.10	**2.4**	**4**	98.04
PSO		150.00	50.00	3.00	6.4	11	93.20
HC		158.17	52.90	2.99	4.0	-	98.28
Proposed	149.69 Pattern-7	147.66	69.00	2.14	**2.2**	**4**	98.64
PSO		147.63	70.30	2.10	5.0	9	98.62
HC		132.96	74.70	1.78	4.0	-	88.82
Proposed	181.06 Pattern-8	179.90	70.00	2.57	**1.6**	**3**	99.36
PSO		156.20	71.00	2.20	8.0	14	86.26
HC		169.00	65.00	2.60	4.0	-	93.33

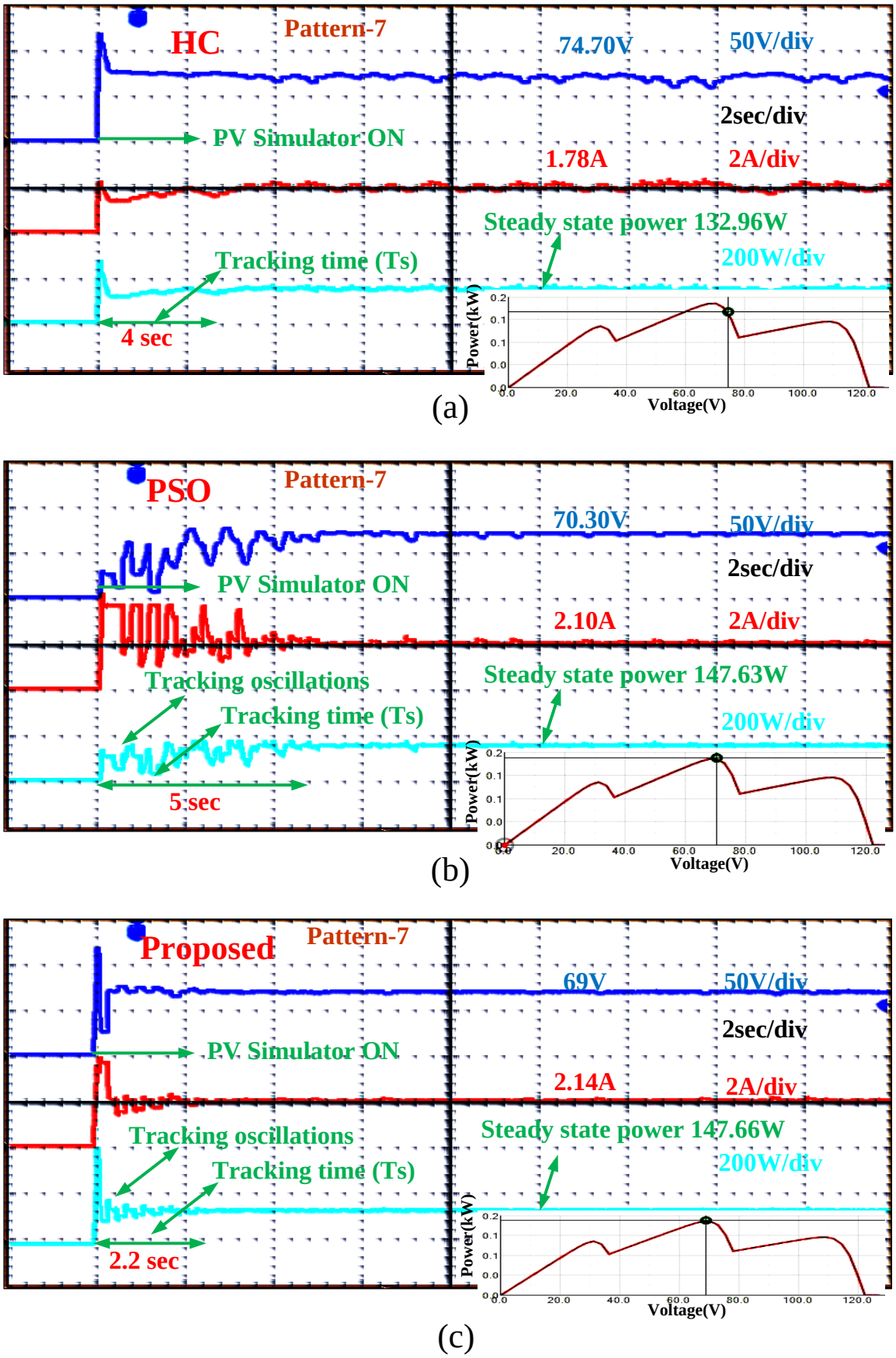

Figure 4.21 Experimental results for shading pattern-7 of 6S PV array of: (a) HC, (b) PSO, and (c) Proposed VPSO-LF algorithm.

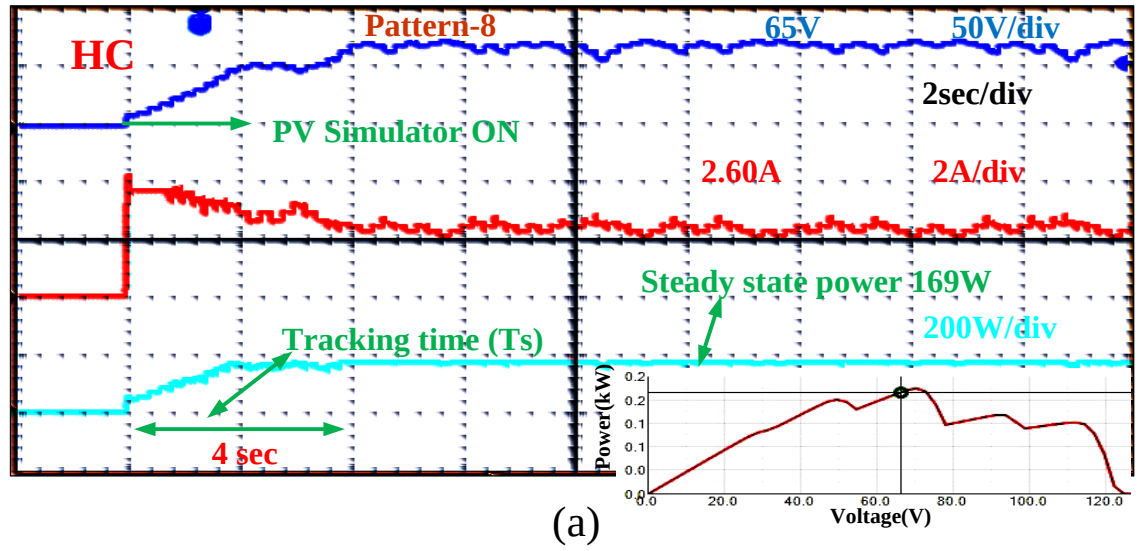

(a)

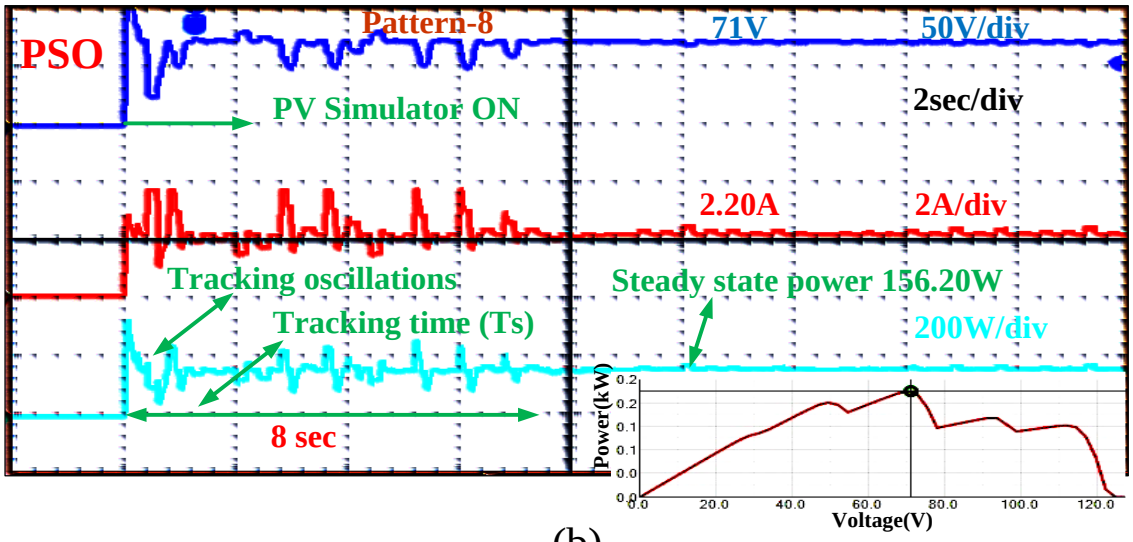

(b)

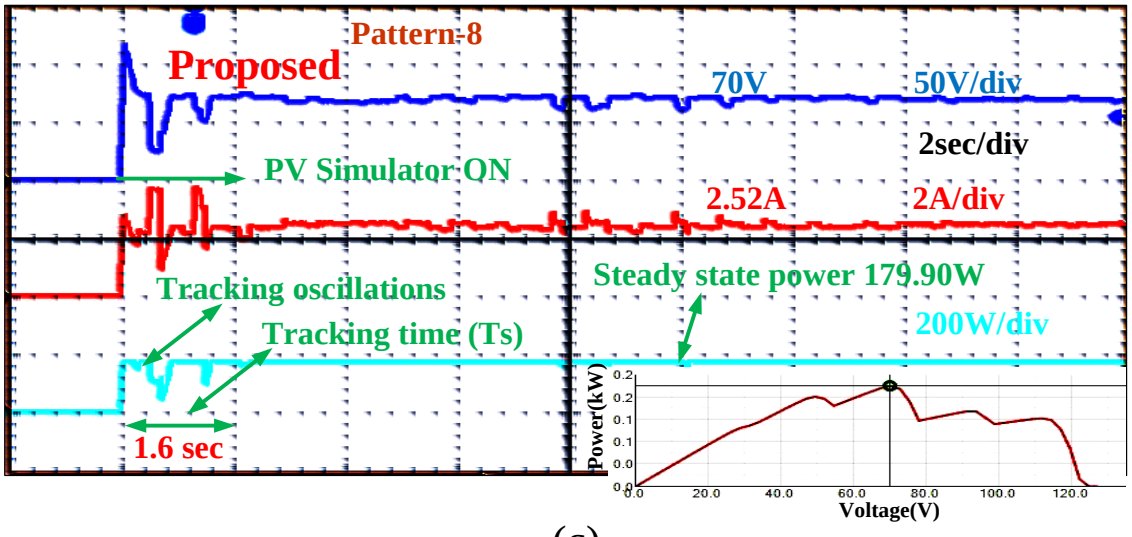

(c)

Figure 4.22 Experimental results for shading pattern-8 of 6S PV array of: (a) HC, (b) PSO, and (c) Proposed VPSO-LF algorithm.

4.6 Comparative Study of Proposed VPSO-LF Algorithm with Existing Algorithms

The proposed VPSO-LF algorithm reduces tracking time, number of iterations, as well as steady-state oscillations around global peak and has more tracking efficiency compared to particle swarm optimization and hill climbing algorithms. The velocity of PSO is updated with Levy Flights distribution in small steps in order to achieve convergence of the global peak without tuning parameters, but in PSO, the velocity update uses three tuning parameters (w, C_1, C_2), because of which it is unable to converge at global peak, and uses more iterations to reach GP. The comparison of velocity particle of VPSO-LF with PSO is shown in Figure 4.8. The problems occurring in HC algorithm are because of its step size, and its inability to tune its step size when change of irradiance or PSC occur. The performance results of the proposed VPSO-LF algorithm with PSO and HC are explained clearly under eight patterns of PV array in Table 4.4. Tracking power, tracking time, efficiency and iterations verses number of pattern of PV array of all three algorithms are shown in Figure 4.23. Flower Pollination Algorithm (FPA) is mentioned in introduction where it is established that the algorithm is unable to find Global Peak (GP) with fewer initial duty cycles but the proposed VPSO-LF algorithm in our study located GP with three duty initialization very little time [85]. Leader-PSO (LPSO) tracked GP with five initial particles and weight tuning parameter but the proposed VPSO-LF algorithm was implemented with no tuning parameter [86]. Modified Particle Velocity based PSO (MPV-PSO) algorithm discards the tuning of weight of PSO, while also showings the nature of deterministic behaviour and adaptive and tuning of cognitive factors with the current position [24]. A Hybrid between the Adaptive Perturb and Observe and Particle Swarm Optimization (HAPO &PSO) tracking speed is high but the initial particles are dependent on V_{oc} [87]. The Improved Cuckoo Search (ICS) was considered four initial duties even though its tracking time is more when compare to proposed VPSO-LF method [88]. These comparisons are shown in Table 4.5.

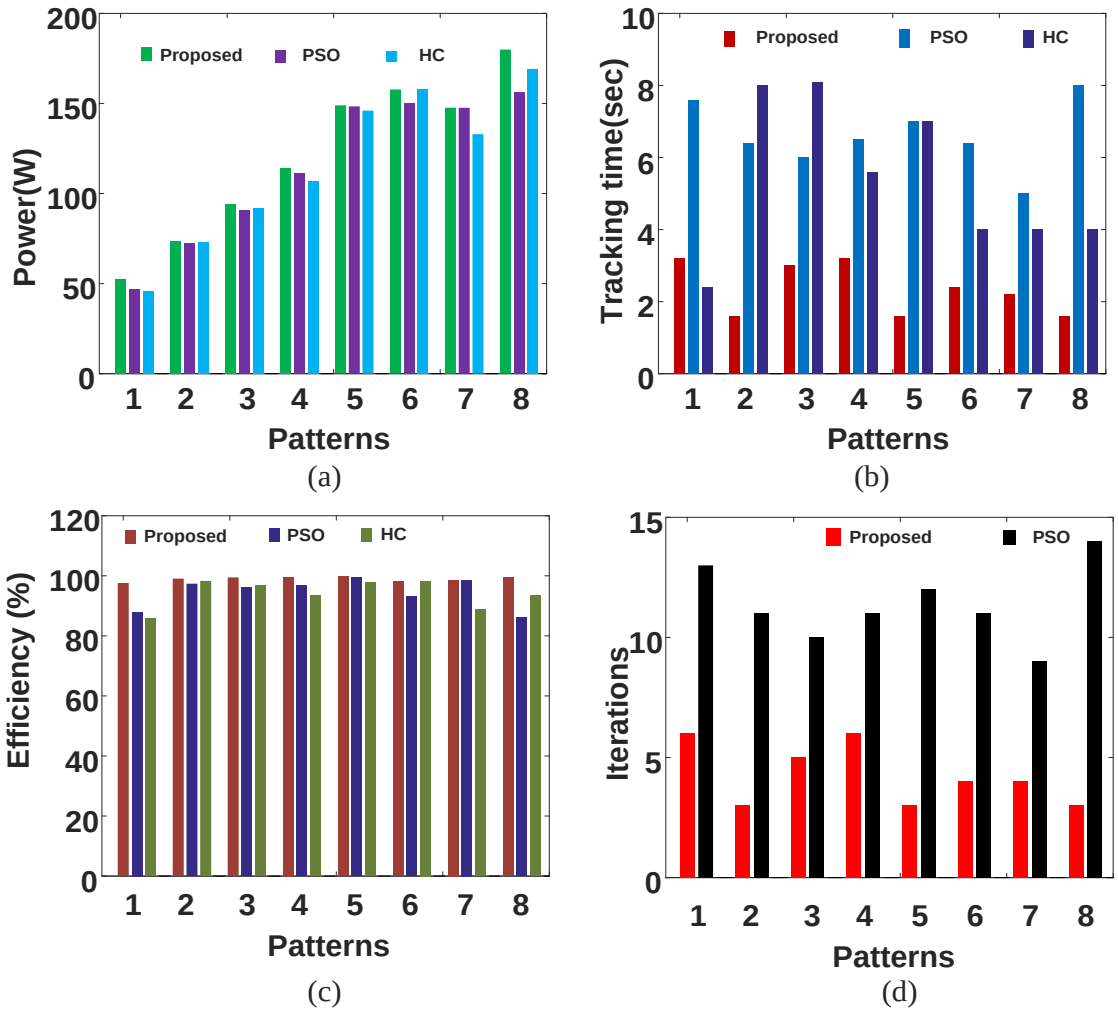

Figure 4.23 Experimental results comparison of proposed VPSO-LF algorithm with PSO, and HC algorithms of: (a) Power, (b) Tracking time, (c) Efficiency, and (d) Iterations with respect to each shading pattern.

Table 4.5 Qualitative comparison of the proposed VPSO-LF algorithm with existing MPPT algorithms

Parameters/ Method	**PSO [20]**	**LPSO [86]**	**FPA [85]**	**ICS [88]**	**MPV-PSO [24]**	**HAPO & PSO [87]**	**Proposed**
Tracking speed	Moderate	fast	Fast	Moderate	Fast	Fast	**Fast**
Iterations	More	Less	Less	Less	Less	Less	**Less**
Tuning parameters	3	1	Nil	Nil	2	Nil	**Nil**
Initial particles	Independent	Independent	Independent	Independent	Dependent	Dependent	**Independent**
Population size	5	5	5	4	3	3	**3**

4.7 Results and Conclusions

In this chapter, the velocity of PSO based on Levy Flight (VPSO-LF) algorithm was proposed, developed and validated experimentally for GMPP tracking of PV array under PSC. *In the proposed VPSO-LF algorithm, the velocity is updated with Levy flights distribution to reach GMPP with low tracking time and reduced number of iterations without any limitations on velocity*. The proposed method also reduces steady-state oscillations around global peak effectively, initial duty independent of the PV system and also does not needs the tuning of velocity parameters. The testing of the proposed VPSO-LF algorithm was carried out along with conventional PSO and HC algorithms to validate the results. From these results, the proposed VPSO-LF method gave better results than conventional PSO and HC methods. The proposed VPSO-LF algorithm can locate GP with any shading pattern of PV array, showing higher efficiency under PSC. In this chapter, the control parameters are more, which increases computations per each iteration and also influences the exploitation process.

Chapter 5

Jaya Algorithm based on Lévy Flight for Global MPPT under Partial Shading in Photovoltaic System

Chapter 5

Jaya Algorithm based on Lévy Flight for Global MPPT under Partial Shading in Photovoltaic System

5.1 Introduction

Many control parameters in an algorithm, creates a poor exploitation process while searching for global best position. For Jaya algorithm having few specific parameters, its performance is good for exploration process, but poor at exploitation process. This chapter proposes Jaya algorithm based on Lévy Flight (Jaya-LF) for better convergence process in GMPPT under Partial Shading Conditions (PSC) of PV array. The proposed technique tracks GMPP with fewer iterations without adaptive control parameters, leading to reduction of transient, steady-state oscillations and minimum tracking period (time) under static condition and with re-initialization of parameters under dynamic shading condition of PV arrays. To validate the performance of proposed Jaya-LF method, simulation and experimental comparisons are made under six cases (patterns) of shaded conditions of PV array. This results of proposed Jaya-LF algorithm are compared with Jaya and PSO algorithms to show the effectiveness of proposed Jaya-LF algorithm under static and dynamic conditions.

5.2 Implementation of GMPPT Algorithms

5.2.1 Jaya Algorithm for GMPPT

Jaya algorithm is based on the attractive and repulsive PSO (ARPSO) [89]. It has recently been improved for solving unconstrained and economic dispatch optimization problems [90], [91]. It is very simple and efficient and does not have many specific parameters for convergence. Power 'P_{pv}' is assumed to be an objective function for maximization problem. The idea is to find the best particle X_{best} and worst particle X_{worst} among all solution after initializing the particle positions i.e., duty cycles of boost converter. Based on best and worst particle updated, new particle position (X_i^{k+1}) is determined as follows:

$$X_i^{k+1} = X_i^k + R_1\left(X_{best} - X_i^k\right) - R_2\left(X_{worst} - X_i^k\right) \tag{5.1}$$

X_i^k and X_i^{k+1} are present and updated duty cycles, and R_1 and R_2 are random number generation from uniform distribution $U[0,1]$. The term $R_1\left(X_{best} - X_i^k\right)$ brings the particle closer to its best position while $R_2\left(X_{worst} - X_i^k\right)$ term brings out of worst condition solution.

The objective functions for each updated particle position is calculated according to equation (5.1).

5.2.2 Jaya Algorithm based on Lévy Flight (Jaya-LF) for GMPPT

Jaya algorithm which can be implemented to GMPPT is a very simple and efficient algorithm with few specific parameters. The Jaya algorithm equation (5.1) has two random numbers because of which random nature exploration is good enough for initial tracking but its exploitation process is poor. Due to minimum number of control parameters, it's tracking oscillations and convergence time is more in Jaya algorithm. So in order to improve exploration and exploitation process, Jaya algorithm is implemented based on Lévy Flights (LF) called Jaya-LF. The proposed Jaya-LF algorithm flowchart is shown in Figure 5.1 and its procedure is explained below.

The Lévy Flights (LF) imply random nature, which can be implemented along with Jaya algorithm for rapid convergence [80]-[84], [92]. Its nature is to search in small steps for exploitation process; otherwise it takes a long jump from one area to another area for the purpose of exploration purpose [83]. Based on the LF concept supporting Jaya algorithm, the tracking time to reach global power is low and also it uses minimum iteration. The proposed Jaya-LF algorithm population is updated based on the condition given in the proposed algorithm flowchart and is rand < 0.25 for proper search operation to achieve global MPPT [84].

Two steps are required for the creation of random numbers with the help of Lévy flight, i.e., the choice of random direction and the production of steps which obey the selected Lévy distribution [83] & [90]. Random walks are captured from Lévy stable distribution. The simple formula for power-law $L(s) \sim |s|^{-1-\beta}$ where $0 < \beta < 2$ is an index [84]. Mathematically, Lévy distribution can be defined as,

$$L(s,\gamma,\mu) = \begin{cases} \sqrt{\frac{\gamma}{2\pi}} \; exp\left[-\frac{\gamma}{2(s-\mu)}\right] \frac{1}{(s-\mu)^{3/2}} & , \quad 0 < \mu < s < \infty \\ 0 & otherwise, \end{cases} \tag{5.2}$$

where μ parameter is location or shift parameter, s is step length and γ is a scale parameter.

In general, Lévy distribution should be defined in terms of Fourier transform

$$F(k) = exp\left[-\alpha|k|^{\beta}\right], \quad 0 < \beta \leq 2 \tag{5.3}$$

where α is a scale factor between [-1, 1], k is distribution variable and β is lévy index. The small value of β allows the variable to jumps long-distance in a search area and keeps away from local optima; the large value of β continues to obtain new values around the variable. As a result, by employing lévy flights on updating the population, variables are able to take short jumps together with occasionally long-distance jumps toward the best value, thereby enhancing the population diversity and facilitating the algorithm to achieve stronger global exploration throughout the search area. In this study, Lévy Flights applied to each variable of the present iteration using the following equation:

$$X_i^{k+1} = Levy\ walk\left(X_i^k\right) + R_1 \times \left(X_{best} - X_i^k\right) - R_2 \times \left(X_{worst} - X_i^k\right) \tag{5.4}$$

where

$$Levy\ walk\left(X_i^k\right) = X_i^k + step\ size \tag{5.5}$$

where

$$step\ size = 0.01 \times step \times \left(X_i^k - P_{best}\right) \tag{5.6}$$

the factor 0.01 comes from the fact that *step*/100 should be the typical *step size* of walks where *step* is a typical length scale; otherwise, Lévy Flights may become so aggressive, which makes new solutions jump outside of the domain and thus waste evaluations.

For random walk, the value of *step* can be calculated by Mantegna's algorithm as:

$$step = \frac{u}{|v|^{1/\beta}} \tag{5.7}$$

here β plays an important role in distributions, by assigning different values for β, the distribution is changed differently. In this study, 1.5 is chosen as the constant value for β [84]. The other two parameters u and v are drawn from normal distributions with standard deviation σ_u and σ_v given by:

$$u \sim N(0, \sigma_u^2), \quad v \sim N(0, \sigma_v^2)$$

where

$$\sigma_u = \left(\frac{\Gamma(1+\beta) \times \sin(\pi \times \beta/2)}{\Gamma\left(\left(\frac{1+\beta}{2}\right)\right) \times \beta \times (2)^{\left(\frac{\beta-1}{2}\right)}} \right)^{\frac{1}{\beta}} \text{ and } \sigma_v = 1 \tag{5.8}$$

where $\Gamma(.)$ is the standard Gamma function

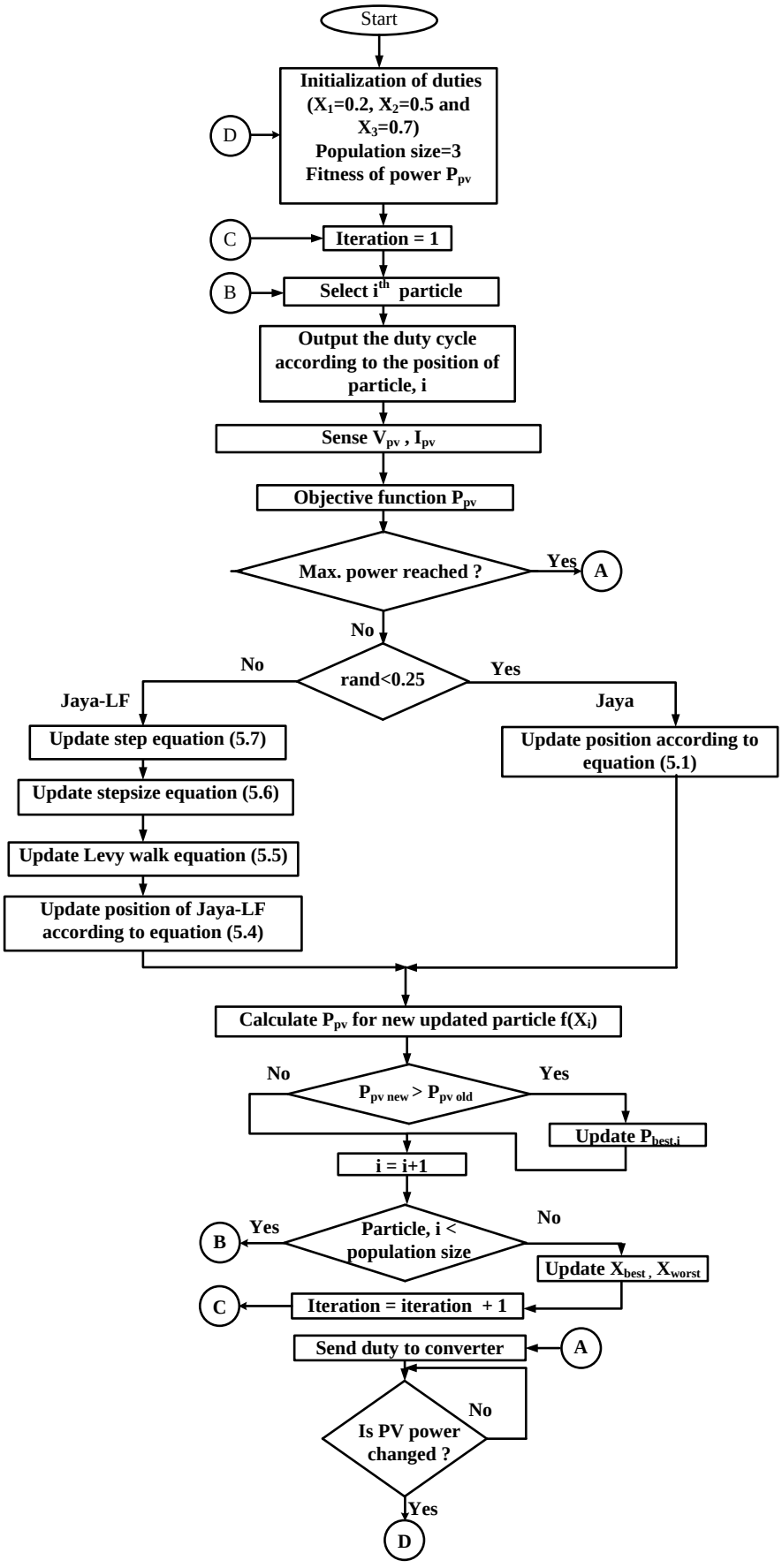

Figure 5.1 Flowchart of proposed Jaya-LF algorithm.

5.2.2.1 Steps to Implement Proposed Jaya-LF Algorithm

Step-1: Initialize the particles at fixed positions between 0.1 and 0.9 of the duty cycle.

Step-2: Measure the power 'P_{pv}' from the output of PV array at each location of particle (duty) by sensing 'V_{pv}' and 'I_{pv}' corresponding duty cycle to boost converter to ' $P_{pv} = V_{pv} \times I_{pv}$'.

Step-3: Update the best fitness powers.

Step-4: Update global best fitness and worst fitness powers from best fitness powers.

Step-5: Update the modified updated positions equations according to (5.1) and (5.6) as per condition given in flowchart (Figure 5.1).

Step-6: Repeat steps 2 and 5 till to reach global peak of P-V curve.

Step-7: If any new shading pattern occurs then re-initialize the parameters.

Step-8: The change of PV pattern is recognized by proposed algorithm with the following power equation:

$$\frac{|P_{n+1} - P_n|}{P_n} \geq \delta \tag{5.9}$$

The term P_n, P_{n+1} are present and future power output of PV system, δ (percentage change of power) is considered as 2% [78].

5.3 The Solar PV Array under Partial Shaded Condition

The performance of the proposed Jaya-LF algorithm can be established with two kinds of PV arrays under PSC. The first one involves three PV modules in series such that two combinations are in parallel and labeled 3S2P as shown in Figure 5.2 (a). The second one is implemented with a four series connected PV module such that two combinations are in parallel and labeled 4S2P as shown in Figure 5.2 (b). The corresponding P-V characteristics under different shaded PV array scenarios or patterns are shown in Figure 5.3 and in each scenario the multiple peaks are different due to shading where the irradiance level pertaining to each case is presented in Table 5.1 and each PV module is designed for 60W, which is shown in Table 3.1 in Chapter 3.

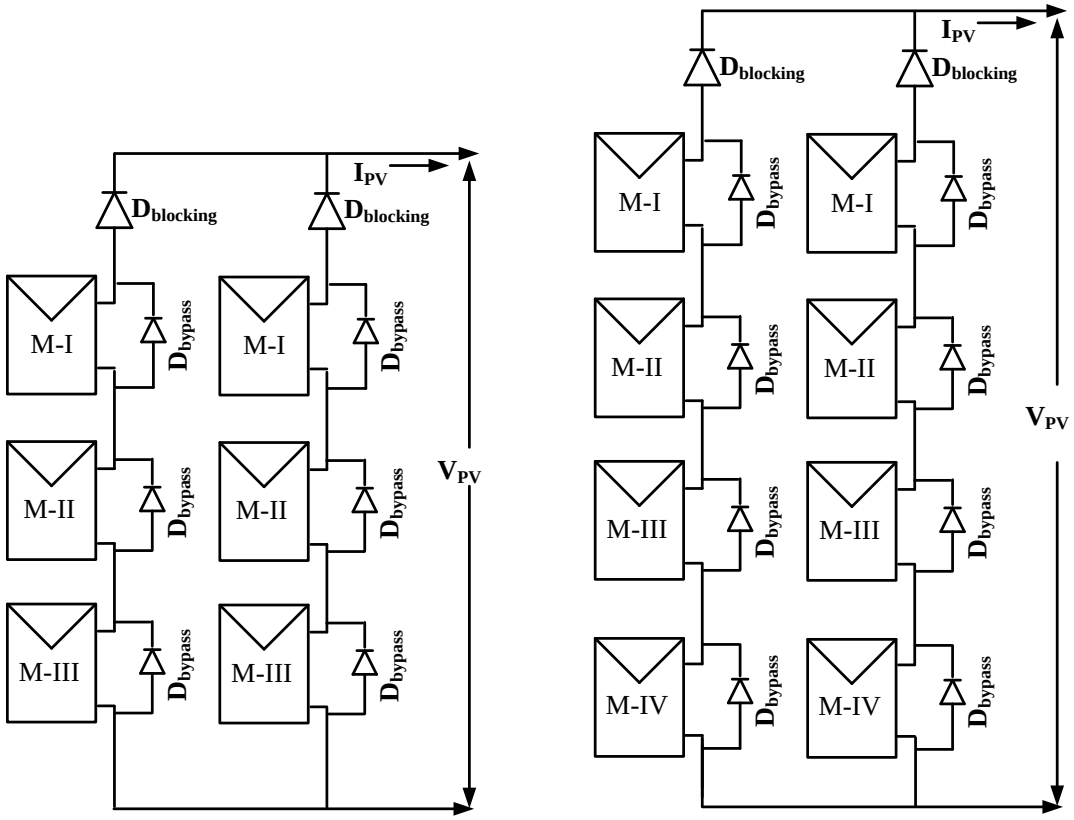

(a) (b)

Figure 5.2 PV array configuration under partial shading conditions of: (a) Three PV modules in series and two path such modules in parallel (3S2P), and (b) Four PV modules in series and two path such modules in parallel (4S2P).

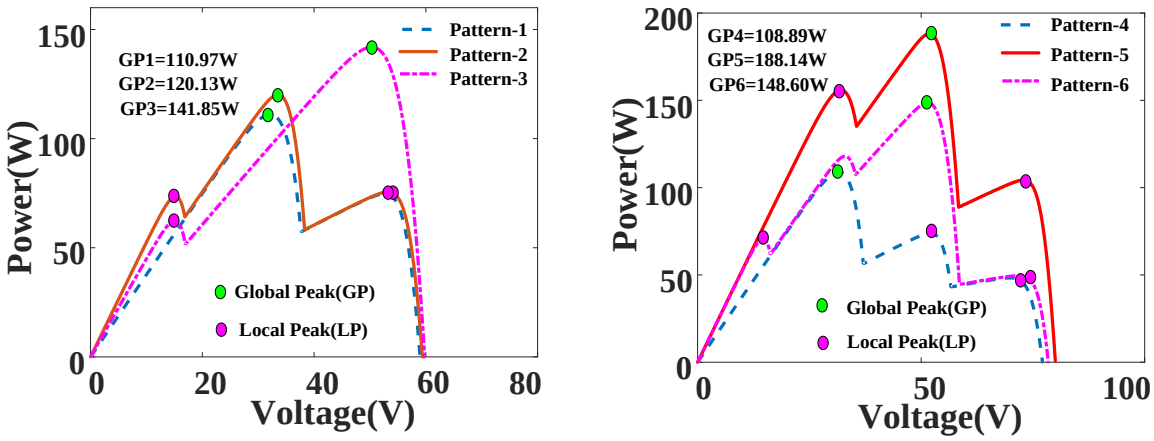

(a) (b)

Figure 5.3 PV array characteristics under partial shading conditions of: (a) 3S2P, and (b) 4S2P.

Table 5.1 Irradiance (W/m^2) of each module in PV array configuration

Module (M)	Pattern-1	Pattern-2	Pattern -3	Pattern-4	Pattern-5	Pattern-6
M-I	500	700	600	500	700	700
M-II	500	500	400	500	700	500
M-III	200	200	400	200	500	400
M-IV	-	-	-	100	200	100

5.4 Simulation Results

The simulation work is implemented in MATLAB/SIMULINK according to the schematic circuit diagram of boost converter along with PV array as shown in Figure 5.4. The proposed algorithm generates duty by sensing voltage and current from the PV array output. The proposed algorithm is modelled in Simulink using s-function as per flowchart shown in Figure 5.1. Modelling of PV array is implemented based on the parameters of PV module as shown in Table 3.1 at Chapter 3. The PV modules are connected in series and parallel with blocking and bypass diodes, as shown in Figure 5.2. The proposed Jaya-LF algorithm is verified under six cases (patterns) of PV array scenarios in order to show the superiority over conventional Jaya and PSO algorithms during partial shading effect. In the first three scenarios, the global Maximum Power Point (MPP) of 3S2P with left peak, middle peak and right peak are considered in P-V characteristics. The next three scenarios of global MPPs involve first peak, second peak and third peak from left of P-V curve at 4S2P. The initial particles of three algorithms, termed as duty cycle to boost the converter, with points are $x_1 = 0.2$, $x_2 = 0.5$ and $x_3 = 0.7$ considered without depending on PV system. The remaining parameters of boost converter and algorithms are represented in Table 5.2.

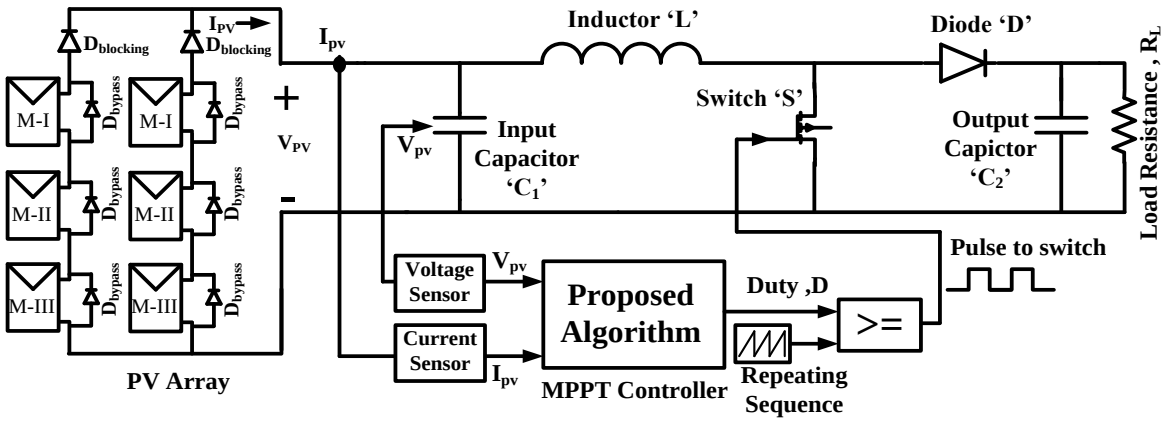

Figure 5.4 Application of PV array to boost converter with MPPT controller.

Table 5.2 Designed parameters of algorithms and boost converter

Particulars	**Specifications**
Proposed	$\beta = 1.5$
PSO	$C_{1,min} = 1$, $C_{1,max} = 2$, $C_{2,min} = 1, C_{2,max} = 2$, $w_{min} = 0.1,\ w_{max} = 1.$
Boost coverter	$L = 1.5mH, C_1 = C_2 = 100\mu F$, $F_s = 10kHz,$ Diode $-$ MUR860, MOSFET $-$ IRFP460, 100Ω 10A Variable Rheostat load.
Sampling period (T_s)	Population size $= 3$ For simulation $T_s = 50ms$, For experimental $T_s = 200ms$.

5.4.1 Simulation Results of 3S2P PV Array Configuration

In the PV array configuration, six PV modules are used to form 3S2P, as shown in Figure 5.2 (a); in pattern-1 (case-1) the irradiance of first, second and third rows are 500W/m^2, 500W/m^2 and 200W/m^2. Out of that two irradiances are same, while one is different. Therefore the corresponding P-V curve has two peaks where the first peak (left peak) is global peak, shown in Figure 5.3 (a). Consider 3S2P as PV source to boost converter and operate switch (MOSFET) of boost converter by providing pulse from the proposed Jaya-LF algorithm; the Jaya-LF will execute based on V_{pv} and I_{pv} of PV array output voltage and current. The PSO algorithm is applied to the proposed system and the tracking time to reach global MPP (110.60 Watt) is 1.38 sec with 10 iterations. The time required is substantial for PSO due to three tuning parameters, these being weight and acceleration parameters (i. e. , w, C_1 and C_2) which are unable to find optimum values during tracking. In order to reach global MPP (110.60 Watt) of Jaya algorithm, the time required is 0.75 sec with 5 iterations and many transient oscillations. *The proposed Jaya-LF algorithm only takes 0.37 sec along with 3 iterations for GMPP (110.60 Watt) of pattern-1. The Jaya-LF yields better results compared to conventional Jaya and PSO algorithms in terms of tracking time and number of iterations for GMPPT*. The proposed Jaya-LF algorithm gives better result compared to PSO and Jaya algorithm because the PSO has more control parameters to get global optima, whereas with PSO, the random numbers help to jump from one location to another location for initial searching, implying the exploration process is good. In order to converge to global peak, it

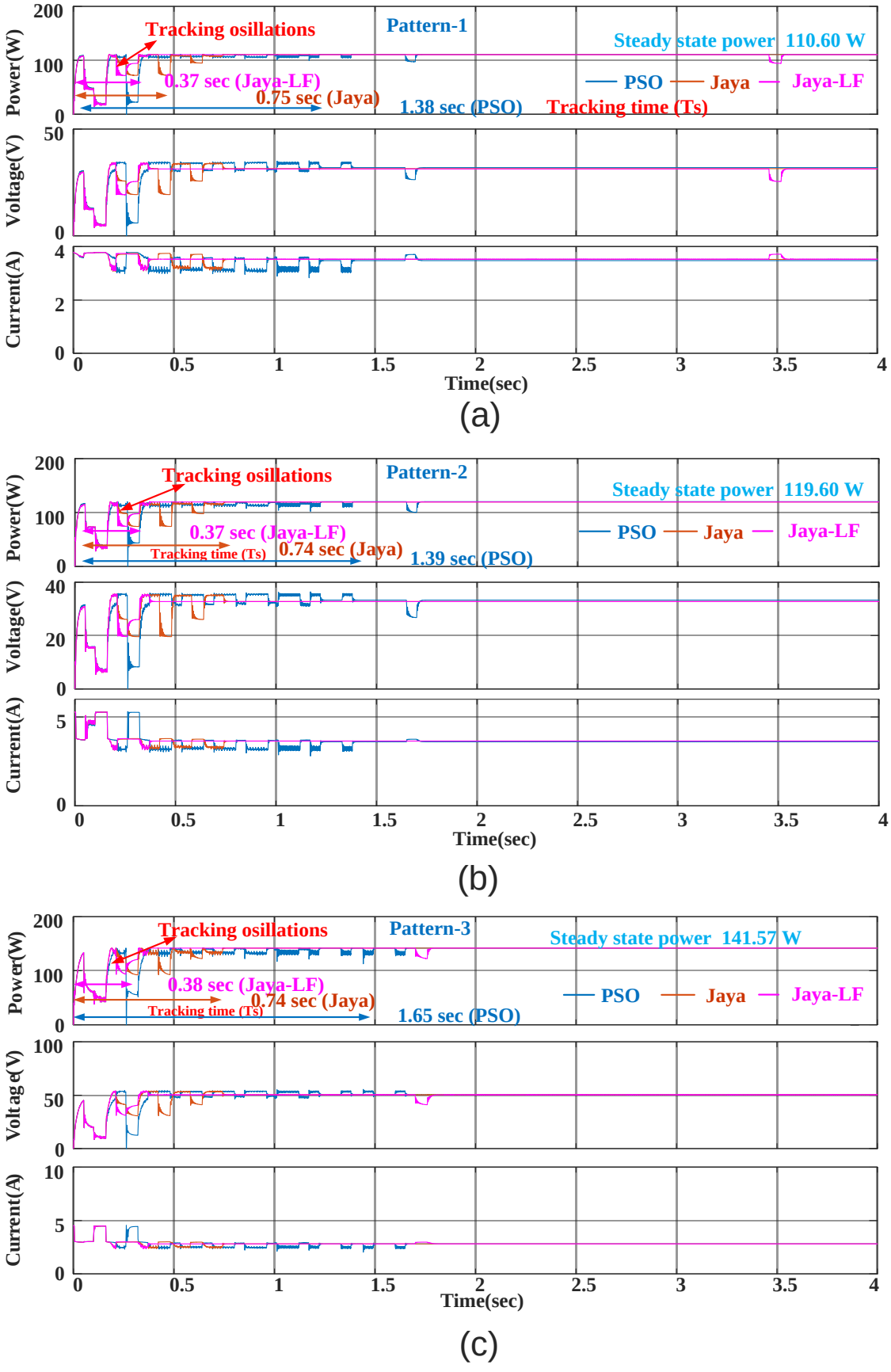

Figure 5.5 Simulation results for 3S2P PV array configuration during shading: (a) Pattern-1, (b) Pattern-2, and (c) Pattern-3.

takes time due to three tuning factors (w, C_1, C_2) ; because the algorithm is unable to arrive at the exact value through iterations, it takes more time to converge, making the exploitation process poor. Jaya algorithm is highly easy to work with and efficient in this aspect and does not have many specific parameters for convergence. Its exploration process is good with the presence of random numbers, but exploitation process is poor due to fewer control parameters. The variation at steady-state power is not constant but oscillating, and so the exploitation is poor. In order to improve exploration and exploitation process, lévy flights are added to Jaya algorithm. The Lévy Flights (LF) imply random nature, which can be implemented along with Jaya algorithm for rapid convergence. By employing lévy flights on updating the population, variables are able to take short jumps and long-distance jumps to improve the process of exploitation and exploration. The simulation results of pattern-1 are shown in Figure 5.5 (a) and performance details are presented in Table 5.3. Similar to pattern-1, the other two patterns of middle peak and right peak called patten-2 and pattern-3 of 3S2P configuration have also been applied as PV source to converter and its irradiance levels and performance results are shown in Table 5.1 and Table 5.3, respectively. The P-V curves and simulation results are shown in Figure 5.3 (a) and Figures 5.5 (b) & 5.5 (c). In these cases also, Jaya-LF overcomes the disadvantages of PSO and Jaya algorithm. Further, the tracking performances of these three MPPT algorithms can be described by MPPT efficiency η, which can be calculated as follows:

$$\text{MPPT efficiency } \eta = \frac{P_1}{P_2} \times 100\% \tag{5.12}$$

Term P_1 means the output power is in the stable mode of the PV system under the Jaya-LF MPPT algorithm and P_2 is the maximum output power of the PV array pattern under a certain PSC conditions.

5.4.2 Simulation Results of 4S2P PV Array Configuration

In the setup, the PV array is implemented with eight PV modules to form 4S2P as shown in Figure 5.2 (b). System complexity is increased compared to 3S2P. The 4S2P array is taken into consideration in order to prove that the proposed method works well for complex PV configurations also. The three patterns are first, second and third peaks from left of P-V curve as shown in Figure 5.3 (b) and its irradiance (W/m^2) levels shown in Table 5.1. In pattern-4,

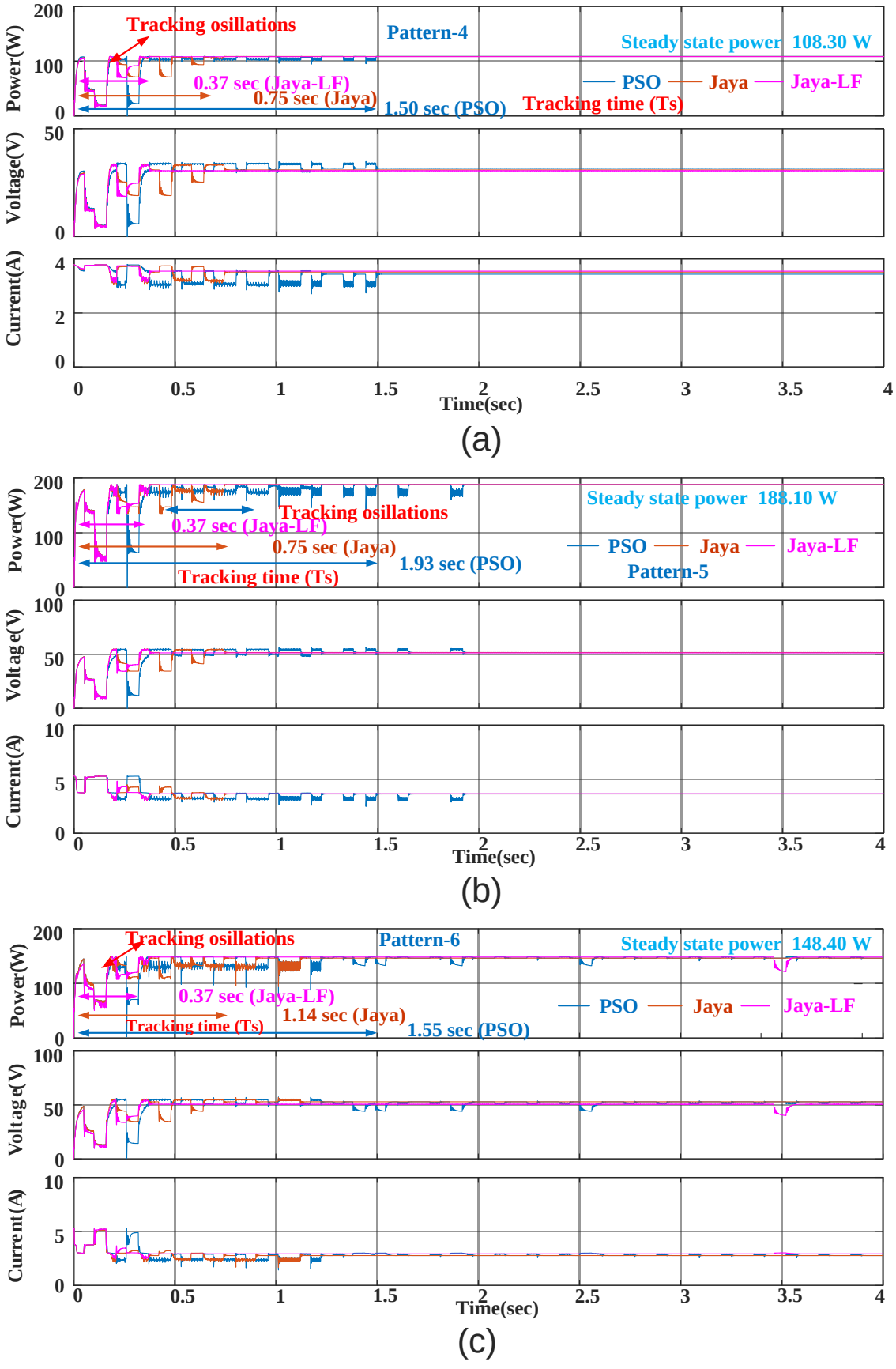

Figure 5.6 Simulation results for 4S2P PV array configuration during shading of: (a) Pattern-4, (b) Pattern-5, and (c) Pattern-6.

the PSO algorithm takes time to locate global peak power (108.30Watt) in 1.5 sec with 10 iterations. Jaya algorithm tracks global peak power (108.30Watt) in 0.75 sec with 5 iteration while *the proposed Jaya-LF algorithm takes 0.37 sec to track global peak (108.30Watt) with 3 iterations. So with 4S2P array also, the proposed algorithm gives best performance compared to Jaya and PSO in terms of tracking oscillation, tracking time with fewer iterations and without tuning parameters*. The advantages of pattern-5 and patten-6 are the same as that of pattern-4. The simulation results of voltage, current and power 4S2P waveforms are shown in Figure 5.6, while the simulation performance of 4S2P PV array results is presented in Table 5.3.

Table 5.3 Simulation performance analysis of 3S2P, and 4S2P PV array configurations

Technique/ Parameter	**Rated Power of PV array (Watt)**	**Extracted Output Power of PV (Watt)**	**Tracking time(sec)**	**Iterations**	**Tracking Efficiency (%)**
Proposed	110.97 Pattern-1	110.60	**0.37**	**03**	99.66
Jaya		110.60	0.75	05	99.66
PSO		110.60	1.38	10	99.66
Proposed	120.13 Pattern-2	119.60	**0.37**	**03**	99.55
Jaya		119.60	0.74	05	99.55
PSO		119.60	1.39	10	99.55
Proposed	141.85 Pattern-3	141.57	**0.38**	**03**	99.80
Jaya		141.57	0.74	05	99.80
PSO		141.57	1.65	11	99.80
Proposed	108.89 Pattern-4	108.30	**0.37**	**03**	99.45
Jaya		108.30	0.75	05	99.45
PSO		108.30	1.50	10	99.45
Proposed	188.14 Pattern-5	188.10	**0.37**	**03**	99.97
Jaya		188.10	0.75	05	99.97
PSO		188.10	1.93	11	99.97
Proposed	148.60 Pattern-6	148.40	**0.37**	**03**	99.86
Jaya		146.30	1.14	08	98.45
PSO		146.30	1.55	11	98.45

Simulation Results of Pattern-1 and Pattern-2 during Dynamics: The dynamics in simulation are observed from pattern-2 to pattern-1 in comparison with PSO, Jaya and the proposed Jaya-LF algorithms. Actually, when one of the shading pattern-2 is considered it will track global peak power (119.60Watt) with the proposed Jaya-LF method, maintain constant power up to 4 sec. After that pattern-1 is applied to the system and then the proposed Jaya-LF algorithm recognizes the system as per the power equation given in (5.9). If it is confirmed by proposed algorithm that there has been a change of pattern, the algorithm has

to re-initialize the initial parameters and then start tracking new global peak power (110.60Watt) according to pattern-1. *Finally, the Jaya-LF method proves advantageous under dynamic conditions compared to Jaya and PSO algorithms results as shown in Figure 5.7 in terms of tracking time and tracking oscillations with reduced number of iterations.*

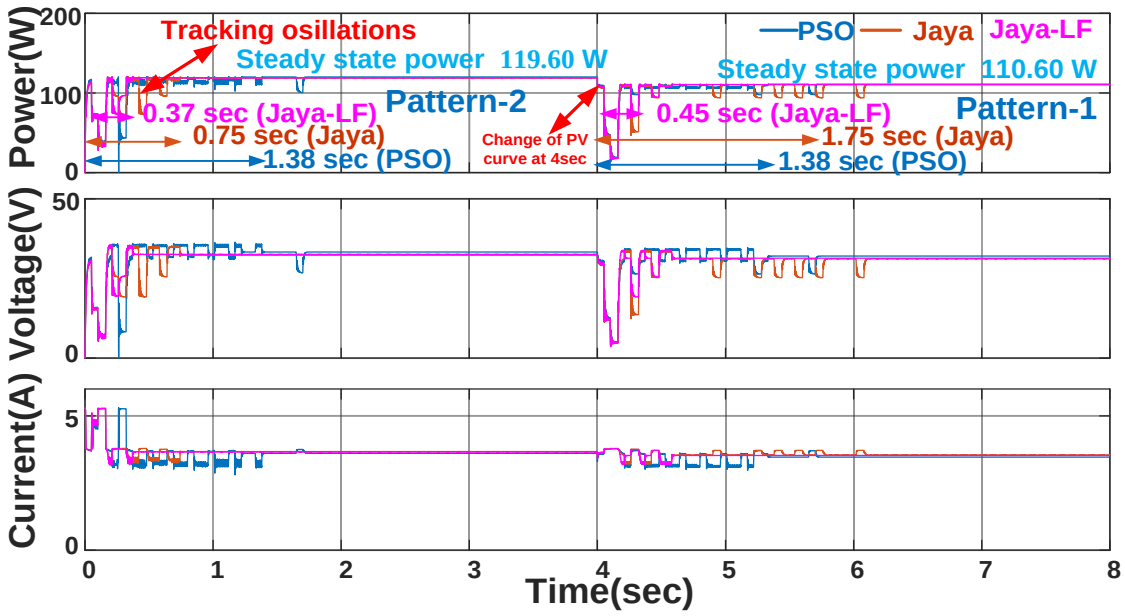

Figure 5.7 Simulation results for proposed Jaya-LF algorithm compared with Jaya, and PSO algorithms during dynamics of shading pattern-1, and shading pattern-2 of 3S2P PV array.

5.5 Experimental Results

An experimental prototype of PV system design is shown in Figure 5.8; it consists of programmable PV simulator followed by boost converter. In real time, the proposed Jaya-LF algorithm can be implemented by dSPACE 1104 controller installed using MATLAB software. Here the PV array configurations were replaced by programmable PV simulator (Magna power electronics XR600-9.9/415+PPPE+HS). The pulse generation for boost converter switch emerged from control algorithm provided by sensing voltage (LV25-p) and current sensor (LA55-p) from output of PV simulator. The parameters considered for experiments were the same as for simulation and the advantages of the proposed Jaya-LF algorithm was verified to be the same as observed during simulation work compared to Jaya and PSO algorithms with six cases of PV patterns under partial shading conditions for GMPPT.

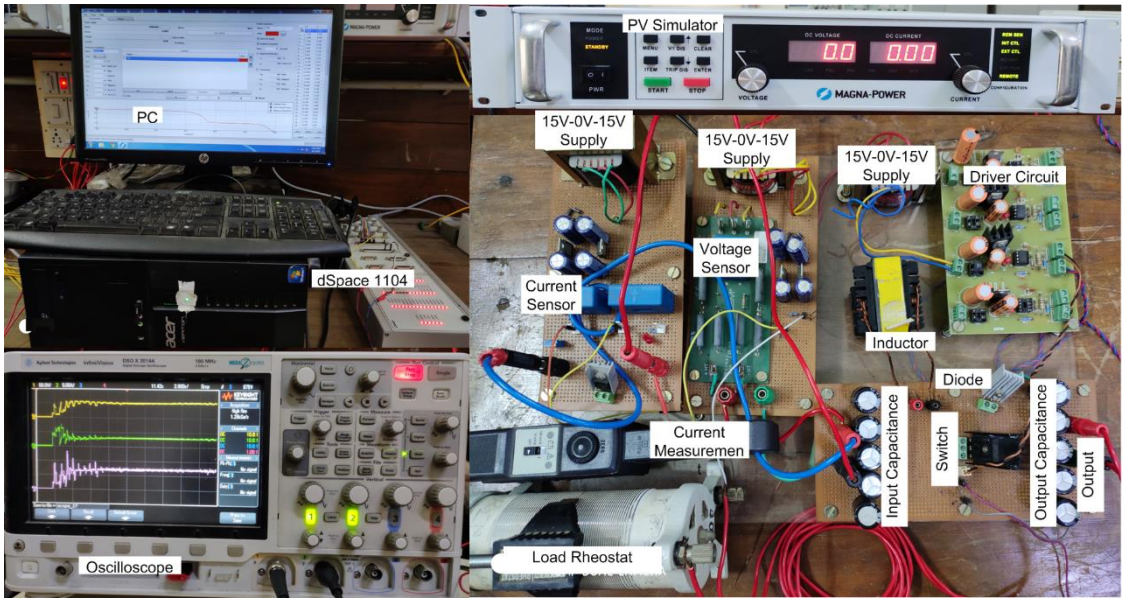

Figure 5. 8 Experimental setup for proposed Jaya-LF algorithm.

5.5.1 Experimental Results of 3S2P PV Array Configuration

The PV array patterns were applied through the PV simulator. In the 3S2P configuration, three PV patterns of left, middle and right peaks were considered in this configuration. In order to verify maximum voltage and maximum current with respect to global power of a particular PV array pattern, the screen shot of P-V curve operating point and I-P curve was taken from PV simulator software by operating the point on global peak on each curve and placing that in each experimental result below the right side bottom corner. The performance results of 3S2P are presented in Table 5.4.

In pattern-1 (case-1), the PSO algorithm tracks global power of 95.87 Watt with a tracking time of 6.5 sec in 11 iterations and from the results shown in Figure 5.9, both tracking and steady state oscillations were observed. The tracking time was more in PSO due to three tuning parameters (w, C_1 and C_2). The power obtained by Jaya algorithm was 110.05 Watt with a tracking time of 4.75 sec to reach global peak of P-V curve in 8 iterations; the observations from using Jaya algorithm are: oscillationsand power loss during initial tracking due to fewer specific parameters. *The proposed Jaya-LF algorithm consumes power of 110.40Watt with a time of 2.5 sec and takes 4 iterations, while showing fewer oscillations during tracking compared to Jaya and PSO algorithm. So during experiment phase too, Jaya-LF outperformed both Jaya and PSO algorithm in terms of minimum tracking time, fewer iterations and without using tuning parameter*. Similar advantages were obtained for

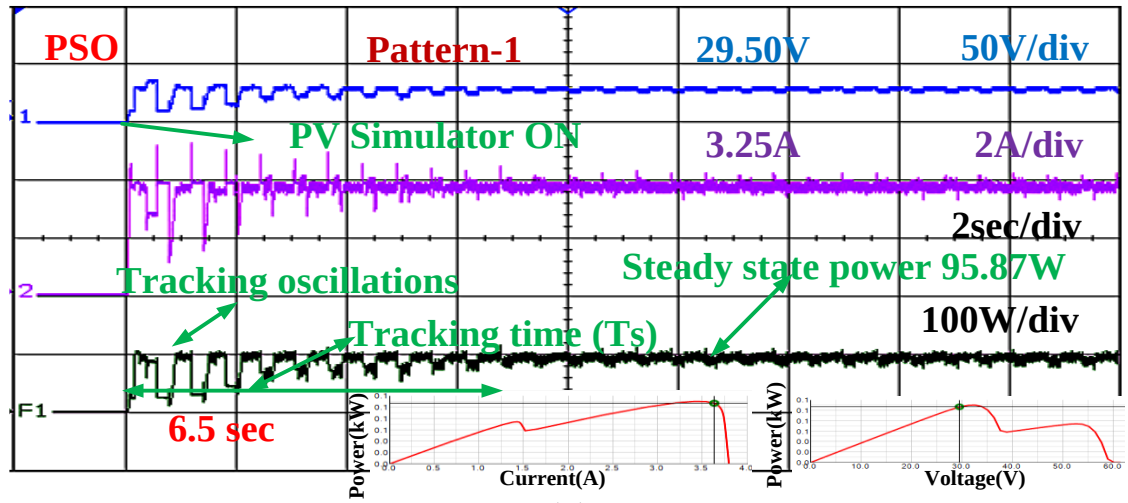

(a)

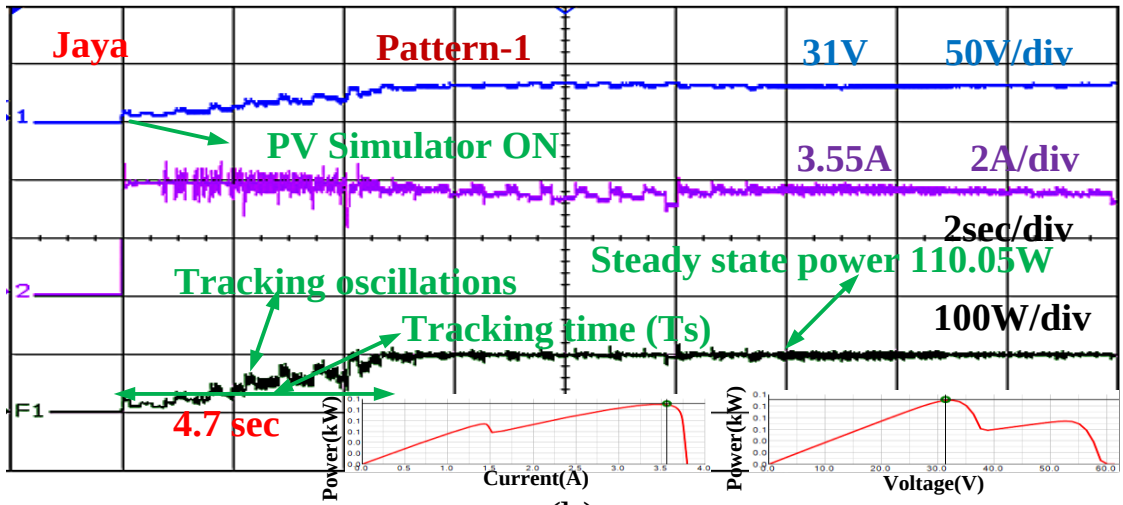

(b)

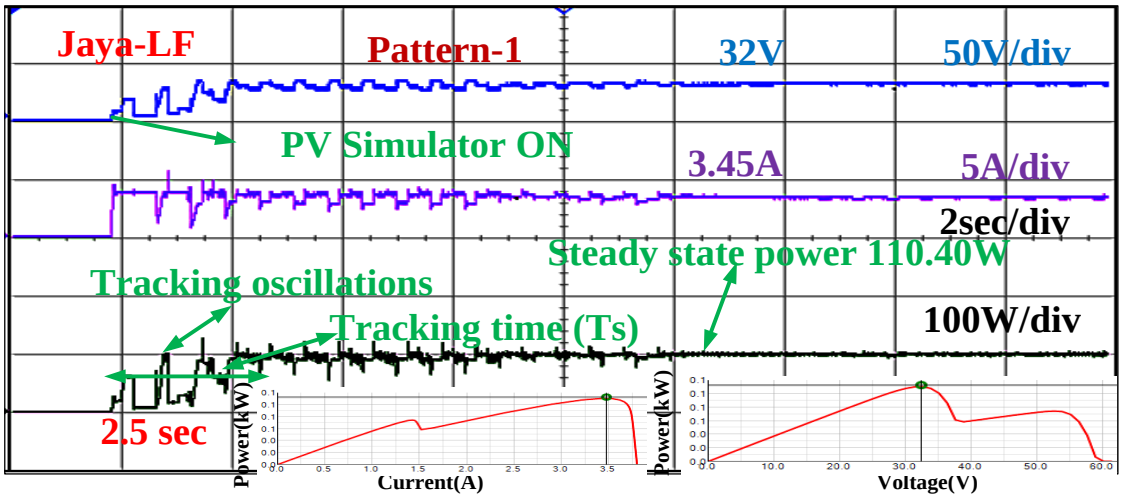

(c)

Figure 5.9 Experimental results for shading pattern-1 of 3S2P PV array of: (a) PSO, (b) Jaya, and (c) Proposed Jaya-LF algorithm.

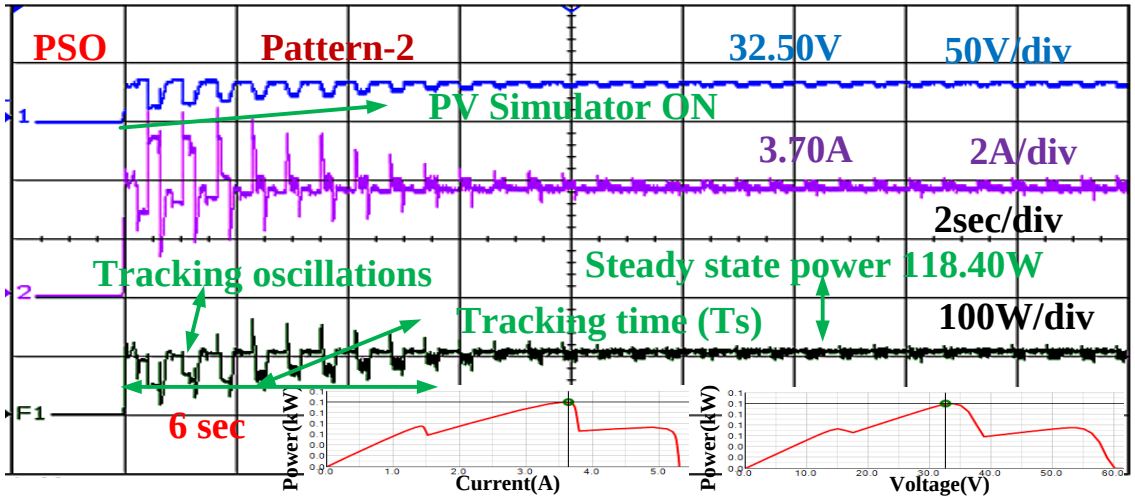

(a)

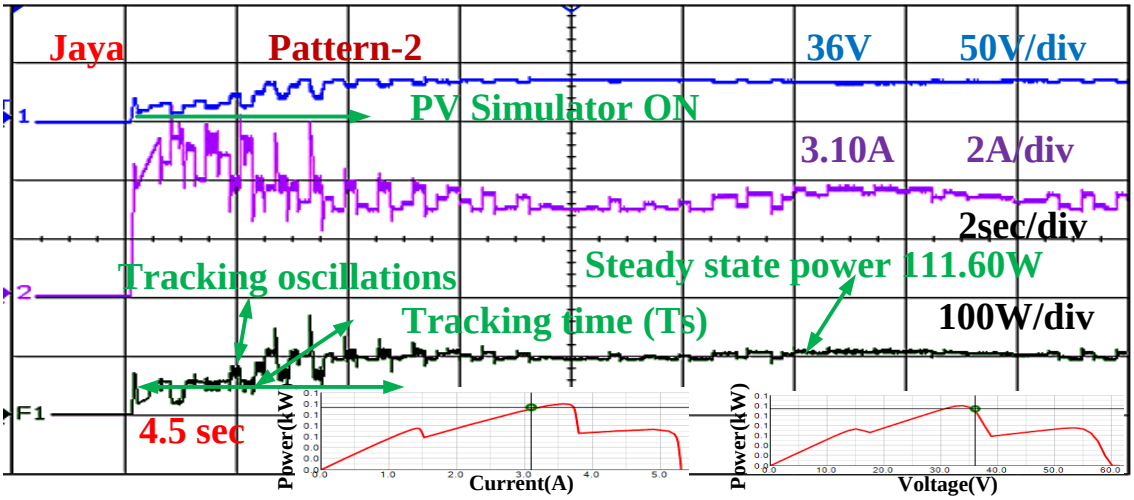

(b)

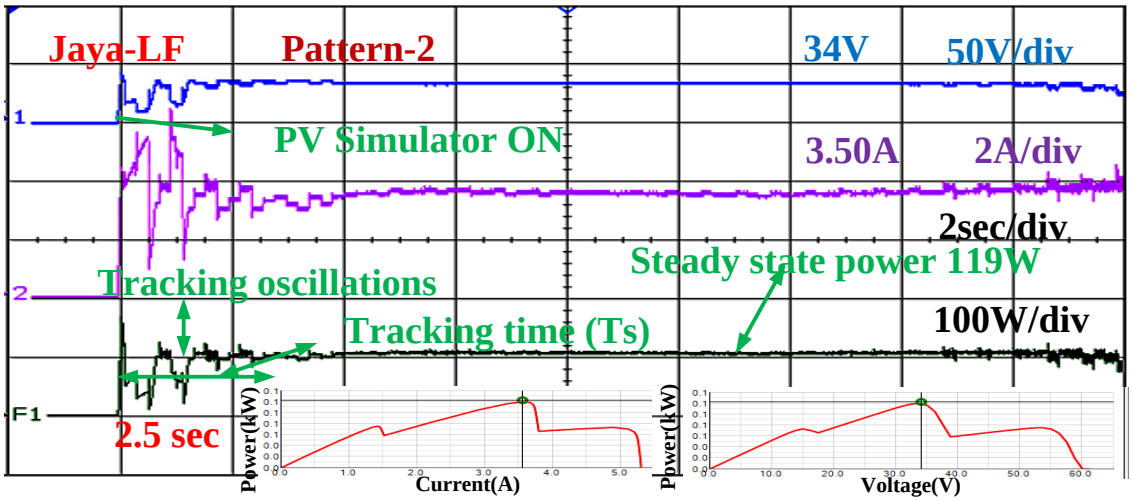

(c)

Figure 5.10 Experimental results for shading pattern-2 of 3S2P PV array of: (a) PSO, (b) Jaya, and (c) Proposed Jaya-LF algorithm.

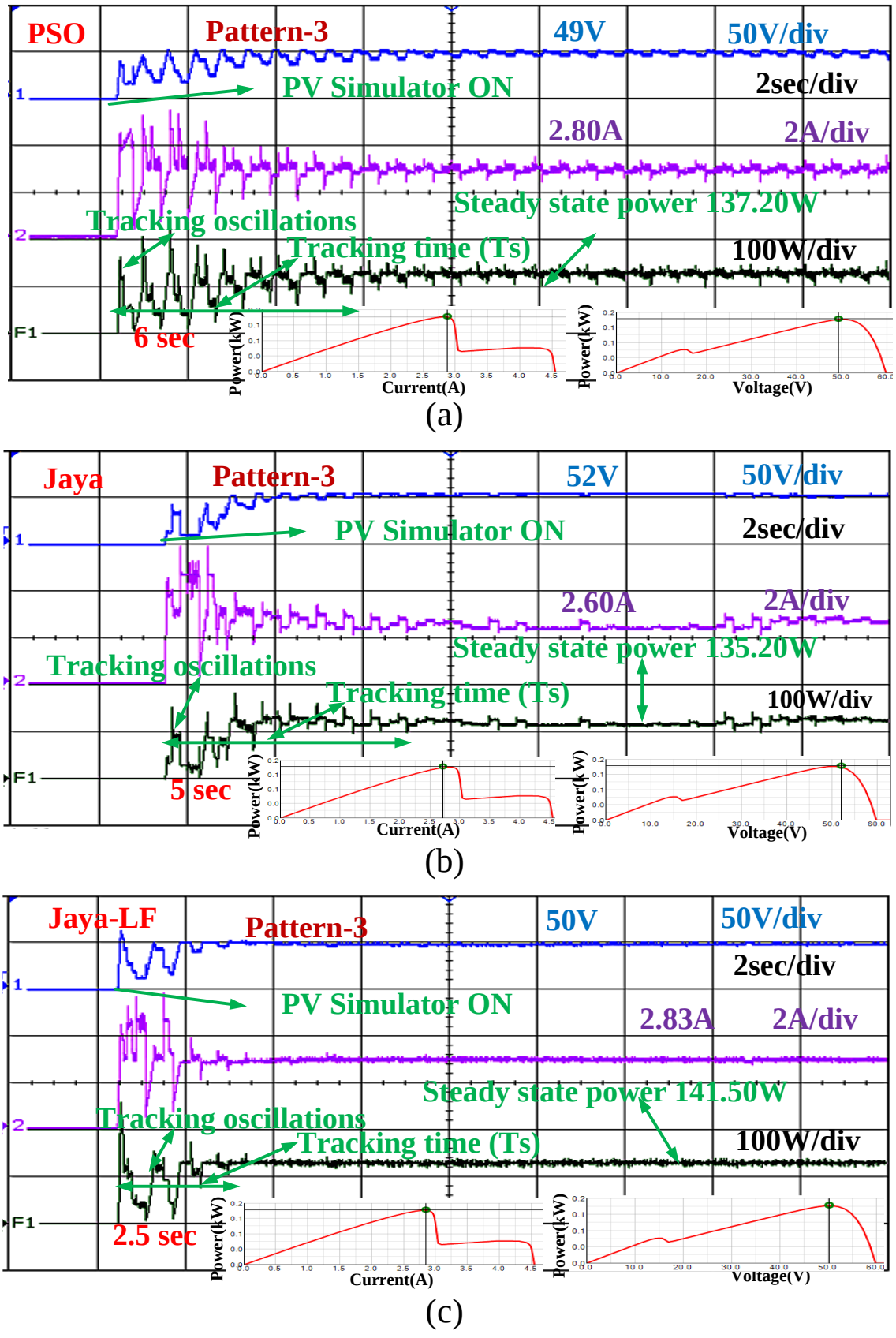

Figure 5.11 Experimental results for shading pattern-3 of 3S2P PV array of: (a) PSO, (b) Jaya, and (c) Proposed Jaya-LF algorithm.

pattern-2 of PSO, Jaya and the proposed Jaya-LF algorithms, with tracking time of (6 sec, 4.5 sec and 2.5 sec) and iterations of (10, 8 and 4) respectively. In pattern-3, the tracking time was (6, 5 and 4) sec with (10, 9 and 4) iterations for PSO, Jaya and the proposed Jaya-LF algorithms. The results are shown in Figures 5.10 & 5.11 for pattern-2 and pattern-3, and the corresponding results are presented in Table 5.4.

5.5.2 Experimental Results of 4S2P PV Array Configuration

The first, second and third peak from left side of P-V curve of 4S2P configuration were considered. In pattern-4, the power generated by PSO is 106.75Watt in 5 sec along with 9 iterations to reach GMPPT, Jaya tracked power of 104Watt in 4 sec and 7 iterations for GMPPT while *the proposed Jaya-LF algorithm tracks global power of 107.10Watt in 2 sec and 3 iterations*. The proposed Jaya-LF algorithm overcomes the problems connected with Jaya and PSO. Its experimental results are shown in Figure 5.12 and details presented in Table 5.4.

In a similar way, in pattern-5, Jaya, PSO and the proposed Jaya-LF algorithms track GMPP with a time of (6, 5 and 3) sec and iterations of (10, 9 and5), respectively. In pattern-6, GMPP is located with (6.5, 5.5 and 2) sec and in (11, 9 and 3) iterations for PSO, Jaya and proposed Jaya-LF algorithm, respectively. The results of pattern-5 and pattern-6 are shown in Figures 5.13 & 5.14 while a detailed explanation is provided in Table 5.4. The operating point on global peak of P-V curve I-P curve are shown in the respective results on right side bottom corner for the sake of convenience.

Experimental Results of Pattern-1 and Pattern-2 during Dynamics: Verification of the proposed Jaya-LF algorithm for sudden change of shading occurs on PV system. According to Figure 5.15 pattern-2 was applied tracks global power of (118.80, 112.20 and 119)Watt with a tracking time (7, 5.5 and 3) sec of PSO, Jaya and proposed Jaya-LF algorithm and continues up to (15, 12 and 16) sec then suddenly the pattern-1 was initiated immediately the algorithm recognize newly updated PV array based on power equation (5.9) , the algorithm has to re-initialize the initial parameters and tracks the GMMP of pattern-1 (110.40, 105.60 and 110.40)Watt with time of (9, 6 and 3) sec. From this, the proposed Jaya-LF algorithm performs well compared with PSO and Jay algorithms even in dynamic conditions also.

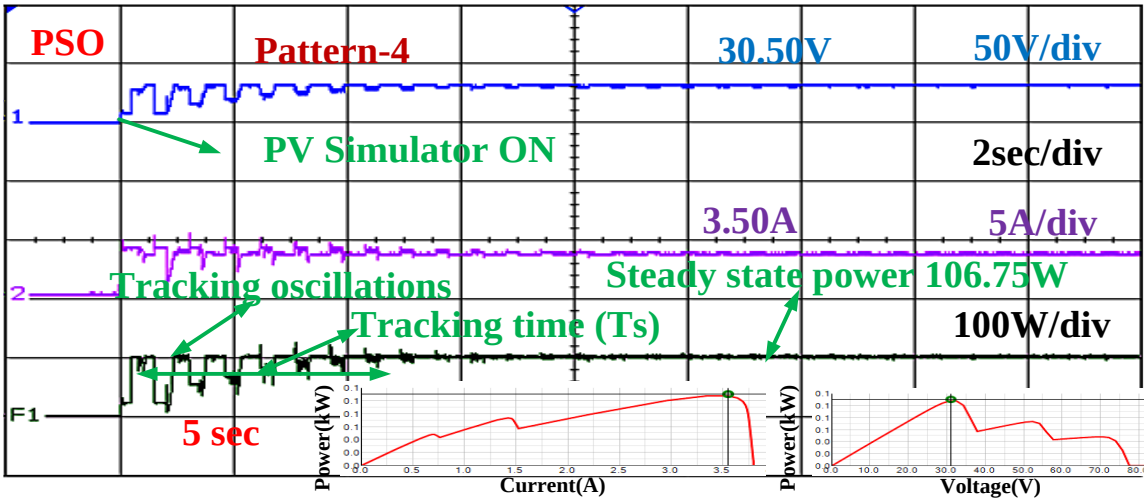

(a)

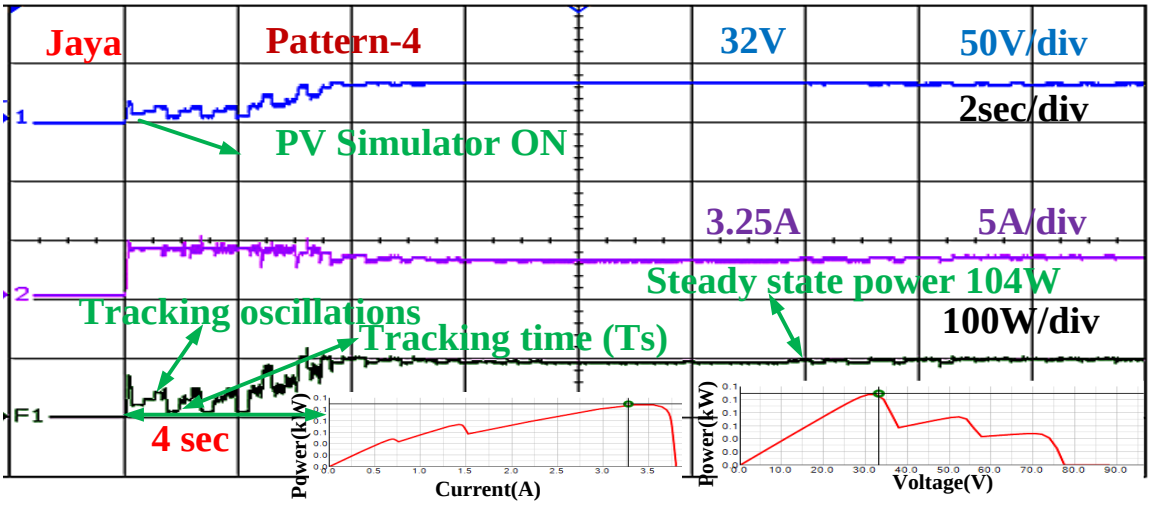

(b)

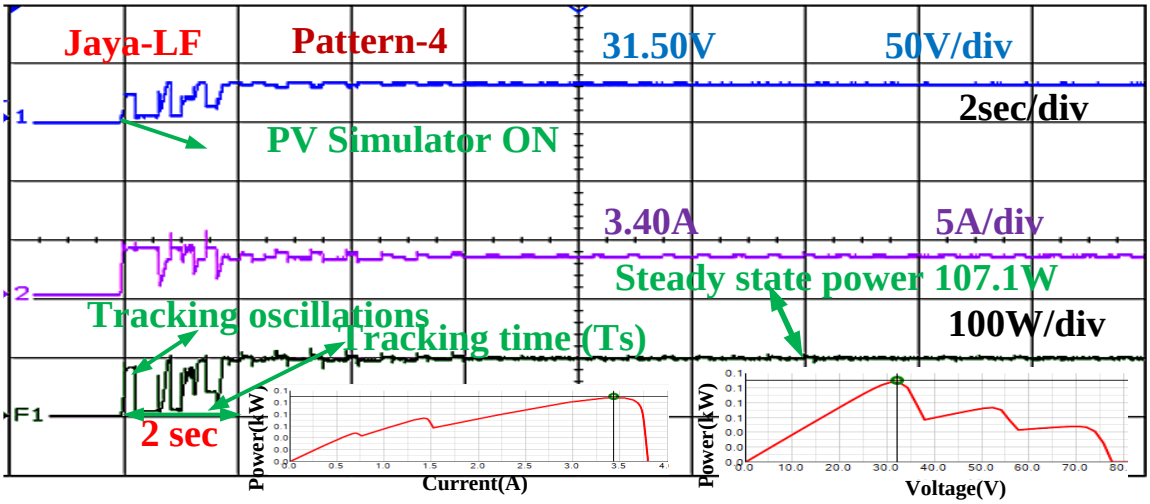

(c)

Figure 5.12 Experimental results for shading pattern-4 of 4S2P PV array of: (a) PSO, (b) Jaya, and (c) Proposed Jaya-LF algorithm.

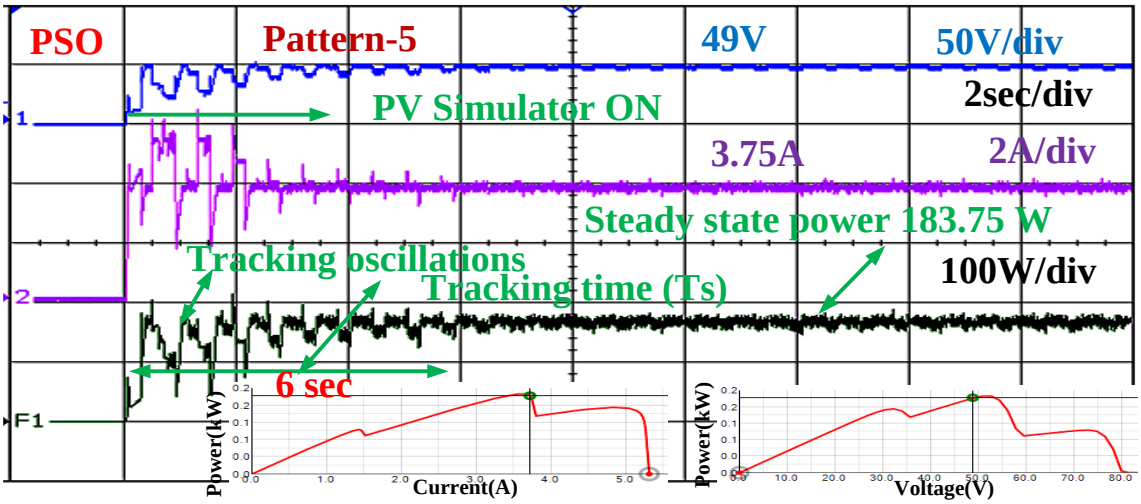

(a)

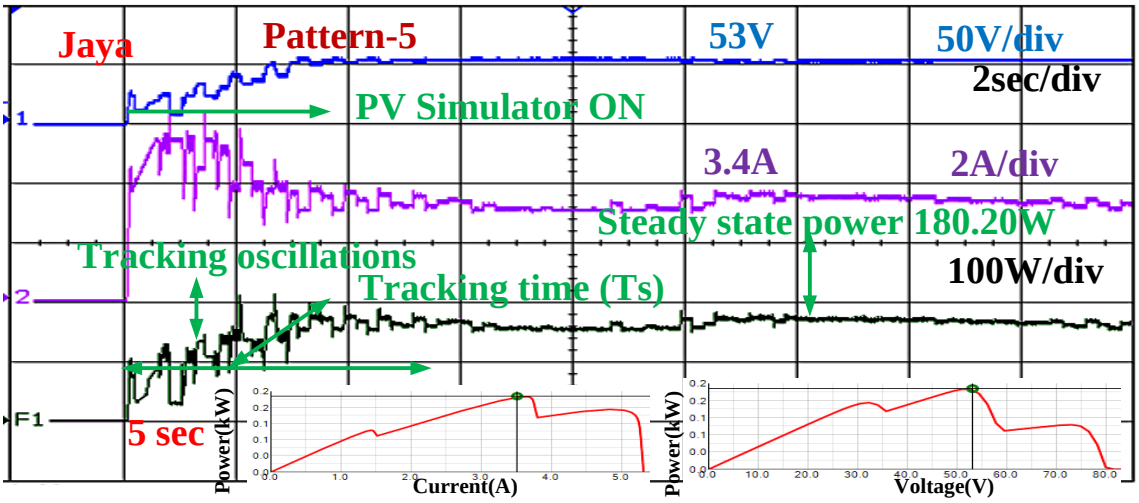

(b)

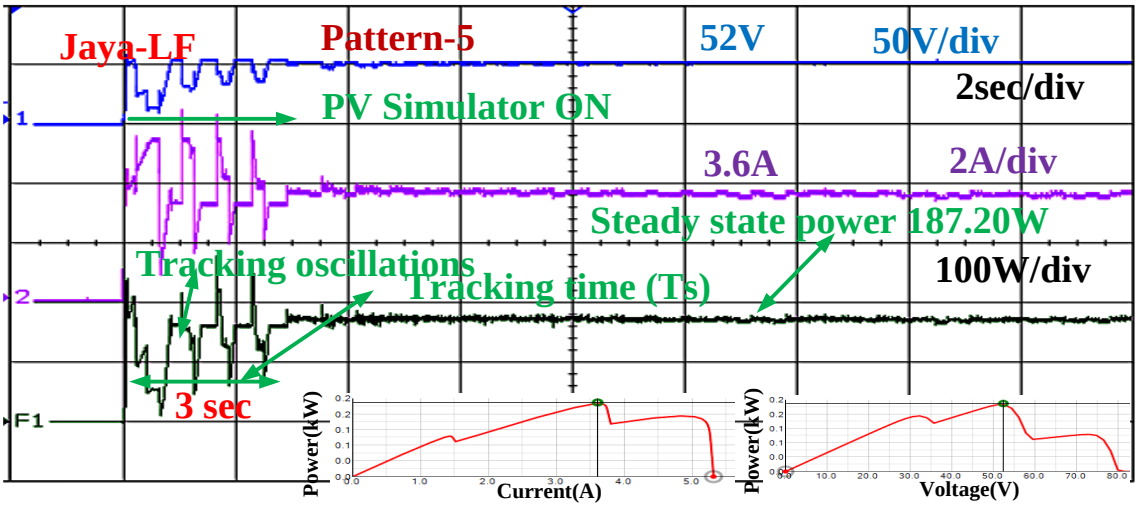

(c)

Figure 5.13 Experimental results for shading pattern-5 of 4S2P PV array of: (a) PSO, (b) Jaya, and (c) Proposed Jaya-LF algorithm.

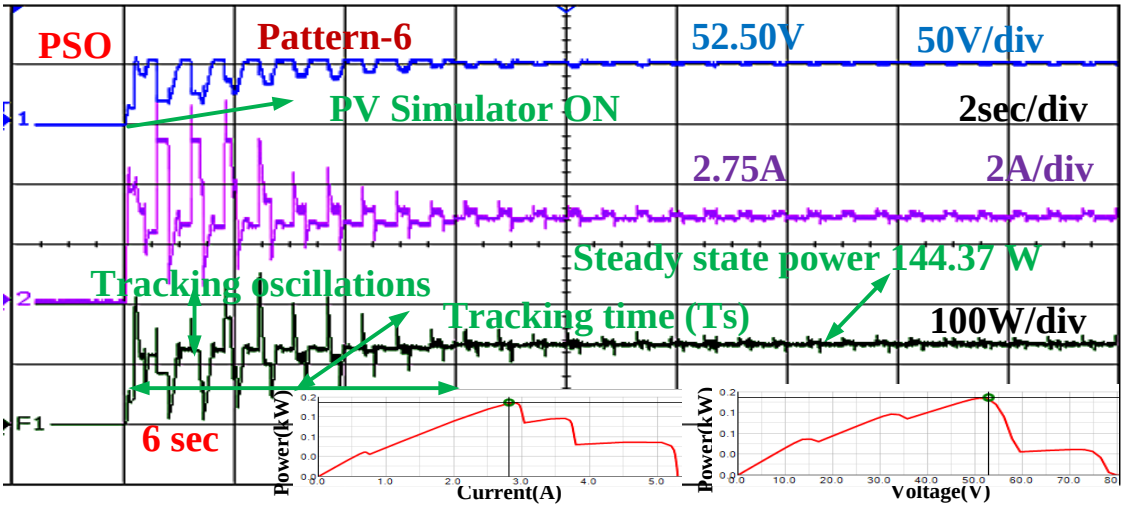

(a)

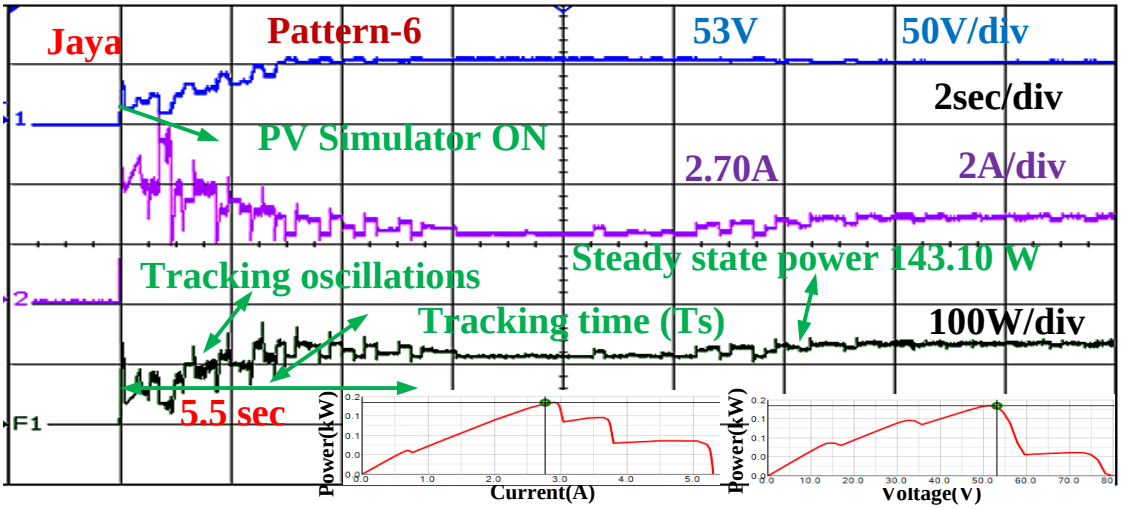

(b)

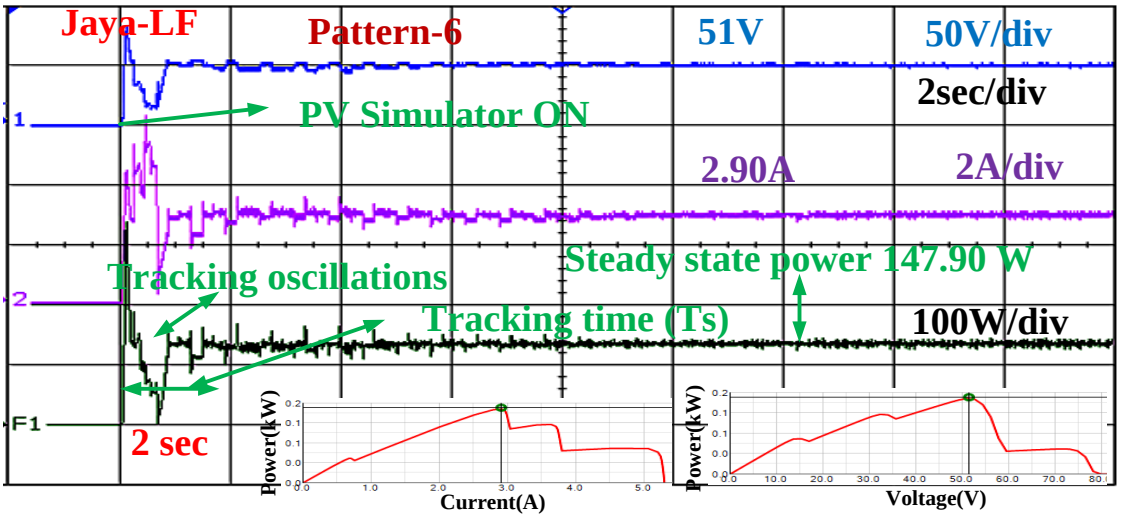

(c)

Figure 5.14 Experimental results for shading pattern-6 of 4S2P PV array of: (a) PSO, (b) Jaya, and (c) Proposed Jaya-LF algorithm.

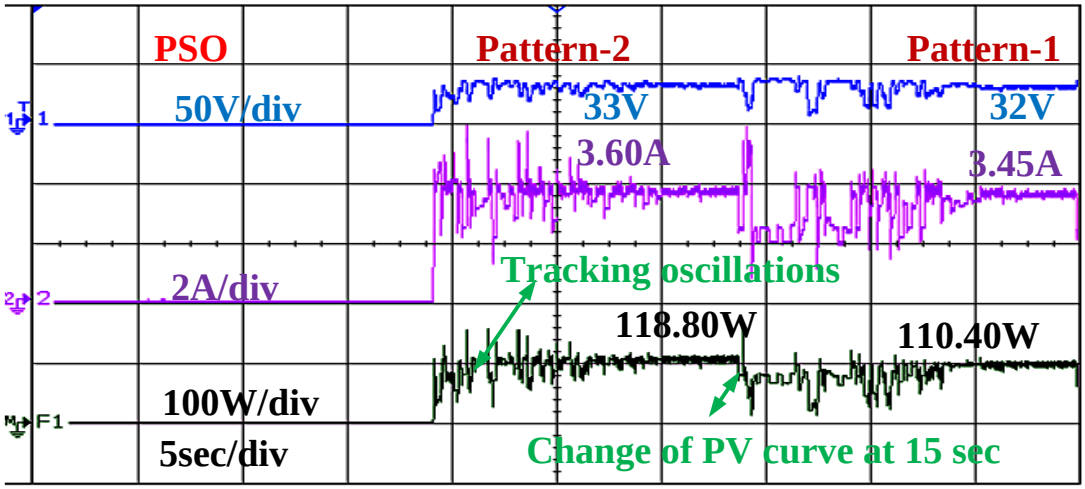

(a)

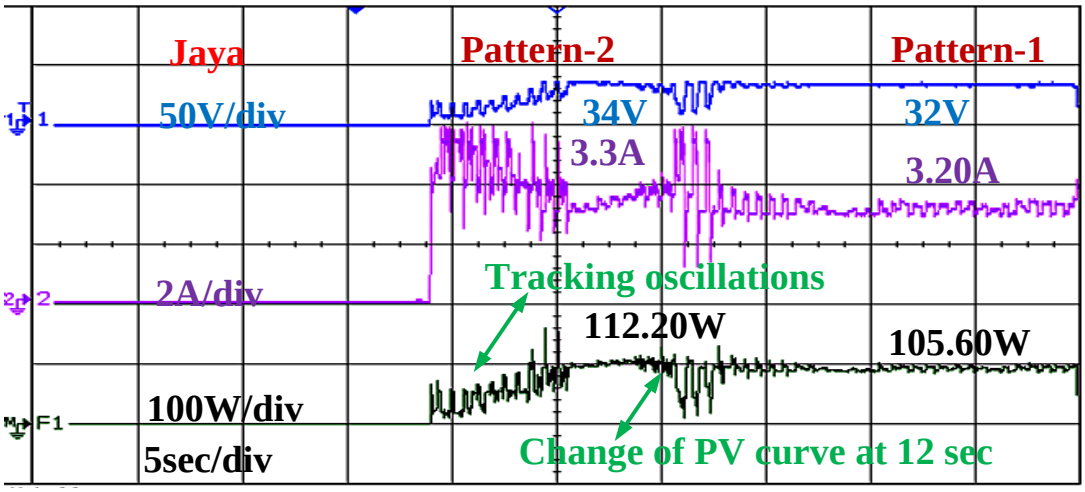

(b)

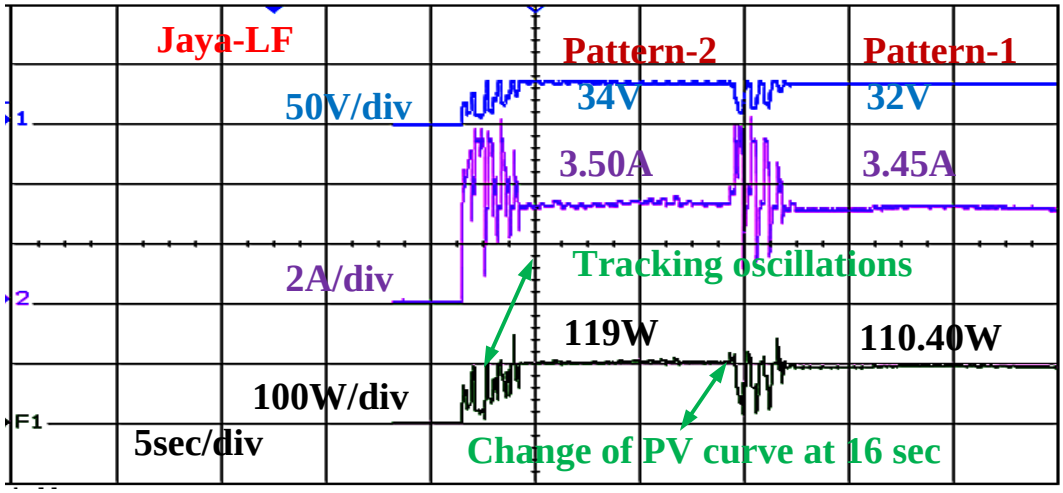

(c)

Figure 5.15 Experimental results during dynamics of shading pattern-1, and shading pattern-2 of 3S2P PV array of: (a) PSO, (b) Jaya, and (c) Proposed Jaya-LF algorithm.

Table 5.4 Experimental performance analysis of 3S2P, and 4S2P PV array configurations

Technique/ Parameter	Rated Power of PV array (Watt)	Extracted Output Power of PV (Watt)	Tracking time(sec)	Iterations	Tracking Efficiency (%)
Proposed	110.97 Pattern-1	110.40	**2.5**	**04**	99.48
Jaya		110.05	4.7	08	99.17
PSO		95.87	6.5	11	86.39
Proposed	120.13 Pattern-2	119.00	**2.5**	**04**	99.05
Jaya		111.60	4.5	08	92.89
PSO		118.40	6.0	10	98.55
Proposed	141.85 Pattern-3	141.50	**2.5**	**04**	99.75
Jaya		135.20	5.0	09	95.31
PSO		137.20	6.0	10	96.72
Proposed	108.89 Pattern-4	107.10	**2.0**	**03**	98.35
Jaya		104.00	4.0	07	95.50
PSO		106.75	5.0	09	98.03
Proposed	188.14 Pattern-5	187.20	**3.0**	**05**	99.50
Jaya		180.20	5.0	09	95.77
PSO		183.75	6.0	10	97.66
Proposed	148.60 Pattern-6	147.90	**2.0**	**03**	99.52
Jaya		143.10	5.5	09	96.29
PSO		144.37	6.0	11	97.15

5.6 Comparative Study of Proposed Jaya-LF Algorithm with Existing Algorithms

The PSO algorithm takes more time to capture global peak of multiple peaks on a P-V curve due to (w, C_1, C_2) factors as these factors contribute to the inability of tuning optimum value during the course of iterations to attain global peak location faster [20]. Adaptive Radial Movement Optimization (ARMO) tracks location(s) of GMPP faster but it is implemented by considering dependent initial particle, the particles are more than five and three tuning parameters [33]. Grey Wolf Optimization (GWO) algorithm is applied for GMPP with one tuning parameter over the course of iterations, but the parameters are not re-initialized when the change of PV pattern occurs and there is delay in convergence as well due to linear control tuning parameter [29]. The recent a Hybrid between the Adaptive Perturb and Observe and Particle Swarm Optimization (HAPO & PSO) algorithm have rapid convergence but the initial parameters are dependent [87]. The natural cubic-spline-guided Jaya (S-Jaya) algorithm, promises improved performance compared to Jaya algorithm but it is implemented with five dependent parameters [25]. Modified Particle Velocity-based Particle Swarm

Optimisation (MPV-PSO) algorithm performs better compared to PSO, the reason being MPV-PSO is achieved by removing weight factor while cognitive factors are updated with current particle by tuning them with PV system voltage [24]. The Hybrid GWO and Fuzzy Logic Controller (GWO-FLC) algorithm is considered for higher power levels with an average of 5 to 10 member initial population [30]. Due to more particles initialization, there is computational burden on the system per each iteration. In this chapter, the proposed Jaya-LF algorithm enables faster convergence compared to Jaya and PSO methods. The Jaya algorithm response is slow for GMPPT application because of fewer specific parameters. In order to improve the performance of Jaya, it is represented by a combination of Lévy flight for fast convergence. The Lévy Flights (LF) imply random nature, which can be implemented along with Jaya algorithm for rapid convergence. By employing Lévy Flights on updating the population, variables are able to take short jumps and long-distance jumps to improve the process of exploitation and exploration.The concept behind LF is searching in small steps for exploitation process while taking a long jump for exploration process from one place to another before commencing searching; this improves the overall performance of Jaya-LF algorithm. The comparison of the proposed Jaya-LF technique with seven recent GMPPT techniques was made, details of which given in Table 5.5, and the results of proposed Jaya-LF algorithm compared with Jaya, PSO are also shown in Figure 5.16 using experiment based tracking time and iteration with respect to each PV pattern of three algorithms.

Table 5.5 Qualitative comparison of the proposed Jaya-LF algorithm with existing MPPT Algorithms

Parameters/ Method	PSO [20]	ARMO [33]	GWO [29]	HAPO & PSO [87]	S-Jaya [25]	MPV-PSO[24]	GWO-FLC [30]	**Proposed**
Tracking speed	Moderate	Fast	Moderate	Fast	Fast	Fast	Fast	**Fast**
Iterations	More	Less	Moderate	Less	Less	Less	Less	**Less**
Tuning parameters	3	3	1	Nil	Nil	2	1	**Nil**
Initial particles	Independent	Dependent	Independent	Dependent	Dependent	Dependent	Independent	**Independent**
Population size	5	> 5	3	3	5	3	> 5	**3**
Efficiency	High	High	High	High	High	High	High	**Very High**
Re-initialization	Conside red	Conside red	Not conside red	Conside red	Conside red	Conside red	Conside red	**Conside red**

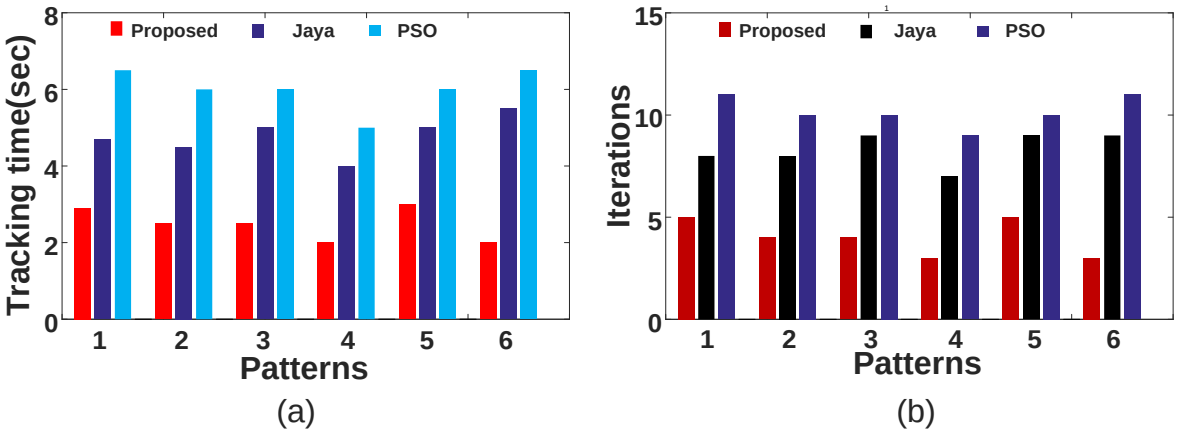

Figure 5.16 Experimental results comparison of proposed Jaya-LF algorithm with PSO, and Jaya algorithms of: (a) Tracking time, and (b) Iterations with respect to each shading pattern.

5.7 Results and Conclusions

In this chapter a novel Jaya algorithm based on Lévy Flight (Jaya-LF) was proposed, simulated and implemented experimentally for tracking global peak power during partial shading of PV arrays. *The proposed Jaya-LF algorithm tracks global peak power with fewer iterations and lower convergence time. The oscillations at steady state and transient state are reduced without any tuning parameter; the three initial particles are independent of the PV system*. To highlight the benefits of the proposed Jaya-LF algorithm, a detailed verification with conventional Jaya and PSO algorithms is presented. The proposed Jaya-LF algorithm performed far better than Jaya and PSO methods and could track GP under all shaded conditions of PV array with superior performance even under dynamic shaded conditions, with higher and more reliable efficiency. The reduced control parameters are considered in the proposed Jaya-LF algorithm compared with MGWO algorithm in Chapter 3 and VPSO-LF algorithm in Chapter 4.

Chapter 6

Conclusions and Scope for Future Research

Chapter 6

Conclusions and Scope for Future Research

6.1 Conclusions

The solar photovoltaic system is the most attractive source of electricity in renewable power generation system due to the abundant availability of sunlight. However, it has some drawbacks, such as weather inconstancy, low tracking efficiency. Extensive research has been conducted so far on improving the efficiency of MPPT power extraction from PV systems under different climatic conditions. However, selecting the best MPPT for a specific PV system configuration and requirements has always been difficult. In order to accomplish this, we have explored and studied the most important and recent evolutionary optimization strategies introduced in our proposed methods, revealing the features of each strategy under partial shading conditions. Most standard MPPT algorithms struggle to obtain reliable GMPP under fast changing of irradiance and partial shading conditions, according to the findings. However, improved evolutionary optimization algorithms outperform traditional algorithms in tracking the GMPP under partial shading conditions.

The proposed MGWO algorithm is used for tracking GMPP during shaded conditions of PV array in Chapter 3. This proposed MGWO algorithm enhances performance of existing GWO algorithm by using modified updated-position and non-linear variation of control parameter for better convergence factor. This proposed MGWO algorithm was tested by considering different PV array configurations. In which six patterns (cases) were formed under partial shaded conditions (PSC). During PSC, the corresponding P-V curves shows multiple peaks. *The proposed MGWO algorithm developed and validated experimentally for tracking the global peak (GP) power under shaded condition of PV array with reduced number of iterations and less tracking period. The steady-state oscillations also reduced around global peak point successfully and implemented only one tuning control parameter; initial particles were independent of PV system*.

The tuning nature of control parameter was eliminated in the proposed algorithm of Chapter 4. To improve convergence factor, the velocity of Particle Swarm Optimization is

updated based on Lévy Flights which is called VPSO-LF algorithm. The Lévy Flights (LF) are random walks, which improves the exploitation process with small steps and takes long jump for the purpose of exploration process. So the proposed VPSO-LF improved the performance of PV array under partial shaded conditions. The VPSO-LF algorithm was proposed with reduced tuning parameters, developed and validated experimentally for GMPP tracking with eight cases (patterns) of PV array under PSC. *In this proposed VPSO-LF algorithm, the velocity is updated with Lévy Flights distribution to reach GMPP with less tracking time and reduced number of iterations and without considering limitations on velocity. The proposed VPSO-LF algorithm also reduces steady-state oscillations around global peak effectively, this method considered initial duty independent of the PV system and also does not needs the tuning of velocity parameters.*

The control parameters were reduced, the algorithm proposed in Chapter 5. Here the Jaya algorithm is having less number of control parameters and suitable for tracking global peak power under partial shaded conditions of PV array. This Jaya algorithm is good for exploration search process with the presence of random number but shows poor exploitation process with less number of control parameters which delay convergence time. To improve convergence time, a Jaya algorithm proposed based on Lévy Flights (Jaya-LF). The proposed Jaya-LF was simulated and implemented experimentally for tracking global peak power during partial shading of PV arrays with low number of control parameters. *The Jaya-LF algorithm tracks global peak power with fewer iterations and lower convergence time.* The oscillations at steady-state and transient state are reduced without tuning parameters; the three initial particles are independent of the PV system. To highlight the benefits of the proposed algorithms, a detailed comparison is made in terms of extracted PV array power, convergence time, number of iterations and tracking efficiency. During the sudden change of PV array pattern, the proposed algorithms had re-initialized the parameters to know the effectiveness of proposed methods. This also compared with existing algorithms in terms of population size, tracking time, iterations, number of tuning parameters, dependency of initial particles, and re-initialization of parameters. The controlled parameters were reduced in Jaya-LF algorithm compared with VPSO-LF and MGWO algorithms.

6.2 Scope for Future Research

- In three-phase systems, two-stage and single-stage grid connected SPV systems are commonly used topologies. The two stage system consists of two conversion stages as DC-DC converter stage for MPP tracking and voltage boosting, and a DC-AC inverter stage for interfacing the PV system to the grid. These proposed algorithms in the present research can further be used on PV integrated to grid-tied systems to improve tracking efficiency of PV system. On the other hand, a single-stage topology have gained attention especially in low voltage applications due to high efficiency when compared to two-stage conversion. However, the efficiency of conversion stage is improved in single-stage grid connected PV system.

- Grid connected PV system has facing challenge of intermittent energy production with the dynamic power demand. To overcome this, energy storage system is added to the grid connected PV system. The improved evolutionary optimization techniques can be applied for hybrid systems to increase the efficiency and to maintain constant voltage. The energy management is required during non-PV hours, supply power to DC-loads. The battery energy storage is connected to dc-link of Voltage Source Converter (VSC) through a bi-directional DC-DC converter to meet the requisite of power management in the grid and load environment. In single-stage PV-battery grid connected system, both VSC and bi-directional DC-DC converter are responsible for MPP tracking and real power injection to grid. For that, co-ordination between VSC and bi-directional DC-DC converter is required for MPP tracking.

- The MPPT algorithms are applied to enhance the performance of the grid-connected permanent magnet synchronous generator driven by variable speed wind turbine (PMSG-VSWT). The MPPT algorithms provides minimum integral squared error (ISE) for the input errors of PI controllers that are controlling the RMS voltage of PMSG and grid, the DC link voltage, and generated power real power.

Journal Publications

Published:

1. Rambabu Motamarri, Nagu Bhookya, "GMPPT by using PSO based on Lévy Flight for Photovoltaic System under Partial Shading Conditions," in *IET Renewable Power Generation*, vol. 14, no. 7, pp. 1143-1155, Jan. 2020.

2. Rambabu Motamarri, Nagu Bhookya, "Jaya Algorithm based on Lévy Flight for Global MPPT under Partial Shading in Photovoltaic System," in *IEEE Journal of Emerging and Selected Topics in Power Electronics*, doi: 10.1109/JESTPE.2020.3036405.

3. Rambabu Motamarri, Nagu Bhookya and B. Chitti babu, "Modified Grey Wolf Optimization for Global MPPT under Partial Shading Conditions in Photovoltaic System" in *Wiley International Journal of Circuit Theory and Applications*, https://doi.org/10.1002/cta.3018.

References

[1] M. Z. Shams El-Dein, M. Kazerani, and M. M. A. Salama, “Optimal Photovoltaic Array Reconfiguration to Reduce Partial Shading Losses,” in *IEEE Transactions on Sustainable Energy*, vol. 4, no. 1, pp. 145-153, Jan. 2013.

[2] H. Patel and V. Agarwal, “MATLAB-based Modeling to Study the Effects of Partial Shading on PV Array Characteristics,” in *IEEE Transactions on Energy Conversion*, vol. 23, no. 1, pp. 302-310, March 2008.

[3] S. Hosseini, S. Taheri, M. Farzaneh, and H. Taheri, “A High-Performance Shade-Tolerant MPPT based on Current-Mode Control,” in *IEEE Transactions Power Electron*ics, vol. 34, no. 10, pp. 10327-10340, Oct. 2019.

[4] E. Karatepe, Syafaruddin, and T. Hiyama, “Simple and High-Efficiency Photovoltaic System under Non-Uniform Operating Conditions,” in *IET Renewable Power Generation*, vol. 4, no. 4, pp. 354-368, July 2010.

[5] N. Femia, G. Petrone, G. Spagnuolo and M. Vitelli, "Optimization of Perturb and Observe Maximum Power Point Tracking Method," in *IEEE Transactions on Power Electronics*, vol. 20, no. 4, pp. 963-973, July 2005.

[6] W. Xiao and W. G. Dunford, "A Modified Adaptive Hill Climbing MPPT Method for Photovoltaic Power Systems," in *IEEE Power Electronics Specialists Conference*, Vol.3, pp. 1957-1963, 2004.

[7] W. Zhu, L. Shang, P. Li, and H. Guo, "Modified Hill Climbing MPPT Algorithm with Reduced Steady-State Oscillation and Improved Tracking Efficiency," in *the Journal of Engineering*, vol. 2018, no. 17, pp. 1878-1883, Nov. 2018.

[8] L. Piegari, and R. Rizzo, “Adaptive Perturb and Observe Algorithm for Photovoltaic Maximum Power Point Tracking,” in *IET Renewable Power Generation*, vol. 4, no. 4, pp. 317–328, 2010.

[9] N. Femia, D. Granozio, G. Petrone, G. Spagnuolo and M. Vitelli, "Predictive & Adaptive MPPT Perturb and Observe Method," in *IEEE Transactions on Aerospace and Electronic Systems*, vol. 43, no. 3, pp. 934-950, July 2007.

[10] S. K. Kollimalla and M. K. Mishra, "Variable Perturbation Size Adaptive P&O MPPT Algorithm for Sudden Changes in Irradiance," in *IEEE Transactions on Sustainable Energy*, vol. 5, no. 3, pp. 718-728, Jul. 2014.

[11] A. K. Abdelsalam, A. M. Massoud, S. Ahmed, and P. N. Enjeti, "High-Performance Adaptive Perturb and Observe MPPT Technique for Photovoltaic-based Microgrids," in *IEEE Transactions Power Electronics*, vol. 26, no. 4, pp. 1010-1021, Apr. 2011.

[12] G. Petrone, G. Spagnuolo, and M. Vitelli, "A Multivariable Perturb-And Observe Maximum Power Point Tracking Technique Applied to A Single Stage Photovoltaic Inverter," in *IEEE Transactions on Industrial Electronics*, vol. 58, no. 1, pp. 76-84, Jan. 2011.

[13] M. A. Elgendy, B. Zahawi, and D. J. Atkinson, "Assessment of the Incremental Conductance Maximum Power Point Tracking Algorithm," in *IEEE Transactions on Sustainable Energy*, vol. 4, no. 1, pp. 108-117, Jan. 2013.

[14] K. S. Tey and S. Mekhilef, "Modified Incremental Conductance Algorithm for Photovoltaic System Under Partial Shading Conditions and Load Variation," in *IEEE Transactions on Industrial Electronics*, vol. 61, no. 10, pp. 5384-5392, Oct. 2014.

[15] T. L. Nguyen and K. Low, "A Global Maximum Power Point Tracking Scheme Employing DIRECT Search Algorithm for Photovoltaic Systems," in *IEEE Transactions on Industrial Electronics*, vol. 57, no. 10, pp. 3456-3467, Oct. 2010.

[16] H. Patel and V. Agarwal, "Maximum Power Point Tracking Scheme for PV Systems Operating Under Partially Shaded Conditions," in *IEEE Transactions on Industrial Electronics*, vol. 55, no. 4, pp. 1689-1698, April 2008.

[17] K. Alireza, I. Hossein and A. Behzad, "A New Maximum Power Point Tracking Strategy for PV Arrays Under Uniform and Non-Uniform Insolation Conditions, " in *Solar Energy*, vol. 91, pp. 221–232, May.2013.

[18] J. Ahmed and Z. Salam, "An Improved Method to Predict the Position of Maximum Power Point During Partial Shading for PV Arrays," in *IEEE Transactions on Industrial Informatics*, vol. 11, no. 6, pp. 1378-1387, Dec. 2015.

[19] J. P. Ram, T. S. Babu, and N. Rajasekar, “A Comprehensive Review on Solar PV Maximum Power Point Tracking Techniques,” in *Renewable and Sustainable Energy Reviews*, vol. 67, pp. 826-847, Jan. 2017.

[20] Y. Liu, S. Huang, J. Huang and W. Liang, "A Particle Swarm Optimization-Based Maximum Power Point Tracking Algorithm for PV Systems Operating Under Partially Shaded Conditions," in *IEEE Transactions on Energy Conversion*, vol. 27, no. 4, pp. 1027-1035, Dec. 2012.

[21] K. Ishaque and Z. Salam, "A Deterministic Particle Swarm Optimization Maximum Power Point Tracker for Photovoltaic System Under Partial Shading Condition," in *IEEE Transactions on Industrial Electronics*, vol. 60, no. 8, pp. 3195-3206, Aug. 2013.

[22] W. Li, G. Zhang, T. Pan, Z. Zhang, Y. Geng and J. Wang, "A Lipschitz Optimization-Based MPPT Algorithm for Photovoltaic System Under Partial Shading Condition," in *IEEE Access*, vol. 7, pp. 126323-126333, Sep. 2019.

[23] T. Sudhakar Babu, N.Rajasekar and K. Sangeetha, “Modified Particle Swarm Optimization Technique based Maximum Power Point Tracking for Uniform and under Partial Shading Condition,” in *Applied Soft Computing*, vol. 34, pp. 613–624, Sep.2015.

[24] T. Sen, N. Pragallapati, V. Agarwal and R. Kumar, "Global Maximum Power Point Tracking of PV Arrays under Partial Shading Conditions using A Modified Particle Velocity-based PSO Technique," in *IET Renewable Power Generation*, vol. 12, no. 5, pp. 555-564, Feb 2018.

[25] C. Huang, L. Wang, R. S. Yeung, Z. Zhang, H. S. Chung and A. Bensoussan, "A Prediction Model-Guided Jaya Algorithm for the PV System Maximum Power Point Tracking," in *IEEE Transactions on Sustainable Energy*, vol. 9, no. 1, pp. 45-55, Jan. 2018.

[26] J. Lian, M. Douglas and P. Jagdish, "A Novel Ant Colony Optimization-based Maximum Power Point Tracking for Photovoltaic Systems Under Partially Shaded Conditions, " in *Energy Buildings*, vol.58, pp. 227–236, March. 2012.

[27] K. Sundareswaran, P. Sankar, P. S. R. Nayak, S. P. Simon and S. Palani, "Enhanced Energy Output from a PV System Under Partial Shaded Conditions Through Artificial Bee Colony," in *IEEE Transactions on Sustainable Energy*, vol. 6, no. 1, pp. 198-209, Jan. 2015.

[28] K. Sundareswaran, S. Peddapati and S. Palani, "MPPT of PV Systems Under Partial Shaded Conditions Through a Colony of Flashing Fireflies," in *IEEE Transactions on Energy Conversion*, vol. 29, no. 2, pp. 463-472, June 2014.

[29] S. Mohanty, B. Subudhi and P. K. Ray, "A New MPPT Design Using Grey Wolf Optimization Technique for Photovoltaic System Under Partial Shading Conditions," in *IEEE Transactions on Sustainable Energy*, vol. 7, no. 1, pp. 181-188, Jan. 2016.

[30] A. M. Eltamaly and H. M.H.Farh, "Dynamic Global Maximum Power Point Tracking of the PV Systems under Variant Partial Shading using Hybrid GWO–FLC, " in *Solar Energy*, vol.177, pp. 306–316, Jan.2019.

[31] D. Yousri, T. S. Babu, D. Allam, V. K. Ramachandaramurthy and M. B. Etiba, "A Novel Chaotic Flower Pollination Algorithm for Global Maximum Power Point Tracking for Photovoltaic System under Partial Shading Conditions," in *IEEE Access*, vol. 7, pp. 121432-121445, Aug. 2019.

[32] H. Li, D. Yang, W. Su, J. Lü and X. Yu, "An Overall Distribution Particle Swarm Optimization MPPT Algorithm for Photovoltaic System Under Partial Shading," in *IEEE Transactions on Industrial Electronics*, vol. 66, no. 1, pp. 265-275, Jan. 2019.

[33] M. Seyedmahmoudian, T. K. Soon, B. Horan, A. Ghandhari, S. Mekhilef and A. Stojcevski, "New ARMO-based MPPT Technique to Minimize Tracking Time and Fluctuation at Output of PV Systems under Rapidly Changing Shading Conditions," in *IEEE Transactions on Industrial Informatics*, doi: 10.1109/TII.2019.2895066.

[34] J. P. Ram, D. S. Pillai, N. Rajasekar and S. M. Strachan, "Detection and Identification of Global Maximum Power Point Operation in Solar PV Applications Using A Hybrid ELPSO-P&O Tracking Technique," in *IEEE Journal of Emerging and Selected Topics in Power Electronics*, vol. 8, no. 2, pp. 1361-1374, June 2020.

[35] M.A. Husain, A. Jain, A. Tariq and A. Iqbal, “Fast and Precise Global Maximum Power Point Tracking Techniques for Photovoltaic System,” in *IET Renewable Power Generation*, vol. 13, no. 14, pp. 2569-2579, Oct. 2019.

[36] R. K. Venkata, and N. B. Muralidhar, “A Novel Global MPP Tracking Scheme based on Shading Pattern Identification using Artificial Neural Networks for Photovoltaic Power Generation During Partial Shaded Condition,” in *IET Renewable Power Generation*, vol. 13, no. 10, pp. 1647-1659, July2019.

[37] S. Selvakumar, M. Madhusmita, C. Koodalsamy, S. P. Simon and Y. R. Sood, "High-Speed Maximum Power Point Tracking Module for PV Systems," in *IEEE Transactions on Industrial Electronics*, vol. 66, no. 2, pp. 1119-1129, Feb. 2019.

[38] H. J. M¨oller, “Semiconductors for Solar Cells,” in *Norwood, MA: Artech House*, 1993.

[39] A. L. Fahrenbruch and R. H. Bube, “Fundamentals of Solar Cells,” in*San Francisco, CA: Academic*, 1983.

[40] L. Casta˜ner and S. Silvestre, “Modeling Photovoltaic Systems Using PSpice,” in *New York: Wiley*, 2002.

[41] A. Guechi and M. Chegaar, “Effects of Diffuse Spectral Illumination on Microcrystalline Solar Cells,” in *Journal of Electron Devices*, vol. 5, pp. 116–121,2007.

[42] C. Riordan and R. Hulstron, "What is an air mass 1.5 spectrum? (Solar Cell Performance Calculations)," in *IEEE Conference on Photovoltaic Specialists, Kissimmee, FL, USA*, vol.2, pp. 1085-1088, 1990.

[43] A. Guechi and M. Chegaar, “Effects of Diffuse Spectral Illumination on Microcrystalline Solar Cells,” in *Journal of Electron Devices*, vol. 5, pp. 116–121, Jan.2007.

[44] Weidong Xiao, W. G. Dunford and A. Capel, "A Novel Modeling Method for Photovoltaic Cells," in *IEEE Annual Power Electronics Specialists Conference, Aachen, Germany*, vol.3, pp. 1950-1956, 2004.

[45] M. G. Villalva, J. R. Gazoli and E. R. Filho, "Comprehensive Approach to Modeling and Simulation of Photovoltaic Arrays," in *IEEE Transactions on Power Electronics*, vol. 24, no. 5, pp. 1198-1208, May. 2009.

[46] D. Sera, R. Teodorescu and P. Rodriguez, "PV Panel Model Based on Datasheet Values," in *IEEE International Symposium on Industrial Electronics*, Vigo, pp. 2392-2396, 2007.

[47] W. De Soto, S. A. Klein, andW. A. Beckman, "Improvement and Validation of A Model for Photovoltaic Array Performance," in *Solar Energy*, vol. 80, no. 1, pp. 78–88, Jan. 2006.

[48] C. Carrero, J.Amador, and S. Arnaltes, "A Single Procedure for Helping PV Designers to Select Silicon PV Module and Evaluate the Loss Resistances," in *Renewable Energy*, vol. 32, no. 15, pp. 2579–2589, Dec. 2007.

[49] P. A. Lynn, "Electricity from Sunlight: An Introduction to Photovoltaics,"in*John Wiley &Sons*, pp. 238, 2010.

[50] T. Markvart, "Solar electricity," in *Wiley*, p. 280, 2000.

[51] C. S. Solanki, "Solar Photovoltaics—Fundamentals, Technologies and Applications," in *New Delhi*, India: PHI Learning, 2011.

[52] "Trends in Photovoltaic Applications. Survey Report of Selected IEA Countries between1992 and 2009," International Energy Agency, Report IEA-PVPS Task 1 T119:2010,2010.[Online].Available:http://www.ieapvps.org/products/download/Trends-in-Photovoltaic_2010.pdf [Accessed 28/10/2010].

[53] D. J. Flood, "Advanced Space Photovoltaic Technology: Applications To Telecommunication Systems," in *Proceedings of Power and Energy Systems in Converging Markets, Melbourne, Victoria, Australia*, pp. 647-652, 1997.

[54] J. H. R. Enslin, M. S. Wolf, D. B. Snyman and W. Swiegers, "Integrated Photovoltaic Maximum Power Point Tracking Converter," in *IEEE Transactions on Industrial Electronics*, vol. 44, no. 6, pp. 769-773, Dec. 1997.

[55] B. Subudhi and R. Pradhan, "A Comparative Study on Maximum Power Point Tracking Techniques for Photovoltaic Power Systems," in *IEEE Transactions on Sustainable Energy*, vol. 4, no. 1, pp. 89-98, Jan. 2013.

[56] F. Belhachat and C. Larbes, "A Review of Global Maximum Power Point Tracking Techniques of Photovoltaic System under Partial Shading Conditions," in *Renewable and Sustainable Energy Reviews*, vol. 92, pp.513–553,2018.

[57] L. Guiqiang, Y. Jin, M.W. Akram, X. Chen and J. Jie, "Application of Bio-Inspired Algorithms in Maximum Power Point Tracking for PV Systems under Partial Shading Conditions – A Review," in *Renewable and Sustainable Energy Reviews*, vol. 81, pp. 840–873, 2018.

[58] L. L.Jiang, R. Srivatsan and L. Maskell, "Computational Intelligence Techniques for Maximum Power Point Tracking in PV Systems: A Review," in *Renewable and Sustainable Energy Reviews*, vol. 85, pp. 14-45, 2018.

[59] A. M. Eltamaly, H. M.H. Farh and M. F. Othmanc, "A Novel Evaluation Index for the Photovoltaic Maximum Power Point Tracker Techniques," in *Solar Energy*, vol. 174, pp. 940–956, 2018.

[60] M. Seyedmahmoudian et al., "Simulation and Hardware Implementation of New Maximum Power Point Tracking Technique for Partially Shaded PV System Using Hybrid DEPSO Method," in *IEEE Transactions on Sustainable Energy*, vol. 6, no. 3, pp. 850-862, July 2015.

[61] S. Silvestre, A. Boronat, and A. Chouder, "Study of Bypass Diodes Configuration on PV Modules," in *Applied Energy*, vol. 86, no. 9, pp.1632–1640, 2009.

[62] S. K. Dash, S. Nema, R. K. Nema and D. Verma, "A Comprehensive Assessment Of Maximum Power Point Tracking Techniques under Uniform and Non-Uniform Irradiance and its Impact on Photovoltaic Systems: A Review," in *Journal of Renewable and Sustainable Energy*, vol. 7, no. 6, pp. 063-113, 2015.

[63] R. C. Eberhart and K. James, "A New Optimizer using Particle Swarm Theory, "in *MHS'95. Proceedings of the Sixth International Symposium on Micro Machine and Human Science*, pp. 39-43, Oct. 1995.

[64] M. Miyatake, M.Veerachary, F. Toriumi, N. Fujii and H. Ko, “Maximum Power Point Tracking of Multiple Photovoltaic Arrays: A PSO Approach,” in *IEEE Transection on Aerospace Electronic System*, vol. 47, no. 1, pp. 367–380, 2011.

[65] Y. Shi, and R. C. Eberhart, “Parameter Selection in Particle Swarm Optimization,” in *Proceedings of the 7th international conference on evolutionary programming VII*, pp. 591–600, 1998.

[66] K. Socha and M. Dorigo, “Ant Colony Optimization for Continuous Domains,” in *European Journal of Operational Research*, vol. 185, no. 3, pp. 1155-1173, March 2008.

[67] K. Sundareswaran, V. Vigneshkumar, P. Sankar, S. P. Simon, P. Srinivasa Rao Nayak and S. Palani, "Development of an Improved P&O Algorithm Assisted Through a Colony of Foraging Ants for MPPT in PV System," in *IEEE Transactions on Industrial Informatics*, vol. 12, no. 1, pp. 187-200, Feb. 2016.

[68] A. H. Besheer and M. Adly, "Ant Colony System Based PI Maximum Power Point Tracking for Stand-Alone Photovoltaic System," in *IEEE International Conference on Industrial Technology, Athens*, pp. 693-698, 2012.

[69] D. Karaboga, “An Idea Based on Honey Bee Swarm for Numerical Optimization,” in *Technical Report-TR06, Erciyes University, Engineering Faculty, Computer Engineering Department*, 2005.

[70] A. S. Benyoucef, A. Chouder, K. Kara, S. Silvestre and O. A. sahed,“Artificial Bee Colony based Algorithm for Maximum Power Point Tracking (MPPT) for PV Systems Operating under Partial Shaded Conditions,” in *Applied Soft Computing*, vol. 32, pp. 38–48, July 2015.

[71] X. S. Yang, “Nature-Inspired Metaheuristic Algorithms,” in*2nd edition. Luniver Press*, 2010.

[72] D. F. Teshome, C. H. Lee, Y. W. Lin and K. L. Lian, "A Modified Firefly Algorithm for Photovoltaic Maximum Power Point Tracking Control Under Partial Shading," in *IEEE Journal of Emerging and Selected Topics in Power Electronics*, vol. 5, no. 2, pp. 661-671, June 2017.

[73] N. Kumar, I. Hussain, B. Singh and B. K. Panigrahi, "Maximum Power Peak Detection of Partially Shaded PV Panel by Using Intelligent Monkey King Evolution Algorithm," in *IEEE Transactions on Industry Applications*, vol. 53, no. 6, pp. 5734-5743, Dec. 2017.

[74] K. Kaced, C. Larbes, N. Ramzan, M. Bounabi and Z. Dahmane, "Bat Algorithm Based Maximum Power Point Tracking for Photovoltaic System under Partial Shading Conditions," in *Solar Energy*, vol. 158, pp. 490–503, 2017.

[75] S. Mirjalili, S. M. Mirjalili and A. Lewis, "Grey Wolf Optimizer," in *Advances in Engineering Software*, vol. 69, pp. 46-61, 2016.

[76] L. Wen, J. Jianjun, L. Ximing and T. Mingzhu, "An Exploration-Enhanced Grey Wolf Optimizer to Solve High-Dimensional Numerical Optimization," in *Engineering Applications of Artificial Intelligence*, vol. 68, pp. 63-80, 2018.

[77] N. Mittal, U. Singh, and B. S. Sohi, "Modified Grey Wolf Optimizer for Global Engineering Optimization," in *Applied Computational Intelligence and Soft Computing*, vol.2016, pp. 1-16, 2016.

[78] M. A. Ghasemi, H. M. Foroushani and M. Parniani, "Partial Shading Detection and Smooth Maximum Power Point Tracking of PV Arrays Under PSC," in *IEEE Transactions on Power Electronics*, vol. 31, no. 9, pp. 6281-6292, Sept. 2016.

[79] S. Mohanty, B. Subudhi and P. K. Ray, "A Grey Wolf-Assisted Perturb & Observe MPPT Algorithm for a PV System," in *IEEE Transactions on Energy Conversion*, vol. 32, no. 1, pp. 340-347, March 2017.

[80] Hakli, H., Uguz, H.: 'A Novel Particle Swarm Optimization Algorithm with Lévy Flight', in *Applied Soft Computing*, vol. 23, pp. 333–345, 2014.

[81] A.V.Chechkin, R.Metzler, J. Klafter, and V. Y. Gonchar, "Introduction to the Theory of Lévy Flights," in *John Wiley & Sons, Hoboken, New Jersey, United States*, pp. 129–162, July 2008.

[82] X. Yang and Suash Deb, "Cuckoo Search via Lévy Flights," in *World Congress on Nature & Biologically Inspired Computing (NaBIC), Coimbatore*, pp. 210-214, 2009.

[83] J. Ahmed, Z. Salam, “A Maximum Power Point Tracking (MPPT) for PV System using Cuckoo Search with Partial Shading Capability,” in *Applied Energy*, vol. 119, pp. 118–130, April 2014.

[84] R. Jensi, J. G. Wiselin, “An Enhanced Particle Swarm Optimization with Lévy Flight for Global Optimization,” in *Applied Soft Computing*, vol. 43, no. C, pp. 248–261, June 2016.

[85] R. J. Prasanth, N. Rajasekar, “A New Global Maximum Power Point Tracking Technique for Solar Photovoltaic (PV) System under Partial Shading Conditions (PSC),” In *Energy*, vol. 118, pp. 512–525, Jan.2017.

[86] R. J. Prasanth, N. Rajasekar, “A New Robust, Mutated and Fast Tracking LPSO Method for Solar PV Maximum Power Point Tracking under Partial Shaded Conditions," in *Applied Energy*, vol. 201, pp. 45–59, Sep. 2017.

[87] M. Kermadi, Z. Salam, J. Ahmed and E. M. Berkouk, "An Effective Hybrid Maximum Power Point Tracker of Photovoltaic Arrays for Complex Partial Shading Conditions," in *IEEE Transactions on Industrial Electronics*, vol. 66, no. 9, pp. 6990-7000, Sept. 2019.

[88] J.Y. Shi, F. Xue, Z.J. Qin, W. Zhang, L.T. Ling and T. Yang, “Improved Global Maximum Power Point Tracking for Photovoltaic System via Cuckoo Search under Partial Shaded Conditions,” In *Journal of Power Electronics*, vol. 16, no. 1, pp. 287-296, Jan. 2016 .

[89] J. Riget and J. S. Vesterstrøm, “A Diversity-Guided Particle Swarm Optimizer - the ARPSO,” EVALife Project Group, Aarhus University, Denmark, EVALife Technical Report no. 2002-02, 2002.

[90] M. -K. Baek, J. -B. Park, and K. Y. Lee, “An Improved Attractive and Repulsive Particle Swarm Optimization for Nonconvex Economic Dispatch Problems,” Proc. The IFAC and CIGR/CIRED workshop on Control of Transmission and Distribution Smart Grids (CTDSG 2016), Prague Czech Republic, October 11-13, 2016.

[91] R. V. Rao, "Jaya: A Simple and New Optimization Algorithm for Solving Constrained and Unconstrained Optimization Problems," in *International Journal of Industrial Engineering Computations*, vol.7, pp. 19–34, Aug. 2016.

[92] J. Yu, C. Kim, A. Wadood, T. Khurshaid and S. Rhee, "Jaya Algorithm with Self-Adaptive Multi-Population and Lévy Flights for Solving Economic Load Dispatch Problems," in *IEEE Access*, vol. 7, pp. 21372-21384, Feb.2019.

Appendix-I: Flowchart for the Hill Climbing Algorithm

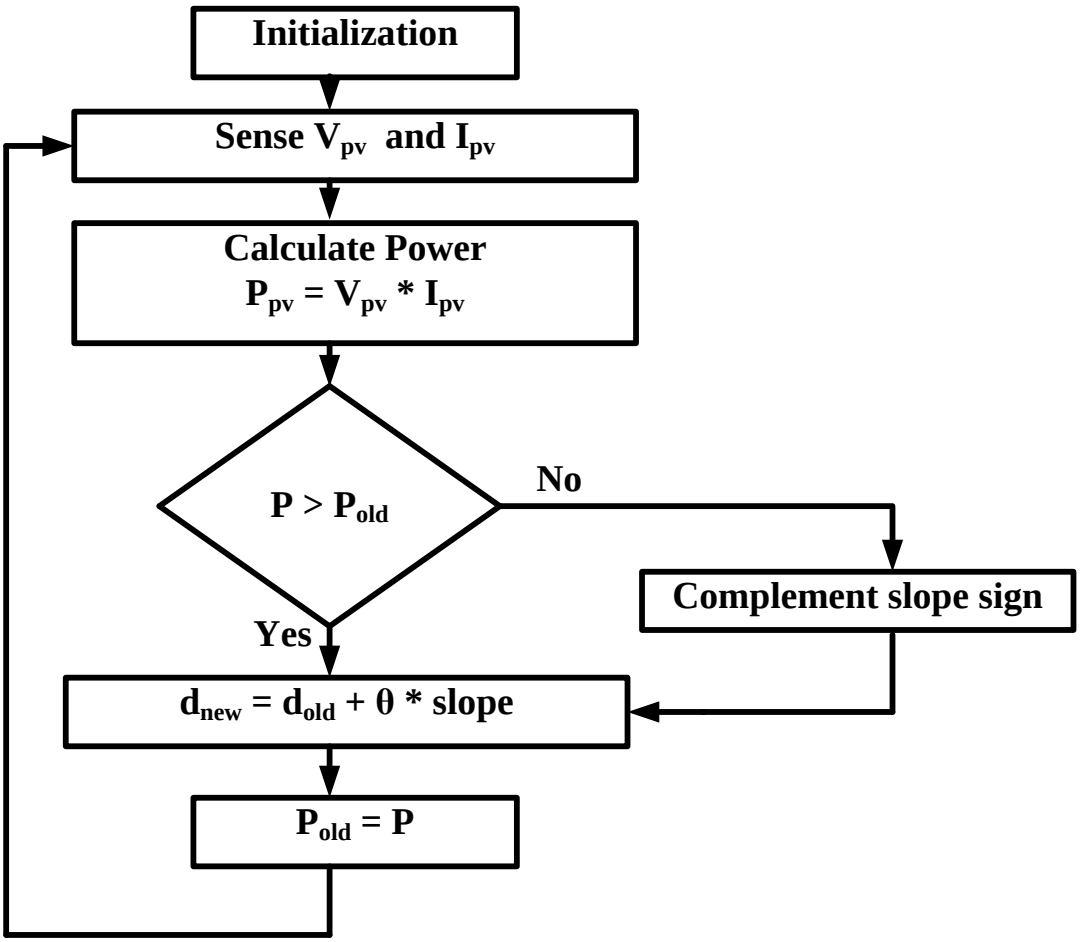

Appendix-II: Flowchart for the PSO Algorithm

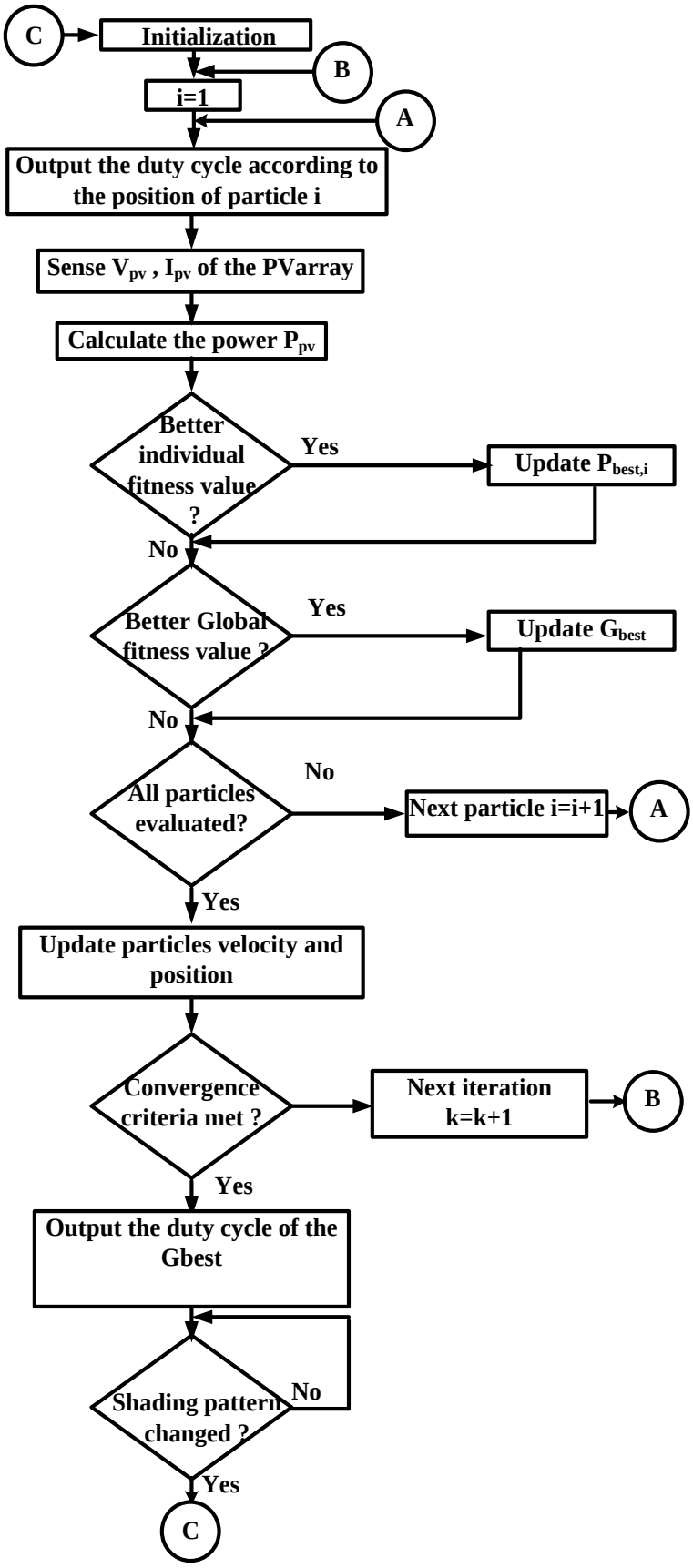

Curriculum-Vitae

Name	:	Rambabu Motamarri
Date of Birth	:	10th July 1988
Marital status	:	Married
Gender	:	Male
Contact number	:	+91-9703712445
Email id	:	ramu77motamarri@student.nitw.ac.in

Academic Qualifications:

Program	Institution	% / CGPA	Year of completion
PhD (Electrical Engineering)	National Institute of Technology Warangal,(NITW) Telangana	-	2021
M. Tech. (Power Electronics & Drives)	Visvesvaraya National Institute of Technology, Nagpur (VNIT).	8.1	2013
B. Tech. (Electrical and Electronics Engg.)	Chaitanya Engineering College under JNTU Kakinada University Visakhapatanm.	65.28	2010